Finite Space Direct and Inverse Problem in Quantum Mechanical Scattering Theory Using the Born Approximation

by

Said Mohammad Said Al-Amoudi

A Thesis Presented to the

FACULTY OF THE COLLEGE OF GRADUATE STUDIES

KING FAHD UNIVERSITY OF PETROLEUM & MINERALS

DHAHRAN, SAUDI ARABIA

In Partial Fulfillment of the
Requirements for the Degree of

MASTER OF SCIENCE

In

PHYSICS

June, 1993

Order Number 1354106

Finite space direct and inverse problem in quantum mechanical scattering theory using the Born approximation

Al-Amoudi, Said Mohammad Said, M.S.

King Fahd University of Petroleum and Minerals (Saudi Arabia), 1993

U·M·I
300 N. Zeeb Rd.
Ann Arbor, MI 48106

FINITE SPACE DIRECT AND INVERSE PROBLEM IN QUANTUM MECHANICAL SCATTERING THEORY USING THE BORN APPROXIMATION

BY

SAID MOHAMMAD SAID AL-AMOUDI

A Thesis Presented to the

FACULTY OF THE COLLEGE OF GRADUATE STUDIES

KING FAHD UNIVERSITY OF PETROLEUM & MINERALS

DHAHRAN, SAUDI ARABIA

In Partial Fulfillment of the
Requirements for the Degree of

MASTER OF SCIENCE

In

PHYSICS

JUNE 1993

KING FAHD UNIVERSITY OF PETROLEUM AND MINERALS
DHAHRAN, SAUDI ARABIA
COLLEGE OF GRADUATE STUDIES

This thesis, written by **Said Mohammad Al-Amoudi** (Student I.D. No. **846413**) under the direction of his Thesis Advisor and approved by his Thesis Committee, has been presented to and accepted by the Dean of the College of Graduate Studies, in partial fulfillment of the requirements for the degree of **MASTER OF SCIENCE**.

THESIS COMMITTEE

Dr. H. A. Mavromatis, Thesis Advisor

Dr. Riazuddin, Member

Dr. Bahlouli, Member

Chairman, Physics Department
Dr. Abdulaziz Al-Harthi

Date : _____

Dean, College of Graduate Studies
Dr. Ala Al-Rabeh

Date: ١٤٢٥-١٢-٠٩

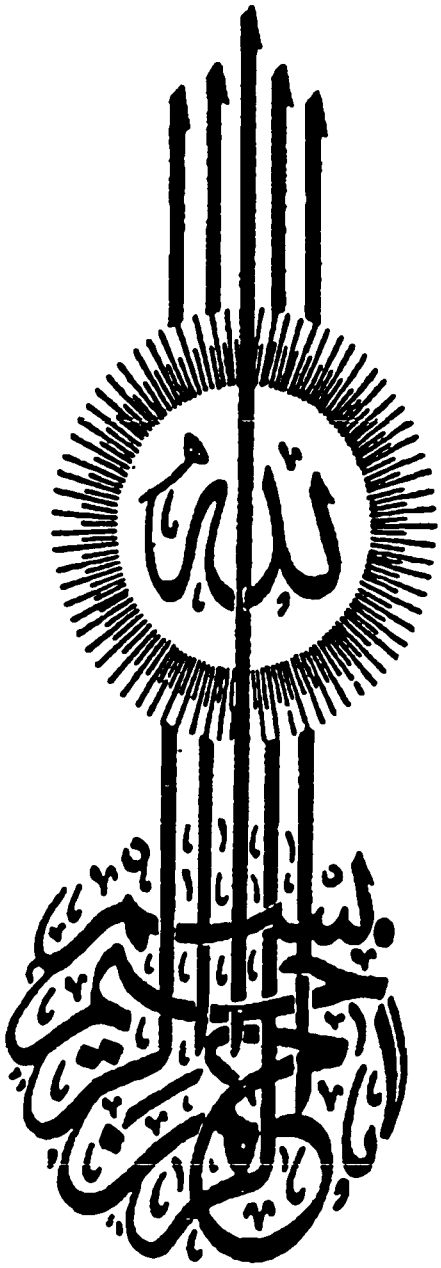
بسم الله الرحمن الرحيم

إهـــــداء

إلى من شغف قلبي بحبهما

إلى والدي الحبيبين

ACKNOWLEDGMENT

I would like to thank my thesis advisor Prof. Harry Mavromatis, who spent a lot of time directing and guiding me, and my other thesis committee members, Prof. Riazuddin and Dr. Bahlouli.

Also, I would like to thank Dr. Isam Ayoubi, from the Mathematics Department, who helped me with some of the numerical calculations.

TABLE OF CONTENTS

خلاصة الرسالة

الاسم : سعيد محمد سعيد العمودي

العنوان : المسألة المباشرة للتناثر في فضاء محدود و عكسها في نظرية علم حركة الكم باستعمال تقريب بورن

التخصص : فيزياء

التاريخ : ذوالحجة ١٤١٣

لقد درست المسألة المباشرة للتناثر في فضاء محدود بنشر التابع الموجي النصف قطري لجسيم كتلته μ محتوى بداخل كرة نصف قطرها a بحدود توابع بسل الكروية غير المستمرة. لقد تم اشتقاق التابع الموجي الجزئي للفضاء المحدود لتقريب بورن وتم تطوير طريقتين لقلبه . فالأولى تتضمن استعمال مقلوب التابع $j_l^2(r)$ بينما تتضمن الثانية تبسيط المسألة لجملة معادلات خطية Ax=b ثم قلب مصفوفة هذه المعادلات A والتي وجدت بأنها شاذة. ومع أن المصفوفة شاذة فقد تمكنا من قلبها باستعمالنا مفاهيم وتقنيات القلب المعممة. وخلال تطويرنا لطريقة القلب الأولى توصلنا إلى بعض العلاقات الرياضية الجديدة . كما أن طريقة قلب الفضاء اللامحدود المشروحة في المرجع (٧) قد حسنت بقلب التابع الموجي الجزئي الثاني لتقريب بورن بدلا من قلب التابع الجزئي الأول لتقريب بورن.

درجة الماجستير في العلوم

جامعة الملك فهد للبترول والمعادن

الظهران - المملكة العربية السعودية

ذوالحجة ١٤١٣ هـ

ABSTRACT

NAME : SAID MOHAMMAD SAID AL-AMOUDI

TITLE : FINITE SPACE DIRECT AND INVERSE PROBLEM IN QUANTUM MECHANICAL SCATTERING THEORY USING THE BORN APPROXIMATION

MAJOR : PHYSICS

DATE : JUNE 1993

The direct scattering problem in a finite space was studied by expanding the radial wave function of a particle of mass μ, confined within a three-dimensional sphere of radius a in terms of a set of discrete spherical Bessel functions. The finite space version of the partial wave Born approximation was derived and two inversion techniques were developed to invert it. The first, involves using the inverse function of $j_\ell^2(r)$ while the second involves reducing the problem to a matrix equation $Ax = b$ and then inverting the matrix A, which turns out to be *singular. Although the matrix A is singular, we manage to invert it using generalized inverse concepts and techniques.* In the course of developing the first of the above inversion techniques, *some new and relevant mathematical relations were obtained.* Furthermore, the infinite space inversion techniques developed in ref. [7] were improved by inverting the second partial wave Born approximation rather than the first partial wave Born approximation.

MASTER OF SCIENCE DEGREE

KING FAHD UNIVERSITY OF PETROLEUM AND MINERALS

DHAHRAN, SAUDI ARABIA

JUNE 1993

INTRODUCTION

The inverse problem in quantum mechanical scattering theory is of interest in nuclear physics because it enables us to understand various aspects of nuclear behaviour in terms of the two-body forces derived from nucleon-nucleon scattering. Using the phase shifts produced by the scattering of two nucleons in the angular momentum channel ℓ, and which can be determined experimentally, one wishes to determine the interaction (or equivalently the potential) and the forces between these nucleons, in contrast to the direct problem where the interaction between the nucleons is known and one wishes to calculate the phase shifts produced by that known potential.

This problem has been extensively discussed in the literature and yet there is no completely satisfactory solution to this problem. An excellent exposition can be found in the recent book by Chadan and Sabatier [1].

In order to solve the inverse problem in quantum mechanical scattering theory, the Gel'fand-Levitan-Marchenko equation must be solved [2], but this approach to the inverse scattering problem is quite difficult. In order to simplify the mathematical derivation, a discrete version of the inverse scattering problem was developed [3], [4] and [5]. Although the mathematical derivation in the discrete version of the inverse scattering problem is simpler than in the continuous one, it is still involved.

However, it is possible to invert a simple approximate expression which relates the scattering potential $V_\ell(r)$ and the phase shifts $\delta_\ell(k)$ produced by this scattering potential. This expression is the partial-wave Born approximation and it is given by [6]:

$$\frac{-\hbar^2}{2\mu}\frac{\delta_\ell(k)}{k} \approx \int_0^\infty j_\ell^2(kr)V_\ell(r)r^2dr, \tag{0.1}$$

where

$V_\ell(r)$: is the scattering potential in the angular momentum channel ℓ.

$j_\ell(r)$: is the spherical Bessel function.

μ : is the mass of the scattered particle.

k : is the momentum of the scattered particle, in units of $\hbar$, which is given by

$$k = \sqrt{\frac{2\mu E}{\hbar^2}}$$

E : is the energy of the particle.

This approximation is valid for channels where the scattering potential is weak.

Recently [7], Eqn. (0.1) was inverted in an infinite space using two different inversion techniques which will be discussed in chapter 2.

In this thesis, a counterpart of the partial-wave Born approximation in finite spaces was derived (see chapter 6), by considering a particle of mass μ, confined within a three-dimensional sphere of radius a and scattered off a finite potential $V_\ell(r)$ located near the origin of the sphere. This finite space partial wave Born approximation is given by

$$-\frac{\hbar^2}{2\mu}\frac{k_{\ell n}^2-\gamma_{\ell n}^2}{N_{\ell n}^2} \approx \int_0^a r^2 j_\ell^2(k_{\ell n}r)V_\ell(r)dr, \tag{0.2}$$

where

$k_{\ell n}$: is the momentum, in units of $\hbar$, of the nth state of a free particle of mass μ in the angular momentum channel ℓ,

$\gamma_{\ell n}$: is the momentum, in units of $\hbar$, of the nth state of the particle in the presence of a scattering potential $V_\ell(r)$ in the angular momentum channel ℓ,

$N_{\ell n}$: is a normalization constant.

It is interesting to invert the finite-space partial-wave Born approximation since there one can use the concept of complete discrete sets to expand the radial wave function of the particle and the potential, which then simplify the calculations and may improve the result which is obtained in the infinite space.

Furthermore, in finite spaces, one can easily obtain, at least numerically, the

phase shifts of potentials which depend explicitly on momentum (see section 4.1) such as [8]:

$$V_\ell(r,p) = V_\ell^{(1)}(r) + \frac{p^2}{\mu} V_\ell^{(2)}(r) + V_\ell^{(2)}(r) \frac{p^2}{\mu},$$

whereas in infinite spaces this is very difficult.

Two inversion techniques were developed to invert the finite-space partial-wave Born approximation (see chapter 6). The first technique, involves using the inverse function of $j_\ell^2(r)$, namely $g_\ell(r)$ (see chapter 1), where the discrete version of this function was derived and consequently some *new mathematical relations were obtained.* The second technique involves expanding the potential in terms of a complete discrete set and then reducing the problem to solving the matrix equation $Ax = b$. To obtain the potential $V_\ell(r)$, one needs to invert the matrix A which turns out to be *singular. Although the matrix A is singular, we manage to invert it using generalized inverse concepts and techniques*, see chapter 1.

In this thesis, we found that the inversion techniques which extract the potential from the partial-wave Born approximation in finite and infinite spaces are *mass dependent.* In chapter 7, we show the usefulness of this dependence to improve the results obtained in [7].

CHAPTER 1

Mathematical Introduction

Before going into the details of the direct and inverse scattering problem in a finite space, it is convenient to introduce here some mathematical relations which will be used throughout this thesis.

1.1 Orthonormal Functions

The representation of functions by expansions in orthonormal functions forms a powerful technique that can be used in a large class of problems. The choice of a particular orthonormal set depends on the symmetries of the problem involved.

Following the notation of Jackson [9], the orthonormality condition on the functions $U_n(\xi)$ is given by

$$\int_a^b U_n^*(\xi)\, U_m(\xi)\, d\xi = \delta_{nm}, \tag{1.1}$$

where $U_n(\xi)$, $n = 1, 2, \ldots$, are square integrable and orthonormal on the interval $[a, b]$.

Then, any square integrable function $f(\xi)$ on the interval $[a, b]$ can be expanded by $U_n(\xi)$ as follows:

$$f(\xi) = \sum_{n=1}^{\infty} c_n\, U_n(\xi), \tag{1.2}$$

where

$$c_n = \int_a^b U_n^*(\xi)\, f(\xi)\, d\xi, \tag{1.3}$$

if the orthonormal set of functions $\{U_n(\xi)\}$ is complete. The completeness relation is given by

$$\sum_{n=1}^{\infty} U_n^*(\xi')\, U_n(\xi) = \delta(\xi' - \xi). \tag{1.4}$$

For our purpose, it is convenient to work with the spherical Bessel functions $j_\ell(r)$ as the complete set, because of the spherical symmetry of our problem, since we are going to consider a particle confined within a three-dimensional sphere of radius a, and because it is then easier to invert the finite-space partial-wave Born approximation, eqn. (0.2), as will be seen in chapter 6.

Spherical Bessel functions $j_\ell(x)$ are related to the Bessel functions $J_p(x)$ as follows [10]:

$$j_\ell(x) = \sqrt{\frac{\pi}{2x}} J_{\ell+1/2}(x), \tag{1.5}$$

or

$$J_{\ell+1/2}(x) = \sqrt{\frac{2x}{\pi}}\, j_\ell(x). \tag{1.6}$$

Since $\{j_\ell(r)\}$ forms a complete set, any function $f(r)$ on the interval $0 \leq r \leq a$ can be expanded in terms of $j_\ell(r)$, i.e.

$$f(r) = \sum_{n=1}^{\infty} b_{\ell n} j_\ell(\frac{\alpha_{\ell n}}{a} r), \tag{1.7}$$

where $\alpha_{\ell n}$ is the nth root of $j_\ell(r)$. Note that the roots of $j_\ell(x)$ are the same as the roots of $J_{\ell+1/2}(x)$, since

$$J_{\ell+1/2}(\alpha_{\ell n}) = \sqrt{\frac{2\alpha_{\ell n}}{\pi}} j_\ell(\alpha_{\ell n}) = 0.$$

The first 50 roots of $j_0(r)$, $j_1(r)$ and $j_2(r)$ are given in ref. [11].

These roots of $j_\ell(r)$ can be obtained by setting $j_\ell(\alpha_{\ell n})$ to zero. For example, for $\ell = 0$,

$$\frac{\sin(\alpha_{0n})}{\alpha_{0n}} = 0$$

$$\Rightarrow \qquad \sin(\alpha_{0n}) = 0.$$

Thus

$$\alpha_{0n} = n\pi, \qquad n = 1, 2, 3, \ldots. \tag{1.8}$$

The orthogonality condition and the completeness relation of $j_\ell(x)$ can be easily obtained from the orthogonality condition and the completeness relation of Bessel functions $J_p(x)$.

The orthogonality relation of Bessel functions for $0 \leq x \leq a$ is given by [12]:

$$\int_0^a J_p(\frac{\alpha_{pm}}{a}x)\, J_p(\frac{\alpha_{pn}}{a}x)\, x\, dx \;=\; \delta_{mn}\frac{a^2}{2}\left[J_{p+1}\left(k_{pn}a\right)\right]^2 \tag{1.9}$$

where α_{pn} is the nth root of $J_p(x)$:

$$J_p(\alpha_{pn}) \;=\; 0, \qquad n = 1,2,3,\ldots.$$

Let $p = \ell + 1/2$ in eqn. (1.9), one then obtains

$$\int_0^a J_{\ell+1/2}(\frac{\alpha_{(\ell+1/2)m}}{a}x)\, J_{\ell+1/2}(\frac{\alpha_{(\ell+1/2)n}}{a}x)\, x\, dx \;=\; \delta_{mn}\frac{a^2}{2}\left[J_{\ell+3/2}\left(k_{(\ell+1/2)n}a\right)\right]^2 \tag{1.10}$$

Define

$$k_{\ell n} \;\equiv\; \frac{\alpha_{(\ell+1/2)n}}{a}. \tag{1.11}$$

Using the definitions in eqns. (1.6) and (1.11), eqn. (1.10) becomes

$$\int_0^a \frac{2r}{\pi}\sqrt{k_{\ell m}\, k_{\ell n}}\, j_\ell(k_{\ell m}r)\, j_\ell(k_{\ell n}r)\, r\, dr \;=\; \delta_{mn}\frac{a^2}{2}\left[\frac{2k_{\ell n}a}{\pi}\, j^2_{\ell+1}(k_{\ell n}a)\right]$$

$$\Rightarrow \qquad \int_0^a j_\ell(k_{\ell m}r)\, j_\ell(k_{\ell n}r)\, r^2\, dr \;=\; \delta_{mn}\frac{a^3}{2}\,\frac{k_{\ell n}}{\sqrt{k_{\ell m}\, k_{\ell n}}}\, j^2_{\ell+1}(k_{\ell n}a). \tag{1.12}$$

<u>If $m = n$</u>, then

$$\int_0^a j^2_\ell(k_{\ell n}r)\, r^2\, dr \;=\; \frac{a^3}{2}\, j^2_{\ell+1}(k_{\ell n}a).$$

But, if $m \neq n$, then

$$\int_0^a j_\ell(k_{\ell m} r)\, j_\ell(k_{\ell n} r)\, r^2\, dr \;=\; 0.$$

Thus

$$\int_0^a j_\ell(k_{\ell m} r)\, j_\ell(k_{\ell n} r)\, r^2\, dr \;=\; \delta_{mn}\, \frac{a^3}{2}\, j_{\ell+1}^2(k_{\ell n} a). \tag{1.13}$$

The orthonormality condition is obtained by requiring

$$\int_0^a N_{\ell m}\, j_\ell(k_{\ell m} r)\, N_{\ell n} j_\ell(k_{\ell n} r)\, r^2\, dr \;=\; \delta_{mn}, \tag{1.14}$$

where $N_{\ell n}$ is the normalization constant.

If $m = n$, then

$$\begin{aligned} N_{\ell n}^2 \int_0^a j_\ell^2(k_{\ell n} r)\, r^2\, dr &= 1 \\ N_{\ell n}^2 \frac{a^3}{2} j_{\ell+1}^2(k_{\ell n} a) &= 1 \\ N_{\ell n}^2 &= \frac{2}{a^3 j_{\ell+1}^2(k_{\ell n} a)}. \end{aligned}$$

Thus

$$N_{\ell n} \;=\; \left| \sqrt{\frac{2}{a^3}}\, \frac{1}{j_{\ell+1}(k_{\ell n} a)} \right|. \tag{1.15}$$

For example, if $\ell = 0$, then

$$\begin{aligned} N_{0n} &= \left| \sqrt{\frac{2}{a^3}}\, \frac{1}{\left(\frac{\sin k_{0n} a}{(k_{0n} a)^2} - \frac{\cos k_{0n} a}{k_{0n} a} \right)} \right| \\ &= \left| \sqrt{\frac{2}{a^3}}\, (k_{0n} a) \right| \\ &= \left| \sqrt{\frac{2}{a}}\, k_{0n} \right|. \end{aligned}$$

The completeness relation of Bessel functions for a continuous parameter k is given by [13]

$$\int_0^\infty J_p(k\rho)\, J_p(k\rho')\, k\, dk = \frac{1}{\rho}\delta(\rho - \rho'). \tag{1.16}$$

Setting $p = \ell + 1/2$ and using eqn. (1.6), eqn. (1.16) becomes

$$\int_0^\infty \sqrt{\frac{2k\rho}{\pi}}\, j_\ell(k\rho) \sqrt{\frac{2k\rho'}{\pi}}\, j_\ell(k\rho')\, k\, dk = \frac{1}{\rho}\delta(\rho - \rho').$$

Thus

$$\int_0^\infty j_\ell(k\rho)\, j_\ell(k\rho')\, k^2\, dk = \frac{\pi}{2\rho^2}\delta(\rho - \rho'). \tag{1.17}$$

1.2 The $g_\ell(kr)$ Functions

In the course of developing some techniques in the inverse problem in quantum mechanical scattering theory, a set of inverse functions of $j_\ell^2(kr)$, namely $g_\ell(kr)$, was obtained to invert the partial wave Born approximation, eqn. (0.1). These $g_\ell(kr)$ functions are defined

1) in terms of a generalized hypergeometric series as [14]:

$$g_\ell(\rho) = \frac{-8\rho^2}{\pi(2\ell+1)}\, {}_1F_2\left(\frac{3}{2}; \frac{1}{2}-\ell,\ \ell+\frac{3}{2}; -\rho^2\right), \tag{1.18}$$

where ${}_1F_2$ is a generalized hypergeometric series.

2) in an integral representation as [15]:

$$g_\ell(\rho) = \frac{(-1)^\ell 16\rho^{3+\ell}\Gamma(\frac{1}{2}-\ell)}{\pi^{3/2}(\ell+\frac{1}{2})B(\frac{3}{2},\ell)} \int_0^1 y^{\ell+3}(1-y^2)^{\ell-1}\, n_\ell(2\rho y)dy, \quad \ell > 0, \tag{1.19}$$

where $n_\ell(r)$ are the spherical Neumann functions [16].

3) in a differential representation as [17]:

$$g_\ell(\rho) = \frac{-4}{\pi}\rho^{2\ell+2}\left(\frac{d}{d\rho}\frac{1}{2\rho}\right)^\ell \frac{d}{d\rho}\left(\frac{d}{d\rho}\frac{1}{2\rho}\right)^\ell \sin(2\rho), \tag{1.20}$$

4) in terms of a finite sum as [18]:

$$g_\ell(\rho) = -(-1)^\ell\frac{8}{\pi}\rho^2\cos(2\rho) + \frac{(-1)^\ell 16\ell(\ell+1)}{\pi}\sum_{k=0}^{\ell}\frac{(-1)^k 2^k(\ell+k)!}{(k+1)!(\ell-k)!}\rho^2\frac{j_k(2\rho)}{(2\rho)^k}, \tag{1.21}$$

where $j_\ell(r)$ are the spherical Bessel functions.

The values and the plots of the first three $g_\ell(\rho)$ functions are given in ref. [7] and fig. 1.1 respectively. The plots of the first three $\frac{g_\ell(\rho)}{\rho^2}$ are given in fig. 1.2.

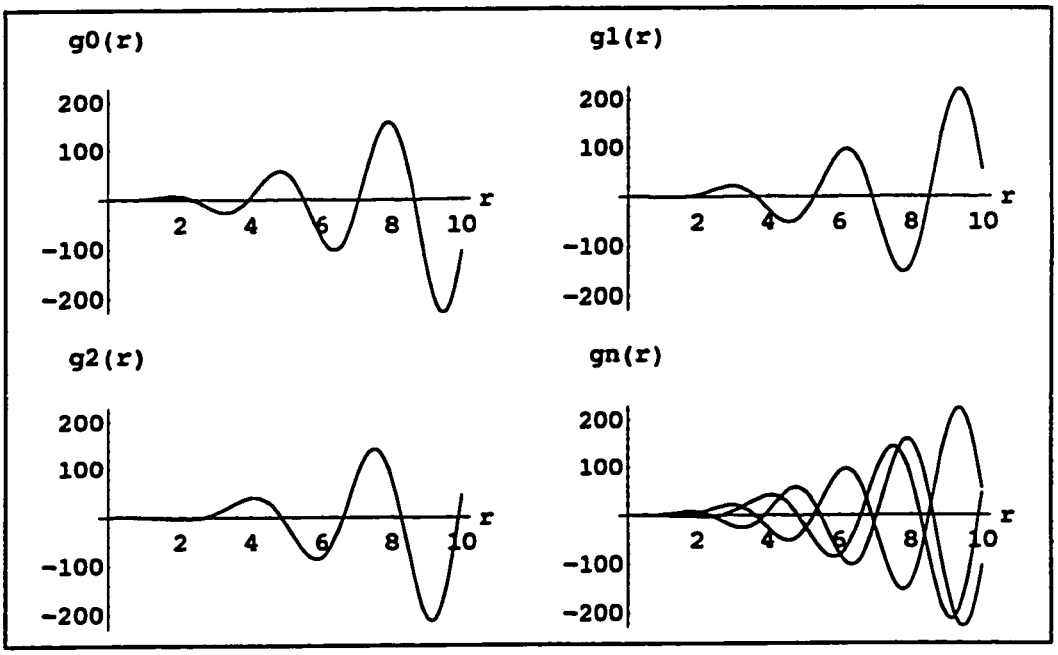

Fig. 1.1 : The plots of $g_0(r)$, $g_1(r)$ and $g_2(r)$.

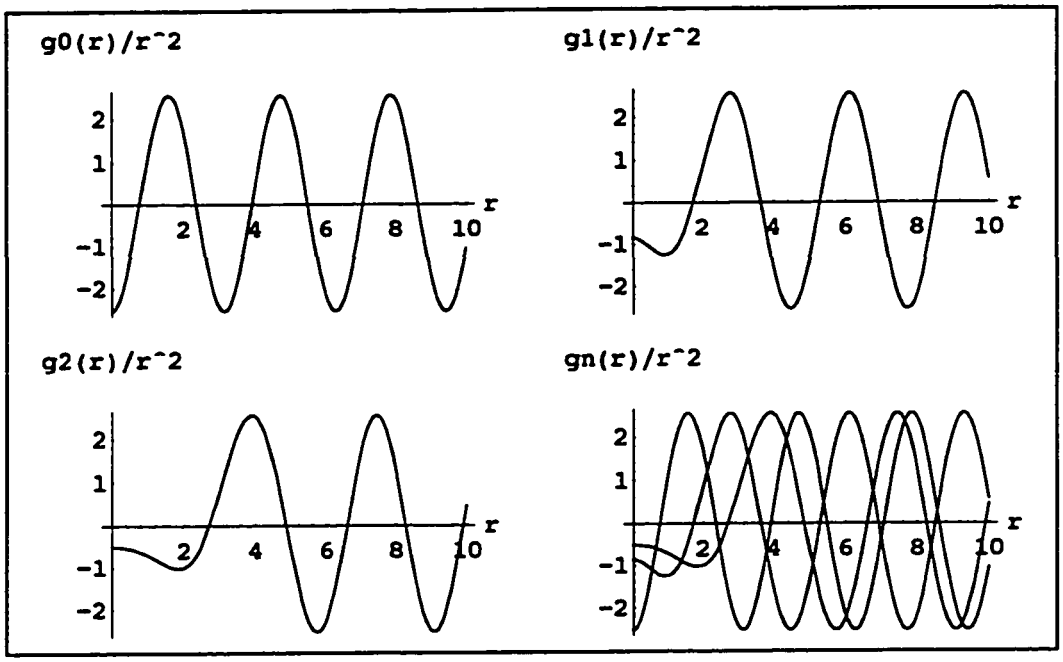

Fig. 1.2 : The plots of $g_0(r)/r^2$, $g_1(r)/r^2$ and $g_2(r)/r^2$.

These $g_\ell(kr)$ functions were designated as the inverse functions of $j_\ell^2(kr)$, because they satisfy the following property [19]:

$$\int_0^\infty j_\ell^2(kr) g_\ell(kr') dk = \frac{r'^2}{r^2}\left\{\delta(r-r') + \delta(r+r') - 2(-1)^\ell \delta(r')\right\}, \qquad (1.22)$$

or equivalently

$$\frac{r^2}{r'^2}\int_0^\infty j_\ell^2(kr) g_\ell(kr') dk - (-1)^{\ell+1} 2\delta(r') = \delta(r-r') + \delta(r+r'). \qquad (1.23)$$

Another useful property of the g_ℓ's which will be used throughout this thesis is [20]:

$$\int_0^\infty \frac{g_\ell(kr)}{k^2 r^2} dk = 4(-1)^{\ell+1}\delta_\ell(r). \qquad (1.24)$$

Using eqn. (1.24), eqn. (1.23) can be put in a more convenient form as follows

$$\frac{r^2}{r'^2}\int_0^\infty j_\ell^2(kr)\, g_\ell(kr')\, dk - \frac{1}{2}\int_0^\infty \frac{g_\ell(kr')}{(kr')^2}\, dk \;=\; \delta(r-r') + \delta(r+r'),$$

or

$$\int_0^\infty k^2 r^2\, j_\ell^2(kr)\, \frac{g_\ell(kr')}{k^2 r'^2}\, dk - \frac{1}{2}\int_0^\infty \frac{g_\ell(kr')}{(kr')^2}\, dk \;=\; \delta(r-r') + \delta(r+r'),$$

which can be written as

$$\int_0^\infty \left(k^2 r^2\, j_\ell^2(kr) - \frac{1}{2}\right)\frac{g_\ell(kr')}{k^2 r'^2} dk \;=\; \delta(r-r') + \delta(r+r'). \qquad (1.25)$$

For $r > 0$ and $r' > 0$, the second term on the RHS of eqn. (1.25), namely $\delta(r+r')$, vanishes because $r + r'$ is strictly greater than zero and from the definition of the delta-function, $\delta(x) = 0$ if $x \neq 0$. Thus

$$\int_0^\infty \left(k^2 r^2\, j_\ell^2(kr) - \frac{1}{2}\right)\frac{g_\ell(kr')}{k^2 r'^2} dk \;=\; \delta(r-r') \qquad \text{if} \quad r > 0, r' > 0. \qquad (1.26)$$

For small values of ρ, $g_\ell(\rho)$ have a simple form [21]:

$$\lim_{\rho \to 0} g_\ell(\rho) = -\frac{8\rho^2}{\pi(2\ell+1)}$$

or

$$\lim_{\rho \to 0} \frac{g_\ell(\rho)}{\rho^2} = -\frac{8}{\pi(2\ell+1)}. \tag{1.27}$$

Notice that the $g_\ell(\rho)$'s are even functions, since

$$\begin{aligned} g_\ell(\rho) &= \frac{-4}{\pi}\rho^{2\ell+2}\left(\frac{d}{d\rho}\frac{1}{2\rho}\right)^\ell \frac{d}{d\rho}\left(\frac{d}{d\rho}\frac{1}{2\rho}\right)^\ell \sin(2\rho) \\ &= \frac{-4}{\pi}(-\rho)^{2\ell+2}\left(\frac{d}{d(-\rho)}\frac{1}{2(-\rho)}\right)^\ell \frac{d}{d(-\rho)}\left(\frac{d}{d(-\rho)}\frac{1}{2(-\rho)}\right)^\ell \sin(-2\rho) \\ &= g_\ell(-\rho). \end{aligned}$$

An interesting point to observe is that $\frac{g_0(kr)}{k^2r^2}$ forms a complete set since

$$\int_0^\infty \frac{g_0(kr)}{k^2r^2}\frac{g_0(k'r)}{k'^2r^2}dr = \frac{16}{\pi}\delta(k-k') \qquad \text{if} \quad k>0, k'>0. \tag{1.28}$$

This result can be proved easily as follows

$$\begin{aligned} \int_0^\infty \frac{g_0(kr)}{k^2r^2}\frac{g_0(k'r)}{k'^2r^2}dr &= \frac{64}{\pi^2}\int_0^\infty \cos(2kr)\cos(2k'r)dr \\ &= \frac{32}{\pi^2}\int_{-\infty}^\infty \cos(2kr)\cos(2k'r)\,dr. \end{aligned}$$

However

$$\cos(x)\cos(y) = \frac{1}{2}\left\{\cos(x+y)+\cos(x-y)\right\}.$$

Therefore

$$\int_0^\infty \frac{g_0(kr)}{k^2r^2}\frac{g_0(k'r)}{k'^2r^2}dr = \frac{16}{\pi^2}\int_{-\infty}^\infty \left\{\cos(2(k+k)r)+\cos(2(k-k')r)\right\}dr. \tag{1.29}$$

But

$$\frac{16}{\pi^2}\int_{-\infty}^{\infty} i\left\{\sin(2(k+k')r)+\sin(2(k-k')r)dr\right\} = 0, \tag{1.30}$$

since $\sin(x)$ is an odd function integrated from $-\infty$ to $+\infty$. Then one can add eqn. (1.30) to eqn. (1.29) to obtain

$$\int_0^{\infty}\frac{g_0(kr)}{k^2r^2}\frac{g_0(k'r)}{k'^2r^2}dr = \frac{8}{\pi^2}\int_{-\infty}^{\infty} e^{2i(k+k')r}+e^{2i(k-k')r}d(2r),$$

or

$$\int_0^{\infty}\frac{g_0(kr)}{k^2r^2}\frac{g_0(k'r)}{k'^2r^2}dr = \frac{16}{\pi}\left\{\delta(k+k')+\delta(k-k')\right\}, \tag{1.31}$$

since

$$\frac{1}{2\pi}\int_{-\infty}^{\infty} e^{iqx}dx = \delta(q).$$

For strictly positive k and k', eqn. (1.31) becomes

$$\int_0^{\infty}\frac{g_0(kr)}{k^2r^2}\frac{g_0(k'r)}{k'^2r^2}dr = \frac{16}{\pi}\delta(k-k') \qquad \text{if} \quad k>0, k'>0.$$

One can now ask the following question; is it generally true that the $\frac{g_\ell(kr)}{k^2r^2}$'s form a complete set ? Equivalently, does the following relation hold for any ℓ ?

$$\int_0^{\infty}\frac{g_\ell(kr)}{k^2r^2}\frac{g_\ell(k'r)}{k'^2r^2}dr \stackrel{?}{=} C_\ell\,\delta(k-k'), \qquad \text{if} \quad k>0, k'>0, \tag{1.32}$$

where C_ℓ is a constant.

Recall that

$$\frac{g_\ell(kr)}{(kr)^2} = -(-1)^\ell\frac{8}{\pi}\cos(2kr)+\frac{(-1)^\ell 16\ell(\ell+1)}{\pi}\sum_{n=0}^{\ell}\frac{(-1)^n 2^n(\ell+n)!}{(n+1)!(\ell-n)!}\frac{j_n(2kr)}{(2kr)^n}.$$

Thus

$$\int_0^\infty \frac{g_\ell(kr)}{(kr)^2}\frac{g_\ell(k'r)}{(k'r)^2}dr = \frac{64}{\pi^2}\int_0^\infty \cos(2kr)\cos(2k'r)dr$$
$$- \frac{8}{\pi}\frac{16\ell(\ell+1)}{\pi}\sum_{n=0}^{\ell}\frac{(-1)^n 2^n(\ell+n)!}{(n+1)!(\ell-n)!}\int_0^\infty \cos(2k'r)\frac{j_n(2kr)}{(2kr)^n}dr$$
$$- \frac{8}{\pi}\frac{16\ell(\ell+1)}{\pi}\sum_{n=0}^{\ell}\frac{(-1)^n 2^n(\ell+n)!}{(n+1)!(\ell-n)!}\int_0^\infty \cos(2kr)\frac{j_n(2kr')}{(2kr')^n}dr$$
$$+ \left(\frac{16\ell(\ell+1)}{\pi}\right)^2\sum_{n=0}^{\ell}\sum_{m=0}^{\ell}\frac{(-1)^{n+m}2^{n+m}(\ell+n)!(\ell+m)!}{(n+1)!(m+1)!(\ell-n)!(\ell-m)!}\int_0^\infty \frac{j_n(2kr)}{(2kr)^n}\frac{j_m(2k'r)}{(2k'r)^m}dr. \tag{1.33}$$

The first term in the RHS of eqn. (1.33) reduces, as was shown previously, to

$$\frac{64}{\pi^2}\int_0^\infty \cos(2kr)\cos(2k'r)dr = \frac{16}{\pi}\left\{\delta(k+k') + \delta(k-k')\right\}.$$

Consider the second term in the RHS of eqn. (1.33)

$$S_2 \equiv -\frac{8}{\pi}\frac{16\ell(\ell+1)}{\pi}\sum_{n=0}^{\ell}\frac{(-1)^n 2^n(\ell+n)!}{(n+1)!(\ell-n)!}\int_0^\infty \cos(2k'r)\frac{j_n(2kr)}{(2kr)^n}dr.$$

But

$$\int_0^\infty \cos(2k'r)\frac{j_n(2kr)}{(2kr)^n}dr = \sqrt{\frac{\pi}{2}}\int_0^\infty \cos(2k'r)\frac{J_{n+\frac{1}{2}}(2kr)}{(2kr)^{n+\frac{1}{2}}}dr,$$

since

$$j_\ell(2kr) = \sqrt{\frac{\pi}{4kr}}J_{\ell+1/2}(2kr).$$

Thus

$$S_2 = -\frac{64\ell(\ell+1)}{\pi^{3/2}}\sum_{n=0}^{\ell}\frac{(-1)^n(\ell+n)!}{(n+1)!(\ell-n)!}\frac{1}{k^{n+\frac{1}{2}}}\int_0^\infty \frac{\cos(2k'r)J_\nu(2kr)}{r^\nu}dr,$$

where

$$\nu = n + \frac{1}{2}.$$

But [22]

$$D_\nu^{(1)}(\alpha,\beta) \equiv \int_0^\infty \frac{J_\nu(\alpha x)\cos(\beta x)}{x^\nu}dx = \begin{cases} \frac{\sqrt{\pi}\alpha^{\nu-1}}{2^\nu\Gamma\left(\frac{2\nu+1}{2}\right)} \times \ {}_2F_1\left(\frac{1}{2}, \frac{-2\nu+1}{2}; \frac{1}{2}; \frac{\beta^2}{\alpha^2}\right) & \text{if } 0<\beta<\alpha \\ 0 & \text{if } 0<\alpha<\beta \end{cases}$$

where [23]

$${}_2F_1(a,b;c;x) = 1 + \frac{ab}{c}\frac{x}{1!} + \frac{a(a+1)b(b+1)}{c(c+1)}\frac{x^2}{2!} + \cdots \tag{1.34}$$

Notice that if $k \neq k'$, then either the second or the third term in the RHS of eqn. (1.33) will vanish depending on the values of k and k'.

Thus the sum of the second and the third terms, $S_\ell(k,k')$, in eqn. (1.33) can be represented as follows

$$S_\ell(k,k') = -\frac{64\ell(\ell+1)}{\pi^{3/2}}\sum_{n=0}^{\ell}\frac{(-1)^n(\ell+n)!}{(n+1)!(\ell-n)!}\frac{1}{k_>^{n+\frac{1}{2}}}\left\{D_{n+\frac{1}{2}}^{(1)}(2k_>,2k_<) + D_{n+\frac{1}{2}}^{(1)}(2k,2k)\delta_{kk'}\right\}, \tag{1.35}$$

where $k_>$ ($k_<$) represents the larger (smaller) of k and k'. Notice that the RHS of eqn. (1.35) contains $\delta_{kk'}$ which indicates that for $k = k'$, the sum of the second and third terms in eqn. (1.33) is twice the sum when $k \neq k'$.

Consider the fourth term in the RHS of eqn. (1.33)

$$T_\ell(k,k') \equiv \left(\frac{16\ell(\ell+1)}{\pi}\right)^2 \sum_{n=0}^{\ell}\sum_{m=0}^{\ell}\frac{(-1)^{n+m}2^{n+m}(\ell+n)!(\ell+m)!}{(n+1)!(m+1)!(\ell-n)!(\ell-m)!}\int_0^\infty \frac{j_n(2kr)}{(2kr)^n}\frac{j_m(2k'r)}{(2k'r)^m}dr. \tag{1.36}$$

Using relation (1.6), the integral in eqn. (1.36) can be written as

$$\begin{aligned}\int_0^\infty \frac{j_n(2kr)j_m(2k'r)}{(2kr)^n(2k'r)^m}dr &= \frac{\pi}{2}\int_0^\infty \frac{J_{n+\frac{1}{2}}(2kr)}{(2kr)^{n+\frac{1}{2}}}\frac{J_{m+\frac{1}{2}}(2k'r)}{(2k'r)^{m+\frac{1}{2}}}dr \\ &= \frac{\pi}{2}\frac{1}{2^{n+m+1}k^{n+1\frac{1}{2}}k'^{m+\frac{1}{2}}}\int_0^\infty \frac{J_{n+\frac{1}{2}}(2kr)J_{m+\frac{1}{2}}(2k'r)}{r^{n+m+1}}dr.\end{aligned}$$

Thus

$$\begin{aligned}T_\ell(k,k') &= \frac{\pi}{4}\left(\frac{16\ell(\ell+1)}{\pi}\right)^2\sum_{n=0}^{\ell}\sum_{m=0}^{\ell}\frac{(-1)^{n+m}(\ell+n)!(\ell+m)!}{(n+1)!(m+1)!(\ell-n)!(\ell-m)!}\frac{1}{k^{n+\frac{1}{2}}k'^{m+\frac{1}{2}}} \\ &\quad\times\int_0^\infty \frac{J_\nu(2kr)J_\mu(2k'r)}{r^{\nu+\mu}}dr,\end{aligned}$$

where

$$\nu = n+\frac{1}{2} \qquad \text{and} \qquad \mu = m+\frac{1}{2}.$$

But [24]

$$\begin{aligned}D^{(2)}_{\nu\mu}(\alpha,\beta) &\equiv \int_0^\infty \frac{J_\nu(\alpha x)J_\mu(\beta x)}{x^{\nu+\mu}}dx \\ &= \begin{cases}\frac{\sqrt{\pi}\beta^\mu}{2^{\nu+\mu}\alpha^{-\nu+1}\Gamma\left(\frac{2\nu+1}{2}\right)\Gamma(\mu+1)} \times {}_2F_1\left(\frac{1}{2},\frac{-2\nu+1}{2};\mu+1;\frac{\beta^2}{\alpha^2}\right) & \text{if } 0<\beta<\alpha \\ \frac{\sqrt{\pi}\alpha^{\mu+\nu-1}\Gamma(\mu+\nu)}{2^{\nu+\mu}\Gamma\left(\frac{2\mu+1}{2}\right)\Gamma\left(\frac{2\mu+2\nu+1}{2}\right)\Gamma\left(\frac{-2\mu+1}{2}\right)} & \text{if } \alpha=\beta>0\end{cases}\end{aligned}$$

Hence

$$\begin{aligned}T_\ell(k,k') &= \frac{\pi}{4}\left(\frac{16\ell(\ell+1)}{\pi}\right)^2\sum_{n=0}^{\ell}\sum_{m=0}^{\ell}\frac{(-1)^{n+m}(\ell+n)!(\ell+m)!}{(n+1)!(m+1)!(\ell-n)!(\ell-m)!}\times \\ &\quad\frac{1}{k^{n+\frac{1}{2}}k'^{m+\frac{1}{2}}}D^{(2)}_{n+\frac{1}{2}m+\frac{1}{2}}(2k,2k'). \qquad (1.37)\end{aligned}$$

Eqn. (1.33) can be written in a simpler form using eqns. (1.31), (1.35) and (1.37) as follows

$$\int_0^\infty \frac{g_\ell(kr)}{(kr)^2}\frac{g_\ell(k'r)}{(k'r)^2}dr = \frac{16}{\pi}\{\delta(k+k')+\delta(k-k')\} + S_\ell(k,k') + T_\ell(k,k'). \quad (1.38)$$

For $k > 0$ and $k' > 0$, eqn. (1.38) becomes

$$\int_0^\infty \frac{g_\ell(kr)}{(kr)^2}\frac{g_\ell(k'r)}{(k'r)^2}dr = \frac{16}{\pi}\delta(k-k') + S_\ell(k,k') + T_\ell(k,k'). \tag{1.39}$$

In general, the last two terms do not vanish. To clarify this point consider a simple case, where $\ell = 1$, $k = 1$ and $k' = 2$.

In order to evaluate $S_1(1,2)$ and $T_1(1,2)$, the following integrals are needed :

$$\begin{aligned}
\int_0^\infty \frac{J_{1/2}(4x)\cos(2x)}{x^{1/2}}dx &= \frac{\sqrt{\pi}}{2\sqrt{2}}\,{}_2F_1\left(\frac{1}{2},0;\frac{1}{2};\frac{1}{4}\right) = \frac{\sqrt{\pi}}{2\sqrt{2}}.\\
\int_0^\infty \frac{J_{3/2}(4x)\cos(2x)}{x^{3/2}}dx &= \frac{\sqrt{\pi}2}{2^{3/2}\Gamma(2)}\,{}_2F_1\left(\frac{1}{2},-1;\frac{1}{2};\frac{1}{4}\right)\\
&= \frac{\sqrt{\pi}}{\sqrt{2}}\times\frac{3}{4}.
\end{aligned}$$

$$\begin{aligned}
\int_0^\infty \frac{J_{1/2}(4x)J_{1/2}(2x)}{x}dx &= \frac{\sqrt{\pi}\sqrt{2}}{2\sqrt{4}\underbrace{\Gamma\left(\frac{3}{2}\right)}_{\frac{\sqrt{\pi}}{2}}}\,{}_2F_1\left(\frac{1}{2},0;\frac{3}{2};\frac{1}{4}\right) = \frac{\sqrt{2}}{2}.\\
\int_0^\infty \frac{J_{1/2}(4x)J_{3/2}(2x)}{x^2}dx &= \frac{\sqrt{\pi}2\sqrt{2}}{42\Gamma\left(\frac{5}{2}\right)}\,{}_2F_1\left(\frac{1}{2},0;\frac{5}{2};\frac{1}{4}\right) = \frac{\sqrt{2}}{3}.\\
\int_0^\infty \frac{J_{3/2}(4x)J_{1/2}(2x)}{x^2}dx &= \frac{\sqrt{\pi}\sqrt{2}}{44^{-1/2}\Gamma\left(\frac{3}{2}\right)}\,{}_2F_1\left(\frac{1}{2},-1;\frac{3}{2};\frac{1}{4}\right) = \frac{11\sqrt{2}}{12}.\\
\int_0^\infty \frac{J_{3/2}(4x)J_{3/2}(2x)}{x^3}dx &= \frac{4\sqrt{\pi}\sqrt{2}}{8\Gamma\left(\frac{5}{2}\right)}\,{}_2F_1\left(\frac{1}{2},-1;\frac{5}{2};\frac{1}{4}\right)\\
&= \frac{2\sqrt{2}}{3}\times\frac{19}{20} = \frac{19\sqrt{2}}{30}.
\end{aligned}$$

Thus

$$\begin{aligned} S_1(1,2) &= -\frac{128}{\pi^{3/2}}\left\{\frac{1}{\sqrt{2}}\times\frac{\sqrt{\pi}}{2\sqrt{2}} - \frac{2!}{2!\times 2^{3/2}}\times\frac{\sqrt{\pi}}{\sqrt{2}}\cdot\frac{3}{4}\right\} \\ &= -\frac{128}{\pi^{3/2}}\left\{\frac{\sqrt{\pi}}{4} - \frac{3\sqrt{\pi}}{16}\right\} = -\frac{32}{\pi}\left\{1-\frac{3}{4}\right\} \\ &= -\frac{8}{\pi}. \end{aligned}$$

and

$$\begin{aligned} T_1(1,2) &= -\frac{256}{\pi}\left\{\frac{1}{\sqrt{2}}\times\frac{\sqrt{\pi}}{2} - \frac{2!}{2!\times\sqrt{2}}\times\frac{\sqrt{2}}{3} - \frac{2!}{2!2^{3/2}}\times\frac{\sqrt{2}\times 11}{12}\right. \\ &\qquad \left. + \frac{2!\times 2!}{2!\times 2!\times 2^{3/2}}\times\frac{19\sqrt{2}}{30}\right\} \\ &= \frac{256}{\pi}\left\{\frac{1}{2} - \frac{1}{3} - \frac{11}{24} + \frac{19}{60}\right\} = \frac{256}{\pi}\left\{\frac{60-40-55+38}{120}\right\} \\ &= \frac{32}{5\pi}. \end{aligned}$$

Hence

$$S_1(1,2) + T_1(1,2) = \frac{32}{5\pi} - \frac{8}{\pi} = -0.51.$$

Therefore

$$\int_0^\infty \frac{g_1(r)}{r^2}\frac{g_1(2r)}{(2r)^2}dr = \frac{32}{5\pi} - \frac{8}{\pi} \neq 0, \tag{1.40}$$

implying

$$\int_0^\infty \frac{g_1(kr)}{(kr)^2}\frac{g_1(k'r)}{(k'r)^2} \neq C_1\,\delta(k-k'), \qquad \text{if } k>0, k'>0,$$

Figure 1.3 below shows the values of $S_1(k,2) + T_1(k,2)$ for $1 \leq k \leq 3$. From the figure and the calculations above one observes directly that $S_1(k,2) + T_1(k,2)$ do not vanish and consequently eqn. (1.32) does not hold for $\ell = 1$ which implies that **the functions $\frac{g_\ell(kr)}{k^2r^2}$ do not form a complete set in general.**

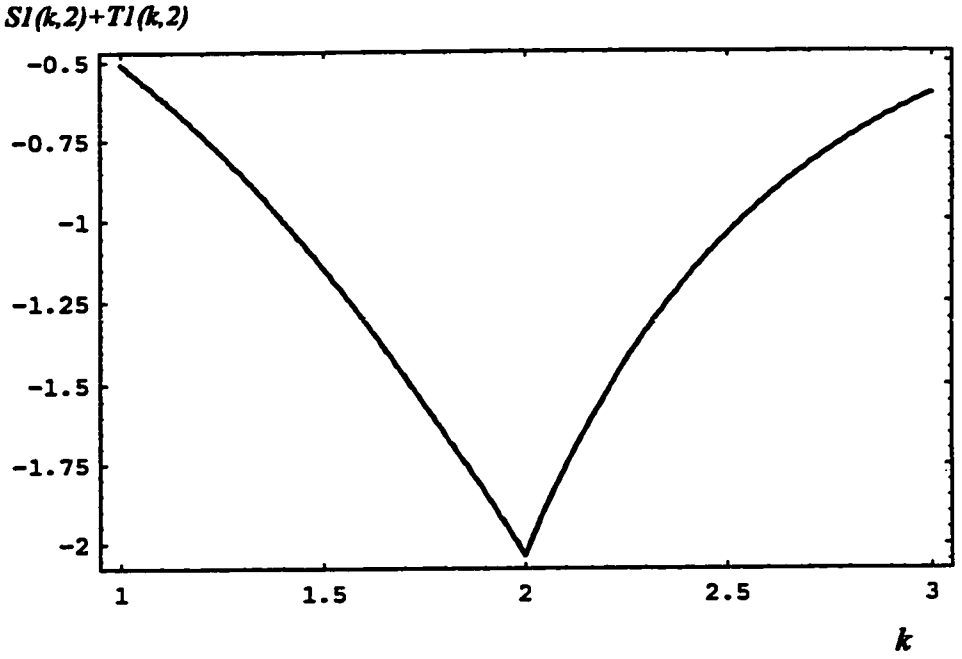

Fig. 1.3 : The sum of $S_\ell(k,k')$ and $T_\ell(k,k')$ for the special case; ℓ=1, k'=2 and $1 \leq k \leq 3$.

Recall that one can expand any square integrable function $f(\xi)$ on $\xi > 0$ in terms of the continuum complete set $\{U(\xi,\eta)\}$ as follows

$$f(\xi) = \int_0^\infty a(\eta)\, U(\xi,\eta)\, d\eta,$$

where

$$a(\eta') = \int_0^\infty f(\xi)\, U^*(\xi,\eta')\, d\xi,$$

which is obtained by using the orthogonality relation of $U(\xi,\eta)$ and its conjugate $U^*(\xi,\eta)$

$$\int_0^\infty U^*(\xi,\eta)\, U(\xi,\eta')\, d\xi = \delta(\eta - \eta').$$

An interesting point to observe is that **although** $\frac{g_\ell(kr)}{k^2r^2}$ **do not form a complete set** (unless $\ell = 0$), i.e.

$$\int_0^\infty \frac{g_\ell(kr)}{k^2r^2}\frac{g_\ell(k'r)}{k'^2r^2}dr \neq C_\ell\,\delta(k-k'), \qquad \text{if } k>0, k'>0$$

one still can expand any square integrable function $f(r)$ **on** $r>0$ **in terms of these functions.** This is because the existence of a "conjugate" function to $\frac{g_\ell(kr)}{k^2r^2}$, namely $\left(k^2r^2j_\ell^2(kr)-\frac{1}{2}\right)$, which are related to each other as in eqn. (1.26), namely

$$\int_0^\infty \left(k^2r^2j_\ell^2(kr)-\frac{1}{2}\right)\frac{g_\ell(kr')}{k^2r'^2}dk = \delta(r-r'), \qquad \text{for } r>0, r'>0.$$

Thus if one expands $f(r)$ in terms of $\frac{g_\ell(kr)}{k^2r^2}$, i.e.

$$f(r) = \int_0^\infty a_\ell(k)\frac{g_\ell(kr)}{(kr)^2}dk, \tag{1.41}$$

then

$$a_\ell(k) = \int_0^\infty f(r')\left[k^2r'^2j_\ell^2(kr')-\frac{1}{2}\right]dr'. \tag{1.42}$$

To check

$$\begin{aligned} f(r) &= \int_0^\infty \frac{g_\ell(kr)}{(kr)^2}dk\int_0^\infty f(r')\left[k^2r'^2j_\ell^2(kr')-\frac{1}{2}\right]dr' \\ &= \int_0^\infty dr'\,f(r')\underbrace{\int_0^\infty\left[k^2r'^2j_\ell^2(kr')-\frac{1}{2}\right]\frac{g_\ell(kr)}{(kr)^2}\,dk}_{\delta(r-r')} \\ &= \int_0^\infty f(r')\delta(r-r')dr' \\ &= f(r). \end{aligned}$$

Similarly, one can expand any square integrable function $f(r)$ on $r > 0$ in terms of $\left(k^2r^2j_\ell^2(kr) - \frac{1}{2}\right)$ because the existence of the "conjugate" function to these functions, namely $\frac{g_\ell(kr)}{k^2r^2}$.

To illustrate the above discussion, consider the following function

$$f(r) = r^2e^{-r^2} \tag{1.43}$$

Let us expand $f(r)$ in terms of $\frac{g_1(kr)}{(kr)^2}$

$$\frac{g_1(kr)}{(kr)^2} = \frac{8}{\pi}\left\{\left(1 - \frac{2}{(kr)^2}\right)\cos(2kr) + \left(\frac{1}{(kr)^3} - \frac{2}{kr}\right)\sin(2kr)\right\}.$$

Then

$$a_1(k) = \int_0^\infty r'^2\left[k^2r'^2j_1^2(kr') - \frac{1}{2}\right]dr'.$$

But

$$\begin{aligned}
k^2r'^2j_1^2(kr') &= \left(\frac{\sin kr'}{kr'} - \cos kr'\right)^2 \\
&= \frac{\sin^2 kr'}{(kr')^2} + \cos^2 kr' - \frac{\sin(2kr')}{(kr')} \\
k^2r'^2j_1^2(kr') - \frac{1}{2} &= \frac{\sin^2 kr'}{(kr')^2} - \frac{\sin(2kr')}{(kr')} + \cos^2 kr' - \frac{1}{2} \\
&= \frac{\sin^2 kr'}{(kr')^2} - \frac{\sin(2kr')}{(kr')} + \frac{\cos(2kr')}{2} \\
&= \frac{1 - \cos(2kr')}{2(kr')^2} - \frac{\sin(2kr')}{(kr')} + \frac{\cos(2kr')}{2}.
\end{aligned}$$

Thus

$$\begin{aligned}
a_1(k) &= \int_0^\infty dr' r'^2 e^{-r'^2} \left\{ \frac{1}{2(kr')^2} - \frac{\cos(2kr')}{2(kr')^2} - \frac{\sin(2kr')}{kr'} + \frac{\cos(2kr')}{2} \right\} \\
&= \int_0^\infty dr' \left\{ \frac{e^{-r'^2}}{2k^2} - \frac{\cos(2kr')e^{-r'^2}}{2k^2} - \frac{r'\sin(2kr')e^{-r'^2}}{k} + \frac{1}{2} r'^2 \cos(2kr')e^{-r'^2} \right\} \\
&= \frac{1}{2k^2}\int_0^\infty e^{-r'^2} dr' - \frac{1}{2k^2}\int_0^\infty \cos(2kr')e^{-r'^2} dr' - \frac{1}{k}\int_0^\infty r'\sin(2kr')e^{-r'^2} dr \\
&\quad + \frac{1}{2}\int_0^\infty r^2 e^{-r'^2}\cos(2kr')dr' \\
&= \frac{1}{2k^2}\frac{\sqrt{\pi}}{2} - \frac{1}{2k^2}\left(\frac{\sqrt{\pi}}{2}e^{-4k^2/4}\right) - \frac{1}{k}\left(\frac{2k\sqrt{\pi}}{4}e^{-4k^2/4}\right) \\
&\quad + \frac{\sqrt{\pi}}{2}\left(\frac{2-4k^2}{8}\right)e^{-4k^2/4} \\
&= \frac{\sqrt{\pi}}{4k^2} - \frac{\sqrt{\pi}}{4k^2}e^{-k^2} - \frac{\sqrt{\pi}}{2}e^{-k^2} + \frac{\sqrt{\pi}}{8}e^{-k^2} - \frac{\sqrt{\pi}}{4}k^2 e^{-k^2} \\
&= \frac{\sqrt{\pi}}{4k^2} - \frac{\sqrt{\pi}}{4k^2}e^{-k^2} - \frac{3\sqrt{\pi}}{8}e^{-k^2} - \frac{\sqrt{\pi}}{4}k^2 e^{-k^2}.
\end{aligned}$$

Hence

$$f(r) = \int_0^\infty a_1(k)\frac{g_1(kr)}{(kr)^2}\,dk. \tag{1.44}$$

Figure 1.4 shows the plot of the function $f(r)$ using eqn. (1.44), the dotted curve, and compares the actual values of $f(r)$, eqn. (1.43), with the ones obtained using the expansion in eqn. (1.44).

Similarly, one can expand

$$f(r) = r^2 e^{-r^2}$$

in terms of $\left(k^2r^2j_\ell^2(kr) - \frac{1}{2}\right)$. In this case, one can easily show that[1]

$$c_1(k) = -\frac{6}{\sqrt{\pi}}e^{-k^2} - \frac{8}{\sqrt{\pi}k^2}e^{-k^2} - \frac{4}{\sqrt{\pi}}k^2e^{-k^2} + \frac{4}{k^3}\,\mathrm{erf}(k),$$

where $\mathrm{erf}(k)$ is the error function which is given by [25]

$$\mathrm{erf}(k) = \frac{2}{\sqrt{\pi}}\int_0^k e^{-\xi^2}\,d\xi$$

Thus

$$f(r) = \int_0^\infty c_1(k)\left(k^2r^2j_\ell^2(kr) - \frac{1}{2}\right)\,dk, \tag{1.45}$$

Figure 1.5 shows the plot of the function $f(r)$ using eqn. (1.45), the dotted curve, and compares the actual values of $f(r)$, eqn. (1.43), with the ones obtained using the expansion in eqn. (1.45).

[1]This result was obtained using *Mathematica*

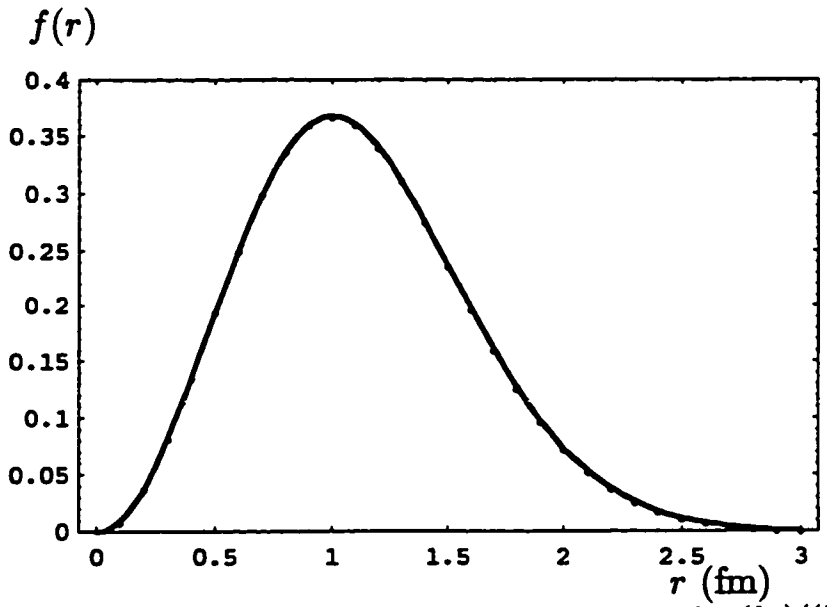

Fig. 1.4 : Expansion of $f(r)$ in eqn. (1.43) in terms of $g_1(kr)/(kr)^2$. The dotted curve is the plot of $f(r)$ using eqn. (1.44) while the continuous is the plot of $f(r)$ using eqn. (1.43). The integral in eqn. (1.44) was evaluated numerically from $k = 0.01$ to $k = 25$.

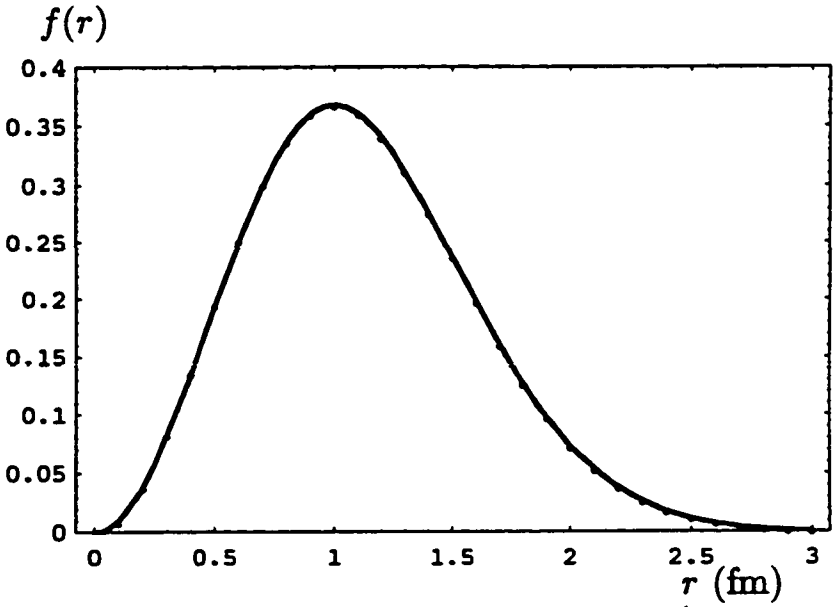

Fig. 1.5 : Expansion of $f(r)$ in eqn. (1.43) in terms of $\left(k^2r^2j_1^2(kr) - \frac{1}{2}\right)$. The dotted curve is the plot of $f(r)$ using eqn. (1.45) while the continuous is the plot of $f(r)$ using eqn. (1.43). The integral in eqn. (1.45) was evaluated numerically from $k = 0.01$ to $k = 15$.

1.2.1 Finite Space $g_\ell(kr)$-Functions

Since our aim is to study the finite space inverse scattering problem in the Born approximation, one wishes to obtain a relation between $j_\ell^2(kr)$ and $g_\ell(kr)$ in the finite space analogous to the one in the infinite space, namely

$$\int_0^\infty \left(k^2 r^2 j_\ell^2(kr) - \frac{1}{2}\right) \frac{g_\ell(kr')}{k^2 r'^2} dk = \delta(r - r') + \delta(r + r'). \tag{1.46}$$

Since $g_\ell(kr)$ is an even function, eqn. (1.46) can be written as

$$\frac{1}{2}\int_{-\infty}^\infty \left(k^2 r^2 j_\ell^2(kr) - \frac{1}{2}\right) \frac{g_\ell(kr')}{k^2 r'^2} dk = \delta(r - r') + \delta(r + r'). \tag{1.47}$$

Note that the integration on the interval $I \equiv (-\infty, \infty)$ in the above equation is over the continuous parameter k, the momentum of the particle (in units of $\hbar$). However, in finite spaces, the energy states of the particle, and consequently the momenta, are discrete. Thus the finite space version of eqn. (1.47) can be obtained by replacing the integration over the continuous parameter k by a summation over the discrete set of states $\{k_{\ell n}\}$, where $k_{\ell n}$ is the momentum of the nth state in the angular momentum channel ℓ. This set of numbers, $\{k_{\ell n}\}$, with

$$\cdots\cdots < -k_{\ell n} < -k_{\ell n-1} < \cdots < -k_{\ell 1} < k_{\ell 0} = 0 < k_{\ell 1} < \cdots < k_{\ell n-1} < k_{\ell n} < \cdots\cdots,$$

is called (using mathematical terminology) a **partition**, P, of I.

Define

$$k_{\ell(-n)} \equiv -k_{\ell n}$$

Thus the partition P of the interval I can be demonstrated as

$$\cdots\cdots < k_{\ell(-n)} < k_{\ell(-n+1)} < \cdots < k_{\ell(-1)} < k_{\ell 0} = 0 < k_{\ell 1} < \cdots < k_{\ell n-1} < k_{\ell n} < \cdots\cdots$$

Thus, for finite spaces

$$\begin{aligned} k &\longrightarrow k_{\ell n}, \\ j_\ell(kr) &\longrightarrow j_\ell(k_{\ell n} r), \\ g_\ell(kr) &\longrightarrow g_\ell(k_{\ell n} r), \\ \int_{-\infty}^{\infty} dk &\longrightarrow \sum_P \Delta k_{\ell n} \end{aligned} \tag{1.48}$$

where $\sum_P$ represents the summation over the partition P and

$$\Delta k_{\ell n} \equiv k_{\ell(n+1)} - k_{\ell n}.$$

Making the transformations in eqn. (1.48), eqn. (1.47) becomes

$$\frac{1}{2}\sum_{n=-\infty}^{\infty}\left(k_{\ell n}^2 r^2 j_\ell^2(k_{\ell n} r) - \frac{1}{2}\right)\frac{g_\ell(k_{\ell n} r')}{(k_{\ell n} r')^2}\Delta k_{\ell n} = \delta(r-r') + \delta(r+r') \tag{1.49}$$

Define

$$f_{\ell n}(k_{\ell n}, r, r') \equiv \left(k_{\ell n}^2 r^2 j_\ell^2(k_{\ell n} r) - \frac{1}{2}\right)\frac{g_\ell(k_{\ell n} r')}{(k_{\ell n} r')^2}$$

Thus eqn. (1.49) becomes

$$\begin{aligned} \frac{1}{2}\sum_{n=-\infty}^{\infty} f_{\ell n}(k_{\ell n}, r, r')\Delta k_{\ell n} &= \frac{1}{2}\sum_{n=-\infty}^{n=-1} f_{\ell n}(k_{\ell n}, r, r')\Delta k_{\ell n} + \frac{1}{2} f_{\ell 0}(k_{\ell 0}, r, r')\, k_{\ell 1} \\ &+ \frac{1}{2}\sum_{n=1}^{n=\infty} f_{\ell n}(k_{\ell n}, r, r')\Delta k_{\ell n} \\ &= \delta(r-r') + \delta(r+r') \end{aligned}$$

But (using eqn. (1.27))

$$f_{\ell 0}(k_{\ell 0}, r, r') = \lim_{k_{\ell n}\to 0}\left(k_{\ell n}^2 r^2 j_\ell^2(k_{\ell n} r) - \frac{1}{2}\right)\frac{g_\ell(k_{\ell n} r')}{(k_{\ell n} r')^2}$$
$$= \frac{4}{\pi(2\ell+1)},$$

and

$$\sum_{n=1}^{n=\infty} f_{\ell n}(k_{\ell n}, r, r')\Delta k_{\ell n} = \sum_{n=-\infty}^{n=-1} f_{\ell n}(k_{\ell n}, r, r')\Delta k_{\ell n}$$

Thus

$$\frac{2\,k_{\ell 1}}{\pi(2\ell+1)} + \sum_{n=1}^{\infty} f_{\ell n}(k_{\ell n}, r, r')\Delta k_{\ell n} = \delta(r-r') + \delta(r+r')$$

or

$$\frac{2\,k_{\ell 1}}{\pi(2\ell+1)} + \sum_{n=1}^{\infty}\left(k_{\ell n}^2 r^2 j_\ell^2(k_{\ell n} r) - \frac{1}{2}\right)\frac{g_\ell(k_{\ell n} r')}{(k_{\ell n} r')^2}\Delta k_{\ell n} = \delta(r-r') + \delta(r+r') \quad (1.50)$$

Eqn. (1.50) is the finite space counterpart relation of eqn. (1.46).

Consider the case where $\underline{\ell = 0}$, then

$$k_{0n} = \frac{n\pi}{a}, \qquad n = 1, 2, \ldots \quad (1.51)$$

where a is the dimension of the sphere.

Substituting g_0 from table 1.2 and eqn. (1.51) in eqn. (1.50), one obtains

$$\frac{2}{a} + \sum_{n=1}^{\infty}\underbrace{\left(\sin^2\left(\frac{n\pi}{a}r\right) - \frac{1}{2}\right)}_{-\frac{1}{2}\cos\left(\frac{2n\pi}{a}r\right)}\left(\frac{-8}{\pi}\cos\left(\frac{2n\pi}{a}r'\right)\right)\frac{\pi}{a} = \delta(r-r') + \delta(r+r')$$

$$\Rightarrow \quad \frac{2}{a} + \frac{4}{a}\sum_{n=1}^{\infty}\cos\left(\frac{2n\pi}{a}r\right)\cos\left(\frac{2n\pi}{a}r'\right) = \delta(r-r') + \delta(r+r') \quad (1.52)$$

Let $2r = x$ and $2r' = x'$. Thus eqn. (1.52) becomes

$$\begin{aligned} \frac{2}{a} + \frac{4}{a}\sum_{n=1}^{\infty} \cos\left(\frac{n\pi}{a}x\right)\cos\left(\frac{n\pi}{a}x'\right) &= \delta\left(\frac{1}{2}(x-x')\right) \\ &= 2\,\delta(x-x') \end{aligned} \tag{1.53}$$

where $\delta(x+x')$ vanishes for $0 < x \leq a$. Thus

$$\frac{2}{a}\left\{\frac{1}{2} + \sum_{n=1}^{\infty} \cos\left(\frac{n\pi}{a}x\right)\cos\left(\frac{n\pi}{a}x'\right)\right\} = \delta(x-x') \tag{1.54}$$

which is a standard expansion of the delta function, see for example [26]. For $\ell > 0$, this result, eqn. (1.54), does not appear to be known, and we plot this equation for $\ell = 1, 2$ for purposes of illustration.

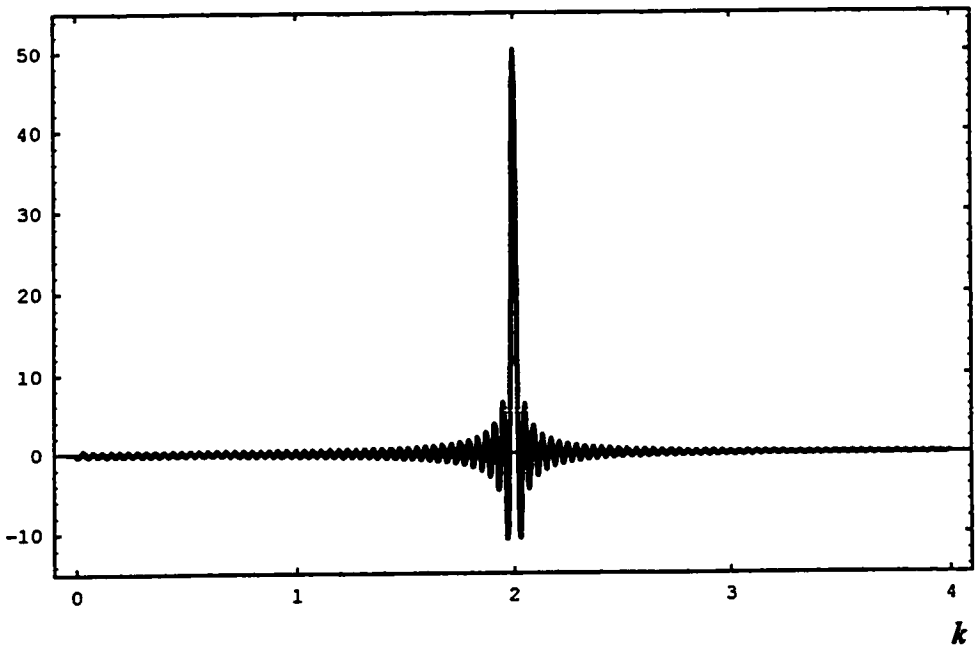

Fig. 1.6 : The plot of eqn. (1.54) for ℓ=1, k'=2 and k varying from $k = 0.005$ to k=4.000 in steps of 0.005. The summation was done numerically up to n =250

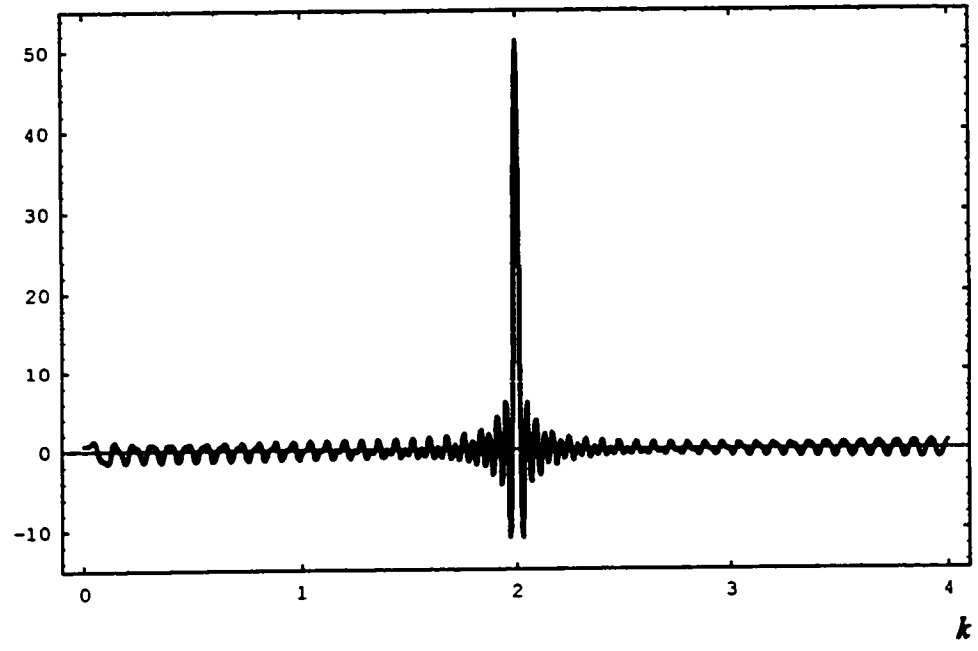

Fig. 1.7 : The plot of eqn. (1.54) for ℓ=2, k'=2 and k varying from $k = 0.005$ to k=4.000 in steps of 0.005. The summation was done numerically up to n =250

1.3 Matrix Algebra

1.3.1 Singular Value Decomposition

The spectral theorem (see for example [27], [28] and [29]) shows that for a symmetric matrix A, there exists an orthogonal matrix V and a diagonal matrix Λ such that $A = V\Lambda V^T$. Using such a decomposition, one can easily predict the behaviour of various kinds of operations when they applied to symmetric matrices.

It is therefore natural to ask if an analogous decomposition exists for any general $n \times m$ rectangular matrix A. This analog is called the **singular value decomposition (SVD)** [30].

Theorem 1 (*SVD Theorem*) : Let $A \in \mathbf{R}^{n\times m}$ have rank r. Then there exist $U \in \mathbf{R}^{n\times n}$, $\Sigma \in \mathbf{R}^{n\times m}$ and $V \in \mathbf{R}^{m\times m}$, such that U and V are orthogonal, Σ has the form

$$\Sigma = \left(\begin{array}{ccc|c} \sigma_1 & & 0 & \\ & \sigma_2 & & 0 \\ & \ddots & & \\ 0 & & \sigma_r & \\ \hline & 0 & & 0 \end{array}\right) \begin{array}{l} \left.\begin{array}{l} \\ \\ \\ \\ \end{array}\right\} r \\ \left.\begin{array}{l} \\ \end{array}\right\} n-r \end{array}$$

$$\underbrace{\qquad\qquad}_{m-r}$$

where $\sigma_1 \geq \sigma_2 \geq \cdots \geq \sigma_r > 0$ are called the *singular values* of A and

$$A = U\Sigma V^T.$$

1.3.2 The generalized Inverse

A matrix has an inverse only if it is square and nonsingular. However, in numerous areas of science in recent years a need has arisen for some kind of an inverse of a matrix that is singular or even rectangular, see for example [31] and [32]. For this reason, the concept of a generalized inverse has been introduced. This concept seems to have been first mentioned in print in 1903 by Fredholm [33]. Since 1955 hundreds of papers on various aspects of generalized inverses have appeared.

A generalized inverse of a given matrix A means a matrix X associated in some way with A that [34]

1) exists for a class of matrices larger than the class of nonsingular matrices,
2) has some properties of the usual inverse, and
3) reduces to the usual inverse when A is nonsingular.

Definition : The generalized inverse of a matrix A is any matrix X satisfying the following relation

$$AXA = A. \tag{1.55}$$

Let A be nonsingular square matrix. Multiplying both sides of eqn. (1.55) by A^{-1} from the left and from the right, one obtains

$$\underbrace{A^{-1}A}_{I} X \underbrace{AA^{-1}}_{I} = \underbrace{A^{-1}A}_{I} A^{-1}$$

$$X = A^{-1}$$

which illustrates the third property of the generalized inverse.

One of the most important applications of the generalized inverse concept is solving a system of simultaneous linear equations

$$Ax = b \tag{1.56}$$

where b is a given vector and x is an unknown vector. If A is a nonsingular square matrix, then there is a unique solution for x, given by

$$x = A^{-1}b.$$

However, in the general case, when A may be singular or rectangular, there may sometimes be no solutions or a multiplicity of solutions. It has been shown [35], in the general case when eqn. (1.56) has many solutions, that if X is any matrix satisfying $AXA = A$, then $Ax = b$ has a solution given by

$$x = Xb,$$

and the most general solution is given by

$$x = Xb + (I - XA)y,$$

where y is an arbitrary vector.

Different Classes of Generalized Inverse

Let A and $X \in \mathbf{C}^{n\times m}$, the set of all $n \times m$ complex matrices. Consider the following matrix equations

$$AXA = A \tag{1.57}$$

$$XAX = X \tag{1.58}$$

$$(XA)^H = XA \tag{1.59}$$

$$(AX)^H = AX \tag{1.60}$$

where H represents the conjugate transpose.

Definition [36]

(i) X is a *generalized inverse* if eqn. (1.57) is satisfied

(ii) X is called *reflexive generalized inverse* if eqns. (1.57) and (1.58) are satisfied.

(iii) X is called *left weak generalized inverse* if eqns. (1.57), (1.58) and (1.59) are satisfied.

(iv) X is called *right weak generalized inverse* if eqns. (1.57), (1.58) and (1.60) are satisfied.

(v) X is called *pseudoinverse* or *Moore–Penrose generalized inverse* if eqns. (1.57), (1.58), (1.59) and (1.60) are all satisfied. Furthermore, this pseudoinverse is unique.

The Pseudoinverse

The pseudoinverse, or the Moore-Penrose generalized inverse, of a matrix A, namely A^+, is given by

$$A^+ = V\Sigma^+ U^T \tag{1.61}$$

where

$$\Sigma^+ = \left(\begin{array}{ccc|c} \sigma_1^{-1} & & 0 & \\ & \sigma_2^{-1} & & 0 \\ & & \ddots & \\ 0 & & \sigma_r^{-1} & \\ \hline & 0 & & 0 \end{array}\right) \in \mathbf{R}^{m\times n}$$

It can be shown [37], that the above definition of A^+ satisfies the four matrix equations, eqns. (1.57) to (1.60), of the pseudoinverse.

One of our techniques to invert the finite-space partial-wave Born approximation involves reducing some system of equations to the matrix equation

$$Ax = b,$$

where A is a singular $n \times n$ matrix. In this technique, the pseudoinverse concept turns out to be very useful in inverting the finite space partial wave Born approximation.

CHAPTER 2

Preliminary Discussion

Before going into the details of the inverse scattering problem in the Born approximation, it is convenient to study the simplest collision problem: the non-relativistic scattering of two particles which interact through a potential $V_\ell(\mathbf{r})$ depending only on their relative coordinate $\mathbf{r}$.

Consider a non-relativistic system of two particles, with masses m_1 and m_2, coordinates $\mathbf{r}_1$ and $\mathbf{r}_2$ measured from some fixed origin O in the lab. coordinate system, see fig. 2.1, and momenta $\mathbf{p}_1$ and $\mathbf{p}_2$. It is assumed that these two particles interact through a potential $V_\ell(|\mathbf{r}_1 - \mathbf{r}_2|)$ which depends only on the relative coordinate $\mathbf{r}_1 - \mathbf{r}_2$. The time-independent wave function $\phi(\mathbf{r}_1,\mathbf{r}_2)$ of the system satisfies the following Schrödinger equation [38]

$$\left(-\frac{\hbar^2}{2m_1}\nabla^2_{\mathbf{r}_1} - \frac{\hbar^2}{2m_2}\nabla^2_{\mathbf{r}_2} + V_\ell(|\mathbf{r}_1 - \mathbf{r}_2|)\right)\phi(\mathbf{r}_1,\mathbf{r}_2) = E_{\text{tot}}\,\phi(\mathbf{r}_1,\mathbf{r}_2) \qquad (2.1)$$

Fig. 2.1.

Eqn. (2.1) can be simplified by introducing the relative coordinate vector $\mathbf{r}$ and the center of mass vector $\mathbf{R}$ which are related to the coordinates $\mathbf{r}_1$ and $\mathbf{r}_2$ by the following relations

$$\mathbf{r} = \mathbf{r}_1 - \mathbf{r}_2 \tag{2.2}$$

$$\mathbf{R} = \frac{m_1\mathbf{r}_1 + m_2\mathbf{r}_2}{m_1 + m_2} \tag{2.3}$$

Using the above coordinate transformation, eqn. (2.1) can be rewritten as follows

$$\left(-\frac{\hbar^2}{2M}\nabla^2_{\mathbf{R}} - \frac{\hbar^2}{2\mu}\nabla^2_{\mathbf{r}} + V_\ell(r)\right)\Phi(\mathbf{R},\mathbf{r}) = E_{\text{tot}}\,\Phi(\mathbf{R},\mathbf{r}) \tag{2.4}$$

where $\Phi(\mathbf{R},\mathbf{r})$ is the wave function of the system in the new coordinate system,

$$M = m_1 + m_2$$

is the total mass and

$$\mu = \frac{m_1 m_2}{m_1 + m_2}$$

is the reduced mass of the two particles.

Since the potential depends only on the relative coordinate, the wave function $\Phi(\mathbf{R}, \mathbf{r})$ can be put in a separable form, i.e.

$$\Phi(\mathbf{R}, \mathbf{r}) = \varphi(\mathbf{R})\psi(\mathbf{r})$$

where the functions $\varphi(\mathbf{R})$ and $\psi(\mathbf{r})$ satisfy the following equations

$$-\frac{\hbar^2}{2M} \nabla^2_{\mathbf{R}} \varphi(\mathbf{R}) = E_{\text{c.m.}} \varphi(\mathbf{R}) \tag{2.5}$$

and

$$\left(-\frac{\hbar^2}{2\mu} \nabla^2_{\mathbf{r}} + V_\ell(r)\right) \psi(\mathbf{r}) = E \psi(\mathbf{r}) \tag{2.6}$$

with

$$E_{\text{tot}} = E_{\text{c.m.}} + E$$

Since translational motion of the system as a whole is uninteresting from the standpoint of the energy levels, scattering cross sections etc., we may choose the origin for the coordinate system to be the center of mass of the particles, i.e. $\mathbf{R} \equiv 0$, and need not be concerned by the motion of the center of mass, see fig. 2.1b.

Thus, the non-relativistic scattering problem of two particles which interact through a central potential $V_\ell(r)$ is equivalent to the scattering of a particle of

reduced mass μ by the potential $V_\ell(r)$ in the center of mass system and the wave function of this particle, $\psi(\mathbf{r})$, satisfies eqn. (2.6).

Because the potential is central, $\psi(\mathbf{r})$ can be written in a separable form as

$$\psi(\mathbf{r}) = R_\ell(r)\, Y_\ell^m(\theta,\phi) = \frac{u_\ell(r)}{r}\, Y_\ell^m(\theta,\phi)$$

The above expression can be substituted in eqn. (2.6) and then one can solve for the radial wave function $R_\ell(r)$ which can be shown to satisfy the following differential equation [39]:

$$\left[-\frac{\hbar^2}{2\mu}\frac{d}{dr}\left(r^2\frac{d}{dr}\right) + \frac{\hbar^2\ell(\ell+1)}{2\mu r^2} + V_\ell(r)\right] R_\ell(r) = E_\ell R_\ell(r), \qquad (2.7)$$

or in terms of $u_\ell(r)$

$$\left[-\frac{\hbar^2}{2\mu}\frac{d^2}{dr^2} + \frac{\hbar^2\ell(\ell+1)}{2\mu r^2} + V_\ell(r)\right] u_\ell(r) = E_\ell u_\ell(r). \qquad (2.8)$$

Consider now the special case of the above collision problem where the first particle, of mass m_1, is moving with initial speed v and scattered by the second particle, of mass m_2, which is initially at rest in the laboratory coordinate system and the masses of the two particles are equal or the difference between them can be neglected, as in the case of a proton and a neutron. In this special case, the following relations hold [40]:

$$\mu = \frac{m_1}{2}$$

$$E = \frac{1}{2}E_{lab}$$

$$k = \frac{1}{2}k_{lab}$$

where

E: is the center-of-mass energy or the kinetic energy of relative motion

k: is the center-of-mass momentum or the momentum of relative motion

E_{lab}: is the energy in the laboratory coordinate system

k_{lab}: is the momentum in the laboratory coordinate system (in units of $\hbar$).

Thus, the problem of a particle of mass m_1, moving with initial speed v, scattered by another particle of mass m_2, initially at rest in the laboratory coordinate system, can be reduced to an equivalent one-body problem in the center of mass coordinate system by studying a particle of mass $\mu = \frac{m_1 m_2}{m_1+m_2}$ moving with initial relative speed v and relative kinetic energy $E = \frac{1}{2}\mu v^2$ scattered from a scattering potential $V_\ell(r)$, where r is the radial distance of the particle μ from the scattering potential, in the angular momentum channel ℓ.

Throughout this thesis, we will work in the relative coordinate system, bearing in mind that one can transform to the laboratory system using the above relations which relate the two systems.

In principle, if the potential $V_\ell(r)$ is known, then one can solve eqn. (2.8) for a given ℓ, analytically or numerically, and calculate the corresponding wave function $\psi(\mathrm{r})$, the scattered radial wave function and the corresponding phase shifts of

the scattered particle at different energies, (direct problem). But in fact we are interested in the inverse problem, i.e. what is the potential, or the force which acts between the two particles, if the phase shifts, which can be deduced directly from experimental measurements, are known at many different energies. Indeed much progress has been made in understanding features of nuclear behaviour in terms of the two-body forces alone, although one cannot expect the force between two isolated protons to be precisely the same as that between two protons the same distance apart in a nucleus.

In order to solve the inverse problem in quantum mechanical scattering theory, the Gel'fand-Levitan-Marchenko equation must be solved. However, it is possible to invert a simple approximate expression which relates the scattering potential $V_\ell(r)$ and the phase shifts $\delta_\ell(k)$ produced by this scattering potential. This expression is the partial wave Born approximation and it is given by

$$\frac{-\hbar^2}{2\mu}\frac{\delta_\ell(k)}{k} \approx \int_0^\infty j_\ell^2(kr)V_\ell(r)r^2dr, \tag{2.9}$$

where

$V_\ell(r)$: is the scattering potential in the angular momentum channel ℓ.

$j_\ell(r)$: is the spherical Bessel function.

μ : is the mass of the scattered particle.

k : is the momentum of the scattered particle, in units of $\hbar$, which is given by

$$k = \sqrt{\frac{2\mu E}{\hbar^2}}$$

E : is the energy of the particle.

This approximation is valid for channels where the scattering potential is weak.

Recently, Eqn. (2.9) was inverted using two different inversion techniques. The first technique, involved using the inverse function of $j_\ell^2(r)$, namely $g_\ell(r')$, which satisfies the following relation

$$\int_0^\infty j_\ell^2(kr) g_\ell(kr') dk = \frac{r'^2}{r^2} \left\{ \delta(r - r') + \delta(r + r') - (-1)^\ell 2\delta(r') \right\}. \qquad (2.10)$$

Premultiplying Eqn. (2.9) by $g_\ell(kr')$ and integrating over k from 0 to ∞, one obtains

$$\int_0^\infty \left(\frac{-\hbar^2}{2\mu} \frac{\delta_\ell(k)}{k} \right) g_\ell(kr') dk = \int_0^\infty \int_0^\infty j_\ell^2(kr) g_\ell(kr') dk \cdot V_\ell(r) r^2 dr.$$

Using eqn. (2.10) in the above equation, one gets

$$\int_0^\infty \left(\frac{-\hbar^2}{2\mu} \frac{\delta_\ell(k)}{k} \right) g_\ell(kr') dk = \int_0^\infty \frac{r'^2}{r^2} \left\{ \delta(r - r') + \delta(r + r') - (-1)^\ell 2\delta(r') \right\} V_\ell(r) r^2 dr. \qquad (2.11)$$

The second term in the RHS of eqn. (2.11), namely

$$\int_0^\infty \frac{r'^2}{r^2} \delta(r + r') r^2 V_\ell(r) dr,$$

vanishes because $\delta(r+r')$ cannot be zero for $r \geq 0$ unless $r = r' = 0$. Thus

$$\int_0^\infty \left(\frac{-\hbar^2}{2\mu}\frac{\delta_\ell(k)}{k}\right) g_\ell(kr')dk = r'^2 V_\ell(r') - 2(-1)^\ell r'^2 \delta_\ell(r') \int_0^\infty V_\ell(r)dr \qquad (2.12)$$

which can be written as

$$V_\ell(r') = \frac{1}{r'^2}\int_0^\infty \left(\frac{-\hbar^2}{2\mu}\frac{\delta_\ell(k)}{k}\right) g_\ell(kr')dk + 2(-1)^\ell \delta_\ell(r') \int_0^\infty V_\ell(r)dr. \qquad (2.13)$$

The second term on the RHS of eqn. (2.13) contains the potential $V_\ell(r)$ which makes this inversion technique impractical since the unknown quantity which is the potential, appears also on the RHS of eqn. (2.13). However, by examining eqn. (2.9) for large k, in which limit this approximation is most appropriate, one can get rid of this troublesome term.

Consider eqn. (2.9) for large k, then

$$\lim_{k\to\infty}\left\{\frac{-\hbar^2}{2\mu}\frac{\delta_\ell(k)}{k}\right\} \longrightarrow \int_0^\infty \lim_{k\to\infty}\left(j_\ell^2(kr)\right) V_\ell(r) r^2 dr.$$

But

$$\lim_{k\to\infty} j_\ell(kr) \longrightarrow \frac{\sin(kr - \ell\pi/2)}{kr}.$$

hence

$$\lim_{k\to\infty}\left(\frac{-\hbar^2}{2\mu}\frac{\delta_\ell(k)}{k}\right) \longrightarrow \int_0^\infty \left(\frac{\sin^2(kr-\ell\pi/2)}{k^2}\right) V_\ell(r)dr.$$

But

$$\begin{aligned}\sin^2(kr - \ell\pi/2) &= \frac{1}{2} - \frac{1}{2}\cos[2kr - \ell\pi] \\ &= \frac{1}{2} - \frac{1}{2}\left\{\cos(2kr)\underbrace{\cos(\ell\pi)}_{(-1)^\ell} + \sin(2kr)\underbrace{\sin(\ell\pi)}_{0}\right\} \\ &= \frac{1}{2} - \frac{1}{2}(-1)^\ell\cos(2kr).\end{aligned}$$

Thus

$$\lim_{k\to\infty}\left(\frac{-\hbar^2}{2\mu}\frac{\delta_\ell(k)}{k}\right) \longrightarrow \frac{1}{2k^2}\int_0^\infty \left[1 - (-1)^\ell\cos(2kr)\right] V_\ell(r)dr.$$

The second term on the RHS of the above expression, namely

$$\int_0^\infty \cos(2kr)\, V_\ell(r)dr,$$

goes to zero as k tends to infinity due to the rapid oscillations of $\cos(2kr)$ in this limit. Hence

$$\lim_{k\to\infty}\left(k^2\left[\frac{-\hbar^2}{2\mu}\frac{\delta_\ell(k)}{k}\right]\right) = \frac{1}{2}\int_0^\infty V_\ell(r)dr. \tag{2.14}$$

Replacing the second term on the RHS of eqn. (2.13) by the equivalent term from eqn. (2.14), one obtains

$$V_\ell(r') = \frac{1}{r'^2}\int_0^\infty\left(\frac{-\hbar^2}{2\mu}\frac{\delta_\ell(k)}{k}\right) g_\ell(kr')dk + 4(-1)^\ell\delta(r')\lim_{k'\to\infty}\left\{\frac{-\hbar^2}{2\mu}k'\delta_\ell(k')\right\} \tag{2.15}$$

However, the functions $g_\ell(kr)$ have the following property

$$\int_0^\infty \frac{g_\ell(kr)}{k^2r^2}dk = 4(-1)^{\ell+1}\delta_\ell(r) \tag{2.16}$$

Replacing the second term on the RHS of eqn. (2.15) by the equivalent term from eqn. (2.16), one gets

$$V_\ell(r') = \frac{1}{r'^2}\int_0^\infty \left(\frac{-\hbar^2}{2\mu}\frac{\delta_\ell(k)}{k}\right) g_\ell(kr')dk + \left(\frac{1}{r'^2}\int_0^\infty \frac{g_\ell(kr')}{k^2}dk\right) \lim_{k\to\infty}\left(\frac{-\hbar^2}{2\mu}k'\delta_\ell(k')\right)$$

which can be rewritten in a simpler form as

$$V_\ell(r) = \frac{1}{r^2}\int_0^\infty \left(\frac{-\hbar^2}{2\mu}\frac{\delta_\ell(k)}{k} - \frac{L}{k^2}\right) g_\ell(kr)dk \tag{2.17}$$

where we replace, for simplicity, r' by r and we define L as

$$L \equiv \lim_{k'\to\infty}\left\{\frac{-\hbar^2}{2\mu}k'\delta_\ell(k')\right\}.$$

The second technique, involved using the following useful operator [41]:

$$\hat{\Theta}_\ell(\rho) \equiv \left(\frac{d}{d\rho^2}\right)^\ell \frac{d}{d\rho}\left(\frac{d}{d\rho^2}\right)^\ell$$

which has the property

$$\hat{\Theta}_\ell(\rho)\left(\rho^{2\ell+2}j_\ell^2(\rho)\right) = \sin(2\rho),$$

where

$$\frac{d}{d\rho^2} \equiv \frac{1}{2\rho}\frac{d}{d\rho}$$

Multiplying both sides of eqn. (2.9) by $k^{2\ell+2}$ and then Operating $\hat{\Theta}_\ell(k)$, one gets

$$\begin{aligned}
\hat{\Theta}_\ell(k)\left(k^{2\ell+2}\left\{\frac{-\hbar^2}{2\mu}\frac{\delta_\ell(k)}{k}\right\}\right) &\approx \int_0^\infty \left(\frac{d}{dk^2}\right)^\ell \frac{d}{dk}\left(\frac{d}{dk^2}\right)^\ell \left(k^{2\ell+2} j_\ell^2(kr)\right) V_\ell(r) r^2 dr \\
&\approx \int_0^\infty \frac{r^{4\ell+1}}{r^{4\ell+1}}\left(\frac{d}{dk^2}\right)^\ell \frac{d}{dk}\left(\frac{d}{dk^2}\right)^\ell \left(k^{2\ell+2} j_\ell^2(kr)\right) V_\ell(r) r^2 dr \\
&\approx \int_0^\infty \underbrace{\left(\frac{d}{d(kr)^2}\right)^\ell \frac{d}{d(kr)}\left(\frac{d}{d(kr)^2}\right)^\ell \left((kr)^{2\ell+2} j_\ell^2(kr)\right)}_{\sin(2kr)} V_\ell(r) r^{2\ell+1} dr \\
&\approx \int_0^\infty \sin(2kr)\, V_\ell(r)\, r^{2\ell+1}\, dr \qquad (2.18)
\end{aligned}$$

Multiplying both sides of eqn. (2.18) by $(4/\pi)\sin(2kr')$ and integrating over k from 0 to ∞, one gets

$$\begin{aligned}
&\frac{4}{\pi}\int_0^\infty \sin(2kr')\hat{\Theta}_\ell(k)\left(k^{2\ell+2}\left\{\frac{-\hbar^2}{2\mu}\frac{\delta_\ell(k)}{k}\right\}\right) dk \\
&\qquad \approx \frac{4}{\pi}\int_0^\infty \sin(2kr') \int_0^\infty \sin(2kr)\, V_\ell(r)\, r^{2\ell+1}\, dr\, dk \\
&\qquad \approx \frac{4}{\pi}\int_0^\infty \int_0^\infty \sin(2kr)\, \sin(2kr')\, V_\ell(r)\, r^{2\ell+1}\, dk\, dr \qquad (2.19)
\end{aligned}$$

But

$$\frac{4}{\pi}\int_0^\infty \int_0^\infty \sin(2kr)\, \sin(2kr')\, dk = \delta(r-r') - \delta(r+r') \qquad (2.20)$$

Replacing the RHS of eqn. (2.19) by the equivalent term from eqn. (2.20), one then obtains

$$V_\ell(r') \approx \frac{4}{\pi\, r'^{2\ell+1}} \int_0^\infty \left(\frac{d}{dk^2}\right)^\ell \frac{d}{dk}\left(\frac{d}{dk^2}\right)^\ell \left(k^{2\ell+2}\left\{\frac{-\hbar^2}{2\mu}\frac{\delta_\ell(k)}{k}\right\}\right) \sin(2kr')\, dk$$

CHAPTER 3

Inverse Scattering Problem in Second Born Approximation

As an improvement to the results obtained in [7], which was shown in the previous chapter, one can use the second partial wave Born approximation, which relates a scattering potential $V_\ell(r)$ to the phase shift $\delta_\ell(k)$ that this potential produces in a more complicated way than in the first partial wave Born approximation, to extract the potential and express it as an integral involving the phase shifts.

From the partial wave expansion, which is discussed fully in the literature (see for example [42]), the phase shift is related to the potential as follows

$$-\frac{\hbar^2}{2\mu}\tan(\,\delta_\ell(k)\,) \;=\; k\int_0^\infty j_\ell(kr)\,V_\ell(r)\,R_\ell(k,r)\,r^2\,dr, \tag{3.1}$$

or

$$-\frac{\tan(\,\delta_\ell(k)\,)}{k} \;=\; \int_0^\infty j_\ell(kr)\,U_\ell(r)\,R_\ell(k,r)\,r^2\,dr, \tag{3.2}$$

where $R_\ell(k,r)$[1] is the radial wave function of the particle which satisfies eqn. (2.7), and

$$U_\ell(r) = \frac{2\mu}{\hbar^2} V_\ell(r).$$

This radial wave function satisfies the following integral equation

$$R_\ell(k,r) = j_\ell(kr) + \int_0^\infty G_\ell(r,r')\, U_\ell(r')\, R_\ell(k,r')\, r'^2\, dr', \tag{3.3}$$

where

$$G_\ell(r,r') = k\, j_\ell(kr_<)\, n_\ell(kr_>).$$

$r_<$ ($r_>$) here means the smaller (larger) of r and r'.

Eqn. (3.3) can be solved by successive iterations. Starting from the zeroth-order approximation $R_\ell^{(0)}(k,r') = j_\ell(kr')$, one obtains at once from eqn. (3.2) the *first Born approximation*, namely[2]

$$-\frac{(\tan(\delta_\ell(k)))_{B1}}{k} = \int_0^\infty j_\ell^2(kr)\, U_\ell(r)\, r^2\, dr. \tag{3.4}$$

The *second Born approximation* for $\tan(\delta_\ell)$, $(\tan(\delta_\ell))_{B2}$, is obtained by using $R_\ell^{(0)}(k,r')$ as input on the RHS of eqn. (3.3), i.e.

$$R_\ell(k,r) = j_\ell(kr) + \int_0^\infty G_\ell(r,s)\, U_\ell(s)\, j_\ell(ks)\, s^2\, ds, \tag{3.5}$$

---

[1] It is written here in this form, instead of $R_\ell(r)$, to also show the k dependence.

[2] Because the phase shifts $\delta_\ell(k)$ are small in this approximation, one can use $\delta_\ell(k) \approx \tan(\delta_\ell(k))$.

and substituting the resulting radial wave function, eqn. (3.5), in eqn. (3.2). This yields

$$-\frac{(\tan(\delta_\ell(k)))_{B2}}{k} = \int_0^\infty dr\, j_\ell(kr)\, U_\ell(r)\, r^2 \left(j_\ell(kr) + \int_0^\infty G_\ell(r,s)\, U_\ell(s)\, j_\ell(ks)\, s^2\, ds \right), \tag{3.6}$$

which can be written as

$$-\frac{\tan(\delta_\ell(k))}{k} = \int_0^\infty j_\ell^2(kr)\, U_\ell(r)\, r^2\, dr + \int_0^\infty \int_0^\infty j_\ell(kr)\, U_\ell(r)\, G_\ell(r,s)\, U_\ell(s)\, j_\ell(ks) \times s^2\, r^2\, ds\, dr, \tag{3.7}$$

where the subscript $B2$ was omitted for simplicity.

The integral over s should be performed over two intervals; $[0,r]$ and $[r,\infty)$. **In the first interval,** $[0,r]$, r is larger than s. Hence the Green's function in this interval becomes

$$G_\ell(r,s) = k\, j_\ell(ks)\, n_\ell(kr).$$

However, **In the second interval,** $[r,\infty)$, s is larger than r. Hence the Green's function in this interval becomes

$$G_\ell(r,s) = k\, j_\ell(kr)\, n_\ell(ks).$$

Thus eqn. (3.7) can be written explicitly as

$$-\frac{\tan(\delta_\ell(k))}{k} = \int_0^\infty j_\ell^2(kr) U_\ell(r) r^2 dr + k \left\{ \int_0^\infty dr \int_r^\infty ds j_\ell^2(kr) U_\ell(r) n_\ell(ks) U_\ell(s) \times j_\ell(ks) r^2 s^2 + \int_0^\infty dr \int_0^r ds j_\ell(kr) n_\ell(kr) U_\ell(r) j_\ell^2(ks) U_\ell(s) r^2 s^2 \right\}. \tag{3.8}$$

Eqn. (3.8) can be put in a more readable form as follows

$$\begin{aligned} -\frac{\tan(\delta_\ell(k))}{k} &= \int_0^\infty j_\ell^2(kr)U_\ell(r)r^2dr \\ &+ k\int_0^\infty dr\, j_\ell(kr)\, n_\ell(kr)\, U_\ell(r)\, r^2 \int_0^r ds\, j_\ell^2(ks)\, U_\ell(s)\, s^2 \\ &+ k\int_0^\infty dr j_\ell^2(kr)U_\ell(r)r^2 \int_r^\infty ds\, j_\ell(ks)\, n_\ell(ks)\, U_\ell(s)\, s^2. \quad (3.9) \end{aligned}$$

Eqn. (3.9) can be inverted using the two inversion techniques discussed in chapter 2, namely;

1) The $j_\ell^2(\rho)$–inverse function approach, namely $g_\ell(\rho)$, which satisfies the following relation

$$\int_0^\infty j_\ell^2(kr)g_\ell(kr')dk = \frac{r'^2}{r^2}\left\{\delta(r-r') + \delta(r+r') - 2(-1)^\ell\delta(r')\right\}. \quad (3.10)$$

2) The differential operator approach, namely $\hat{\Theta}_\ell(\rho)$, which has the following property

$$\hat{\Theta}_\ell(\rho)\left(\rho^{2\ell+2}j_\ell^2(\rho)\right) = \sin(2\rho).$$

$g_\ell(\rho)$−Approach

Multiplying both sides of eqn. (3.9) by $g_\ell(kr')$ and integrating over k from 0 to ∞, one obtains

$$\begin{aligned}\int_0^\infty -\frac{\tan(\,\delta_\ell(k)\,)}{k} g_\ell(kr')dk &= \int_0^\infty U_\ell(r)r^2dr \int_0^\infty j_\ell^2(kr)g_\ell(kr')dk \\ &+ \int_0^\infty g_\ell(kr')k\,dk \left\{\int_0^\infty dr\, j_\ell(kr)\, n_\ell(kr)\, U_\ell(r)\, r^2 \times \right. \\ &\left. \int_0^r ds\, j_\ell^2(ks)\, U_\ell(s)\, s^2 \right\} \\ &+ \int_0^\infty g_\ell(kr')k\,dk \left\{\int_0^\infty dr j_\ell^2(kr) U_\ell(r) r^2 \times \right. \\ &\left. \int_r^\infty ds\, j_\ell(ks)\, n_\ell(ks)\, U_\ell(s)\, s^2 \right\}. \end{aligned} \tag{3.11}$$

Substituting eqn. (3.10) in the 1st term of the RHS of eqn. (3.11), one obtains[3]

$$\begin{aligned}\int_0^\infty -\frac{\tan\delta_\ell(k)}{k} g_\ell(kr')dk &= r'^2 U_\ell(r') - 2(-1)^\ell r'^2 \delta(r') \int_0^\infty U_\ell(r)dr \\ &+ \left(\frac{2\mu}{\hbar^2}\right)^2 \{F_1(r') + F_2(r')\}, \end{aligned} \tag{3.12}$$

where

$$\begin{aligned} F_1(r') &\equiv \int_0^\infty g_\ell(kr')k\,dk \int_0^\infty dr\, j_\ell(kr)\, n_\ell(kr)\, V_\ell(r)\, r^2 \int_0^r ds\, j_\ell^2(ks)\, V_\ell(s)\, s^2 \\ F_2(r') &\equiv \int_0^\infty g_\ell(kr')k\,dk \int_0^\infty dr j_\ell^2(kr) V_\ell(r) r^2 \int_r^\infty ds\, j_\ell(ks)\, n_\ell(ks)\, V_\ell(s)\, s^2. \end{aligned} \tag{3.13}$$

[3]Recall that $\delta(r + r')$ does not contribute to the integral as explained before.

Multiplying both sides of eqn. (3.12) by $\frac{\hbar^2}{2\mu}$, one obtains

$$r'^2 V_\ell(r') - 2(-1)^\ell r'^2 \delta(r') \int_0^\infty V_\ell(r) dr = \int_0^\infty -\frac{\hbar^2}{2\mu} \frac{\tan(\delta_\ell(k))}{k} g_\ell(kr') dk - \frac{2\mu}{\hbar^2} \{ F_1(r') + F_2(r') \}. \quad (3.14)$$

Recall that

$$\frac{1}{2} \int_0^\infty V_\ell(r)\, dr = \lim_{k' \to \infty} \left\{ \frac{-\hbar^2}{2\mu} k' \delta_\ell(k') \right\} \equiv L,$$
$$\int_0^\infty \frac{g_\ell(kr')}{k^2 r'^2} dk = 4(-1)^{\ell+1} \delta_\ell(r').$$

Thus, eqn. (3.14) can be written as

$$r'^2 V_\ell(r') + r'^2 L \int_0^\infty \frac{g_\ell(kr')}{k^2 r'^2} dk = \int_0^\infty -\frac{\hbar^2}{2\mu} \frac{\tan(\delta_\ell(k))}{k} g_\ell(kr') dk - \frac{2\mu}{\hbar^2} \{ F_1(r') + F_2(r') \}. \quad (3.15)$$

Hence

$$r'^2 V_\ell(r') = \int_0^\infty \left(-\frac{\hbar^2}{2\mu} \frac{\tan(\delta_\ell(k))}{k} - \frac{L}{k^2} \right) g_\ell(kr') dk - \frac{2\mu}{\hbar^2} \{ F_1(r') + F_2(r') \},$$

or

$$V_\ell(r) = \frac{1}{r^2} \int_0^\infty \left(-\frac{\hbar^2}{2\mu} \frac{\tan(\delta_\ell(k))}{k} - \frac{L}{k^2} \right) g_\ell(kr) dk - \frac{2\mu}{\hbar^2} \left\{ \frac{F_1(r)}{r^2} + \frac{F_2(r)}{r^2} \right\}, \quad (3.16)$$

where r' is replaced by r for convenience.

Notice that the first term on the RHS of eqn. (3.16) is simply the potential obtained by inverting the partial wave in the first Born approximation, $V_\ell^{(B1)}(r)$.

Thus the potential obtained using the second Born approximation yields, as is reasonable, the potential obtained using the first Born approximation plus a correction term.

The second term on the RHS of eqn. (3.16) makes this inversion approach impractical since the potential $V_\ell(r)$ is contained in $F_1(r)$ and $F_2(r)$ as an integral form. However, one can get around this problem by solving $F_1(r)$ and $F_2(r)$ by successive iterations. The first-order approximation of $F_1(r)$ and $F_2(r)$, namely $F_1^{(1)}(r)$ and $F_2^{(1)}(r)$, is obtained by replacing the potential $V_\ell(r)$ in eqn. (3.13) by $V_\ell^{(B1)}(r)$. Thus, the first-order approximation of the potential in the second Born approach is given by

$$V_\ell^{(1)}(r) = \frac{1}{r^2}\int_0^\infty \left(-\frac{\hbar^2}{2\mu}\frac{\tan(\delta_\ell(k))}{k} - \frac{L}{k^2}\right) g_\ell(kr)dk - \frac{2\mu}{\hbar^2}\left\{\frac{F_1^{(1)}(r)}{r^2} + \frac{F_2^{(1)}(r)}{r^2}\right\},$$

where

$$\begin{aligned}
F_1^{(1)}(r') &\equiv \int_0^\infty g_\ell(kr')k\,dk \int_0^\infty dr\, j_\ell(kr)\, n_\ell(kr)\, V_\ell^{(B1)}(r)\, r^2 \int_0^r ds\, j_\ell^2(ks)\, V_\ell^{(B1)}(s)\, s^2, \\
F_2^{(1)}(r') &\equiv \int_0^\infty g_\ell(kr')k\,dk \int_0^\infty dr j_\ell^2(kr) V_\ell^{(B1)}(r) r^2 \int_r^\infty ds\, j_\ell(ks)\, n_\ell(ks)\, V_\ell^{(B1)}(s)\, s^2, \\
V_\ell^{(B1)}(r) &\equiv \frac{1}{r^2}\int_0^\infty \left(-\frac{\hbar^2}{2\mu}\frac{\tan(\delta_\ell(k))}{k} - \frac{L}{k^2}\right) g_\ell(kr)dk.
\end{aligned}$$

The second-order approximation $V_\ell^{(2)}(r)$ is obtained by substituting $V_\ell^{(1)}(r)$ in eqn. (3.16). Thus

$$V_\ell^{(2)}(r) = \frac{1}{r^2}\int_0^\infty \left(-\frac{\hbar^2}{2\mu}\frac{\tan(\delta_\ell(k))}{k} - \frac{L}{k^2}\right) g_\ell(kr)dk - \frac{2\mu}{\hbar^2}\left\{\frac{F_1^{(2)}(r)}{r^2} + \frac{F_2^{(2)}(r)}{r^2}\right\},$$

where

$$F_1^{(2)}(r') \equiv \int_0^\infty g_\ell(kr')k\,dk \int_0^\infty dr\, j_\ell(kr)\, n_\ell(kr)\, V_\ell^{(1)}(r) r^2 \int_0^r ds\, j_\ell^2(ks)\, V_\ell^{(1)}(s)\, s^2,$$
$$F_2^{(2)}(r') \equiv \int_0^\infty g_\ell(kr')k\,dk \int_0^\infty dr j_\ell^2(kr) V_\ell^{(1)}(r) r^2 \int_r^\infty ds\, j_\ell(ks)\, n_\ell(ks)\, V_\ell^{(1)}(s)\, s^2.$$

Higher order approximations for $F_1(r)$ and $F_2(r)$ are obtained by a straightforward generalization of this reasoning. If $F_1^{(n+1)}(r)$ and $F_2^{(n+1)}(r)$ do not differ considerably from $F_1^{(n)}(r)$ and $F_2^{(n)}(r)$, one can approximate the potential $V_\ell(r)$ in eqn. (3.16) by the nth-order approximation of the potential $V_\ell^{(n)}(r)$, i.e.

$$V_\ell(r) \approx V_\ell^{(n)}(r) = \frac{1}{r^2}\int_0^\infty \left(-\frac{\hbar^2}{2\mu}\frac{\tan(\,\delta_\ell(k)\,)}{k} - \frac{L}{k^2}\right) g_\ell(kr)dk - \frac{2\mu}{\hbar^2}\left\{\frac{F_1^{(n)}(r)}{r^2} + \frac{F_2^{(n)}(r)}{r^2}\right\}, \tag{3.17}$$

where

$$F_1^{(n)}(r') \equiv \int_0^\infty g_\ell(kr')k\,dk \int_0^\infty dr\, j_\ell(kr)\, n_\ell(kr)\, V_\ell^{(n-1)}(r)\, r^2 \int_0^r ds\, j_\ell^2(ks)\, V_\ell^{(n-1)}(s)\, s^2,$$
$$F_2^{(n)}(r') \equiv \int_0^\infty g_\ell(kr')k\,dk \int_0^\infty dr j_\ell^2(kr) V_\ell^{(n-1)}(r) r^2 \int_r^\infty ds\, j_\ell(ks)\, n_\ell(ks)\, V_\ell^{(n-1)}(s)\, s^2.$$

$\hat{\Theta}_\ell(\rho)$−Approach

Starting from eqn. (3.9), one can multiply both sides of eqn. (3.9) by $k^{2\ell+2}$ and then operating $\hat{\Theta}_\ell(k)$ on the resulting equation. This yields

$$\hat{\Theta}_\ell(k)\left(k^{2\ell+2}\left\{-\frac{\hbar^2}{2\mu}\frac{\tan(\,\delta_\ell(k)\,)}{k}\right\}\right) = \int_0^\infty \hat{\Theta}_\ell(k)\left(k^{2\ell+2} j_\ell^2(kr)\right) V_\ell(r) r^2 dr + \frac{2\mu}{\hbar^2}\hat{\Theta}_\ell(k)\,\{\eta_1(k) + \eta_2(k)\}, \tag{3.18}$$

where

$$\eta_1(k) \equiv k^{2\ell+3}\int_0^\infty dr\, j_\ell(kr)\, n_\ell(kr)\, V_\ell(r)\, r^2 \int_0^r ds\, j_\ell^2(ks)\, V_\ell(s)\, s^2,$$
$$\eta_2(k) \equiv k^{2\ell+3}\int_0^\infty dr j_\ell^2(kr) V_\ell(r) r^2 \int_r^\infty ds\, j_\ell(ks)\, n_\ell(ks)\, V_\ell(s)\, s^2. \quad (3.19)$$

But

$$\begin{aligned}\hat{\Theta}_\ell(k)\left(k^{2\ell+2} j_\ell^2(kr)\right) &= \left(\frac{d}{dk^2}\right)^\ell \frac{d}{dk}\left(\frac{d}{dk^2}\right)^\ell \left(k^{2\ell+2} j_\ell^2(kr)\right) \\ &= \left(\frac{d}{d(kr)^2}\right)^\ell \frac{d}{d(kr)}\left(\frac{d}{d(kr)^2}\right)^\ell \left((kr)^{2\ell+2} j_\ell^2(kr)\right) r^{2\ell-1} \\ &= \sin(2kr)\, r^{2\ell-1}\end{aligned}$$

Thus

$$\begin{aligned}\hat{\Theta}_\ell(k)\left(k^{2\ell+2}\left\{-\frac{\hbar^2}{2\mu}\frac{\tan(\delta_\ell(k))}{k}\right\}\right) &= \int_0^\infty \sin(2kr)\, V_\ell(r) r^{2\ell+1} dr \\ &+ \frac{2\mu}{\hbar^2}\hat{\Theta}_\ell(k)\left\{\eta_1(k) + \eta_2(k)\right\}. \quad (3.20)\end{aligned}$$

Multiplying both sides of eqn. (3.20) by $(4/\pi)\sin(2kr')$ and integrating over k from 0 to ∞, one obtains

$$\begin{aligned}\frac{4}{\pi}\int_0^\infty \sin(2kr')\,\hat{\Theta}_\ell(k)\left(k^{2\ell+2}\left\{-\frac{\hbar^2}{2\mu}\frac{\tan(\delta_\ell(k))}{k}\right\}\right) dk &= V_\ell(r')\, r'^{2\ell+1} \\ &+ \frac{4}{\pi}\frac{2\mu}{\hbar^2}\int_0^\infty \sin(2kr')\,\hat{\Theta}_\ell(k)\left\{\eta_1(k) + \eta_2(k)\right\} dk, \quad (3.21)\end{aligned}$$

since

$$\frac{4}{\pi}\int_0^\infty \sin(2kr)\,\sin(2kr')\, dk = \delta(r-r') - \delta(r+r').$$

Hence

$$\begin{aligned}V_\ell(r) &= \frac{4}{\pi r^{2\ell+1}}\int_0^\infty dk\,\sin(2kr)\hat{\Theta}_\ell(k)\left(k^{2\ell+2}\left\{-\frac{\hbar^2}{2\mu}\frac{\tan(\delta_\ell(k))}{k}\right\}\right. \\ &\left. - \frac{2\mu}{\hbar^2}\left\{\eta_1(k) + \eta_2(k)\right\}\right). \quad (3.22)\end{aligned}$$

where r' is replaced by r for convenience.

As in the $g_\ell(\rho)$−approach, the RHS of eqn. (3.22) is simply the potential obtained by inverting the partial wave in the first Born approximation, $V_\ell^{(B1)}(r)$, plus some correction terms.

Similarly, the second term on the RHS of eqn. (3.22) makes this inversion approach impractical since the potential $V_\ell(r)$ is contained in $\eta_1(k)$ and $\eta_2(k)$ as an integral form. However, one can get around this problem by solving $\eta_1(k)$ and $\eta_2(k)$ by successive iterations. The first-order approximation of $\eta_1(k)$ and $\eta_2(k)$, namely $\eta_1^{(1)}(k)$ and $\eta_2^{(1)}(k)$, is obtained by replacing the potential $V_\ell(r)$ in eqn. (3.22) by $V_\ell^{(B1)}(r)$. Thus, the first-order approximation of the potential in the second Born approach is given by

$$\begin{aligned} V_\ell^{(1)}(r) &= \frac{4}{\pi r^{2\ell+1}} \int_0^\infty dk\, \sin(2kr) \hat{\Theta}_\ell(k) \left(k^{2\ell+2} \left\{ -\frac{\hbar^2}{2\mu} \frac{\tan(\,\delta_\ell(k)\,)}{k} \right\} \right. \\ &- \left. \frac{2\mu}{\hbar^2} \left\{ \eta_1^{(1)}(k) + \eta_2^{(1)}(k) \right\} \right), \end{aligned}$$

where

$$\begin{aligned} \eta_1^{(1)}(k) &\equiv k^{2\ell+3} \int_0^\infty dr'\, j_\ell(kr')\, n_\ell(kr')\, V_\ell^{(B1)}(r')\, r'^2 \int_0^{r'} ds\, j_\ell^2(ks)\, V_\ell^{(B1)}(s)\, s^2, \\ \eta_2^{(1)}(k) &\equiv k^{2\ell+3} \int_0^\infty dr' j_\ell^2(kr') V_\ell^{(B1)}(r') r'^2 \int_{r'}^\infty ds\, j_\ell(ks)\, n_\ell(ks)\, V_\ell^{(B1)}(s)\, s^2. \end{aligned}$$

The second-order approximation $V_\ell^{(2)}(r)$ is obtained by substituting $V_\ell^{(1)}(r)$ in eqn. (3.22). Thus

$$V_\ell^{(2)}(r) = \frac{4}{\pi r^{2\ell+1}} \int_0^\infty dk \, \sin(2kr) \hat{\Theta}_\ell(k) \left(k^{2\ell+2} \left\{ -\frac{\hbar^2}{2\mu} \frac{\tan(\delta_\ell(k))}{k} \right\} - \frac{2\mu}{\hbar^2} \left\{ \eta_1^{(2)}(k) + \eta_2^{(2)}(k) \right\} \right),$$

where

$$\eta_1^{(2)}(k) \equiv k^{2\ell+3} \int_0^\infty dr' \, j_\ell(kr') \, n_\ell(kr') \, V_\ell^{(1)}(r') \, r'^2 \int_0^{r'} ds \, j_\ell^2(ks) \, V_\ell^{(1)}(s) \, s^2,$$
$$\eta_2^{(2)}(k) \equiv k^{2\ell+3} \int_0^\infty dr' j_\ell^2(kr') V_\ell^{(1)}(r') r'^2 \int_{r'}^\infty ds \, j_\ell(ks) \, n_\ell(ks) \, V_\ell^{(1)}(s) \, s^2.$$

Higher order approximations for $\eta_1(k)$ and $\eta_2(k)$ are obtained by a straightforward generalization of this reasoning. However, if $\eta_1^{(n+1)}(k)$ and $\eta_2^{(n+1)}(k)$ do not differ considerably from $\eta_1^{(n)}(k)$ and $\eta_2^{(n)}(k)$, one can approximate the potential $V_\ell(r)$ in eqn. (3.22) by the nth-order approximation of the potential $V_\ell^{(n)}(r)$, i.e.

$$V_\ell(r) \approx V_\ell^{(n)}(r) = \frac{4}{\pi r^{2\ell+1}} \int_0^\infty dk \, \sin(2kr) \hat{\Theta}_\ell(k) \left(k^{2\ell+2} \left\{ -\frac{\hbar^2}{2\mu} \frac{\tan(\delta_\ell(k))}{k} \right\} - \frac{2\mu}{\hbar^2} \left\{ \eta_1^{(n)}(k) + \eta_2^{(n)}(k) \right\} \right), \tag{3.23}$$

where

$$\eta_1^{(n)}(k) \equiv k^{2\ell+3} \int_0^\infty dr' \, j_\ell(kr') \, n_\ell(kr') \, V_\ell^{(n-1)}(r') \, r'^2 \int_0^{r'} ds \, j_\ell^2(ks) \, V_\ell^{(n-1)}(s) \, s^2,$$
$$\eta_2^{(n)}(k) \equiv k^{2\ell+3} \int_0^\infty dr' j_\ell^2(kr') V_\ell^{(n-1)}(r') r'^2 \int_{r'}^\infty ds \, j_\ell(ks) \, n_\ell(ks) \, V_\ell^{(n-1)}(s) \, s^2.$$

Notice that the correction terms in eqns. (3.17) and (3.23) should be smaller than the amplitude of the potential obtained by inverting the partial wave in the

first Born approximation, $V_\ell^{(B1)}(r)$. In order to investigate the magnitudes of these correction terms and consequently the improvement of the results obtained compared to those obtained using the partial wave Born approximation discussed in [7], one should perform some numerical calculations using the same phase shifts used in [7]. By comparing the potentials obtained using the second Born inversion technique with those obtained in [7], one can determine the magnitudes of these correction terms.

However, studying the second Born inversion technique in detail will take us far away from our main objective, namely studying the *finite space inverse scattering problem.* However, one still can *approximate* the magnitudes of these correction terms by considering the following example. *For simplicity, let us confine our attention to the first approach, namely the $g_\ell(\rho)$−approach.*

Example 3.1 :

Consider a particle of mass $\mu = 1000$ MeV/c^2, scattered from a square well potential of depth $V = -10$ MeV and range $d = 2$ fm, in the angular momentum channel $\ell = 0$. Using the notation in ref. [7], the "experimental" phase shifts[4] and the potential calculated using the partial wave Born approximation inversion technique developed in [7] are given in figs. 3.1 and 3.2 respectively.

[4]This notation is explained in chapter 7.

The magnitude of the correction term in eqn. (3.17) for $\ell = 0$, namely $\frac{2\mu}{\hbar^2}\left\{\frac{F_1^{(n)}(r)}{r^2} + \frac{F_2^{(n)}(r)}{r^2}\right\}$ where

$$F_1^{(n)}(r') \equiv \int_0^\infty g_0(kr')k\,dk \int_0^\infty dr\, j_0(kr)\, n_0(kr)\, V_0^{(n-1)}(r)\, r^2 \int_0^r ds\, j_0^2(ks)\, V_0^{(n-1)}(s)\, s^2,$$

$$F_2^{(n)}(r') \equiv \int_0^\infty g_0(kr')k\,dk \int_0^\infty dr j_0^2(kr) V_0^{(n-1)}(r) r^2 \int_r^\infty ds\, j_0(ks)\, n_0(ks)\, V_0^{(n-1)}(s)\, s^2,$$

can be *approximated* by replacing $V_0^{(n-1)}$ by the exact value of the potential, namely a square well potential of depth $V = -10$ MeV and range $d = 2$ fm. By making this replacement, the potential $V_0^{(n-1)}$ becomes a constant and the above triple integrals can be evaluated simply. A combination of *Mathematica* and FORTRAN-77 program was used to evaluate the above triple integrals. The correction term is plotted in fig. 3.3 while the potential given by eqn. (3.17) is plotted in fig. 3.4. One can see clearly from fig. 3.3 that the *approximate* magnitude of the correction term is, as expected, smaller than the amplitude of $V_\ell^{(B1)}(r)$.

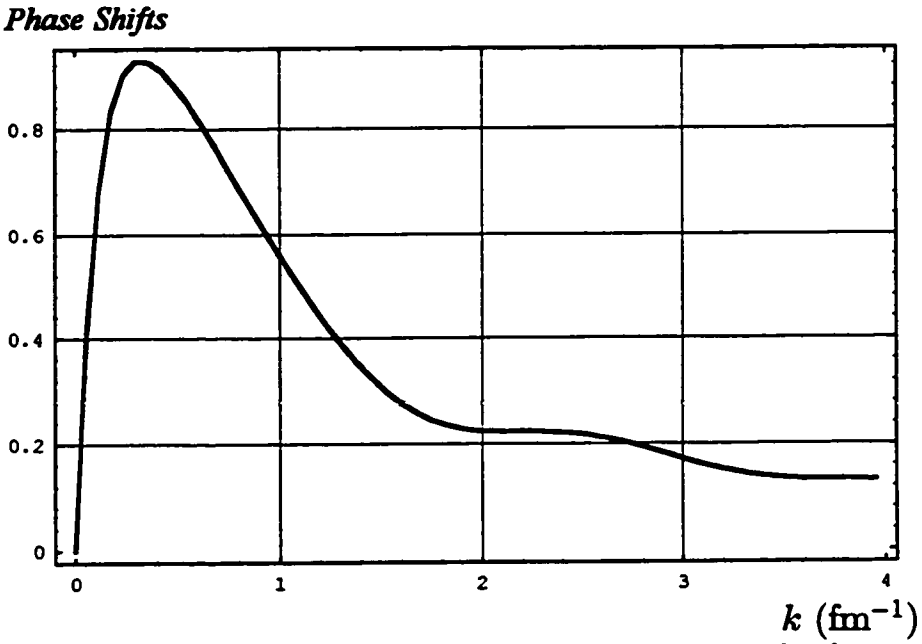

Fig. 3.1 : "Experimental" phase shifts produced by a particle of mass $\mu = 1000$ MeV/c^2 scattered from a square well potential of depth $V = -10$ MeV and range $d = 2$ fm in the angular momentum channel ℓ=0.

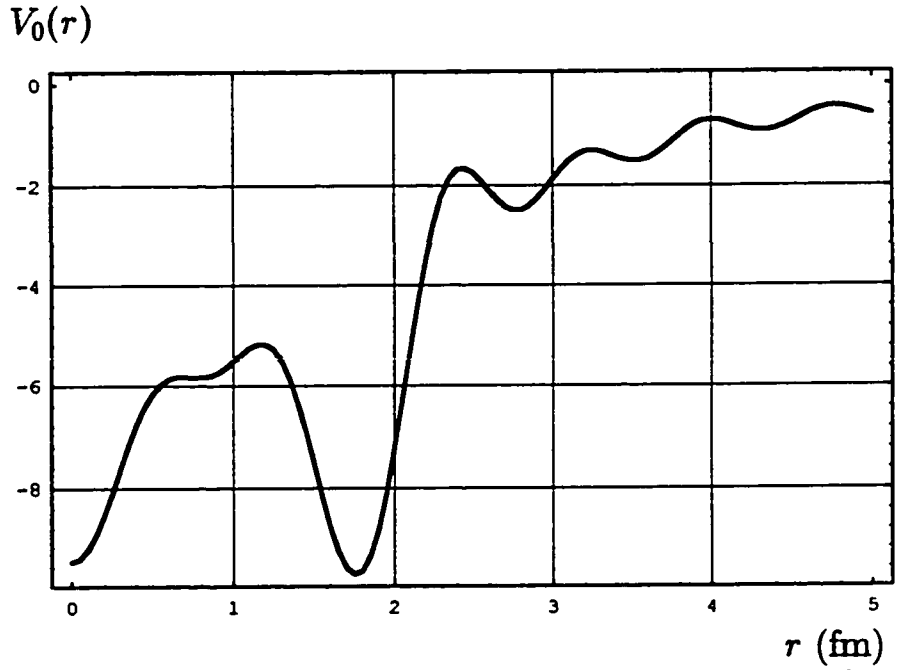

Fig. 3.2 : Potential calculated from eqn. (7.5) using the "experimental" phase shifts shown in the above figure.

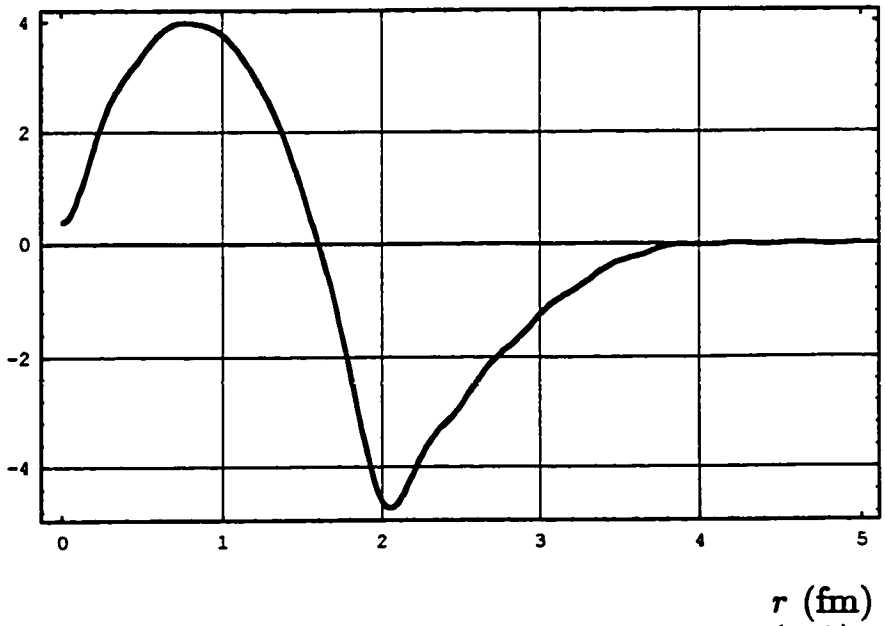

Fig. 3.3 : Approximate values of the correction term in eqn. (3.17) calculated by replacing $V_0^{(n-1)}$ in the triple integrals by a square well potential of depth $V = -10$ MeV and range $d = 2$ fm.

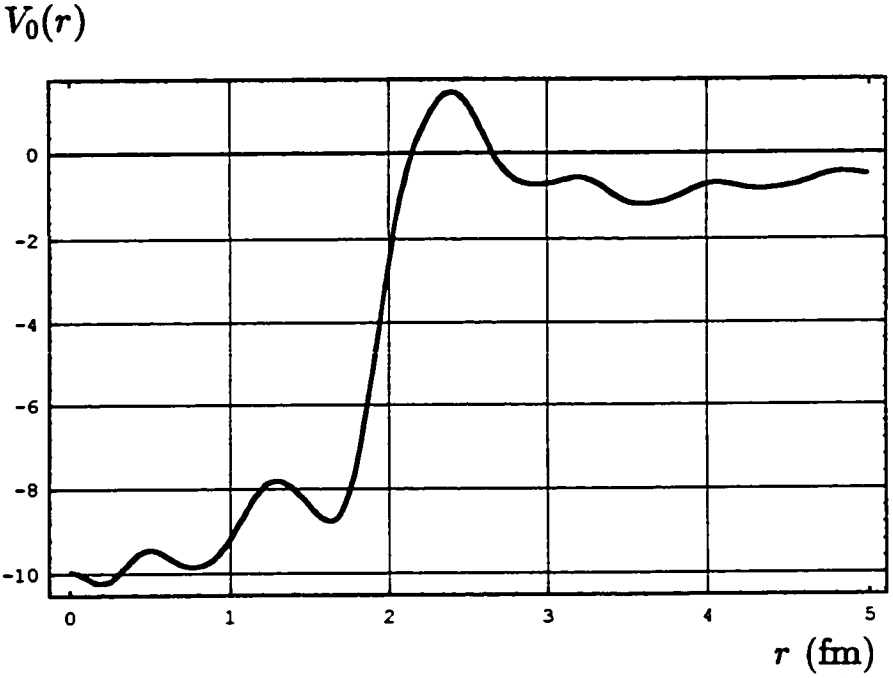

Fig. 3.4 : Potential calculated from eqn. (3.17) using the "experimental" phase shifts shown fig. 3.1 and the correction term in fig. 3.3.

CHAPTER 4

Finite Space Direct Scattering Problem

The problem of a particle of mass m_1, moving with initial speed v, scattered by another particle of mass m_2, initially at rest in the laboratory coordinate system, can be reduced to an equivalent one-body problem in the center of mass coordinate system by studying a particle of mass $\mu = \frac{m_1 m_2}{m_1+m_2}$ moving with initial relative speed v and relative kinetic energy $E = \frac{1}{2}\mu v^2$ scattered from a scattering potential $V_\ell(r)$, where r is the radial distance of the particle μ from the scattering potential, in the angular momentum channel ℓ.

If the masses of the two particles, m_1 and m_2, are equal or the difference between them can be neglected, as in the case of a proton and a neutron, then the following relations hold

$$E = \frac{1}{2}E_{lab}$$

$$k = \frac{1}{2}k_{lab}$$

where

E_{lab}: is the energy in the laboratory coordinate system

k_{lab}: is the momentum in the laboratory coordinate system (in units of $\hbar$).

Thus the finite space direct problem of a moving nucleon with initial relative speed v scattered by a stationary nucleon can be studied by considering a particle of mass μ confined within a three-dimensional sphere of radius a and scattered off a finite potential $V_\ell(r)$ located near the origin of the sphere. In this case, the energy eigenstates - $E_{\ell n}$ - of the particle for different angular momenta ℓ are discrete.

The solution of Schrödinger equation for the scattered wave $\psi_\ell(\mathbf{r})$ of the above problem is [43]:

$$R_\ell(r)Y_\ell^m(\theta,\phi) = \frac{u_\ell(r)}{r}Y_\ell^m(\theta,\phi)$$

and the radial wave function $u_\ell(r)$ satisfies the following differential equation:

$$\hat{H}u_\ell(r) = E_\ell u_\ell(r), \tag{4.1}$$

where

$$\hat{H} = -\frac{\hbar^2}{2\mu}\frac{d^2}{dr^2} + \frac{\hbar^2\ell(\ell+1)}{2\mu r^2} + V_\ell(r). \tag{4.2}$$

We require $u_\ell(0) = 0$ so that $R_\ell(r)$ is finite at $r = 0$ and $u_\ell(a) = 0$ since we are considering a finite spherical space of dimension a.

If $V_\ell(r) = 0$ in eqn. (4.2), then

$$\left(-\frac{\hbar^2}{2\mu}\frac{d^2}{dr^2} + \frac{\hbar^2\ell(\ell+1)}{2\mu r^2}\right) u_\ell(r) = E_\ell u_\ell(r). \tag{4.3}$$

The above equation represents a free particle of mass m and angular momentum ℓ in our finite spherical space. Multiplying both sides of the above equation by $-\frac{2\mu}{\hbar^2}$, one obtains

$$\left(\frac{d^2}{dr^2} - \frac{\ell(\ell+1)}{r^2} + k_\ell^2\right) u_\ell(r) = 0, \tag{4.4}$$

where

$$k_\ell^2 = \frac{2\mu E_\ell}{\hbar^2}. \tag{4.5}$$

The solution of the differential eqn. (4.4) is [44]:

$$u_\ell(r) = r\,R_\ell(r) = Arj_\ell(kr) + Brn_\ell(kr), \tag{4.6}$$

where A and B are constants.

But $u_\ell(0) = 0 \Rightarrow B = 0$, and $u_\ell(a) = 0 \Rightarrow j_\ell(k_\ell a) = 0$, So $k_\ell a$ are the zeros of the spherical Bessel function of the ℓth order. But it is well known that each spherical Bessel function has an infinite discrete number of roots $\alpha_{\ell n}$, where $\alpha_{\ell n}$ is the nth root of $j_\ell(x)$[1]. Moreover, a has a unique value. This implies that $k_{\ell n}$, and $E_{\ell n}$, are discrete, as expected for finite spaces, and $k_{\ell n}$ is given by

$$k_{\ell n} = \frac{\alpha_{\ell n}}{a}. \tag{4.7}$$

[1]See chapter 1, p. 3.

4.1 Radial Wave Function Expansion Approach

If $V_\ell(r) \neq 0$ in eqn (4.2), then the radial wave function of the nth energy state $R_{\ell n}(r)$ can be expanded in terms of the normalized eigenstates of the free particle, namely the spherical Bessel functions $N_{\ell q} j_\ell(k_{\ell q} r)$, i.e.

$$R_{\ell n}(r) = \sum_{q=1}^{\infty} b_{\ell n q} N_{\ell q} j_\ell(k_{\ell q} r) \tag{4.8}$$

or

$$u_{\ell n}(r) = \sum_{q=1}^{\infty} b_{\ell n q} N_{\ell q} r j_\ell(k_{\ell q} r). \tag{4.9}$$

where $N_{\ell q}$ are the normalization constants and $b_{\ell n q}$ are the expansion coefficients.

If the radial wave function, eqn. (4.9), is substituted in eqn. (4.1), then

$$\hat{H} \sum_{q=1}^{\infty} b_{\ell n q} N_{\ell q} r j_\ell(k_{\ell q} r) = E_\ell \sum_{q=1}^{\infty} b_{\ell n q} N_{\ell q} r j_\ell(k_{\ell q} r). \tag{4.10}$$

Multiplying both sides of the above equation by $N_{\ell p} r j_\ell(k_{\ell p} r)$ and integrating over r from 0 to a, we get

$$\sum_{q=1}^{\infty} b_{\ell n q} N_{\ell p} N_{\ell q} \int_0^a r j_\ell(k_{\ell p} r) \hat{H} r j_\ell(k_{\ell q} r) dr = E_\ell \sum_{q=1}^{\infty} b_{\ell n q} N_{\ell p} N_{\ell q} \int_0^a j_\ell(k_{\ell p} r) j_\ell(k_{\ell q} r) r^2 dr. \tag{4.11}$$

Using the orthonormality condition of the spherical Bessel function[2], namely

$$N_{\ell m} N_{\ell n} \int_0^a j_\ell(k_{\ell m} r) j_\ell(k_{\ell n} r) r^2 dr = \delta_{mn}, \tag{4.12}$$

[2]See chapter 1, p. 5.

eqn. (4.11) becomes

$$\sum_{q=1}^{\infty} b_{\ell nq}(\hat{H}_{pq} - \delta_{pq}E_\ell) = 0, \tag{4.13}$$

where

$$\hat{H}_{pq} = \hat{H}_{qp} = N_{\ell p}N_{\ell q}\int_0^a r j_\ell(k_{\ell p}r)\hat{H}r j_\ell(k_{\ell q}r)dr. \tag{4.14}$$

If there exists an integer m such that for any $q > m$

$$\left|\hat{H}_{pq}\right| \ll \left|\hat{H}_{pm}\right|,$$

then the infinite sum in eqn. (4.13) can be approximated by the finite sum

$$\sum_{q=1}^{q=m} b_{\ell nq}(\hat{H}_{pq} - \delta_{pq}E_\ell) = 0. \tag{4.15}$$

Eqn. (4.15) is an eigenvalue equation, which can be solved nontrivially only if the determinant of the coefficients vanishes, i.e.

$$\left|\hat{H}_{pq} - \delta_{pq}E_\ell\right| = 0 \tag{4.16}$$

or

$$\begin{vmatrix} \hat{H}_{11} - E_\ell & \hat{H}_{12} & \hat{H}_{13} & \cdots & \hat{H}_{1m} \\ \hat{H}_{21} & \hat{H}_{22} - E_\ell & \hat{H}_{23} & \cdots & \hat{H}_{2m} \\ \hat{H}_{31} & \hat{H}_{32} & \hat{H}_{33} - E_\ell & \cdots & \hat{H}_{3m} \\ \vdots & & & \ddots & \\ \hat{H}_{m1} & \hat{H}_{m2} & \cdots & & \hat{H}_{mm} - E_\ell \end{vmatrix}. \tag{4.17}$$

Solving this secular equation, which is of order m in E_ℓ, one gets m roots which are the perturbed eigenvalues, $E_{\ell n}$, of $\hat{H}$. We designate these $E_{\ell n}$ as perturbed due to the presence of the potential $V_\ell(r)$ and to differentiate them from the free particle or the unperturbed eigenvalues.

Throughout this thesis, the perturbed momenta will be denoted by $\gamma_{\ell n}$ and the unperturbed ones will be denoted by $k_{\ell n}$.

One can substitute each $E_{\ell n}$ in eqn. (4.15) to get the corresponding values of $b_{\ell n q}$. Thus

$$R_{\ell n}(r) = \sum_{q=1}^{q=m} b_{\ell n q} N_{\ell q} j_\ell(k_{\ell q} r) \tag{4.18}$$

or

$$u_{\ell n}(r) = \sum_{q=1}^{q=m} b_{\ell n q} N_{\ell q} r j_\ell(k_{\ell q} r). \tag{4.19}$$

To illustrate the above discussion, let us consider the following two examples in which $\ell = 0$ and 1, where the scattering potential $V_\ell(r)$ were chosen, for simplicity, to be a square well, or a square barrier, potential.

Example 4.1 : Let $\ell = 0$.

In this case, $N_{0q} = \sqrt{\frac{2}{a}} k_{0q}$ and $k_{0q} = \frac{q\pi}{a}$, $q = 1, 2, 3, \ldots$.

The scattering potential $V_\ell(r)$ is given by:

$$V_\ell(r) = \begin{cases} V & \text{if } r \leq d \\ 0 & \text{if } r > d \end{cases} \tag{4.20}$$

where

V : is the depth (height) of the square well (barrier) potential,

d : is the range of the square well (barrier) potential.

Then,

$$\hat{H}_{pq} = \frac{2}{a}\int_0^a \sin\left(\frac{p\pi}{a}r\right)\hat{H}\sin\left(\frac{q\pi}{a}r\right)dr, \tag{4.21}$$

or

$$\hat{H}_{pq} = \frac{2}{a}\int_0^a \sin\left(\frac{p\pi}{a}r\right)\left(-\frac{\hbar^2}{2\mu}\frac{d^2}{dr^2} + V_\ell(r)\right)\sin\left(\frac{q\pi}{a}r\right)dr. \tag{4.22}$$

Define

$$\hat{H}_{pq} \equiv T_{pq} + V_{pq},$$

where

$$T_{pq} = -\frac{\hbar^2}{2\mu}\frac{2}{a}\int_0^a \sin\left(\frac{p\pi}{a}r\right)\frac{d^2}{dr^2}\sin\left(\frac{q\pi}{a}r\right)dr, \tag{4.23}$$

and

$$V_{pq} = \frac{2}{a}\int_0^a \sin\left(\frac{p\pi}{a}r\right)V_\ell(r)\sin\left(\frac{q\pi}{a}r\right)dr. \tag{4.24}$$

Consider

$$\begin{aligned}\int_0^a \sin\left(\frac{p\pi}{a}r\right)\frac{d^2}{dr^2}\sin\left(\frac{q\pi}{a}r\right)dr &= \frac{q\pi}{a}\int_0^a \sin\left(\frac{p\pi}{a}r\right)\frac{d}{dr}\cos\left(\frac{q\pi}{a}r\right)dr \\ &= -\left(\frac{q\pi}{a}\right)^2\int_0^a \sin\left(\frac{p\pi}{a}r\right)\sin\left(\frac{q\pi}{a}r\right)dr \\ &= -\frac{a}{\pi}\left(\frac{q\pi}{a}\right)^2\int_0^\pi \sin(p\eta)\sin(q\eta)d\eta. \end{aligned} \tag{4.25}$$

If $p = q$ in eqn. (4.25), then

$$\int_0^\pi \sin^2(q\eta)d\eta = \frac{\pi}{2}.$$

But if $p \neq q$, then

$$\int_0^\pi \sin(p\eta)\sin(q\eta)d\eta = \frac{\sin((p-q)\eta)}{2(p-q)} - \frac{\sin((p+q)\eta)}{2(p+q)}\Bigg|_0^\pi = 0.$$

Thus,

$$\int_0^\pi \sin(p\eta)\sin(q\eta)d\eta = \begin{cases} \frac{\pi}{2} & \text{if } p = q \\ 0 & \text{otherwise.} \end{cases} \tag{4.26}$$

Substituting eqn. (4.26) in eqn. (4.25), one gets

$$\int_0^a \sin\left(\frac{p\pi}{a}r\right)\frac{d^2}{dr^2}\sin\left(\frac{q\pi}{a}r\right)dr = \begin{cases} -\frac{a}{2}\left(\frac{q\pi}{a}\right)^2 & \text{if } p = q \\ 0 & \text{otherwise.} \end{cases} \tag{4.27}$$

Hence

$$T_{pq} = \frac{\hbar^2}{2\mu}\begin{cases} \left(\frac{q\pi}{a}\right)^2 & \text{if } p = q \\ 0 & \text{otherwise.} \end{cases} \tag{4.28}$$

Similarly,

$$\begin{aligned} \int_0^a \sin\left(\frac{p\pi}{a}r\right)V_\ell(r)\sin\left(\frac{q\pi}{a}r\right)dr &= V\int_0^d \sin\left(\frac{p\pi}{a}r\right)\sin\left(\frac{q\pi}{a}r\right)dr \\ &= \frac{Va}{\pi}\int_0^{\frac{\pi d}{a}} \sin(p\eta)\sin(q\eta)d\eta. \end{aligned} \tag{4.29}$$

If $p \neq q$, then

$$\int_0^a \sin\left(\frac{p\pi}{a}r\right)V_\ell(r)\sin\left(\frac{q\pi}{a}r\right)dr = \frac{Va}{\pi}\left\{\frac{\sin((p-q)\eta)}{2(p-q)} - \frac{\sin((p+q)\eta)}{2(p+q)}\right\}_{\eta=0}^{\eta=\frac{\pi d}{a}}$$

$$\int_0^a \sin\left(\frac{p\pi}{a}r\right) V_\ell(r) \sin\left(\frac{q\pi}{a}r\right) dr = \frac{Va}{2\pi}\left\{\frac{\sin(\frac{(p-q)\pi d}{a})}{(p-q)} - \frac{\sin(\frac{(p+q)\pi d}{a})}{(p+q)}\right\}. \quad (4.30)$$

But if $p = q$, then

$$\begin{aligned}\int_0^a \sin\left(\frac{p\pi}{a}r\right) V_\ell(r) \sin\left(\frac{q\pi}{a}r\right) dr &= \frac{Va}{\pi}\int_0^{\frac{\pi d}{a}} \sin^2(q\eta)d\eta \\ &= \frac{Vd}{2} - \frac{Va}{2\pi}\frac{1}{2q}\int_0^{\frac{\pi d}{a}} \cos(2q\eta)d(2q\eta) \\ &= \frac{Vd}{2} - \frac{Va}{4\pi q}\sin(\frac{2\pi qd}{a}). \end{aligned} \quad (4.31)$$

Thus

$$V_{pq} = \begin{cases} \frac{Vd}{a} - \left(\frac{V}{2\pi q}\right)\sin(\frac{2\pi qd}{a}) & \text{if } p = q \\ \frac{V}{\pi}\left\{\frac{\sin(\frac{(p-q)\pi d}{a})}{(p-q)} - \frac{\sin(\frac{(p+q)\pi d}{a})}{(p+q)}\right\} & \text{if } p \neq q. \end{cases} \quad (4.32)$$

Hence

$$\hat{H}_{pq} = \begin{cases} \frac{\hbar^2}{2\mu}\left(\frac{q\pi}{a}\right)^2 + \frac{Vd}{a} - \left(\frac{V}{2\pi q}\right)\sin(\frac{2\pi qd}{a}) & \text{if } p = q \\ \frac{V}{\pi}\left\{\frac{\sin(\frac{(p-q)\pi d}{a})}{(p-q)} - \frac{\sin(\frac{(p+q)\pi d}{a})}{(p+q)}\right\} & \text{if } p \neq q. \end{cases} \quad (4.33)$$

Then one can substitute the matrix elements $\hat{H}_{pq}$ in the secular equation, eqn. (4.17), to obtain the energies of the perturbed eigenstates. *Eqns. (4.13) and (4.14) apply to any Hamiltonian, in particular even if V_ℓ also depends explicitly on the momentum* p *(for example, see page xii). In this case, the only additional complication is that the matrix elements of the potential on the LHS of eqn. (4.29) are just a little bit more complicated to evaluate.*

Example 4.2 : Let $\ell = 1$.

In this case, the matrix elements of the Hamiltonian are given by:

$$\hat{H}_{pq} = \frac{N_{1p}N_{1q}}{k_{1p}k_{1q}} \int_0^a \left(\frac{\sin(k_{1p}r)}{k_{1p}r} - \cos(k_{1p}r)\right) \left(-\frac{\hbar^2}{2\mu}\frac{d^2}{dr^2} + \frac{\hbar^2}{\mu r^2} + V_\ell(r)\right) \times \left(\frac{\sin(k_{1q}r)}{k_{1q}r} - \cos(k_{1q}r)\right) dr \qquad (4.34)$$

Similarly, one can define $\hat{H}_{pq}$ as

$$H_{pq} = T_{pq} + V_{pq}^{cf} + V_{pq}, \qquad (4.35)$$

where

$$\begin{aligned} T_{pq} &= C_{pq} \int_0^a \left(\frac{\sin(k_{1p}r)}{k_{1p}r} - \cos(k_{1p}r)\right) \left(-\frac{\hbar^2}{2\mu}\frac{d^2}{dr^2}\right) \left(\frac{\sin(k_{1q}r)}{k_{1q}r} - \cos(k_{1q}r)\right) dr, \\ V_{pq}^{cf} &= C_{pq} \int_0^a \left(\frac{\sin(k_{1p}r)}{k_{1p}r} - \cos(k_{1p}r)\right) \left(\frac{\hbar^2}{\mu r^2}\right) \left(\frac{\sin(k_{1q}r)}{k_{1q}r} - \cos(k_{1q}r)\right) dr, \\ V_{pq} &= C_{pq} \int_0^a \left(\frac{\sin(k_{1p}r)}{k_{1p}r} - \cos(k_{1p}r)\right) V_\ell(r) \left(\frac{\sin(k_{1q}r)}{k_{1q}r} - \cos(k_{1q}r)\right) dr, \end{aligned} \qquad (4.36)$$

and

$$C_{pq} = \frac{N_{1p}N_{1q}}{k_{1p}k_{1q}}. \qquad (4.37)$$

But

$$\frac{d^2}{dr^2}\left(\frac{\sin(k_{1p}r)}{k_{1p}r} - \cos(k_{1p}r)\right) = k_{1q}^2 \cos(k_{1q}r) - \frac{2\cos(k_{1q}r)}{r^2} + \frac{2\sin(k_{1q}r)}{k_{1q}r^3} - \frac{k_{1q}\sin(k_{1q}r)}{r}.$$

Thus

$$T_{pq} = -\frac{\hbar^2 C_{pq}}{2\mu}\int_0^a \left(k_{1q}^2\cos(k_{1q}r) - \frac{2\cos(k_{1q}r)}{r^2} + \frac{2\sin(k_{1q}r)}{k_{1q}r^3} - \frac{k_{1q}\sin(k_{1q}r)}{r}\right)\times \left(\frac{\sin(k_{1p}r)}{k_{1p}r} - \cos(k_{1p}r)\right)dr,$$

which can be factored as

$$T_{pq} = -\frac{\hbar^2 C_{pq}}{2\mu k_{1p}k_{1q}}\int_0^a \left(\frac{\sin(k_{1p}r)}{k_{1p}r} - \cos(k_{1p}r)\right)\times \left(\frac{(k_{1q}^2r^2-2)(k_{1q}r\cos(k_{1q}r) - \sin(k_{1q}r))(\sin(k_{1p}r) - k_{1p}r\cos(k_{1p}r))}{r^4}\right)dr. \quad (4.38)$$

The second term in $\hat{H}_{pq}$, namely V_{pq}^{cf}, can be written in an explicit form as

$$V_{pq}^{cf} = \frac{\hbar^2 C_{pq}}{\mu}\int_0^a \frac{\left(\frac{\sin(k_{1p}r)}{k_{1p}r} - \cos(k_{1p}r)\right)\left(\frac{\sin(k_{1q}r)}{k_{1q}r} - \cos(k_{1q}r)\right)}{r^2}dr. \quad (4.39)$$

Then, one can write the summation of V_{pq}^{cf} and T_{pq} in a factored form as

$$V_{pq}^{cf} + T_{pq} = \frac{\hbar^2 k_{1q} C_{pq}}{2\mu k_{1p}}\int_0^a \frac{(\sin(k_{1q}r) - k_{1q}r\cos(k_{1q}r))(\sin(k_{1p}r) - k_{1p}r\cos(k_{1p}r))}{r^2}dr. \quad (4.40)$$

The matrix elements of the last term, the potential term, are

$$V_{pq} = VC_{pq}\int_0^d \left(\frac{\sin(k_{1p}r)}{k_{1p}r} - \cos(k_{1p}r)\right)\left(\frac{\sin(k_{1q}r)}{k_{1q}r} - \cos(k_{1q}r)\right)dr. \quad (4.41)$$

The integrals in eqns. (4.40) and (4.41) can be evaluated numerically. Then one can substitute eqns. (4.40) and (4.41) in eqn. (4.17) to obtain the matrix elements $\hat{H}_{pq}$.

4.2 Finite Space Phase Shift

The asymptotic radial wave function of the nth state, $R^{as}_{\ell n}(r)$, in the presence of a potential $V_\ell(r)$ is given by

$$R^{as}_{\ell n}(r) = \frac{u^{as}_{\ell n}(r)}{r} = Bj_\ell(\gamma_{\ell n} r) + Cn_\ell(\gamma_{\ell n} r), \tag{4.42}$$

where B and C are constants.

Let

$$B = A\cos(\delta_\ell)$$

and

$$C = -A\sin(\delta_\ell).$$

Then, eqn. (4.42) becomes

$$R^{as}_{\ell n}(r) = \frac{u^{as}_{\ell n}(r)}{r} = A[\cos(\delta_\ell)\cdot j_\ell(\gamma_{\ell n} r) - \sin(\delta_\ell)\cdot n_\ell(\gamma_{\ell n} r)]. \tag{4.43}$$

But the exact radial wave function of the nth state, $R^{ex}_{\ell n}(r)$, at any position r is given by eqn. (4.8). So the radial wave function and its derivative are identical to those of the asymptotic solutions in the region where the potential $V_\ell(r)$ vanishes. Thus, if p is any point where $V_\ell(r)$ vanishes, then for $r \geq p$

$$R^{as}_{\ell n}(r)|_{r=p} = R^{ex}_{\ell n}(r)|_{r=p}$$

and

$$\frac{d}{dr}\left(R^{as}_{\ell n}(r)\right)\Big|_{r=p} = \frac{d}{dr}\left(R^{ex}_{\ell n}(r)\right)\Big|_{r=p}.$$

or

$$(A[\cos(\delta_\ell) \cdot j_\ell(\gamma_{\ell n} r) - \sin(\delta_\ell) \cdot n_\ell(\gamma_{\ell n} r)])_{r=p} = \sum_{q=1}^{q=m} b_{\ell n q} N_{\ell q} (j_\ell(k_{\ell q} r))_{r=p}, \quad (4.44)$$

and

$$(A\gamma_{\ell n}[\cos(\delta_\ell) \cdot j'_\ell(\gamma_{\ell n} r) - \sin(\delta_\ell) \cdot n'_\ell(\gamma_{\ell n} r)])_{r=p} = \sum_{q=1}^{q=m} b_{\ell n q} N_{\ell q} (k_{\ell q} j'_\ell(k_{\ell q} r))_{r=p}, \quad (4.45)$$

where

$$j'_\ell(\gamma_{\ell n} r) \equiv \frac{d}{dr} j_\ell(\gamma_{\ell n} r),$$

and

$$n'_\ell(\gamma_{\ell n} r) \equiv \frac{d}{dr} n_\ell(\gamma_{\ell n} r).$$

Dividing eqn. (4.44) by eqn. (4.45), one gets

$$\left(\frac{1}{\gamma_{\ell n}}\right) \left(\frac{\cos(\delta_\ell).j_\ell(\gamma_{\ell n} r) - \sin(\delta_\ell).n_\ell(\gamma_{\ell n} r)}{\cos(\delta_\ell).j'_\ell(\gamma_{\ell n} r) - \sin(\delta_\ell).n'_\ell(\gamma_{\ell n} r)}\right)_{r=p} = \left(\frac{\sum_{q=1}^{q=m} b_{\ell n q} N_{\ell q} j_\ell(k_{\ell q} r)}{\sum_{q=1}^{q=m} b_{\ell n q} N_{\ell q} k_{\ell q} j'_\ell(k_{\ell q} r)}\right)_{r=p}. \quad (4.46)$$

As an application to the above expression, let us consider the special two cases when $\ell = 0$ and 1.

Example 4.3 : Let $\ell = 0$ in eqn. (4.46).

In this case, $N_{0q} = \sqrt{\frac{2}{a}} k_{0q}$ for any q. Then

$$\frac{1}{\gamma_{0n}} \left\{ \frac{\cos(\delta_0)\left(\frac{\sin(\gamma_{0n}p)}{\gamma_{0n}p}\right) + \sin(\delta_0)\left(\frac{\cos(\gamma_{0n}p)}{\gamma_{0n}p}\right)}{\cos(\delta_0)\left(\frac{\cos(\gamma_{0n}p)}{\gamma_{0n}p} - \frac{\sin(\gamma_{0n}p)}{(\gamma_{0n}p)^2}\right) - \sin(\delta_0)\left(\frac{\cos(\gamma_{0n}p)}{(\gamma_{0n}p)^2} + \frac{\sin(\gamma_{0n}p)}{\gamma_{0n}p}\right)} \right\}$$

$$= \frac{\sum_{q=1}^{q=m} b_{0nq} j_0(k_{0q}r)}{\sum_{q=1}^{q=m} b_{0nq} k_{0q} j_0'(k_{0q}r)}.$$

$$\Rightarrow \frac{1}{\gamma_{0n}} \left\{ \frac{\cos(\delta_0)\sin(\gamma_{0n}p) + \sin(\delta_0)\cos(\gamma_{0n}p)}{\cos(\delta_0)\left(\cos(\gamma_{0n}p) - \frac{\sin(\gamma_{0n}p)}{\gamma_{0n}p}\right) - \sin(\delta_0)\left(\frac{\cos(\gamma_{0n}p)}{\gamma_{0n}p} + \sin(\gamma_{0n}p)\right)} \right\}$$

$$= \frac{\sum_{q=1}^{q=m} b_{0nq}\left(\frac{\sin(k_{0q}p)}{k_{0q}p}\right)}{\sum_{q=1}^{q=m} b_{0nq} k_{0q}\left(\frac{\cos(k_{0q}p)}{k_{0q}p} - \frac{\sin(k_{0q}p)}{(k_{0q}p)^2}\right)}. \tag{4.47}$$

But

$$\sin(x+y) = \sin(x)\cdot\cos(y) + \cos(x)\cdot\sin(y),$$

and

$$\cos(x+y) = \cos(x)\cdot\cos(y) - \sin(x)\cdot\sin(y).$$

Thus eqn. (4.47) becomes

$$\frac{1}{\gamma_{0n}} \left\{ \frac{\sin(\gamma_{0n}p + \delta_0)}{\cos(\gamma_{0n}p + \delta_0) - \frac{\sin(\gamma_{0n}p + \delta_0)}{\gamma_{0n}p}} \right\} = \frac{\sum_{q=1}^{q=m} b_{0nq}\left(\frac{\sin(k_{0q}p)}{k_{0q}p}\right)}{\sum_{q=1}^{q=m} b_{0nq} k_{0q}\left(\frac{\cos(k_{0q}p)}{k_{0q}p} - \frac{\sin(k_{0q}p)}{(k_{0q}p)^2}\right)}. \tag{4.48}$$

Taking $\cos(\gamma_{0n}p + \delta_0)$ as a common factor, one gets

$$\frac{1}{\gamma_{0n}} \left\{ \frac{\tan(\gamma_{0n}p + \delta_0)}{1 - \frac{\tan(\gamma_{0n}p + \delta_0)}{\gamma_{0n}p}} \right\} = \frac{\sum_{q=1}^{q=m} \beta_{0nq}\sin(k_{0q}p)}{\sum_{q=1}^{q=m} \beta_{0nq} k_{0q}\left(\cos(k_{0q}p) - \frac{\sin(k_{0q}p)}{k_{0q}p}\right)}, \tag{4.49}$$

where

$$\beta_{0nq} = \frac{b_{0nq}}{k_{0q}}.$$

Throughout this thesis, $\beta_{\ell nq}$ is defined as follows:

$$\beta_{\ell nq} = \frac{b_{\ell nq}}{k_{\ell q}}.$$

Eqn. (4.49) can be simplified as

$$\frac{\gamma_{0n}p}{\tan(\gamma_{0n}p + \delta_0)} - 1 = \frac{\sum_{q=1}^{q=m} \beta_{0nq} k_{0q} p \cos(k_{0q}p)}{\sum_{q=1}^{q=m} \beta_{0nq} \sin(k_{0q}p)} - 1.$$

$$\Rightarrow \qquad \tan(\gamma_{0n}p + \delta_0) = \gamma_{0n} \frac{\sum_{q=1}^{q=m} \beta_{0nq} \sin(k_{0q}p)}{\sum_{q=1}^{q=m} \beta_{0nq} k_{0q} \cos(k_{0q}p)}. \tag{4.50}$$

Thus,

$$\delta_0(\gamma_{0n}) = \tan^{-1}\left(\gamma_{0n} \frac{\sum_{q=1}^{q=m} \beta_{0nq} \sin(k_{0q}p)}{\sum_{q=1}^{q=m} \beta_{0nq} k_{0q} \cos(k_{0q}p)}\right) - \gamma_{0n}p. \tag{4.51}$$

But $k_{0q} = \frac{q\pi}{a}$,

$$\Rightarrow \qquad \delta_0(\gamma_{0n}) = \tan^{-1}\left[\left(\frac{a\gamma_{0n}}{\pi}\right) \frac{\sum_{q=1}^{q=m} \beta_{0nq} \sin(\frac{q\pi}{a}p)}{\sum_{q=1}^{q=m} q\beta_{0nq} \cos(\frac{q\pi}{a}p)}\right] - \gamma_{0n}p. \tag{4.52}$$

Example 4.4 : Let $\ell = 1$ in eqn. (4.46).

Then the LHS becomes

$$\text{LHS} = \frac{1}{\gamma_{1n}} \text{x}$$

$$\left\{ \frac{\cos(\delta_1)\left(\frac{\sin(\gamma_{1n}p)}{(\gamma_{1n}p)^2} - \frac{\cos(\gamma_{1n}p)}{\gamma_{1n}p}\right) + \sin(\delta_1)\left(\frac{\cos(\gamma_{1n}p)}{(\gamma_{1n}p)^2} + \frac{\sin(\gamma_{1n}p)}{\gamma_{1n}p}\right)}{\cos(\delta_1)\left[\frac{\sin(\gamma_{1n}p)}{\gamma_{1n}p} + 2\left(\frac{\cos(\gamma_{1n}p)}{(\gamma_{1n}p)^2} - \frac{\sin(\gamma_{1n}p)}{(\gamma_{1n}p)^3}\right)\right] + \sin(\delta_1)\left[\frac{\cos(\gamma_{1n}p)}{\gamma_{1n}p} - 2\left(\frac{\cos(\gamma_{1n}p)}{(\gamma_{1n}p)^3} + \frac{\sin(\gamma_{1n}p)}{(\gamma_{1n}p)^2}\right)\right]} \right\}$$

which can be simplified to

$$\text{LHS} = \frac{1}{\gamma_{1n}} \left\{ \frac{\frac{\sin(\gamma_{1n}p+\delta_1)}{\gamma_{1n}p} - \cos(\gamma_{1n}p + \delta_1)}{\sin(\gamma_{1n}p + \delta_1) + \left(\frac{2}{\gamma_{1n}p}\right)\left(\cos(\gamma_{1n}p + \delta_1) - \frac{\sin(\gamma_{1n}p)}{\gamma_{1n}p}\right)} \right\}.$$

Inverting the above expression, one obtains

$$(\text{LHS})^{-1} = \gamma_{1n} \cdot \left\{ \frac{\sin(\gamma_{1n}p + \delta_1)}{\frac{\sin(\gamma_{1n}p+\delta_1)}{\gamma_{1n}} - \cos(\gamma_{1n}p + \delta_1)} \right\} - \frac{2}{p}. \tag{4.53}$$

On the other hand,

$$\text{RHS} = \frac{\sum_{q=1}^{q=m} b_{1nq} N_{1q} \left(\frac{\sin(k_{1q}p)}{(k_{1q}p)^2} - \frac{\cos(k_{1q}p)}{k_{1q}p}\right)}{\sum_{q=1}^{q=m} b_{1nq} N_{1q} k_{1q} \left[\frac{\sin(k_{1q}p)}{k_{1q}p} - \left(\frac{2}{\gamma_{1n}p}\right)\left(\frac{\sin(k_{1q}p)}{(k_{1q}p)^2} - \frac{\cos(k_{1q}p)}{k_{1q}p}\right)\right]}.$$

Similarly, one can invert the above expression to get

$$(\text{RHS})^{-1} = \frac{\sum_{q=1}^{q=m} b_{1nq} N_{1q} \left(\frac{\sin(k_{1q}p)}{p}\right)}{\sum_{q=1}^{q=m} b_{1nq} N_{1q} \left(\frac{\sin(k_{1q}p)}{(k_{1q}p)^2} - \frac{\cos(k_{1q}p)}{k_{1q}p}\right)} - \frac{2}{p}. \tag{4.54}$$

Therefore, for $\ell = 1$ eqn. (4.46) becomes

$$\gamma_{1n} \cdot \left\{ \frac{\sin(\gamma_{1n}p + \delta_1)}{\frac{\sin(\gamma_{1n}p+\delta_1)}{\gamma_{1n}} - \cos(\gamma_{1n}p + \delta_1)} \right\} = \frac{\sum_{q=1}^{q=m} b_{1nq} N_{1q} \left(\frac{\sin(k_{1q}p)}{p}\right)}{\sum_{q=1}^{q=m} b_{1nq} N_{1q} \left(\frac{\sin(k_{1q}p)}{(k_{1q}p)^2} - \frac{\cos(k_{1q}p)}{k_{1q}p}\right)}, \tag{4.55}$$

or

$$\frac{1}{\gamma_{1n}}\left\{\frac{\frac{\sin(\gamma_{1n}p+\delta_1)}{\gamma_{1n}p}-\cos(\gamma_{1n}p+\delta_1)}{\sin(\gamma_{1n}p+\delta_1)}\right\}=\frac{\sum_{q=1}^{q=m}b_{1nq}N_{1q}\left(\frac{\sin(k_{1q}p)}{(k_{1q}p)^2}-\frac{\cos(k_{1q}p)}{k_{1q}p}\right)}{\sum_{q=1}^{q=m}b_{1nq}N_{1q}\left(\frac{\sin(k_{1q}p)}{p}\right)}. \quad (4.56)$$

Eqn. (4.56) can be simplified to

$$\frac{1}{\gamma_{1n}p}-\cot(\gamma_{1n}p+\delta_1)=\frac{\gamma_{1n}\sum_{q=1}^{q=m}\beta_{1nq}N_{1q}\left(\frac{\sin(k_{1q}p)}{k_{1q}p}-\cos(k_{1q}p)\right)}{\sum_{q=1}^{q=m}\beta_{1nq}N_{1q}k_{1q}\sin(k_{1q}p)}.$$

Then,

$$\cot(\gamma_{1n}p+\delta_1)=\frac{1}{\gamma_{1n}p}-\frac{\gamma_{1n}\sum_{q=1}^{q=m}\beta_{1nq}N_{1q}\left(\frac{\sin(k_{1q}p)}{k_{1q}p}-\cos(k_{1q}p)\right)}{\sum_{q=1}^{q=m}\beta_{1nq}N_{1q}k_{1q}\sin(k_{1q}p)}, \quad (4.57)$$

or

$$\tan(\gamma_{1n}p+\delta_1)=\frac{\gamma_{1n}p\sum_{q=1}^{q=m}\beta_{1nq}N_{1q}k_{1q}\sin(k_{1q}p)}{\sum_{q=1}^{q=m}\beta_{1nq}N_{1q}\left\{k_{1q}\sin(k_{1q}p)-\gamma_{1n}^2p\left(\frac{\sin(k_{1q}p)}{k_{1q}p}-\cos(k_{1q}p)\right)\right\}}. \quad (4.58)$$

Thus,

$$\delta_1(\gamma_{1n})=\cot^{-1}\left\{\frac{1}{\gamma_{1n}p}-\frac{\gamma_{1n}\sum_{q=1}^{q=m}\beta_{1nq}N_{1q}\left(\frac{\sin(k_{1q}p)}{k_{1q}p}-\cos(k_{1q}p)\right)}{\sum_{q=1}^{q=m}\beta_{1nq}N_{1q}k_{1q}\sin(k_{1q}p)}\right\}-\gamma_{1n}p, \quad (4.59)$$

or

$$\delta_1(\gamma_{1n})=\tan^{-1}\left\{\frac{\gamma_{1n}p\sum_{q=1}^{q=m}\beta_{1nq}N_{1q}k_{1q}\sin(k_{1q}p)}{\sum_{q=1}^{q=m}\beta_{1nq}N_{1q}\left\{k_{1q}\sin(k_{1q}p)-\gamma_{1n}^2p\left(\frac{\sin(k_{1q}p)}{k_{1q}p}-\cos(k_{1q}p)\right)\right\}}\right\}-\gamma_{1n}p. \quad (4.60)$$

The finite space phase shift expression, eqn.(4.46), can be further simplified by requiring $p = a$, where a is the dimension of the finite space. At $r = a$, the radial wave function vanishes. Then eqn. (4.46) becomes

$$\cos(\delta_\ell) \cdot j_\ell(\gamma_{\ell n} a) - \sin(\delta_\ell) \cdot n_\ell(\gamma_{\ell n} a) = 0. \tag{4.61}$$

Using this value for p, the phase shift for $\ell = 0$ in eqn. (4.61) becomes

$$\delta_0(\gamma_{0n}) = \tan^{-1}(0) - \gamma_{0n} a = n\pi - \gamma_{0n} a, \qquad n = 1, 2, 3, \ldots. \tag{4.62}$$

For $\ell = 1$, in this case the second term in the denominator of eqn. (4.60), namely

$$k_{1q} a j_1(k_{1q} a) = \frac{\sin(k_{1q} a)}{k_{1q} a} - \cos(k_{1q} a),$$

vanishes and eqn. (4.60) becomes

$$\delta_1(\gamma_{1n}) = \tan^{-1}\left\{ \frac{\gamma_{1n} a \sum_{q=1}^{q=m} \beta_{1nq} N_{1q} k_{1q} \sin(k_{1q} a)}{\sum_{q=1}^{q=m} \beta_{1nq} N_{1q} k_{1q} \sin(k_{1q} a)} \right\} - \gamma_{1n} a.$$

Thus

$$\delta_1(\gamma_{1n}) = \tan^{-1}(\gamma_{1n} a) - \gamma_{1n} a. \tag{4.63}$$

For $\ell = 2$, the phase shift is given by

$$\delta_2(\gamma_{2n}) = \tan^{-1}\left\{ \frac{3\gamma_{2n} a}{3 - (\gamma_{2n} a)^2} \right\} - \gamma_{2n} a. \tag{4.64}$$

4.3 Second Approach To The Direct Problem

One can approach the direct problem in a different way, which takes a particularly simple form for our choice of the potential $V_\ell(r)$, namely the square well (or barrier) potential. In this case the Schrödinger equation is

$$\left(-\frac{\hbar^2}{2\mu}\frac{d^2}{dr^2}+\frac{\hbar^2\ell(\ell+1)}{2\mu r^2}+V\right)u_\ell^{int}(r)=E_\ell u_\ell^{int}(r) \quad \text{if } 0\le r\le d \tag{4.65}$$

and

$$\left(-\frac{\hbar^2}{2\mu}\frac{d^2}{dr^2}+\frac{\hbar^2\ell(\ell+1)}{2\mu r^2}\right)u_\ell^{ext}(r)=E_\ell u_\ell^{ext}(r) \quad \text{if } d\le r\le a. \tag{4.66}$$

where

V : is the depth (height) of the square well (barrier) potential.

d : is the range of the square well (barrier) potential.

$u_\ell^{int}(r)$: is the radial solution in the region where the potential is effective. We designate this solution as the internal solution.

$u_\ell^{ext}(r)$: is the radial solution outside the effective region of the potential. We designate this solution as the external solution.

Eqns. (4.65) and (4.66) can be written as

$$\left(\frac{d^2}{dr^2}-\frac{\ell(\ell+1)}{r^2}+K_\ell^2\right)u_\ell^{int}(r)=0 \quad \text{if } 0\le r\le d \tag{4.67}$$

and

$$\left(\frac{d^2}{dr^2}-\frac{\ell(\ell+1)}{r^2}+\gamma_\ell^2\right)u_\ell^{ext}(r)=0 \quad \text{if } d\le r\le a. \tag{4.68}$$

where

$$K_\ell^2 = \frac{2m(E_\ell - V)}{\hbar^2}, \tag{4.69}$$

and

$$\gamma_\ell^2 = \frac{2mE_\ell}{\hbar^2}. \tag{4.70}$$

The solutions of eqns. (4.67) and (4.68) are

$$u_\ell^{int}(r) = Brj_\ell(K_\ell r) + Crn_\ell(K_\ell r), \tag{4.71}$$

and

$$u_\ell^{ext}(r) = Drj_\ell(\gamma_\ell r) + Frn_\ell(\gamma_\ell r), \tag{4.72}$$

Where B, C, D and F are constants.

Imposing the finite space boundary conditions[3] on eqns. (4.71) and (4.72), one obtains

$$u_{\ell n}^{int}(r) = Brj_\ell(K_{\ell n} r), \tag{4.73}$$

and

$$u_{\ell n}^{ext}(r) = Drj_\ell(\gamma_{\ell n} r) + Frn_\ell(\gamma_{\ell n} r). \tag{4.74}$$

Let

$$D = A\cos(\delta_{\ell n}) \quad \text{and} \quad F = -A\sin(\delta_{\ell n}).$$

Then, the external solution in eqn. (4.74) becomes

$$u_{\ell n}^{ext}(r) = Ar\{\cos(\delta_{\ell n})\, j_\ell(\gamma_{\ell n} r) - \sin(\delta_{\ell n})\, n_\ell(\gamma_{\ell n} r)\}. \tag{4.75}$$

[3]See page 61.

Since the radial wave function and its first derivative are continuous inside the space, we require that the internal solution and its first derivative be equal to those of the external solution i.e.

$$u_{\ell n}^{int}(r)\Big|_{r=d} = u_{\ell n}^{ext}(r)\Big|_{r=d},$$

and

$$\frac{d}{dr}\left(u_{\ell n}^{int}(r)\right)\Big|_{r=d} = \frac{d}{dr}\left(u_{\ell n}^{ext}(r)\right)\Big|_{r=d}.$$

or explicitly as

$$\{Brj_\ell(K_{\ell n}r)\}_{r=d} = \{\, Ar[\cos(\delta_\ell)\cdot j_\ell(\gamma_{\ell n}r) - \sin(\delta_\ell)\cdot n_\ell(\gamma_{\ell n}r)]\,\}_{r=d}, \tag{4.76}$$

and

$$\{Brj_\ell(K_{\ell n}r)\}'_{r=d} = \{\, Ar[\cos(\delta_\ell)\cdot j_\ell(\gamma_{\ell n}r) - \sin(\delta_\ell)\cdot n_\ell(\gamma_{\ell n}r)]\,\}'_{r=d} \tag{4.77}$$

where

$$\{\cdots\cdots\}' \equiv \frac{d}{dr}\{\cdots\cdots\}$$

Dividing eqn. (4.76) by eqn. (4.77), one gets

$$\left(\frac{rj_\ell(K_{\ell n}r)}{\{rj_\ell(K_{\ell n}r)\}'}\right)_{r=d} = \left(\frac{r[\cos(\delta_\ell)\cdot j_\ell(\gamma_{\ell n}r) - \sin(\delta_\ell)\cdot n_\ell(\gamma_{\ell n}r)]}{\{r[\cos(\delta_\ell)\cdot j_\ell(\gamma_{\ell n}r) - \sin(\delta_\ell)\cdot n_\ell(\gamma_{\ell n}r)]\}'}\right)_{r=d} \tag{4.78}$$

Also we require that the external solution vanish at the boundary of the space i.e.

$$u_{\ell n}^{ext}(a) = 0 \tag{4.79}$$

Solving eqn. (4.78) and eqn. (4.79) together, one can determine the phase shift and the discrete energy levels of this finite space.

4.3.1 Phase-Shifted Spherical Bessel Functions $\Re_\ell(\rho, \alpha)$

The spherical Bessel functions $j_\ell(\rho)$ are given by [45]:

$$j_\ell(\rho) = (-1)^\ell \rho^\ell \left(\frac{1}{\rho}\frac{d}{d\rho}\right)^\ell \frac{\sin(\rho)}{\rho}, \tag{4.80}$$

and the spherical Neumann functions $n_\ell(\rho)$ are given by [46]:

$$n_\ell(\rho) = -(-1)^\ell \rho^\ell \left(\frac{1}{\rho}\frac{d}{d\rho}\right)^\ell \frac{\cos(\rho)}{\rho}. \tag{4.81}$$

We define the phase-shifted spherical Bessel functions $\Re_\ell(\rho, \alpha)$ as follows:

$$\begin{aligned}
\Re_\ell(\rho, \alpha) &\equiv \cos(\alpha) j_\ell(\rho) - \sin(\alpha) n_\ell(\rho) && (4.82)\\
&\equiv (-1)^\ell \rho^\ell \left(\frac{1}{\rho}\frac{d}{d\rho}\right)^\ell \left(\frac{\sin(\rho)\cos(\alpha) + \cos(\rho)\sin(\alpha)}{\rho}\right) && (4.83)\\
&\equiv (-1)^\ell \rho^\ell \left(\frac{1}{\rho}\frac{d}{d\rho}\right)^\ell \left(\frac{\sin(\rho+\alpha)}{\rho}\right). && (4.84)
\end{aligned}$$

Comparing eqn. (4.84) with eqn. (4.81), one can directly observe that $\Re_\ell(\rho, \alpha)$ differs from $j_\ell(\rho)$ by only a phase factor α which does not depend on ρ and that $\Re_\ell(\rho, \alpha) \longrightarrow j_\ell(\rho)$ as $\alpha \longrightarrow 0$. The values of these phase shifted spherical Bessel functions for $\ell = 0$, 1 and 2 are listed in Table 4.1.

Table 4.1: Phase shifted spherical Bessel functions $\Re_\ell(\rho,\alpha)$ and spherical Bessel functions $j_\ell(\rho)$ for $\ell = 0$, 1 and 2.

$\ell =$	0	1	2
$j_\ell(\rho)$	$\frac{\sin(\rho)}{\rho}$	$\frac{\sin(\rho)}{\rho^2} - \frac{\cos(\rho)}{\rho}$	$\left(\frac{3}{\rho^3} - \frac{1}{\rho}\right)\sin(\rho) - \frac{3}{\rho^2}\cos(\rho)$
$\Re_\ell(\rho,\alpha)$	$\frac{\sin(\rho+\alpha)}{\rho}$	$\frac{\sin(\rho+\alpha)}{\rho^2} - \frac{\cos(\rho+\alpha)}{\rho}$	$\left(\frac{3}{\rho^3} - \frac{1}{\rho}\right)\sin(\rho+\alpha) - \frac{3}{\rho^2}\cos(\rho+\alpha)$

Using these phase-shifted spherical Bessel functions, Eqn. (4.78) and Eqn. (4.79) can be put in a compact form as follows:

$$\left(\frac{rj_\ell(K_{\ell n}r)}{\{rj_\ell(K_{\ell n}r)\}'}\right)_{r=d} = \left(\frac{r\Re_\ell(\gamma_{\ell n}r,\delta_{\ell n})}{\{r\Re_\ell(\gamma_{\ell n}r,\delta_{\ell n})\}'}\right)_{r=d} \tag{4.85}$$

and

$$\Re_\ell(\gamma_{\ell n}a,\delta_{\ell n}) = 0 \tag{4.86}$$

The following two examples illustrate this second approach to the direct problem.

Example 4.7 : Let $\ell = 0$.

In this case, eqn. (4.85) becomes

$$\frac{d\,\frac{\sin(K_{0n}d)}{K_{0n}d}}{\cos(K_{0n}d)} = \frac{d\,\frac{\sin(\gamma_{0n}d+\delta_{0n})}{\gamma_{0n}d}}{\cos(\gamma_{0n}d+\delta_{0n})} \tag{4.87}$$

Thus

$$\frac{\tan(K_{0n}d)}{K_{0n}} = \frac{\tan(\gamma_{0n}d + \delta_{0n})}{\gamma_{0n}} \tag{4.88}$$

and eqn. (4.86) becomes

$$\sin(\gamma_{0n}a + \delta_{0n}) = 0 \tag{4.89}$$

$$\Rightarrow \qquad \delta_{0n} = n\pi - \gamma_{0n}a, \qquad n = 1, 2, 3, \ldots. \tag{4.90}$$

Substituting eqn. (4.90) in eqn. (4.88), one gets the following transcendental equation

$$\frac{\tan(K_{0n}d)}{K_{0n}} = \frac{\tan(\gamma_{0n}(d-a) + n\pi)}{\gamma_{0n}} \tag{4.91}$$

But

$$\tan(x + n\pi) = \tan(x) \qquad \text{for } n = 1, 2, 3, \ldots.$$

Thus eqn. (4.91) becomes

$$\frac{\tan(K_{0n}d)}{K_{0n}} = \frac{\tan(\gamma_{0n}(d-a))}{\gamma_{0n}} \tag{4.92}$$

If $V < 0$ (square well potential):

There are two cases:

1) $E_{0n} > 0$, then

$$K_{0n}^2 = \frac{2\mu(E_{0n} + |V|)}{\hbar^2} = \gamma_{0n}^2 + \frac{2\mu|V|}{\hbar^2} > 0,$$

and

$$\gamma_{0n}^2 = \frac{2\mu E_{0n}}{\hbar^2} > 0.$$

Then, one can solve the transcendental equation, eqn. (4.92), graphically or numerically to obtain the discrete energy levels and the corresponding phase shifts. Fig. 4.1 shows the positive energy levels graphically in the special case when $V = -200$ MeV, $d = 2$ fm and $a = 10$ fm. These arise when the curves corresponding to the left and right sides of eqn. (4.92) intersect.

2) $E_{0n} < 0$, then

$$K_{0n}^2 = \frac{2\mu(|V| - |E_{0n}|)}{\hbar^2} > 0,$$

and

$$\gamma_{0n}^2 = -\frac{2\mu|E_{0n}|}{\hbar^2} < 0.$$

$$\Rightarrow \qquad \gamma_{0n} = i\sqrt{\frac{2\mu|E_{0n}|}{\hbar^2}} \equiv i\xi_{0n}.$$

Thus, eqn. (4.92) becomes

$$\frac{\tan(K_{0n}d)}{K_{0n}} = \frac{\tan(i\xi_{0n}(d-a))}{i\xi_{0n}}. \tag{4.93}$$

But

$$\tan(ix) = i\tanh(x). \tag{4.94}$$

Therefore, eqn. (4.92) becomes

$$\frac{\tan(K_{0n}d)}{K_{0n}} = \frac{\tanh(\xi_{0n}(d-a))}{\xi_{0n}}, \tag{4.95}$$

which can be solved graphically or numerically to obtain the finite number of allowed bounded energy levels. Fig. 4.2 shows these bound states graphically in the special case when $V = -200$ MeV, $d = 2$ fm and $a = 10$ fm. They correspond to the intersections of the two curves corresponding to the left and right hand sides of eqn. (4.95). In this special case, there are only two bounded states, see fig. 4.2.

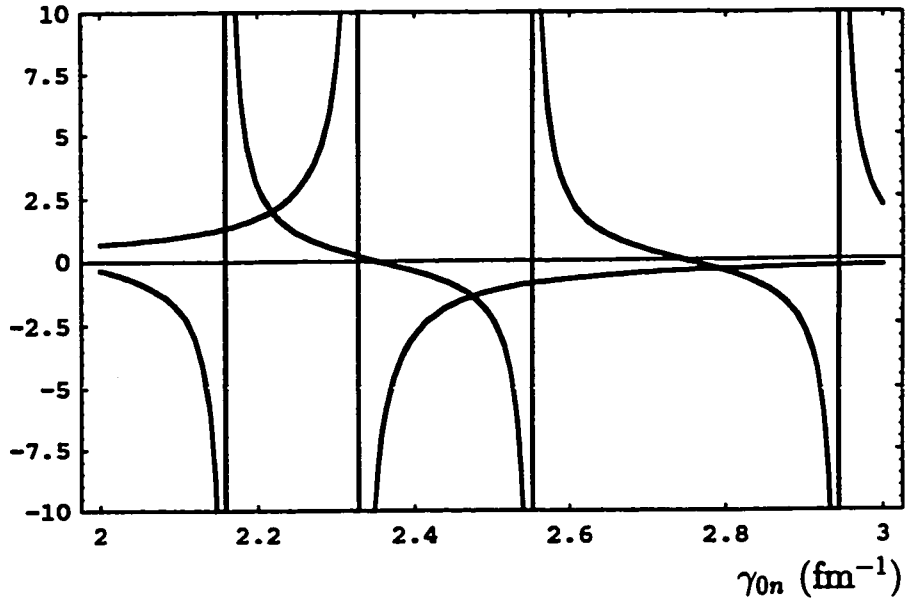

Fig. 4.1 : Graphical solution of the transcendental equation (4.92) for $V = -200$ MeV, $d = 2$ fm, $a = 10$ fm, and $E_{0n} > 0$. The energies at which the intersections of the RHS of eqn. (4.92) with the LHS occur, represents the discrete perturbed energy states.

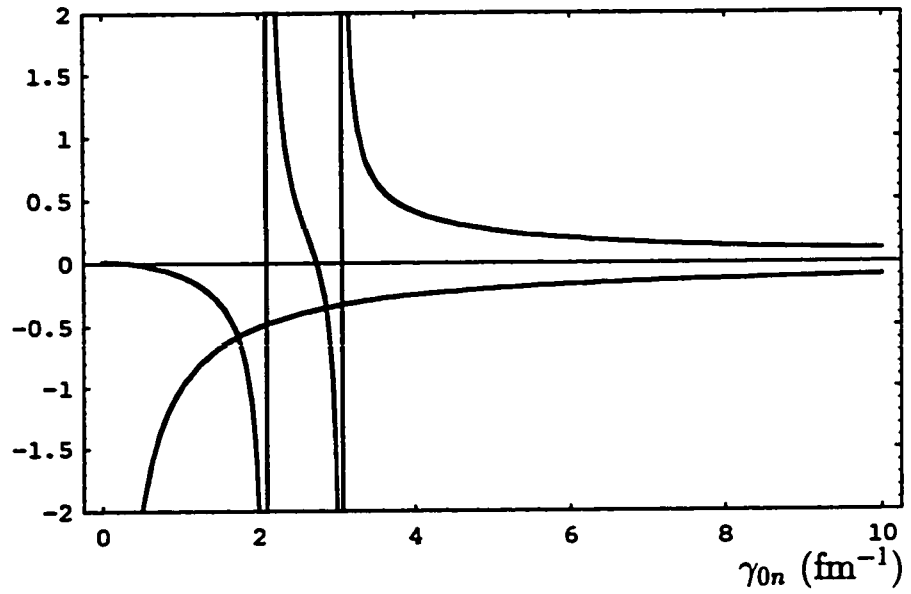

Fig. 4.2 : Graphical solution of the transcendental equation (4.95) for $V = -200$ MeV, $d = 2$ fm and $a = 10$ fm. The energies at which the intersections of the RHS of eqn. (4.95) with the LHS occur, represents the bounded energy states.

If $V > 0$ (square barrier potential)

In this case $E_{0n} > 0$, but still there are two possibilities :

1) $E_{0n} > V$, then

$$K_{0n}^2 = \frac{2\mu(E_{0n} - V)}{\hbar^2} > 0$$

and

$$\gamma_{0n}^2 = \frac{2\mu E_{0n}}{\hbar^2} > 0.$$

Then, one can solve the transcendental equation, eqn. (4.92), graphically or numerically to obtain the discrete energy levels and the corresponding phase shifts. Fig. 4.3 shows a graphical solution of eqn. (4.92) in the special case when $V = 200$ MeV, $d = 2$ fm and $a = 10$ fm.

2) $E_{0n} < V$, then

$$K_{0n}^2 = \frac{2\mu(E_{0n} - V)}{\hbar^2} < 0,$$

and

$$\gamma_{0n}^2 = \frac{2\mu E_{0n}}{\hbar^2} > 0.$$

$$\Rightarrow \qquad K_{0n} = i\sqrt{\frac{2\mu(V - E_{0n})}{\hbar^2}} \equiv i\xi_{0n}$$

Using this value of K_{0n} and eqn. (4.92), the transcendental equation, eqn. (4.92), becomes

$$\frac{\tanh(\xi_{\ell n} d)}{\xi_{\ell n}} = \frac{\tan(\gamma_{\ell n}(d - a))}{\gamma_{\ell n}} \tag{4.96}$$

Fig. 4.4 shows a graphical solution of eqn. (4.96) in the special case when $V = 200$ MeV, $d = 2$ fm and $a = 10$ fm.

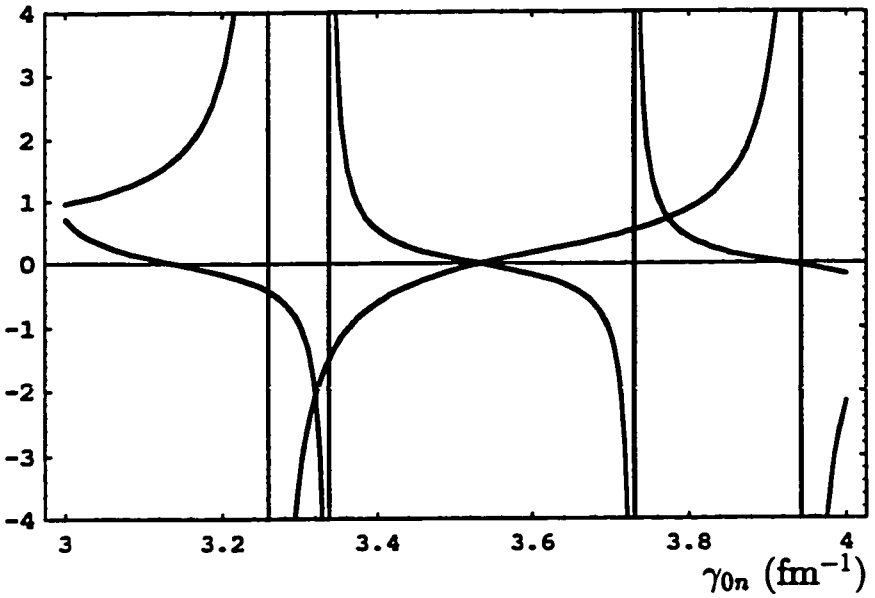

Fig. 4.3 : Graphical solution of the transcendental equation (4.92) for $V = -200$ MeV, $d = 2$ fm, $a = 10$ fm, and $E_{0n} > V$. The energies at which the intersections of the RHS of eqn. (4.92) with the LHS occur, represents the discrete perturbed energy states.

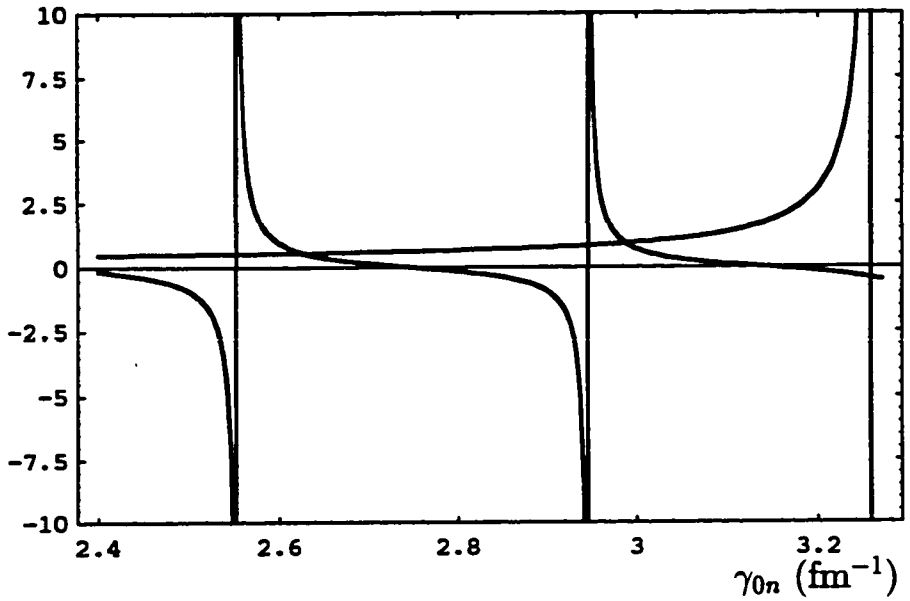

Fig. 4.4 : Graphical solution of the transcendental equation (4.92) for $V = -200$ MeV, $d = 2$ fm, $a = 10$ fm, and $E_{0n} < V$. The energies at which the intersections of the RHS of eqn. (4.92) with the LHS occur, represents the discrete perturbed energy states.

Example 4.8 : Let $\ell = 1$.

In this case, eqn. (4.85) becomes

$$\frac{d\left(\frac{\sin(K_{1n}d)}{(K_{1n}d)^2} - \frac{\cos(K_{1n}d)}{K_{1n}d}\right)}{\left\{d\left(\frac{\sin(K_{1n}d)}{(K_{1n}d)^2} - \frac{\cos(K_{1n}d)}{K_{1n}d}\right)\right\}'} = \frac{d\left(\frac{\sin(\gamma_{1n}d+\delta_{1n})}{(\gamma_{1n}d)^2} - \frac{\cos(\gamma_{1n}d+\delta_{1n})}{K_{1n}d}\right)}{\left\{d\left(\frac{\sin(\gamma_{1n}d+\delta_{1n})}{(\gamma_{1n}d)^2} - \frac{\cos(\gamma_{1n}d+\delta_{1n})}{\gamma_{1n}d}\right)\right\}'},$$

which can be simpified to

$$\frac{\frac{\sin(K_{1n}d)}{K_{1n}d} - \cos(K_{1n}d)}{\left\{\frac{\sin(K_{1n}d)}{K_{1n}d} - \cos(K_{1n}d)\right\}'} = \frac{\frac{\sin(\gamma_{1n}d+\delta_{1n})}{\gamma_{1n}d} - \cos(\gamma_{1n}d+\delta_{1n})}{\left\{\frac{\sin(\gamma_{1n}d+\delta_{1n})}{\gamma_{1n}d} - \cos(\gamma_{1n}d+\delta_{1n})\right\}'}. \tag{4.97}$$

Eqn. (4.97) can be written as

$$\frac{\frac{\sin(K_{1n}d)}{K_{1n}d} - \cos(K_{1n}d)}{\frac{\cos(K_{1n}d)}{d} - \frac{\sin(K_{1n}d)}{K_{1n}d^2} + K_{1n}\sin(K_{1n}d)} = \frac{\frac{\sin(\gamma_{1n}d+\delta_{1n})}{\gamma_{1n}d} - \cos(\gamma_{1n}d+\delta_{1n})}{\frac{\cos(\gamma_{1n}d+\delta_{1n})}{d} - \frac{\sin(\gamma_{1n}d+\delta_{1n})}{\gamma_{1n}d^2} + \gamma_{1n}\sin(\gamma_{1n}d+\delta_{1n})}. \tag{4.98}$$

Inverting both sides of eqn. (4,98), one obtains

$$\frac{\frac{\cos(K_{1n}d)}{d} - \frac{\sin(K_{1n}d)}{K_{1n}d^2} + K_{1n}\sin(K_{1n}d)}{\frac{\sin(K_{1n}d)}{K_{1n}d} - \cos(K_{1n}d)} = \frac{\frac{\cos(\gamma_{1n}d+\delta_{1n})}{d} - \frac{\sin(\gamma_{1n}d+\delta_{1n})}{\gamma_{1n}d^2} + \gamma_{1n}\sin(\gamma_{1n}d+\delta_{1n})}{\frac{\sin(\gamma_{1n}d+\delta_{1n})}{\gamma_{1n}d} - \cos(\gamma_{1n}d+\delta_{1n})},$$

which can be simplified to

$$-\frac{1}{d} + \frac{K_{1n}\sin(K_{1n}d)}{\frac{\sin(K_{1n}d)}{K_{1n}d} - \cos(K_{1n}d)} = -\frac{1}{d} + \frac{\gamma_{1n}\sin(\gamma_{1n}d+\delta_{1n})}{\frac{\sin(\gamma_{1n}d+\delta_{1n})}{\gamma_{1n}d} - \cos(\gamma_{1n}d+\delta_{1n})}. \tag{4.99}$$

$$\Rightarrow \qquad \frac{K_{1n}\sin(K_{1n}d)}{\frac{\sin(K_{1n}d)}{K_{1n}d} - \cos(K_{1n}d)} = \frac{\gamma_{1n}\sin(\gamma_{1n}d+\delta_{1n})}{\frac{\sin(\gamma_{1n}d+\delta_{1n})}{\gamma_{1n}d} - \cos(\gamma_{1n}d+\delta_{1n})}. \tag{4.100}$$

Inverting both sides of eqn. (4.100), one gets

$$\frac{\frac{\sin(K_{1n}d)}{K_{1n}d} - \cos(K_{1n}d)}{K_{1n}\sin(K_{1n}d)} = \frac{\frac{\sin(\gamma_{1n}d+\delta_{1n})}{\gamma_{1n}d} - \cos(\gamma_{1n}d+\delta_{1n})}{\gamma_{1n}\sin(\gamma_{1n}d+\delta_{1n})}.$$

Thus

$$\frac{1}{\gamma_{1n}^2 d} - \frac{\cot(\gamma_{1n}d + \delta_{1n})}{\gamma_{1n}} = \frac{1}{K_{1n}^2 d} - \frac{\cot(K_{1n}d)}{K_{1n}}. \tag{4.101}$$

From eqn. (4.86), one obtains

$$\frac{\sin(\gamma_{1n}a + \delta_{1n})}{\gamma_{1n}a} - \cos(\gamma_{1n}a + \delta_{1n}) = 0. \tag{4.102}$$

$$\Rightarrow \qquad \tan(\gamma_{1n}a + \delta_{1n}) = \gamma_{1n}a.$$

Hence

$$\delta_{1n} = \tan^{-1}(\gamma_{1n}a) - \gamma_{1n}a. \tag{4.103}$$

Substituting eqn. (4.103) in eqn. (4.101), one gets

$$\frac{1}{\gamma_{1n}^2 d} - \frac{\cot(\gamma_{1n}(d-a) + \tan^{-1}(\gamma_{1n}a))}{\gamma_{1n}} = \frac{1}{K_{1n}^2 d} - \frac{\cot(K_{1n}d)}{K_{1n}}. \tag{4.104}$$

Similarly one can solve the transcendental equation, eqn. (4.104), numerically or graphically to obtain the discrete energy levels for the four different cases discussed in example 4.7. Fig. 4.5 shows the positive energy levels graphically in the special case when $V = -200$ MeV, $d = 2$ fm and $a = 10$ fm. These arise when the curves corresponding to the left and right sides of eqn. (4.104) intersect. The phase shifts can be obtained by substituting the corresponding energy levels in eqn. (4.103).

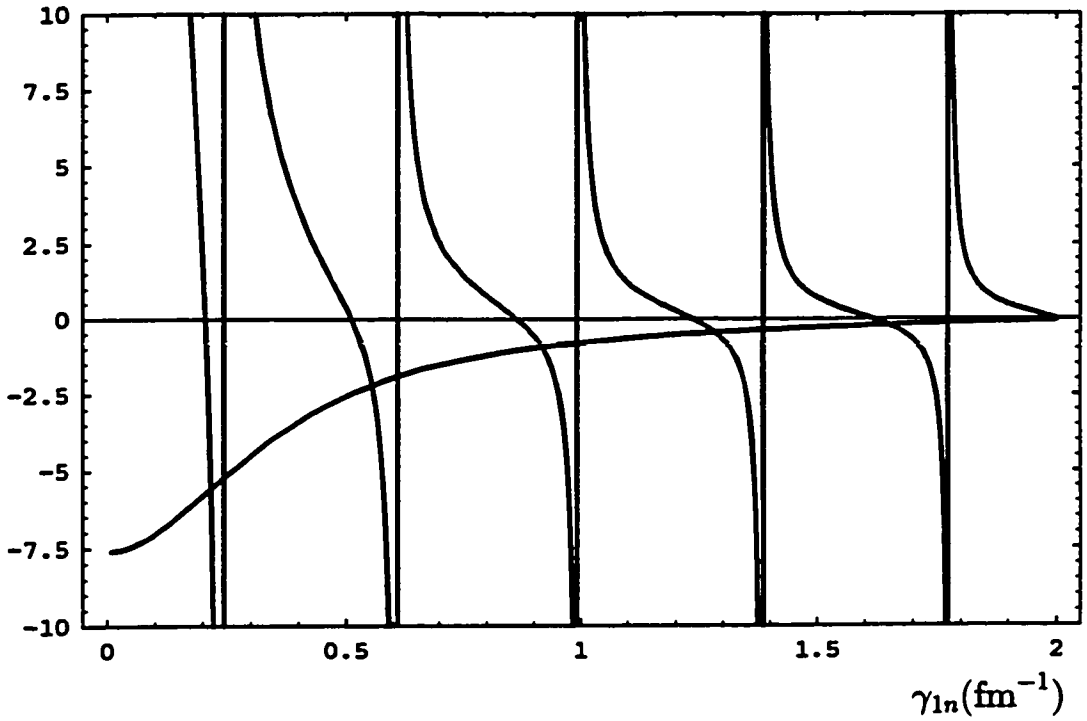

Fig. 4.5 : Graphical solution of the transcendental equation (4.104) for $V = -200$ MeV, $d = 2$ fm, $a = 10$ fm, and $E_{0n} > 0$. The energies at which the intersections of the RHS of eqn. (4.104) with the LHS occur, represents the discrete perturbed energy states.

Comparing examples 4.3 and 4.4 with examples 4.7 and 4.8, one can see the usefulness of the phase-shifted spherical Bessel function in simplifying the calculations.

CHAPTER 5

Numerical Calculations In The Finite Space Direct Scattering Problem

In order to understand the direct problem and the dependence of the energy states on the different parameters of the direct problem, such as the dimension of the space and the depth of the potential, some numerical calculations are performed.

Several aspects of this direct problem can be studied numerically for a particular scattering potential, namely the square well (or barrier) potential, such as :

- Comparison between the bounded energy states in the finite space and those produced in an infinite space.
- The relation between the dimension of the space and the number of states to a certain energy.

- Comparison between the phase shifts produced in the finite space and those produced in an infinite space.

5.1 The Truncation Integer m

In the previous chapter we mentioned that the discrete energies of a particle of mass μ confined within a three-dimensional sphere of radius a can be obtained by solving eqn. (4.13), namely

$$\sum_{q=1}^{q=\infty} b_{\ell nq}(\hat{H}_{pq} - \delta_{pq}E_\ell) = 0,$$

where

$$\hat{H}_{pq} = \hat{H}_{qp} = N_{\ell p}N_{\ell q}\int_0^a r j_\ell(k_{\ell p}r)\left(-\frac{\hbar^2}{2\mu}\frac{d^2}{dr^2} + \frac{\hbar^2\ell(\ell+1)}{2\mu r^2} + V_\ell(r)\right) r j_\ell(k_{\ell q}r)dr,$$

and if there exists an integer m such that for any $q > m$

$$\left|\hat{H}_{pq}\right| \ll \left|\hat{H}_{pm}\right|,$$

then the infinite sum in eqn. (4.13) can be approximated by the finite sum

$$\sum_{q=1}^{q=m} b_{\ell nq}(\hat{H}_{pq} - \delta_{pq}E_\ell) = 0. \tag{5.1}$$

The eigenvalues are then obtained by solving the following secular equation which is of order m in E_ℓ

$$\left|\hat{H}_{pq} - \delta_{pq}E_\ell\right| = 0. \tag{5.2}$$

We designate this integer, m, as the truncation integer because the infinite sum is truncated at m. But what is the magnitude of this m? and will this value of m be affected by the different parameters of the direct problem; namely the dimension of the space a and the depth V (or height) of the square well (or barrier) potential $V_\ell(r)$?

It is very important to answer these questions not only to get precise values for the energy states without summing up to infinity, but also to keep the discrete energies of the particle in the non-relativistic regime, because the concept of potentials is, in general, an approximation, valid only for non-relativistic particles. Thus one expects it to be valid only for particles bound in nuclei or moving with non-relativistic kinetic energies [47]. For nucleons moving with high energies, around 300 MeV, some form of relativistic corrections are necessary. Furthermore, to invert the finite-space partial-wave Born approximation, eqn. (0.2), using the techniques discussed in chapter 6, one should consider experimental phase shifts in the non-relativistic regime. Therefore, the summation in eqn. (5.1) should be truncated, i.e. m should be chosen, before the relativistic regime.

Thus, two factors should be considered in choosing m:

1) The energy states should be as accurate as possible.

2) The energies of the confined particle should be in the non-relativistic regime so that this formalism will be valid physically.

The first factor is studied in this chapter while it is convenient to study the second one in chapter 7. To illustrate the effect of the first factor in choosing m, let us consider the following numerical example.

Example 5.1 :

Consider a particle of mass $\mu = 1000$ MeV, confined in a sphere of radius a, and scattered from a square well (or barrier) potential of depth (or height) V and range $d = 2$ fm, in the angular momentum channel $\ell = 0$. In this case, the matrix elements of the Hamiltonian $\hat{H}_{pq}$ are given by[1]

$$\hat{H}_{pq} = \begin{cases} \frac{\hbar^2}{2\mu}\left(\frac{q\pi}{a}\right)^2 + \frac{Vd}{a} - \left(\frac{V}{2\pi q}\right)\sin\left(\frac{2\pi q d}{a}\right) & \text{if} \quad p = q \\ \frac{V}{\pi}\left\{\frac{\sin\left(\frac{(p-q)\pi d}{a}\right)}{(p-q)} - \frac{\sin\left(\frac{(p-q)\pi d}{a}\right)}{(p+q)}\right\} & \text{if} \quad p \neq q. \end{cases} \tag{5.3}$$

Let us now consider the effect of varying the different parameters of the direct problem on the precision of the calculated values of energies.

5.1.1 V-Dependence

We mean by V-dependence, the dependence of the truncation integer m on the depth (or height), V, of the square potential. In order to study the V-dependence one should fix the dimension of the space and vary the other parameters; namely

[1] We have shown this result in example 4.1.

the strength of the potential and the truncation integer.

A FORTRAN-77 program was used to solve the secular equation, eqn. (5.2), with $\hat{H}_{pq}$ given by eqn. (5.3). The potential range, d, in these calculations is 2.00 fm and the dimension of the space, a, is 10.00 fm, while the potential strength is variable. Energies of the first few states for different values of m and V are given in tables 5.1 through 5.8. The exact (non-relativistic) values of the energy states in these tables were found using the second approach of the direct problem, the numerical method[2].

[2]Using *Mathematica*.

Table 5.1: Energies (in MeV) of the first few states for different values of m using eqn. (5.2). The potential $V_\ell(r)$ is a square well potential of depth $V = -10$ MeV and the dimension of the space is $a = 10$ fm.

m	10	25	50	100	150	200	Exact
E_1	1.057	1.054	1.054	1.054	1.054	1.054	1.054
E_2	5.965	5.962	5.962	5.962	5.962	5.962	5.962
E_3	15.502	15.500	15.500	15.500	15.500	15.500	15.500
E_4	29.488	29.487	29.487	29.487	29.487	29.487	29.487
E_5	47.564	47.563	47.563	47.563	47.563	47.563	47.563
$\vdots$							
E_{10}	195.549	195.451	195.451	195.451	195.451	195.451	195.451

Table 5.2: Energies (in MeV) of the first few states for different values of m using eqn. (5.2). The potential $V_\ell(r)$ is a square well potential of depth $V = -40$ MeV and the dimension of the space is $a = 10$ fm.

m	10	25	50	100	150	200	Exact
$E^{(1)}_{\text{bind}}$	−14.980	−15.082	−15.087	−15.088	−15.088	−15.088	−15.088
E_2	3.196	3.195	3.195	3.195	3.195	3.195	3.195
E_3	12.172	12.169	12.169	12.169	12.169	12.169	12.169
E_4	25.904	25.896	25.895	25.895	25.895	25.895	25.895
E_5	43.435	43.400	43.399	43.398	43.398	43.398	43.398
$\vdots$							
E_{10}	191.472	190.191	190.190	190.190	190.190	190.190	190.190

Table 5.3: Energies (in MeV) of the first few states for different values of m using eqn. (5.2). The potential $V_\ell(r)$ is a square well potential of depth $V = -100$ MeV and the dimension of the space is $a = 10$ fm.

m	10	25	50	100	150	200	Exact
$E^{(1)}_{\text{bind}}$	−67.317	−67.764	−67.787	−67.790	−67.790	−67.790	−67.790
E_2	2.135	2.003	1.997	1.996	1.996	1.996	1.996
E_3	8.193	7.742	7.725	7.723	7.723	7.723	7.723
E_4	18.288	17.645	17.627	17.625	17.624	17.624	17.624
E_5	33.447	32.760	32.748	32.747	32.748	32.748	32.747
⋮							
E_{10}	186.799	180.183	180.163	180.161	180.161	180.161	180.161

Table 5.4: Energies (in MeV) of the first few states for different values of m using eqn. (5.2). The potential $V_\ell(r)$ is a square well potential of depth $V = -200$ MeV and the dimension of the space is $a = 10$ fm.

N	10	25	50	100	150	200	Exact
$E^{(1)}_{\text{bind}}$	−162.409	−163.473	−163.530	−163.537	−163.538	−163.538	−163.538
$E^{(2)}_{\text{bind}}$	−48.198	−59.732	−59.949	−59.975	−59.977	−59.978	−59.978
E_3	3.175	3.063	3.063	3.063	3.063	3.063	3.063
E_4	12.572	12.119	12.118	12.118	12.118	12.118	12.118
E_5	27.901	26.798	26.794	26.794	26.794	26.794	26.794
⋮							
E_{10}	102.662	161.328	161.263	161.258	161.258	161.258	161.258

Table 5.5: Energies (in MeV) of the first few states for different values of m using eqn. (5.2). The potential $V_\ell(r)$ is a square well potential of depth $V = -350$ MeV and the dimension of the space is $a = 10$ fm.

N	10	25	50	100	150	200	Exact
$E^{(1)}_{\text{bind}}$	−308.824	−310.664	−310.776	−310.789	−310.791	−310.791	−310.791
$E^{(2)}_{\text{bind}}$	−161.446	−195.068	−195.547	−195.602	−195.607	−195.608	−195.609
$E^{(3)}_{\text{bind}}$	2.9629	−20.524	−21.455	−21.548	−21.557	−21.559	−21.5611
E_4	11.807	3.415	3.402	3.402	3.401	3.401	3.401
E_5	26.401	13.314	13.287	13.285	13.285	13.285	13.285
⋮							
E_{10}	179.032	146.868	146.806	146.801	146.801	146.801	146.801

Table 5.6: Energies (in MeV) of the first few states for different values of m using eqn. (5.2). The potential $V_\ell(r)$ is a square barrier potential of height $V = +10$ MeV and the dimension of the space is $a = 10$ fm.

m	10	25	50	100	150	200	Exact
E_1	2.294	2.294	2.294	2.294	2.294	2.294	2.294
E_2	9.050	9.048	9.048	9.048	9.048	9.048	9.048
E_3	19.863	19.860	19.860	19.860	19.860	19.860	19.860
E_4	34.126	34.124	34.123	34.123	34.123	34.123	34.123
E_5	51.610	51.608	51.608	51.608	51.608	51.608	51.608
⋮							
E_{10}	199.569	199.454	199.454	199.454	199.454	199.454	199.454

Table 5.7: Energies (in MeV) of the first few states for different values of m using eqn. (5.2). The potential $V_\ell(r)$ is a square barrier potential of height $V = +100$ MeV and the dimension of the space is $a = 10$ fm.

m	10	25	50	100	150	200	Exact
E_1	2.772	2.766	2.765	2.765	2.765	2.765	2.765
E_2	11.070	11.046	11.043	11.043	11.043	11.043	11.043
E_3	24.841	24.782	24.777	24.776	24.776	24.776	24.776
E_4	43.961	43.842	43.939	43.838	43.837	43.837	43.837
E_5	68.157	67.957	67.944	67.942	67.942	67.942	67.942
$\vdots$							
E_{10}	239.894	220.446	220.424	220.422	220.422	220.422	220.422

Table 5.8: Energies (in MeV) of the first few states for different values of m using eqn. (5.2). The potential $V_\ell(r)$ is a square barrier potential of height $V = +350$ MeV and the dimension of the space is $a = 10$ fm.

m	10	25	50	100	150	200	Exact
E_1	2.932	2.910	2.908	2.908	2.908	2.908	2.908
E_2	11.727	11.636	11.629	11.628	11.628	11.628	11.628
E_3	26.388	26.171	26.154	26.152	26.151	26.151	26.151
E_4	46.922	46.498	46.467	46.463	46.463	46.462	46.462
E_5	73.349	72.592	72.544	72.537	72.536	72.536	72.536
$\vdots$							
E_{10}	438.429	286.889	286.656	286.629	286.626	286.625	286.625

From these tables, tables 5.1-5.8, one can observe the following:

1) Unbounded States:

For the unbounded states, the truncation number m is small **even for strong potentials.** For example, in the case of $V = +350$ MeV, table 5.8, the exact value of the fifth energy level, E_5, is 72.536 MeV while the value of the same energy level at $m = 25$ is 72.592 MeV with only 0.08 % percentage error. Table 5.9 shows the values of the fifth and the tenth energy levels for different strengths of the square potential. **For weak potentials,** $m = 10$ is sufficient to produce the exact values of the unbounded states, see tables 5.1 and 5.6.

Table 5.9: Comparison between the exact values of the fifth and the tenth energy levels and those found at $m = 25$ for $a = 10.0$ fm and for different potential strengths.

		Exact	Energy at $m = 25$	Percentage Error %
$V = -100$ MeV	E_5 MeV	32.747	32.760	0.04
	E_{10} MeV	180.161	180.183	0.01
$V = -350$ MeV	E_5 MeV	13.285	13.314	0.22
	E_{10} MeV	146.801	146.868	0.04
$V = 350$ MeV	E_5 MeV	72.536	72.592	0.08
	E_{10} MeV	286.625	286.889	0.09

2) Bounded States:

For the bounded states, the truncation number m is small **for weak potentials**, but for strong potentials the situation is a little bit different. **For strong potentials**, the first bounded energy level can be found exactly even for small values of m, while the other bounded states are obtained with a considerable percentage error if m is small, around $m = 25$. Table 5.10 shows this behavior clearly.

Table 5.10: Comparison between the values of the exact bounded states and those found at $m = 25$ for $a = 10.0$ fm and for different potential depths.

		Exact	Energy at $m = 25$	Percentage Error %
$V = -100$ MeV	$E_{\text{bind}}^{(1)}$	-67.790	-67.764	0.04
$V = -200$ MeV	$E_{\text{bind}}^{(1)}$	-163.538	-163.473	0.04
	$E_{\text{bind}}^{(2)}$	-59.978	-59.732	0.41
$V = -350$ MeV	$E_{\text{bind}}^{(1)}$	-310.791	-310.664	0.04
	$E_{\text{bind}}^{(2)}$	-195.609	-195.068	0.28
	$E_{\text{bind}}^{(3)}$	-21.561	-20.524	5.04

5.1.2 a-Dependence

We mean by a-dependence, the dependence of the truncation integer m on a, the dimension of the space. In order to study this dependence one should fix the strength of the potential. To illustrate this dependence, let us consider a particle of mass 1000 MeV, scattered from a square well potential of depth $V = -100$ MeV and range $d = 2.00$ fm, confined in a sphere of radius a in the angular momentum channel $\ell = 0$. The secular equation, eqn. (5.2), was solved using a FORTRAN-77 program with $\hat{H}_{pq}$ given by eqn. (5.3). Energies of the first few states for different values of m and a are given in tables 5.1 through 5.8. The exact values of the energy states in these tables were found using the second approach of the direct problem, the numerical method[3].

[3]Using *Mathematica*.

Table 5.11: Energies (in MeV) of the first few states for different values of m using eqn. (5.2). The potential $V_\ell(r)$ is a square well potential of depth $V = -100$ MeV and the dimension of the space is $a = 20$ fm.

m	10	25	50	100	150	200	Exact
E_{bind}	−57.255	−67.604	−67.763	−67.787	−67.790	−67.790	−67.790
E_2	0.590	0.510	0.502	0.501	0.501	0.501	0.501
E_3	2.357	2.021	1.989	1.986	1.985	1.985	1.985
E_4	5.290	4.496	4.428	4.422	4.421	4.421	4.421
E_5	9.373	7.916	7.818	7.809	7.808	7.808	7.808
⋮							
E_{10}	46.590	41.150	41.097	41.092	41.092	41.092	41.092

Table 5.12: Energies (in MeV) of the first few states for different values of m using eqn. (5.2). The potential $V_\ell(r)$ is a square well potential of depth $V = -100$ MeV and the dimension of the space is $a = 30$ fm.

m	10	25	50	100	150	200	Exact
E_{bind}	−31.274	−67.105	−67.710	−67.778	−67.787	−67.789	−67.789
E_2	0.255	0.236	0.222	0.222	0.222	0.222	0.222
E_3	1.019	0.944	0.888	0.885	0.334	0.884	0.884
E_4	2.290	2.120	1.989	1.982	1.982	1.982	1.982
E_5	4.068	3.760	3.520	3.507	3.506	3.506	3.506
⋮							
E_{10}	20.609	18.709	17.743	17.723	17.720	17.720	17.720

Table 5.13: Energies (in MeV) of the first few states for different values of m using eqn. (5.2). The potential $V_\ell(r)$ is a square well potential of depth $V = -100$ MeV and the dimension of the space is $a = 40$ fm.

m	10	25	50	100	150	200	Exact
E_{bind}	−16.005	−64.593	−67.601	−67.762	−67.782	−67.787	−67.787
E_2	0.142	0.133	0.126	0.124	0.124	0.124	0.124
E_3	0.567	0.533	0.502	0.497	0.497	0.497	0.497
E_4	1.276	1.200	1.126	1.117	1.116	1.116	1.116
E_5	2.266	2.132	1.998	1.981	1.980	1.980	1.980
⋮							
E_{10}	11.536	10.749	9.992	9.940	9.936	9.935	9.935

Table 5.14: Energies (in MeV) of the first few states for different values of m using eqn. (5.2). The potential $V_\ell(r)$ is a square well potential of depth $V = -100$ MeV and the dimension of the space is $a = 50$ fm.

m	10	25	50	100	150	200	Exact
E_{bind}	−8.628	−55.635	−67.230	−67.732	−67.774	−67.784	−67.784
E_2	0.091	0.085	0.081	0.080	0.080	0.080	0.080
E_3	0.362	0.339	0.323	0.318	0.318	0.318	0.318
E_4	0.814	0.763	0.727	0.715	0.715	0.714	0.714
E_5	1.447	1.356	1.291	1.270	1.269	1.268	1.268
⋮							
E_{10}	7.369	6.851	6.488	6.380	6.374	6.372	6.372

From these tables, tables 5.11-5.14, one can observe the following:

1) Unbounded States:

As the size of the space increases, one needs to go to higher values of m in order to obtain exact values for a certain energy level of the particle. Consider for example, the fifth and the tenth energy levels. The exact energies of these states for $a = 20.00$ fm, see table 5.11, are 7.808 MeV and 41.092 MeV respectively while the calculated ones for $m = 50$ are 7.818 MeV for the fifth energy state with 0.13 % percentage error and 41.097 MeV for the tenth energy state with 0.01 % percentage error. For $m = 100$ the accuracy of the calculated energies are much better, where the calculated values of the fifth and the tenth energy states are 7.809 MeV with 0.01 % percentage error and 41.092 MeV which is the exact value of the tenth energy state.

For $a = 50.00$ fm, the exact values of the fifth and the tenth energy levels, see table 5.11, are 1.268 MeV and 6.372 MeV respectively while the calculated ones for $m = 50$ are 1.292 MeV for the fifth energy state with 1.81 % percentage error and 6.488 MeV for the tenth energy state with 1.82 % percentage error.
For $m = 100$ the accuracy of the calculated energies are much better, where the calculated values of the fifth and the tenth energy states are 1.270 MeV with 0.16 % percentage error and 6.380 MeV with 0.12 % percentage error. Certainly, the errors in the calculated energy levels for a= 50.00 fm are much higher than those for a =

20.00 fm. Table 5.15 shows clearly that as the size of the space increases, the error in obtaining the energy level for a specific state and for a fixed value of m increases.

2) Bounded States:

The one bounded state of the square well potential of depth $V = -100$ MeV shows the same behaviour as the unbounded states, see table 5.16, namely; the error in obtaining the bounded state increases as the dimension of the space increases for certain value of m, but the error in obtaining the value of the bounded state is greater than that of the unbounded states. In order to get an accurate value for the bounded state, one should increase the value of m. For example, the calculated value of the bounded state for $a = 30$ fm and $m = 50$ is -67.710 MeV with 0.12 % percentage error while the percentage error in obtaining the value of the bounded state is 0.02 % for $m = 100$ and $a = 30$ fm.

3) Number of States:

As the dimension of the space increases, the number of energy states up to a certain energy level increases. For example, for $a = 10$ fm, there are only 4 energy states up to 17.624 MeV, see table 5.3, but for $a = 30$ fm, there are 10 states up to 17.720 MeV, table 5.12, while for $a = 50$ fm, there are 16 states up to 17.739 MeV, table 5.14. Recall that one cannot compare the above three cases at a specific energy because of the discreteness of the energy levels.

Table 5.15: Comparison between the exact value of the fifth energy state (in MeV) and those found at $m = 50$ for different values of a, the size of the space. The potential $V_\ell(r)$ is a square well potential of depth $V = -100$ MeV.

		Exact	Energy at $m = 50$	Percentage Error %
$a = 10$ fm	E_5 MeV	32.747	32.748	0.003
	E_{10} MeV	180.161	180.163	0.001
$a = 20$ fm	E_5 MeV	7.808	7.818	0.13
	E_{10} MeV	41.092	41.097	0.01
$a = 30$ fm	E_5 MeV	3.605	3.520	0.40
	E_{10} MeV	17.720	17.743	0.13
$a = 40$ fm	E_5 MeV	1.980	1.998	0.91
	E_{10} MeV	9.935	9.992	0.57
$a = 50$ fm	E_5 MeV	1.268	1.291	1.81
	E_{10} MeV	6.372	6.488	1.82

Table 5.16: Comparison between the exact value of the bounded state (in MeV) and those found at $m = 50$ for different values of a, the dimension of the space. The potential $V_\ell(r)$ is a square well potential of depth $V = -100$ MeV.

		Exact	Energy at $m = 50$	Percentage Error %
$a = 10$ fm	E_{bind} MeV	−67.790	−67.787	0.003
$a = 20$ fm	E_{bind} MeV	−67.790	−67.763	0.04
$a = 30$ fm	E_{bind} MeV	−67.790	−67.710	0.12
$a = 40$ fm	E_{bind} MeV	−67.790	−67.601	0.28
$a = 50$ fm	E_{bind} MeV	−67.790	−67.230	0.83

5.2 Phase Shifts In Finite and Infinite Spaces

The finite space phase shift at a certain energy does not differ from that in the infinite space at the same energy, because the phase shift is a measurable quantity which does not depend on the size of the space; infinite or finite. Let us consider the following example to illustrate this fact.

Example 5.2 :

Consider a particle of mass $\mu = 1000$ MeV, confined in a sphere of radius $a = 30$ fm, and scattered from a square well potential of depth $V = -10$ MeV and range $d = 2$ fm, in the angular momentum channel ℓ.

Let us study the following cases :

Case I : Let $\ell = 0$. In this case, the matrix elements of the Hamiltonian are given by eqn. (5.3) and the finite space phase shift, $\delta_{0n}(\gamma_{0n})$, is given by eqn. (4.62), namely

$$\delta_{0n}(\gamma_{0n}) = n\pi - \gamma_{0n}a, \qquad n = 1,2,3,\ldots,m,$$

while the infinite space phase shift, $\delta_0(k)$, is given by

$$\delta_0(k) = \tan^{-1}\left\{\frac{k\tan(Kd)}{K}\right\} - kd, \tag{5.4}$$

where

$$K^2 = \frac{2\mu}{\hbar^2}(E + |V|).$$

Fig. 5.1 shows the infinite space phase shifts and fig. 5.2 shows the finite space phase shifts which were obtained by solving eqn. (5.2) for $m = 50$. From fig. 5.3, one can see clearly that the finite space phase shift at a certain energy is exactly the same as the infinite phase shift at that energy.

Case II : Let $\ell = 1$. The finite space phase shift, $\delta_{1n}(\gamma_{1n})$, is given by eqn. (4.63), namely

$$\delta_1(\gamma_{1n}) = \tan^{-1}(\gamma_{1n}a) - \gamma_{1n}a,$$

while the infinite space phase shift, $\delta_1(k)$, is given by

$$\delta_1(k) = \tan^{-1}\left[\frac{K^2kd}{K^2 - k^2 + k^2Kd\cot(Kd)}\right] - kd \tag{5.5}$$

Fig. 5.4 shows the infinite space phase shifts while fig. 5.5 compares the infinite space phase shifts with the finite space phase shifts which were obtained by solving eqn. (5.2) for $m = 50$. One can see clearly from fig. 5.5 that for a certain energy, the phase shift in the finite space is exactly the same as that in the infinite space.

Case III : Let $\ell = 2$. The finite space phase shift, $\delta_{2n}(\gamma_{2n})$, is given by eqn. (4.64), namely

$$\delta_2(\gamma_{2n}) = \tan^{-1}\left\{\frac{3\gamma_{2n}a}{3 - (\gamma_{2n}a)^2}\right\} - \gamma_{2n}a,$$

while the infinite space phase shift, $\delta_2(k)$, is given by

$$\delta(k) = \tan^{-1}\frac{(k^3d^3 - 6kd)\phi - 3kd^2\lambda}{(3k^2d^2 - 6)\phi + (k^2d^3 - 3d)\lambda} - kd, \tag{5.6}$$

where

$$\lambda \equiv -6Kd + K^3d^3 + 6\tan Kd - 3K^2d^2\tan Kd$$

$$\phi \equiv 3Kd^2 + \tan(Kd)(K^2d^3 - 3d)$$

Fig. 5.6 shows the infinite space phase shifts while fig. 5.7 compares the infinite space phase shifts with the finite space phase shifts which were obtained by solving eqn. (5.2) for $m = 50$. One can see clearly from fig. 5.7 that for a certain energy, the phase shift in the finite space is exactly the same as that in the infinite space.

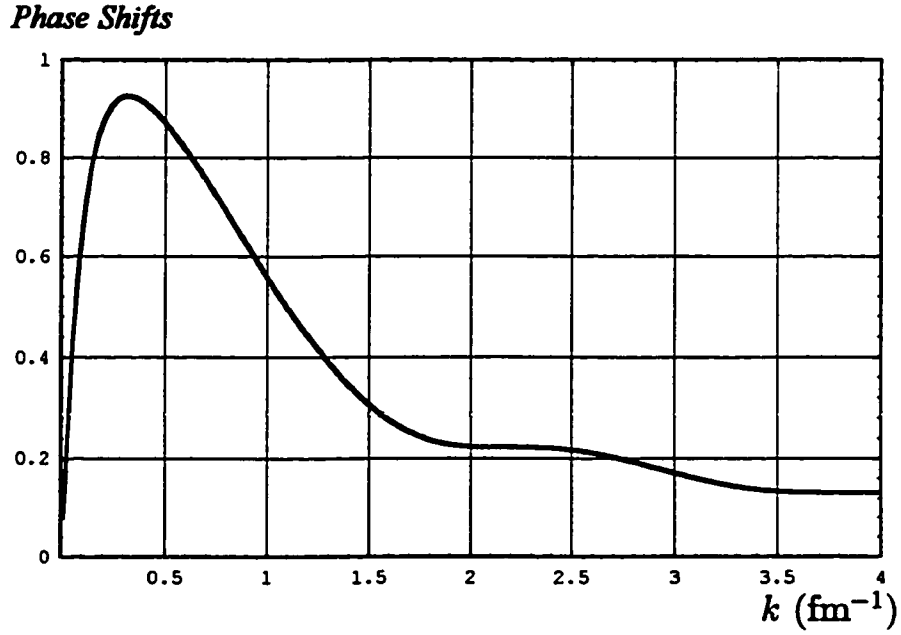

Fig. 5.1 : Phase shifts produced by a particle scattered from a square well potential of depth $V = -10$ MeV and range $d = 2$ fm in the angular momentum channel $\ell = 0$.

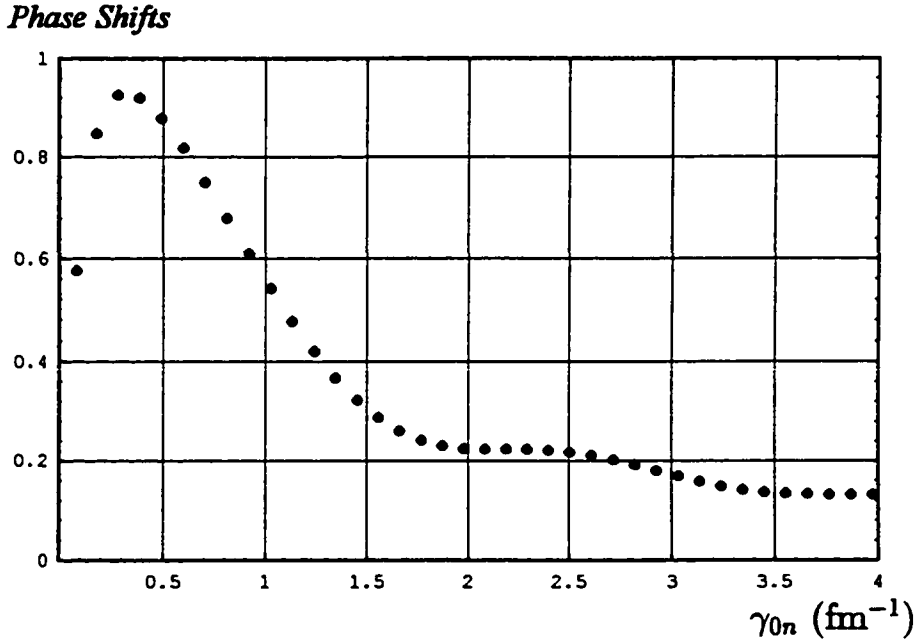

Fig. 5.2 : Discrete phase shifts produced by a particle scattered from a square well potential of depth $V = -10$ MeV and range $d = 2$ fm, in a sphere of radius $a = 30$ fm, in the angular momentum channel $\ell = 0$, using eqn. (5.2) for $m = 50$.

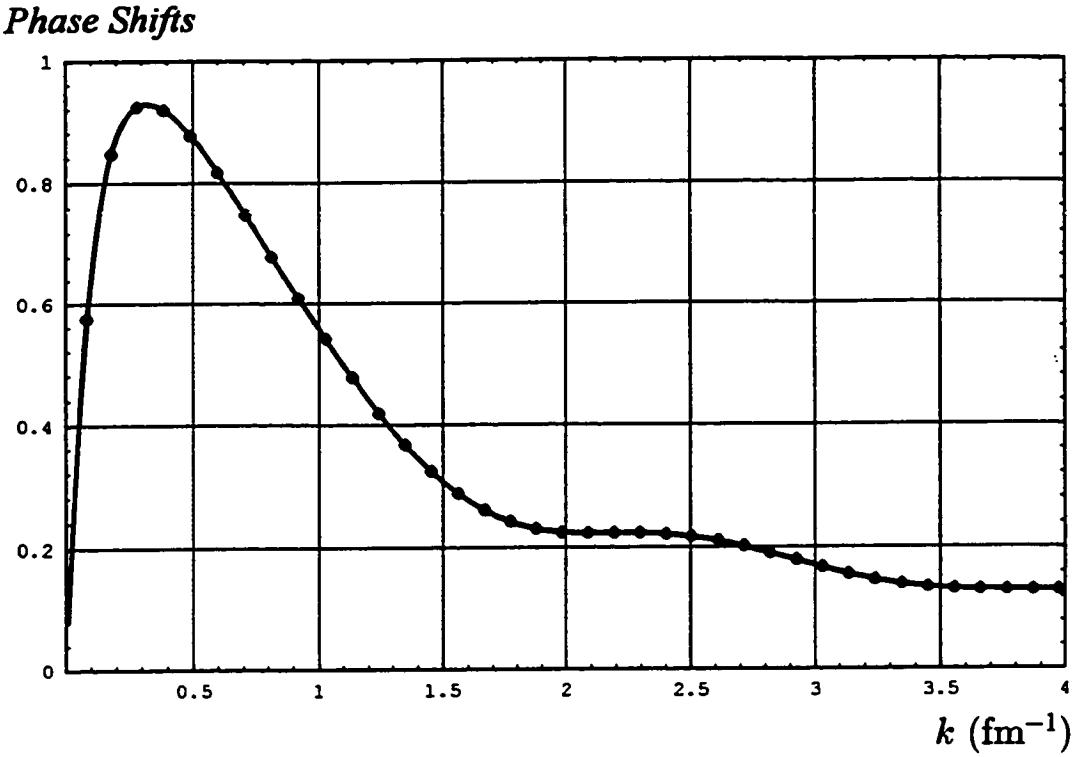

Fig. 5.3 : Comparison between the infinite space phase shifts in fig. 5.1 and the finite space phase shifts in fig. 5.2.

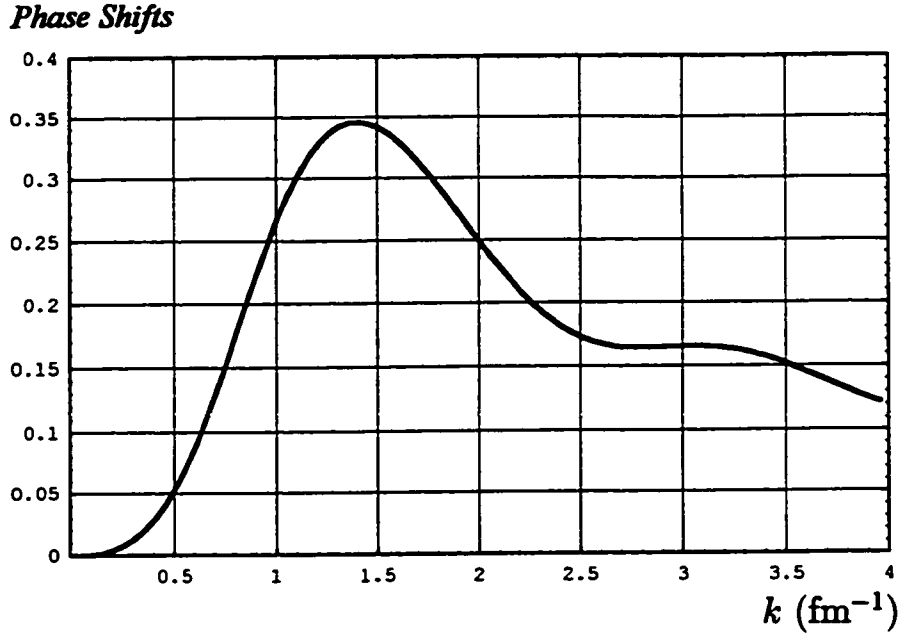

Fig. 5.4 : Phase shifts produced by a particle scattered from a square well potential of depth $V = -10$ MeV and range $d = 2$ fm in the angular momentum channel $\ell = 1$.

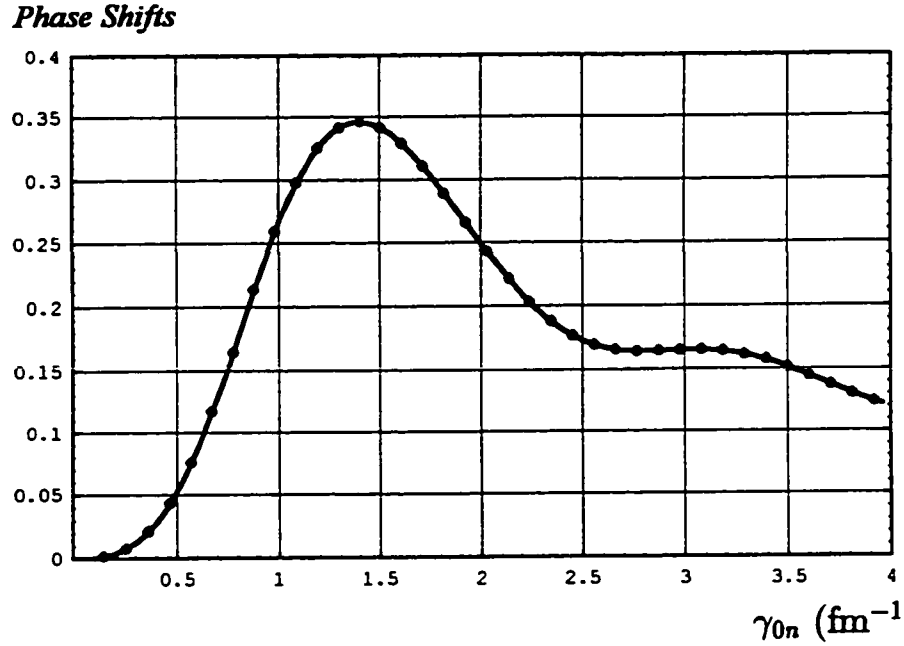

Fig. 5.5 : Comparison between the infinite space phase shifts and the finite space phase shifts produced by a particle scattered from a square well potential of depth $V = -10$ MeV and range $d = 2$ fm, in a sphere of radius $a = 30$ fm, in the angular momentum channel $\ell = 1$, using eqn. (5.2) for $m = 50$.

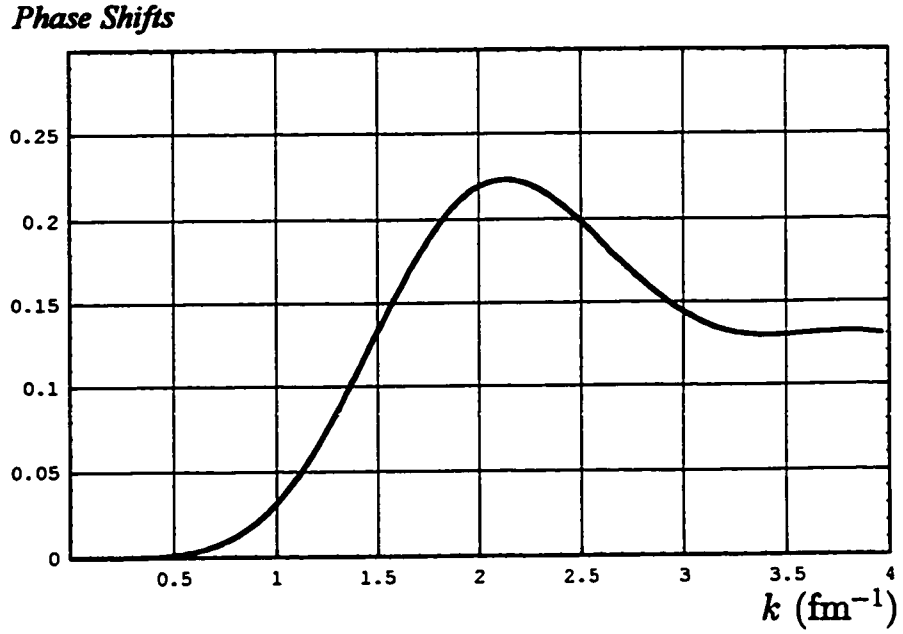

Fig. 5.6 : Phase shifts produced by a particle scattered from a square well potential of depth $V = -10$ MeV and range $d = 2$ fm in the angular momentum channel $\ell = 2$.

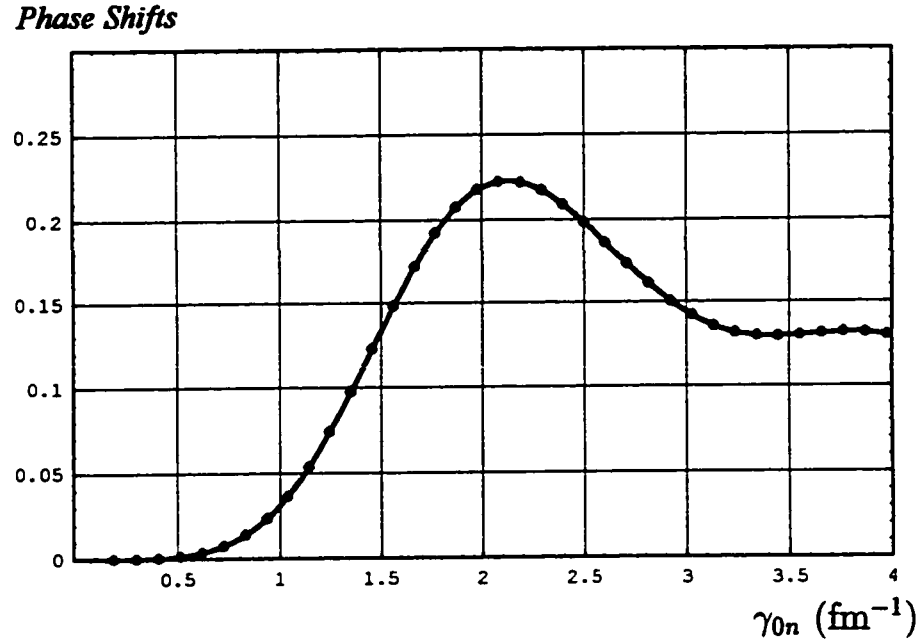

Fig. 5.7 : Comparison between the infinite space phase shifts and the finite space phase shifts produced by a particle scattered from a square well potential of depth $V = -10$ MeV and range $d = 2$ fm, in a sphere of radius $a = 30$ fm, in the angular momentum channel $\ell = 2$, using eqn. (5.2) for $m = 50$.

CHAPTER 6

Finite Space Inverse Scattering Problem

The finite space inverse scattering problem of a moving nucleon with initial relative speed v scattered by a stationary nucleon can be studied by considering a particle of mass μ confined within a three-dimensional sphere of radius a and scattered off a finite potential $V_\ell(r)$ located near the origin of the sphere.

6.1 Finite-Space Partial-Wave Born Approximation

The radial wave function of the scattered particle satisfies the following Shrödinger equation

$$\left[\frac{d^2}{dr^2} - \frac{\ell(\ell+1)}{r^2} - \frac{2\mu}{\hbar^2}V_\ell(r) + \gamma_{\ell n}^2\right] u_{\ell n}(r) = 0, \tag{6.1}$$

where $\gamma_{\ell n}^2$ are discrete and given by

$$\gamma_{\ell n}^2 = \frac{2\mu E_{\ell n}}{\hbar^2}.$$

If $V_\ell(r) = 0$, then

$$\left[\frac{d^2}{dr^2} - \frac{\ell(\ell+1)}{r^2} + k_{\ell r}^2\right] u_{\ell n}(r) = 0. \tag{6.2}$$

The solution of eqn. (6.2) is

$$u_{\ell n}(r) = r j_\ell(k_{\ell n} r). \tag{6.3}$$

Substituting eqn. (6.3) in eqn. (6.2), one obtains

$$\left[\frac{d^2}{dr^2} - \frac{\ell(\ell+1)}{r^2} + k_{\ell n}^2\right] (r j_\ell(k_{\ell n} r)) = 0. \tag{6.4}$$

Premultiplying eqn. (6.1) by $r j_\ell(k_{\ell n} r)$ and eqn. (6.4) by $u_{\ell n}(r)$, then subtracting, one obtains

$$r j_\ell(k_{\ell n} r)\frac{d^2 u_{\ell n}}{dr^2} - u_{\ell n}(r)\frac{d^2}{dr^2}(r j_\ell(k_{\ell n} r)) + \left(\gamma_{\ell n}^2 - k_{\ell n}^2\right)(r j_\ell(k_{\ell n} r))\, u_{\ell n}(r) -$$

$$r j_\ell(k_{\ell n} r) \cdot \frac{2\mu}{\hbar^2} V_\ell(r) u_{\ell n}(r) = 0,$$

which can be put in another form as

$$\frac{d}{dr}\left\{r j_\ell(k_{\ell n} r)\frac{d}{dr}(u_{\ell n}(r)) - u_{\ell n}(r)\frac{d}{dr}(r j_\ell(k_{\ell n} r))\right\}$$

$$= \left(k_{\ell n}^2 - \gamma_{\ell n}^2\right) r\, j_\ell(k_{\ell n} r)\, u_{\ell n}(r) + \left(\frac{2\mu}{\hbar^2}\right) r\, j_\ell(k_{\ell n} r)\, V_\ell(r)\, u_{\ell n}(r). \tag{6.5}$$

Multiplying both sides of eqn. (6.5) by the normalization constant, $N_{\ell n}$, one gets

$$\frac{d}{dr}\left\{N_{\ell n} r j_\ell(k_{\ell n} r)\frac{d}{dr}(u_{\ell n}(r)) - u_{\ell n}(r)\frac{d}{dr}(N_{\ell n} r j_\ell(k_{\ell n} r))\right\}$$

$$= \left(k_{\ell n}^2 - \gamma_{\ell n}^2\right) N_{\ell n} r\, j_\ell(k_{\ell n} r)\, u_{\ell n}(r) + \left(\frac{2\mu}{\hbar^2}\right) N_{\ell n} r\, j_\ell(k_{\ell n} r)\, V_\ell(r)\, u_{\ell n}(r). \tag{6.6}$$

Integrating both sides of eqn. (6.6) with respect to r from 0 to a, the dimension of the space, one gets

$$\left| N_{\ell n} r j_\ell(k_{\ell n} r) \frac{d}{dr}\left(u_{\ell n}(r)\right) - u_{\ell n}(r) \frac{d}{dr}\left(N_{\ell n} r j_\ell(k_{\ell n} r)\right) \right|_0^a$$

$$= \left(k_{\ell n}^2 - \gamma_{\ell n}^2\right) \int_0^a N_{\ell n} r\, j_\ell(k_{\ell n} r)\, u_{\ell n}(r)\, dr + \left(\frac{2\mu}{\hbar^2}\right) \int_0^a N_{\ell n} r\, j_\ell(k_{\ell n} r)\, V_\ell(r)\, u_{\ell n}(r)\, dr. \tag{6.7}$$

But from the finite space boundary conditions,

$$j_\ell(k_{\ell n} a) = u_{\ell n}(0) = u_{\ell n}(k_{\ell n} a) = 0.$$

Thus, the LHS of eqn. (6.7) vanishes.

The radial wave function, $u_{\ell n}(r)$, can be expanded in terms of the normalized spherical Bessel functions, i.e.

$$u_{\ell n}(r) = \sum_{m=1}^{\infty} b_{\ell n m} N_{\ell m} r j_\ell(k_{\ell m} r). \tag{6.8}$$

Substituting the expansion in eqn. (6.8) in the RHS of eqn. (6.7), one obtains

$$\left(k_{\ell n}^2 - \gamma_{\ell n}^2\right) \int_0^a N_{\ell n} r\, j_\ell(k_{\ell n} r) \sum_{m=1}^{\infty} b_{\ell n m} N_{\ell m} r j_\ell(k_{\ell m} r)\, dr + \left(\frac{2\mu}{\hbar^2}\right) \int_0^a N_{\ell n} r\, j_\ell(k_{\ell n} r) \times$$
$$V_\ell(r) \sum_{m=1}^{\infty} b_{\ell n m} N_{\ell m} r j_\ell(k_{\ell m} r)\, dr = 0. \tag{6.9}$$

Consider the 1st part of the LHS of eqn. (6.9)

$$\left(k_{\ell n}^2 - \gamma_{\ell n}^2\right) \int_0^a N_{\ell n} r j_\ell(k_{\ell n} r) \sum_{m=1}^{\infty} b_{\ell n m} N_{\ell m} r j_\ell(k_{\ell m} r) dr$$
$$= \left(k_{\ell n}^2 - \gamma_{\ell n}^2\right) \sum_{m=1}^{\infty} b_{\ell n m} N_{\ell n} N_{\ell m} \int_0^a j_\ell(k_{\ell n} r) j_\ell(k_{\ell m} r) r^2 dr. \tag{6.10}$$

Using the orthonormality relation of the spherical Bessel functions, namely

$$N_{\ell m} N_{\ell n} \int_0^a j_\ell(k_{\ell m} r) j_\ell(k_{\ell n} r) r^2 dr = \delta_{mn}, \tag{6.11}$$

eqn. (6.10) becomes

$$\begin{aligned}(k_{\ell n}^2 - \gamma_{\ell n}^2) \int_0^a N_{\ell n} r j_\ell(k_{\ell n} r) \sum_{m=1}^{\infty} b_{\ell n m} N_{\ell m} r j_\ell(k_{\ell m} r) dr &= \sum_{m=1}^{\infty} b_{\ell n m} \left(k_{\ell n}^2 - \gamma_{\ell n}^2\right) \delta_{nm} \\ &= b_{\ell n n} \left(k_{\ell n}^2 - \gamma_{\ell n}^2\right). \end{aligned} \tag{6.12}$$

For weak potentials, the radial wave function in the 2nd term of the LHS of eqn. (6.9) can be approximated by the free particle radial wave function, **Born Approximation**, i.e.

$$u_{\ell n}(r) = \sum_{m=1}^{\infty} b_{\ell n m} N_{\ell m} r j_\ell(k_{\ell m} r) \approx b_{\ell n n} N_{\ell n} r j_\ell(k_{\ell n} r). \tag{6.13}$$

Substituting eqn. (6.13) in the 2nd part of the LHS of eqn. (6.9), one obtains

$$\begin{aligned}&\frac{2\mu}{\hbar^2} \int_0^a N_{\ell n} r\, j_\ell(k_{\ell n} r)\, V_\ell(r) \sum_{m=1}^{\infty} b_{\ell n m} N_{\ell m} r j_\ell(k_{\ell m} r)\, dr \\ &\qquad \approx \frac{2\mu}{\hbar^2} \int_0^a N_{\ell n} r j_\ell(k_{\ell n} r) V_\ell(r) b_{\ell n n} N_{\ell n} r j_\ell(k_{\ell n} r) dr \\ &\qquad \approx b_{\ell n n} \frac{2\mu}{\hbar^2} \int_0^a \left(N_{\ell n} r j_\ell(k_{\ell n} r)\right)^2 V_\ell(r) dr. \end{aligned} \tag{6.14}$$

Substituting eqns. (6.12) and (6.14) in eqn. (6.9), one gets

$$\begin{aligned}\gamma_{\ell n}^2 - k_{\ell n}^2 &\approx \frac{2\mu}{\hbar^2} \int_0^a N_{\ell n}^2 r^2 j_\ell^2(k_{\ell n} r) V_\ell(r) dr \\ \frac{\hbar^2}{2\mu} \frac{\gamma_{\ell n}^2 - k_{\ell n}^2}{N_{\ell n}^2} &\approx \int_0^a r^2 j_\ell^2(k_{\ell n} r) V_\ell(r) dr, \end{aligned} \tag{6.15}$$

or

$$-\frac{\hbar^2}{2\mu}\frac{k_{\ell n}^2-\gamma_{\ell n}^2}{N_{\ell n}^2}\approx\int_0^a r^2 j_\ell^2(k_{\ell n}r)V_\ell(r)dr. \tag{6.16}$$

Eqn. (6.16) is **the counterpart of the partial wave Born approximation for finite spaces**, where for an infinite space,

$$-\frac{\hbar^2}{2\mu}\frac{\delta_l(k)}{k}\approx\int_0^\infty r^2 j_l^2(kr)V_l(r)dr. \tag{6.17}$$

Although the LHS of eqn. (6.16) does not depend on the phase shift, $\delta_{\ell n}$, explicitly, it does depend on it implicitly. Consider for example the LHS of eqn. (6.16) for $\ell = 0$. In this case, the LHS of eqn. (6.16) becomes

$$\begin{aligned}\text{LHS} &= \frac{\hbar^2}{2\mu}\frac{\gamma_{0n}^2-k_{0n}^2}{N_{0n}^2}\\ &= \frac{\hbar^2}{2\mu}\frac{(\gamma_{0n}-k_{0n})(\gamma_{0n}+k_{0n})}{N_{0n}^2}\end{aligned} \tag{6.18}$$

For $\ell = 0$, the phase shift is given[1] by

$$\delta_{0n} = n\pi - \gamma_{0n}a, \qquad n = 1,2,3,\ldots,m \tag{6.19}$$

Recall that

$$k_{0n} = \frac{n\pi}{a}.$$

Therefore, eqn. (6.19) can be written as

$$\delta_{0n} = k_{0n}a - \gamma_{0n}a, \qquad n = 1,2,3,\ldots,m,$$

[1]See eqn. (4.62)

or

$$\delta_{0n} = (k_{0n} - \gamma_{0n})\, a. \tag{6.20}$$

Hence

$$\frac{\delta_{0n}}{a} = k_{0n} - \gamma_{0n} \tag{6.21}$$

Adding and subtracting k_{0n} to the RHS of eqn. (6.20), one obtains

$$\begin{aligned} \delta_{0n} &= (k_{0n} + k_{0n} - k_{0n} - \gamma_{0n})\, a \\ &= \{2\, k_{0n} - (k_{0n} + \gamma_{0n})\}\, a. \end{aligned} \tag{6.22}$$

Thus,

$$k_{0n} + \gamma_{0n} = 2\, k_{0n} - \frac{\delta_{0n}}{a} \tag{6.23}$$

Substituting eqns. (6.21) and (6.23) in eqn. (6.18), one obtains

$$\frac{\hbar^2}{2\mu}\frac{\gamma_{0n}^2 - k_{0n}^2}{N_{0n}^2} = \frac{\hbar^2}{2\mu}\frac{\frac{\delta_{0n}}{a}\left(\frac{\delta_{0n}}{a} - 2\, k_{0n}\right)}{N_{0n}^2} \tag{6.24}$$

6.2 Finite Space $g_\ell(k_{\ell n} r)$ Approach

The finite-space partial-wave Born approximation, eqn. (6.15), can be inverted using the inverse function of $j_\ell^2(k_{\ell n} r)$, namely $g_\ell(k_{\ell n} r)$, which satisfies the following relation which we have derived and verified in chapter 1:

$$\sum_{n=0}^{\infty}\left(r^2 k_{\ell n}^2 j_\ell^2(k_{\ell n}) - \frac{1}{2}\right)\frac{g_\ell(k_{\ell n} r')}{k_{\ell n}^2 r'^2}\Delta k_{\ell n} = \delta(r - r'), \tag{6.25}$$

or equivalently

$$\frac{2\, k_{\ell 1}}{\pi(2\ell + 1)} + \sum_{n=1}^{\infty}\left(k_{\ell n}^2 r^2 j_\ell^2(k_{\ell n} r) - \frac{1}{2}\right)\frac{g_\ell(k_{\ell n} r')}{(k_{\ell n} r')^2}\Delta k_{\ell n} = \delta(r - r'), \tag{6.26}$$

where

$$\Delta k_{\ell n} = k_{\ell(n+1)} - k_{\ell n}.$$

Multiplying both sides of eqn. (6.15) by $k_{\ell n}^2$, one obtains

$$\frac{\hbar^2}{2\mu}\frac{\gamma_{\ell n}^2 - k_{\ell n}^2}{\aleph_{\ell n}^2} = \int_0^a r^2 k_{\ell n}^2 j_\ell^2(k_{\ell n} r)\, V_\ell(r)\, dr, \tag{6.27}$$

where

$$\aleph_{\ell n} \equiv \frac{N_{\ell n}}{k_{\ell n}}.$$

Consider eqn. (6.27) for large $k_{\ell n}$, i.e. for large n, then

$$\lim_{n\to\infty}\left\{\frac{\hbar^2}{2\mu}\frac{\gamma_{\ell n}^2 - k_{\ell n}^2}{\aleph_{\ell n}^2}\right\} \longrightarrow \int_0^a \lim_{n\to\infty}\left\{k_{\ell n}^2 r^2 j_\ell^2(k_{\ell n} r)\right\} V_\ell(r) dr.$$

But

$$\begin{aligned}
\lim_{n\to\infty}\left\{k_{\ell n}^2 r^2 j_\ell^2(k_{\ell n} r)\right\} &\longrightarrow \sin^2(k_{\ell n} r - \ell\pi/2) \\
&= \frac{1}{2} - \frac{1}{2}\cos\left[2k_{\ell n} r - \ell\pi\right] \\
&= \frac{1}{2} - \frac{1}{2}\left\{\cos(2k_{\ell n} r)\underbrace{\cos(\ell\pi)}_{(-1)^\ell} + \sin(2k_{\ell n} r)\underbrace{\sin(\ell\pi)}_{0}\right\} \\
&= \frac{1}{2} - \frac{1}{2}(-1)^\ell \cos(2k_{\ell n} r).
\end{aligned}$$

Thus

$$\lim_{n\to\infty}\left\{\frac{\hbar^2}{2\mu}\frac{\gamma_{\ell n}^2 - k_{\ell n}^2}{\aleph_{\ell n}^2}\right\} \longrightarrow \int_0^a \left(\frac{1}{2} - \frac{1}{2}(-1)^\ell \cos(2k_{\ell n} r)\right) V_\ell(r)\, dr. \tag{6.28}$$

The second term on the RHS of the above expression, eqn. (6.28), namely

$$\int_0^\infty \cos(2k_{\ell n}r)\, V_\ell(r)dr,$$

goes to zero as n tends to infinity due to the rapid oscillations of $\cos(2k_{\ell n}r)$ in this limit. Hence

$$\lim_{n\to\infty}\left\{\frac{\hbar^2}{2\mu}\frac{\gamma_{\ell n}^2 - k_{\ell n}^2}{\aleph_{\ell n}^2}\right\} = \frac{1}{2}\int_0^a V_\ell(r)\,dr \equiv L \tag{6.29}$$

Subtracting eqn. (6.29) from both sides of eqn. (6.27), one obtains

$$\frac{\hbar^2}{2\mu}\frac{\gamma_{\ell n}^2 - k_{\ell n}^2}{\aleph_{\ell n}^2} - L = \int_0^a V_\ell(r)\left[r^2 k_{\ell n}^2 j_\ell^2(k_{\ell n}r) - \frac{1}{2}\right]dr \tag{6.30}$$

Multiplying eqn. (6.30) by $\frac{g_\ell(k_{\ell n}r')}{k_{\ell n}^2 r'^2}\Delta k_n$ and summing over n, one gets

$$\begin{aligned}
&\sum_{n=1}^\infty\left[\frac{\hbar^2}{2\mu}\frac{\gamma_{\ell n}^2 - k_{\ell n}^2}{\aleph_{\ell n}^2} - L\right]\frac{g_\ell(k_{\ell n}r')}{k_{\ell n}^2 r'^2}\Delta k_{\ell n} \\
&\quad = \sum_{n=1}^\infty\int_0^a V_\ell(r)\left[k_{\ell n}^2 r^2 j_\ell^2(k_{\ell n}r) - \frac{1}{2}\right]\left[\frac{g_\ell(k_{\ell n}r')}{k_{\ell n}^2 r'^2}\right]\Delta k_{\ell n}dr \\
&\quad = \int_0^a V_\ell(r)\left\{\sum_{n=1}^\infty\left(r^2 k_{\ell n}^2 j_\ell^2(k_{\ell n}r) - \frac{1}{2}\right)\frac{g_\ell(k_{\ell n}r')}{k_{\ell n}^2 r'^2}\Delta k_n\right\}dr.
\end{aligned} \tag{6.31}$$

But from eqn. (6.26),

$$\sum_{n=1}^\infty\left(k_{\ell n}^2 r^2 j_\ell^2(k_{\ell n}r) - \frac{1}{2}\right)\frac{g_\ell(k_{\ell n}r')}{(k_{\ell n}r')^2}\Delta k_{\ell n} = \delta(r-r') - \frac{2\,k_{\ell 1}}{\pi(2\ell+1)} \tag{6.32}$$

Thus

$$\begin{aligned}\sum_{n=1}^{\infty}\left[\frac{\hbar^2}{2\mu}\frac{\gamma_{\ell n}^2-k_{\ell n}^2}{\aleph_{\ell n}^2}-L\right]\frac{g_\ell(k_{\ell n}r')}{k_{\ell n}^2 r'^2}\Delta k_{\ell n} &= \int_0^a V_\ell(r)\left(\delta(r-r')-\frac{2\,k_{\ell 1}}{\pi(2\ell+1)}\right)dr \\ &= \left\{V_\ell(r')-\frac{2\,k_{\ell 1}}{\pi(2\ell+1)}\underbrace{\int_0^a V(r)dr}_{2L}\right\} \\ &= V_\ell(r')-\frac{4\,k_{\ell 1}L}{\pi(2\ell+1)} \qquad (6.33)\end{aligned}$$

Hence

$$V_\ell(r')\approx\frac{4k_{\ell 1}L}{\pi(2\ell+1)}+\sum_{n=1}^{\infty}\left[\frac{\hbar^2}{2\mu}\left(\frac{\gamma_{\ell n}^2-k_{\ell n}^2}{\aleph_{\ell n}^2}\right)-L\right]\frac{g_\ell(k_{\ell n}r')}{k_{\ell n}^2 r'^2}\Delta k_{\ell n} \qquad (6.34)$$

Replacing r' by r in eqn. (6.34), one obtains

$$V_\ell(r)\approx\frac{4k_{\ell 1}L}{\pi(2\ell+1)}+\sum_{n=1}^{\infty}\left[\frac{\hbar^2}{2\mu}\left(\frac{\gamma_{\ell n}^2-k_{\ell n}^2}{\aleph_{\ell n}^2}\right)-L\right]\frac{g_\ell(k_{\ell n}r)}{k_{\ell n}^2 r^2}\Delta k_{\ell n} \qquad (6.35)$$

6.3 Potential Expansion Approach

One can approach the inverse scattering problem in a different way by expanding the potential $V_\ell(r)$ in $0 < r \leq a$ in terms of a complete set $\left\{U_p\left(\alpha_{pn}\frac{r}{a}\right)\right\}$, i.e.

$$V_\ell(r)=\sum_{q=1}^{q=\infty} b_q\, U_p\left(\alpha_{pq}\frac{r}{a}\right) \qquad (6.36)$$

where α_{pn} is the nth root of U_p.

As an illustration to this approach, we expand the potential in terms of the spherical Bessel function $j_\ell(k_{\ell n}r)$, i.e.

$$V_\ell(r) = \sum_{q=1}^{q=\infty} b_q\, j_\ell(k_{\ell q}r), \tag{6.37}$$

where

$$k_{\ell q} = \frac{\alpha_{\ell q}}{a},$$

bearing in mind that one can equally expand $V_\ell(r)$ *in terms of any orthonormal set*, e.g. $j_{\ell+1}\left(k_{(\ell+1)q}r\right)$, $g_\ell\left(\alpha_{\ell q}\frac{r}{a}\right)$, ..., etc.

Substituting eqn. (6.37) in eqn. (6.15), one obtains

$$\frac{\hbar^2}{2\mu}\frac{\gamma_{\ell n}^2 - k_{\ell n}^2}{N_{\ell n}^2} = \int_0^a r^2\, j_\ell^2(k_{\ell n}r) \sum_{q=1}^{q=\infty} b_q\, j_\ell(k_{\ell q}r)\, dr.$$

Hence

$$\frac{\hbar^2}{2\mu}\frac{\gamma_{\ell n}^2 - k_{\ell n}^2}{N_{\ell n}^2} = \sum_{q=1}^{\infty} b_q \int_0^a r^2 j_\ell^2(k_{\ell n}r) j_\ell(k_{\ell q}r) dr$$

Define

$$M_{nq} \equiv \int_0^a r^2 j_\ell^2(k_{\ell n}r) j_\ell(k_{\ell q}r) dr$$

Thus,

$$\frac{\hbar^2}{2\mu}\frac{\gamma_{\ell n}^2 - k_{\ell n}^2}{N_{\ell n}^2} = \sum_{q=1}^{\infty} b_q M_{nq} \tag{6.38}$$

If there exists an integer m such that for any $q > m$

$$|M_{nq}| \ll |M_{nm}|,$$

then the infinite sum in eqn. (6.38) can be approximated by the finite sum

$$\frac{\hbar^2}{2\mu}\frac{\gamma_{\ell n}^2 - k_{\ell n}^2}{N_{\ell n}^2} = \sum_{q=1}^{q=m} b_q M_{nq}, \tag{6.39}$$

and the potential $V_\ell(r)$ in eqn.(6.37) can be approximated by

$$V_\ell(r) = \sum_{q=1}^{q=m} b_q \, j_\ell(k_{\ell q} r) \tag{6.40}$$

Eqn. (6.39) can be written in a matrix form as

$$d = Mb \tag{6.41}$$

where

d : is an $m \times 1$ column vector with vector elements $d_n \equiv \frac{\hbar^2}{2\mu} \frac{\gamma_{\ell n}^2 - k_{\ell n}^2}{N_{\ell n}^2}$.

M : is an $m \times m$ matrix with M_{nq} as a matrix element.

b : is an $m \times 1$ column vector with vector elements b_n.

Multiplying both sides of eqn. (6.41) by the inverse of M, M^{-1}, one obtains the set b_q, which is given in a matrix form as

$$b = M^{-1} d. \tag{6.42}$$

Then, these b_q are substituted in eqn. (6.37) to get the potential $V_\ell(r)$

CHAPTER 7

Numerical Calculations In The Finite Space Inverse Scattering Problem

In order to investigate the inversion techniques discussed in the previous chapter and their limitations, one should perform some numerical calculations using phase shifts of *known potentials. By comparing the potentials extracted using one of the inversion techniques with the actual potentials, one can determine the limitations of each of these techniques.*

Before discussing numerical examples, two important points should be noticed; 1) There is a vast body of experimental measurements on nucleon-nucleon scattering in the range $E_{lab} = 0-750$ MeV [48]. For the energy range $E_{lab} = 0-450$ MeV (or in terms of relative energies $E_{rel} \equiv E = 0-225$ MeV), the inelastic effects are small while in the energy range $E_{lab} = 450-750$ MeV (or $E = 225-375$) the inelastic effects are large. Since the inversion techniques discussed previously are valid

where the inelastic effects are small, one should restrict oneself to phase shifts in the range $E_{lab} \approx 0$–450 MeV or ($E \approx 0$–225 MeV).

2) The experimental phase shifts are continuous functions of the energy while in inverting the finite space partial wave Born approximation, namely

$$\frac{\hbar^2}{2\mu}\frac{\gamma_{\ell n}^2 - k_{\ell n}^2}{N_{\ell n}^2} \approx \int_0^a r^2 j_\ell^2(k_{\ell n} r) V_\ell(r)\, dr,$$

the phase shifts are functions of discrete energies. The discrete perturbed energies $E_{\ell n}$ are related to $\gamma_{\ell n}^2$ as follows

$$E_{\ell n} = \frac{\hbar^2 \gamma_{\ell n}^2}{2\mu}.$$

A natural question now arises; how one can determine the perturbed energies, or equivalently $\gamma_{\ell n}$, (in order to use the finite space inversion techniques) from the experimental phase shifts $\delta_\ell^{ex}(k)$?

Recall that the finite space phase shifts are obtained by solving the following equation[1]

$$\cos(\delta_{\ell n}) \cdot j_\ell(\gamma_{\ell n} a) - \sin(\delta_{\ell n}) \cdot n_\ell(\gamma_{\ell n} a) = 0, \tag{7.1}$$

where a is the dimension of the finite space. But

$$\delta_\ell^{ex}(k)|_{k=\gamma_{\ell n}} = \delta_{\ell n}(\gamma_{\ell n}), \tag{7.2}$$

since the phase shifts should not depend on the dimension of the space if it is sufficiently large. Solving the transcendental equation, eqn. (7.2), one can obtain the perturbed momenta $\gamma_{\ell n}$ and consequently the perturbed energies.

[1]See chapter 4, eqn. (4.61)

Throughout this chapter, we consider a nucleon of mass $m_1 = 939$ MeV/c^2 (for a proton $m = 938.2592$ MeV/c^2 while for a neutron $m = 939.5527$ MeV/c^2), moving with initial kinetic energy E_{lab}, in a sphere of radius a, scattered by another nucleon, initially at rest in the laboratory coordinate system. The equivalent one-body problem in the relative coordinate system is a particle of mass $\mu = 469.5$ MeV/c^2 (Recall that $E = \frac{1}{2}E_{lab}$ and $k = \frac{1}{2}k_{lab}$) moving with relative kinetic energy E, in a sphere of radius a, scattered off a scattering potential $V_\ell(r)$, in the angular momentum channel ℓ. For simplicity, we consider square well or barrier potentials of different strengths as the "experimental" phase shifts. Using the phase shifts produced by those potentials, one can use the finite space inversion techniques to reproduce the potentials and then to compare these with the actual ones.

To begin with, we will consider the finite space $g_\ell(k_{\ell n}r)$ approach.

7.1 Finite Space $g_\ell(k_{\ell n}r)$ Approach

Example 7.1 :

Consider a particle of mass $\mu = 469.5$ MeV/c^2 scattered off a square well potential of depth V and range $d = 2$ fm in the angular momentum channel $\ell = 0$, in a sphere of radius a. In this case, the finite space phase shift, eqn. (7.1), reduces to[2]

$$\delta_0(\gamma_{0n}) = n\pi - \gamma_{0n}a, \quad n = 1, 2, \ldots, m, \tag{7.3}$$

where m is the truncation integer. The plot of eqn. (7.3) for n varies from 1 to 7, i.e. $m = 7$, is given in fig. 7.1.

The potential $V_0(r)$, is given by

$$\begin{aligned} V_0(r) &= \frac{4L}{a} + \sum_{n=1}^{\infty}\left[\frac{\hbar^2}{2\mu}\left(\frac{\gamma_{0n}^2 - \left(\frac{n\pi}{a}\right)^2}{\frac{2}{a}}\right) - L\right]\left(\frac{-8}{\pi}\cos\left(\frac{2n\pi}{a}r\right)\right)\frac{\pi}{a} \\ &= \frac{4L}{a} - \frac{8}{a}\sum_{n=1}^{\infty}\left[\frac{a\hbar^2}{4\mu}\left(\gamma_{0n}^2 - \left(\frac{n\pi}{a}\right)^2\right) - L\right]\cos\left(\frac{2n\pi}{a}r\right). \end{aligned} \tag{7.4}$$

Since the "experimental" phase shifts should be considered in the energy range $E \approx 0$–225 MeV, as discussed previously, the summation in eqn. (7.4) should be truncated up to a certain energy state, call it the mth state. Therefore, the infinite sum in eqn. (7.4) should be replaced by the following finite sum

$$V_0(r) = \frac{4L}{a} - \frac{8}{a}\sum_{n=1}^{n=m}\left[\frac{a\hbar^2}{4\mu}\left(\gamma_{0n}^2 - \left(\frac{n\pi}{a}\right)^2\right) - L\right]\cos\left(\frac{2n\pi}{a}r\right). \tag{7.5}$$

[2]See chapter 4, eqn. (4.62)

Let us study the following cases :

Case I) : Consider a square well potential of depth $V = -5$ MeV in a sphere of radius $a = 10$ fm. In this case, the energy of the 7th state is 199.5 MeV while the energy of the 8th state is 260.8 MeV. Thus it is convenient to choose $m = 7$. The "experimental" phase shifts $\delta_0^{ex}(k)$ of this potential are given in fig. 7.2. Solving the transcendental equation, namely

$$\delta_0^{ex}(k)|_{k=\gamma_{0n}} = \delta_0(\gamma_{0n}) = n\pi - \gamma_{0n}a, \quad n = 1, 2, \ldots, m, \tag{7.6}$$

graphically, as in fig. 7.3, or numerically, one can obtain the discrete phase shifts at the discrete perturbed energy states, see fig. 7.4a. Substituting the obtained discrete perturbed energy states γ_{0n} in eqn. (7.5), one can obtain the potential $V_0(r)$, see fig. 7.4b. As can be seen from fig. 7.4b, the potential obtained is, to a very good approximation, a square well potential of depth $V = -5$ MeV.

Notice that the potential in fig. 7.4b was plotted in $0 < r \leq 5 = \frac{a}{2}$. This is because of the symmetry of the potential $V_0(r)$ around $r = \frac{a}{2}$, i.e.

$$V_0(r) = V_0(a - r).$$

This can be shown easily as follows

$$V_0(a-r) = \frac{4L}{a} - \frac{8}{a}\sum_{n=1}^{n=m}\left[\frac{a\hbar^2}{4\mu}\left(\gamma_{0n}^2 - \left(\frac{n\pi}{a}\right)^2\right) - L\right]\cos\left(\frac{2n\pi}{a}(a-r)\right). \tag{7.7}$$

But

$$\begin{aligned}\cos\left(\frac{2n\pi}{a}(a-r)\right) &= \underbrace{\cos(2n\pi)}_{1}\cos\left(\frac{2n\pi}{a}r\right) + \underbrace{\sin(2n\pi)}_{0}\sin\left(\frac{2n\pi}{a}r\right) \\ &= \cos\left(\frac{2n\pi}{a}r\right)\end{aligned}$$

Therefore, eqn. (7.6) becomes

$$\begin{aligned} V_0(a-r) &= \frac{4L}{a} - \frac{8}{a}\sum_{n=1}^{n=m}\left[\frac{a\hbar^2}{4\mu}\left(\gamma_{0n}^2 - \left(\frac{n\pi}{a}\right)^2\right) - L\right]\cos\left(\frac{2n\pi}{a}r\right) \\ &= V_0(r) \end{aligned} \tag{7.8}$$

Eqn. (7.8) implies that the interaction between two nucleons when they are very close to each other is the same as the interaction between them when they are separated by a, the radius of the sphere (recall that r represents the relative distance between the two nucleons), which is not physical, see fig. 7.4c. This ambiguity arises because of the symmetry of the $g_0(k_{0n}r)$ around $r = \frac{a}{2}$. To overcome this problem, one should consider finite spaces of sufficiently large size. The potentials obtained using eqn. (7.5) should be considered in the region $0 \leq r \leq \frac{a}{2}$, since $V_0(r) = V_0(a-r)$. Figs. 7.4c and 7.4d illustrate this behaviour clearly where in fig. 7.4c the radius of the sphere is sufficiently large, $a = 10$ fm, such that if one consider the potential in $0 \leq r \leq \frac{a}{2}$, the analogous potential in the infinite space will be obtained while in fig. 7.4d the radius of the sphere is so small that if one consider the potential in $0 \leq r \leq \frac{a}{2}$, the analogous potential in the infinite space will not be obtained. For $\ell \geq 1$, there is a similar behviour, but not symmetric around $r = \frac{a}{2}$, see figs. 7.4e and 7.4f.

Figures 7.5a and 7.6a, show the discrete finite space phase shifts for the same potential but for $a = 30$ and 50 fm respectively while figures 7.5b and 7.6b show the corresponding potentials. As can be seen from figures 7.4b, 7.5b and 7.6b, increasing the radius of the sphere, or in other words, summing over a larger number of states, does not improve the potential as one may expect.

It is very interesting to observe that using only seven energy states, one can obtain the potential which shows the usefulness of this technique.

Case II) : Consider a square well potential of depth $V = -10$ MeV in a sphere of radius $a = 10$ fm. The "experimental" phase shifts $\delta_0^{ex}(k)$ of this potential is given in fig. 7.7. Solving the transcendental equation, eqn. (7.6), graphically, as in fig. 7.8, or numerically, one can obtain the discrete phase shifts at the discrete perturbed energy states, see fig. 7.9a. Substituting the obtained discrete perturbed energy states γ_{0n} in eqn. (7.5), one can obtain the potential $V_0(r)$, see fig. 7.9b. As can be seen from fig. 7.9b, the potential obtained is, to a good approximation, a square well potential of depth $V = -10$ MeV. Figures 7.10a and 7.11a, show the discrete finite space phase shifts for the same potential but for $a = 30$ and 50 fm respectively while figures 7.10b and 7.11b show the corresponding potentials. As can be seen from figures 7.9b, 7.10b and 7.11b, increasing the radius of the sphere, or in other words, summing over a larger number of states, does not improve the potential as one may expect.

Case III) : Consider a square well potential of depth $V = -20$ MeV. One can use the argument above to obtain the discrete phase shifts at the corresponding perturbed energies. The discrete phase shifts for $a = 10$, 30 and 50 fm are shown in figures 7.12a, 7.13a and 7.14a respectively while the corresponding potentials are given in figures 7.12b, 7.13b and 7.14b. Comparing the potentials obtained in figures 7.12b, 7.13b and 7.14b, one can observe that the potentials do not improve

by increasing the radius of the sphere. Furthermore, the potentials start to deviate from the square well potential shape.

Case IV) : Consider a square well potential of depth $V = -40$ MeV. The discrete phase shifts at the corresponding discrete perturbed energies for $a = 10$, 30, 50 and 100 fm are shown in figures 7.15a, 7.16a, 7.17a and 7.18a while the corresponding potentials are given in figures 7.15b, 7.16b, 7.17b and 7.18b. As can be seen from figures 7.15b, 7.16b, 7.17b and 7.18b, the potentials obtained deviate considerably from the square well potential. Moreover, one can observe from figures 7.19, 7.20 and 7.21 that increasing the radius of the sphere, or in other words, summing over a larger number of states, results in improving the potential up to a certain extent.

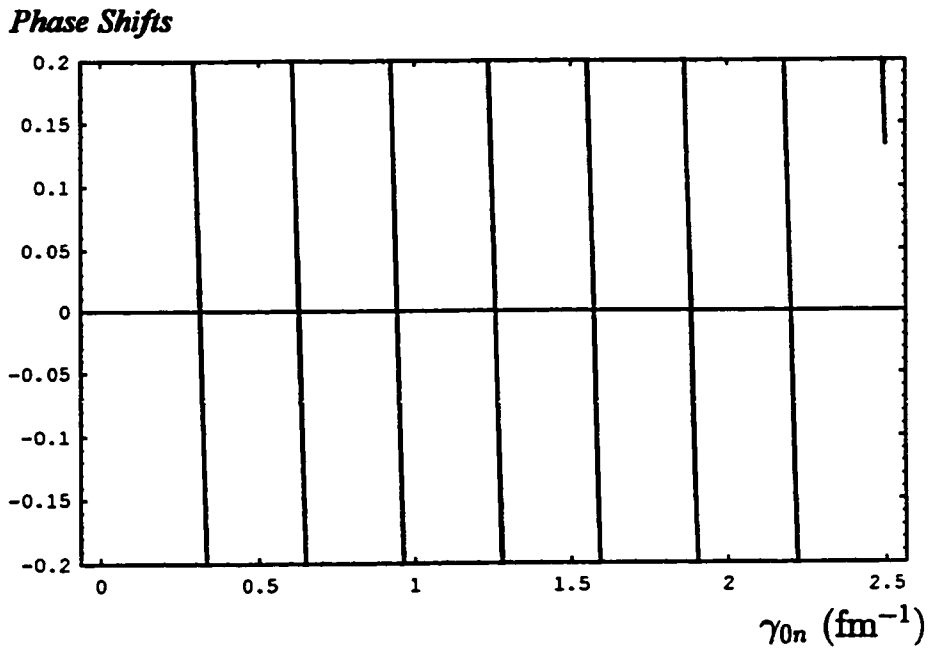

Fig. 7.1 : Plot of eqn. (7.3) for $n = 1$ to $n = 7$.

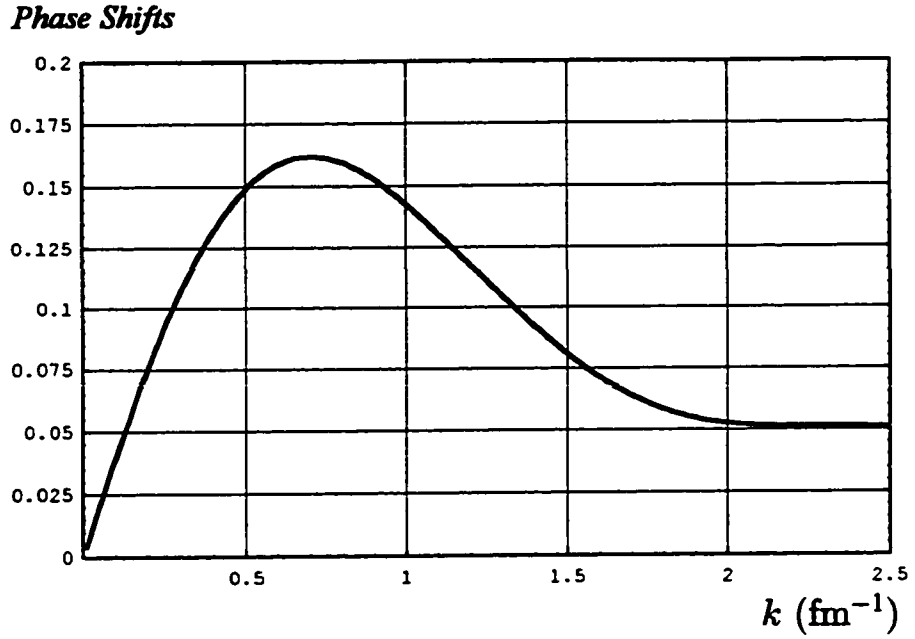

Fig. 7.2 : "Experimental" phase shifts produced by a nucleon scattered off a square well potential of depth $V = -5$ MeV and range $d = 2$ fm, in the angular momentum channel $\ell = 0$.

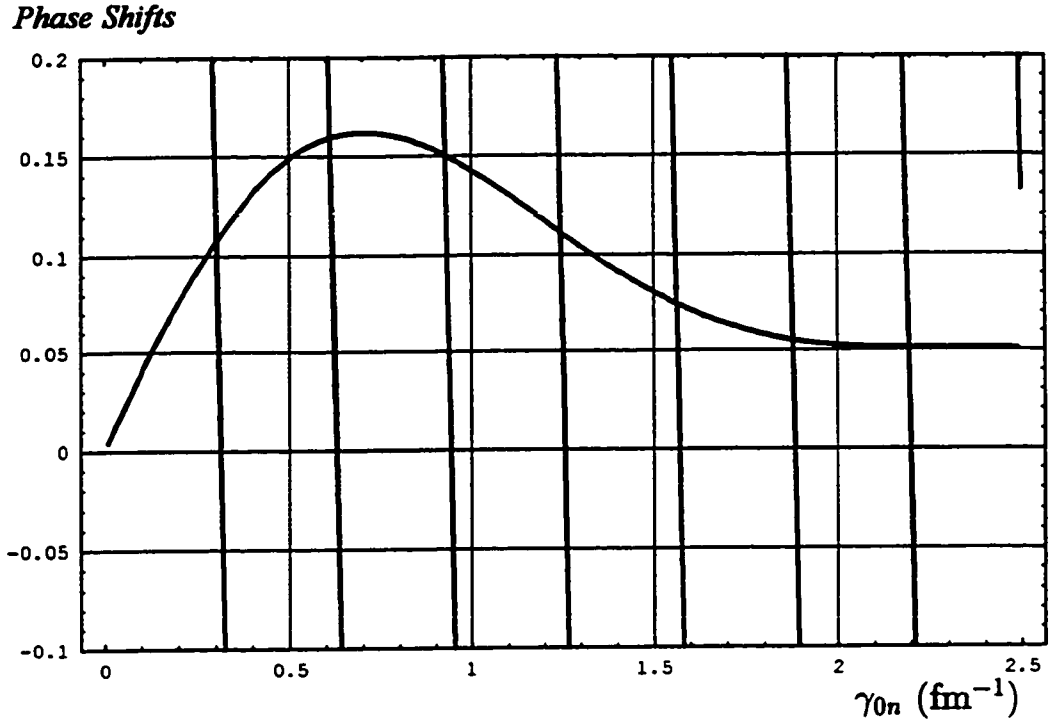

Fig. 7.3 : Graphical solution of the transcendental equation (7.6). The energies at which the intersections of the curve, which represents the "experimental" phase shifts, with the straight lines, which represents the discrete phase shifts, occur represents the discrete perturbed energy states.

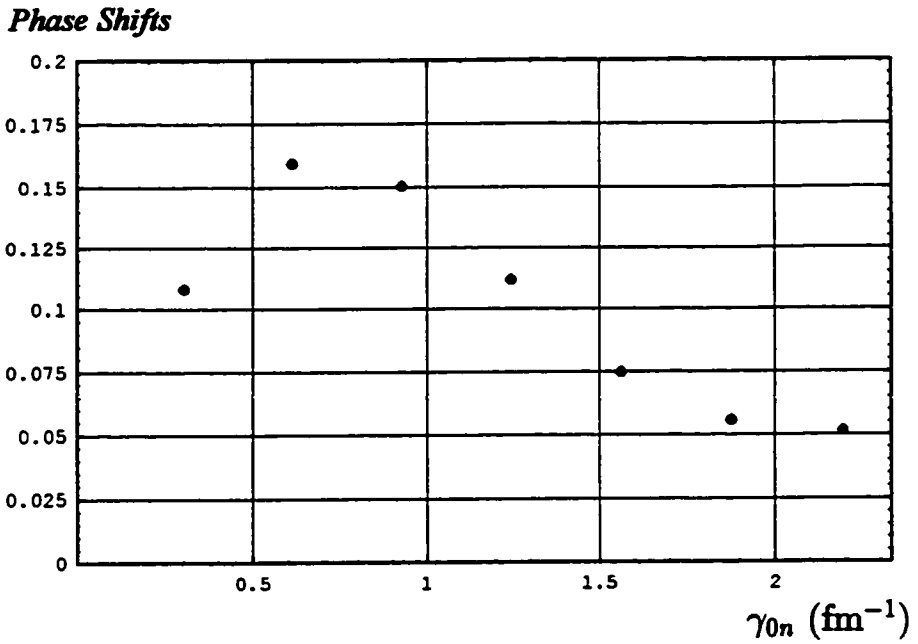

Fig. 7.4a : Discrete phase shifts produced by a nucleon scattered from a square well potential of depth $V = -5$ MeV and range $d = 2$ fm in $\ell = 0$. The discrete energies were obtained by solving the transcendental equation 7.6 for $a = 10$ fm.

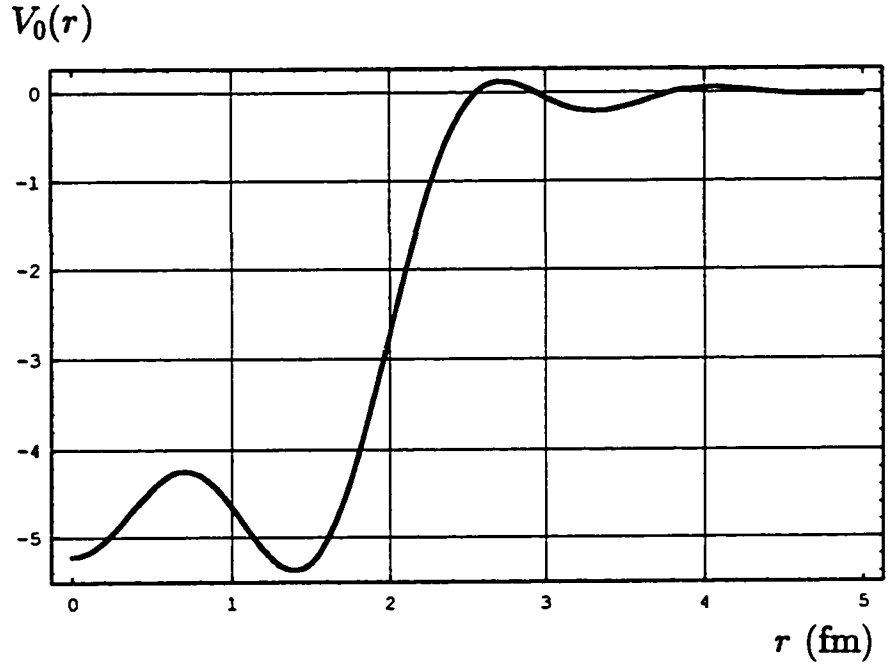

Fig. 7.4b : Potential calculated from eqn. (7.5) using the discrete perturbed energy states obtained in the above figure.

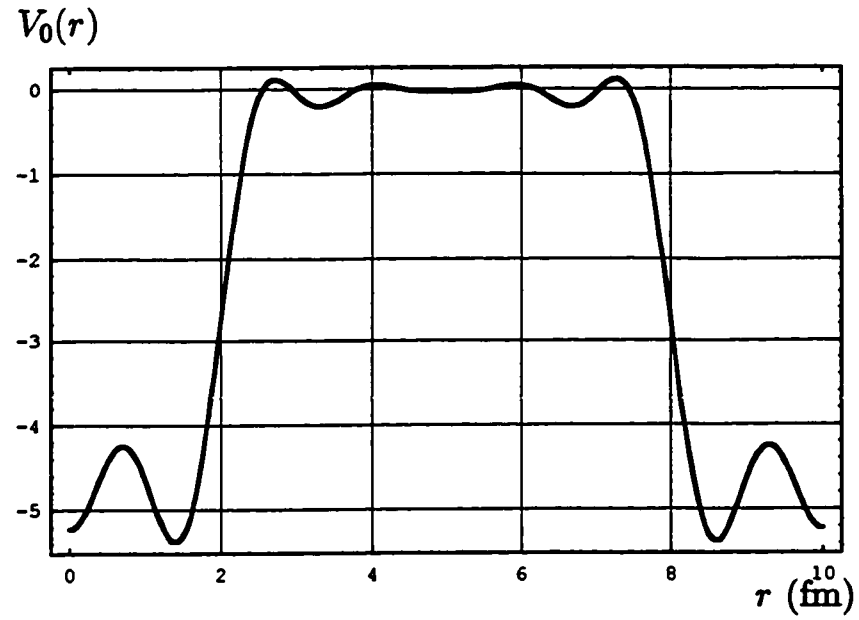

Fig. 7.4c : Potential calculated from eqn. (7.5) using the the discrete energy states of a nucleon in a sphere of radius $a = 10$ fm, scattered from a square well potential of depth $V = -5$ MeV and range $d = 2$ fm in $\ell = 0$. The potential is plotted over the whole space.

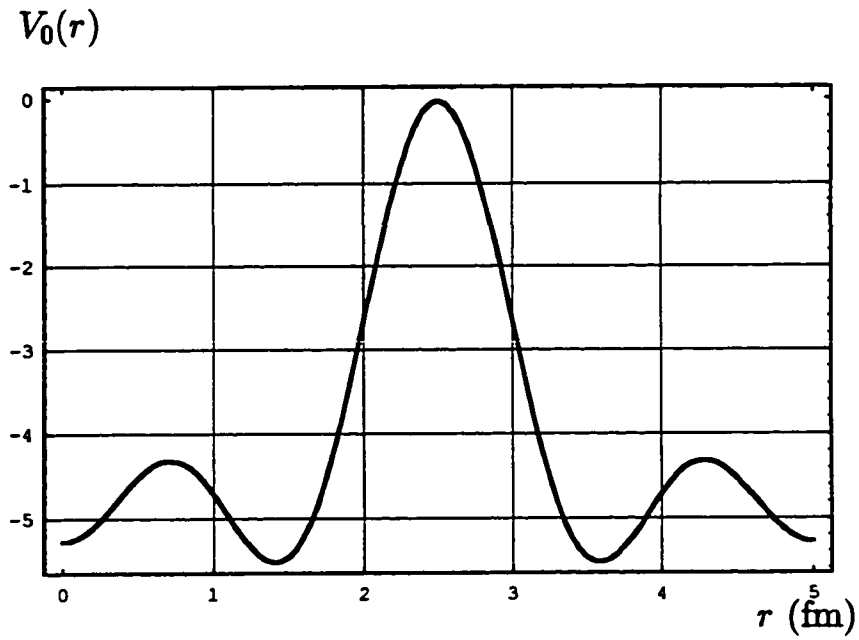

Fig. 7.4d : Potential calculated from eqn. (7.5) using the the discrete energy states of a nucleon in a sphere of radius $a = 5$ fm, scattered from a square well potential of depth $V = -5$ MeV and range $d = 2$ fm in $\ell = 0$. The potential is plotted over the whole space.

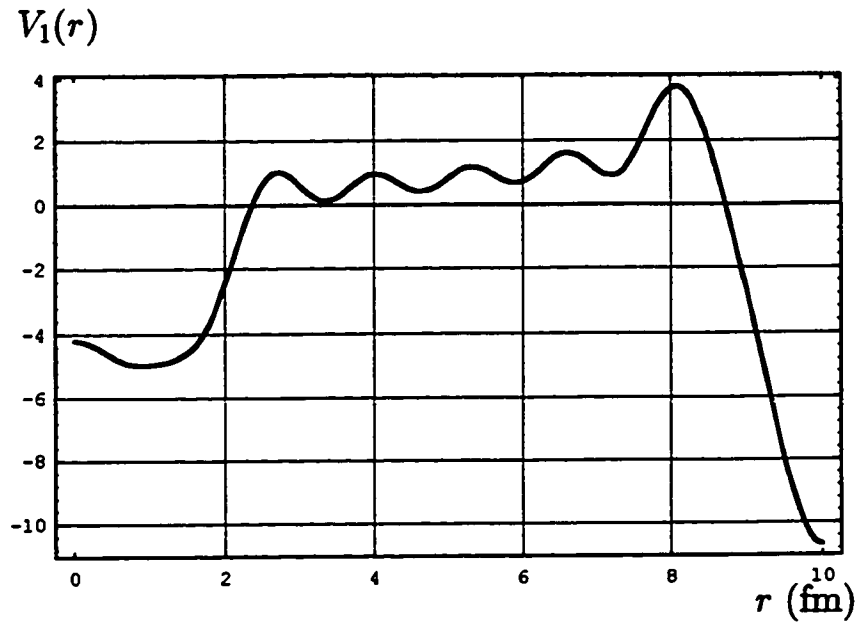

Fig. 7.4e : Potential calculated from eqn. (7.5) using the the discrete energy states of a nucleon in a sphere of radius $a = 10$ fm, scattered from a square well potential of depth $V = -5$ MeV and range $d = 2$ fm in $\ell = 1$. The potential is plotted over the whole space.

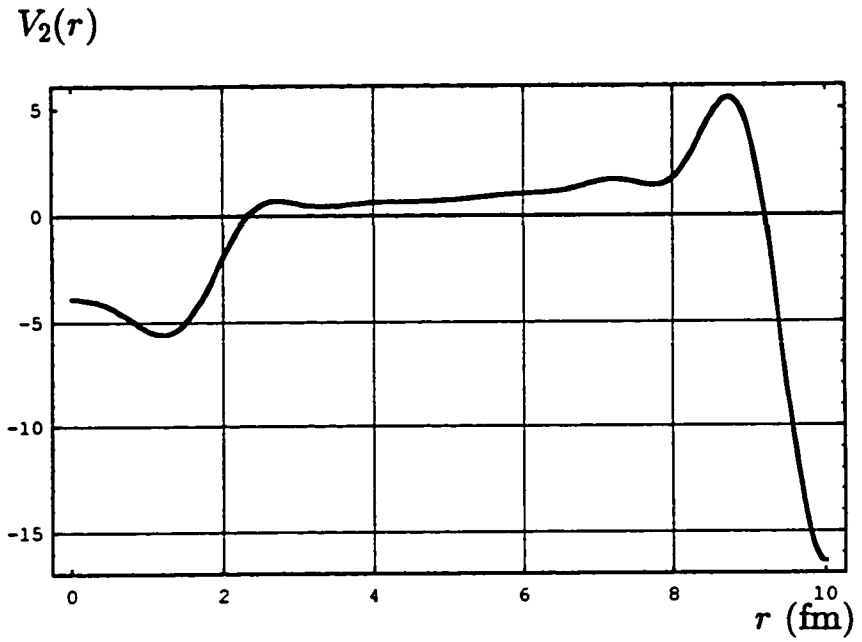

Fig. 7.4f : Potential calculated from eqn. (7.5) using the the discrete energy states of a nucleon in a sphere of radius $a = 10$ fm, scattered from a square well potential of depth $V = -5$ MeV and range $d = 2$ fm in $\ell = 2$. The potential is plotted over the whole space.

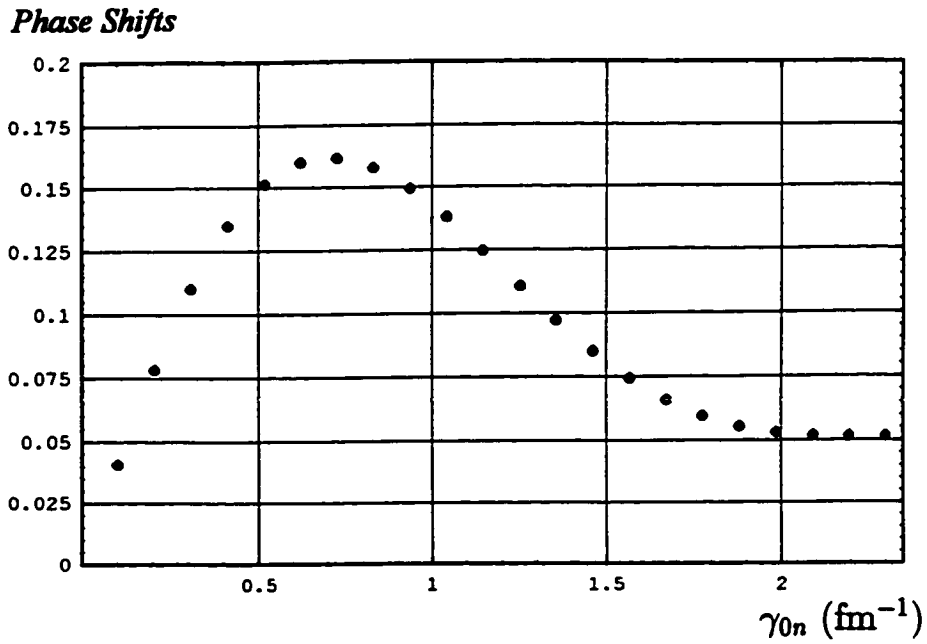

Fig. 7.5a : Discrete phase shifts produced by a nucleon scattered from a square well potential of depth $V = -5$ MeV and range $d = 2$ fm in $\ell = 0$. The discrete energies were obtained by solving the transcendental equation 7.6 for $a = 30$ fm.

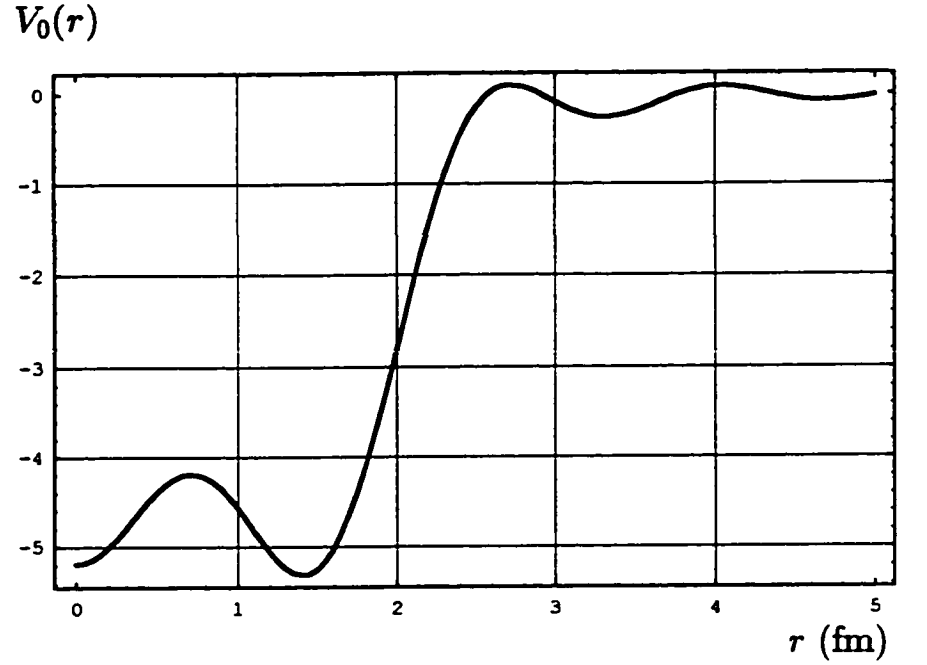

Fig. 7.5b : Potential calculated from eqn. (7.5) using the discrete perturbed energy states obtained in the above figure.

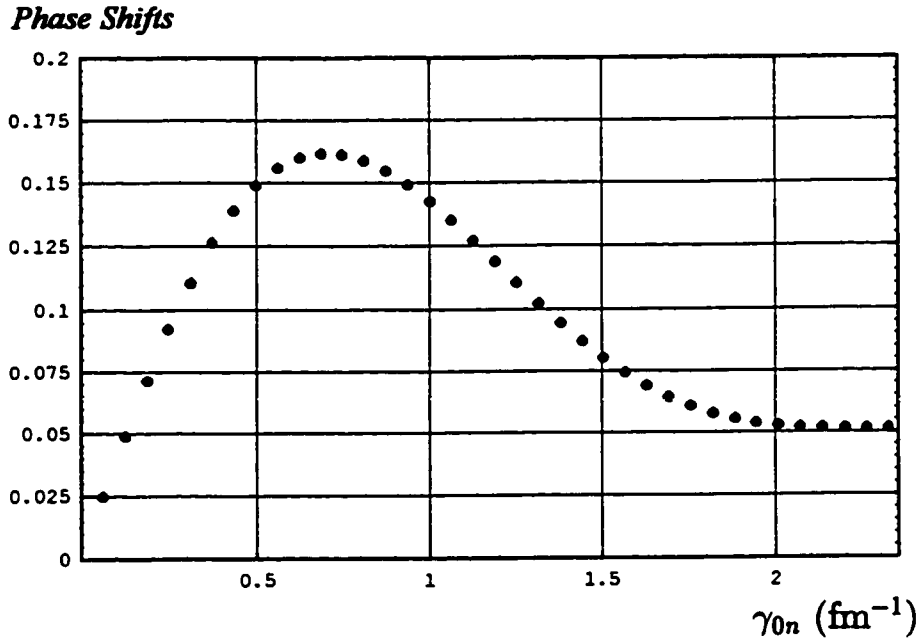

Fig. 7.6a : Discrete phase shifts produced by a nucleon scattered from a square well potential of depth $V = -5$ MeV and range $d = 2$ fm in $\ell = 0$. The discrete energies were obtained by solving the transcendental equation 7.6 for $a = 50$ fm.

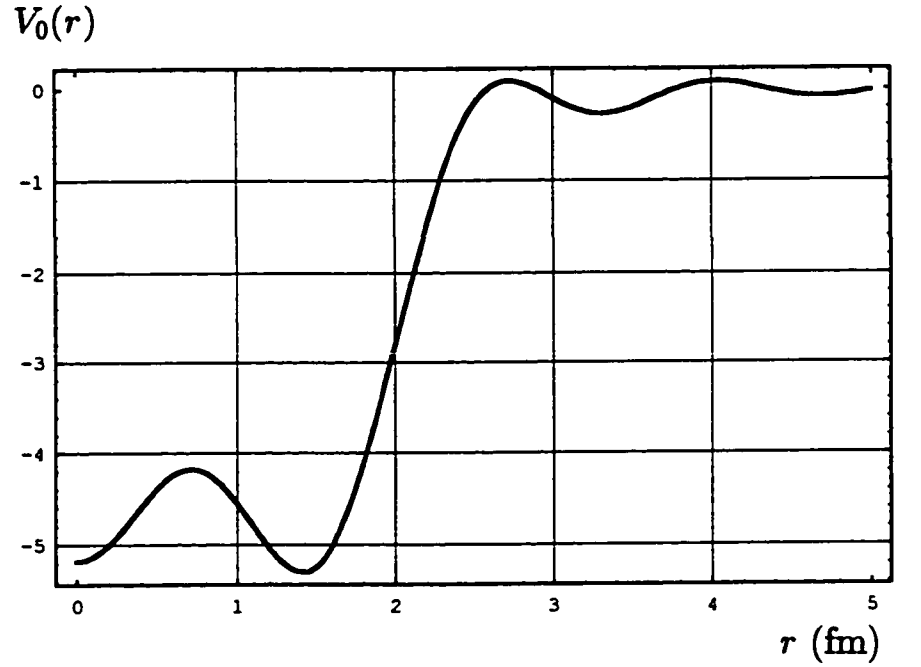

Fig. 7.6b : Potential calculated from eqn. (7.5) using the discrete perturbed energy states obtained in the above figure.

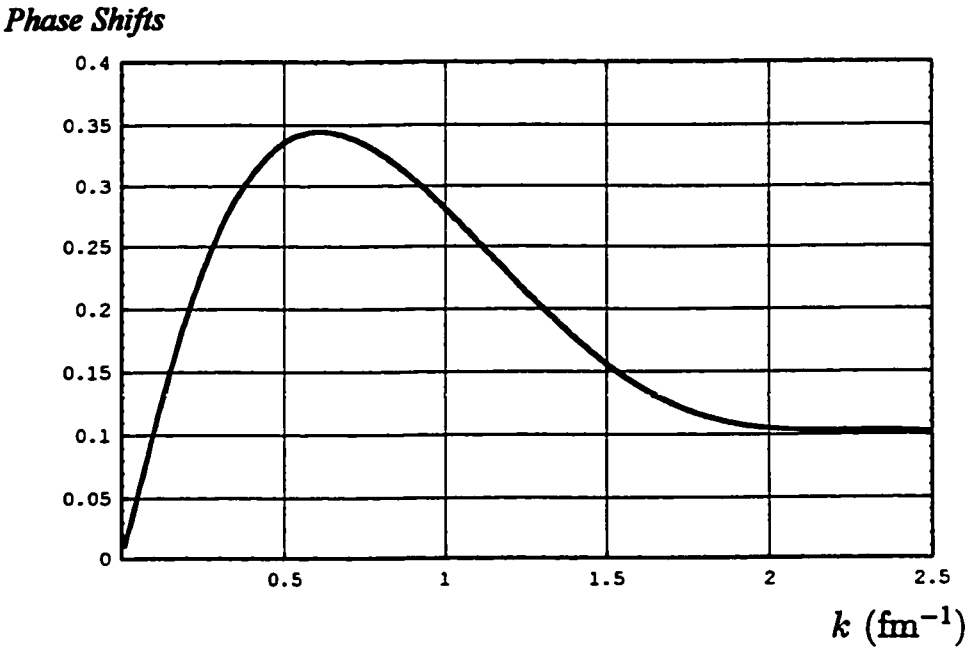

Fig. 7.7 : "Experimental" phase shifts produced by a nucleon scattered off a square well potential of depth $V = -10$ MeV and range $d = 2$ fm.

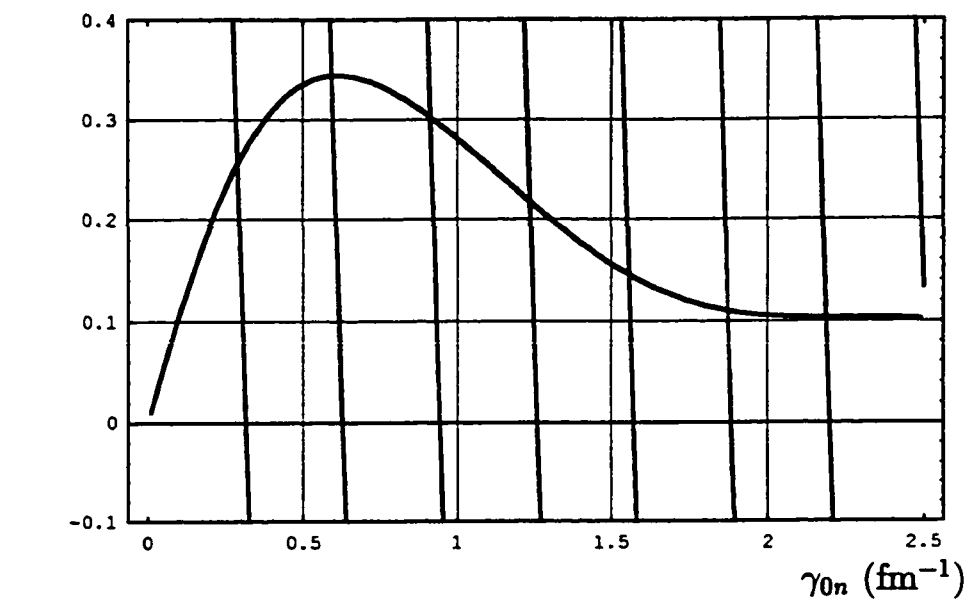

Fig. 7.8 : Graphical solution of the transcendental eqaution (7.6). The energies at which the intersections of the curve with the straight lines occur represents the discrete perturbed energy states.

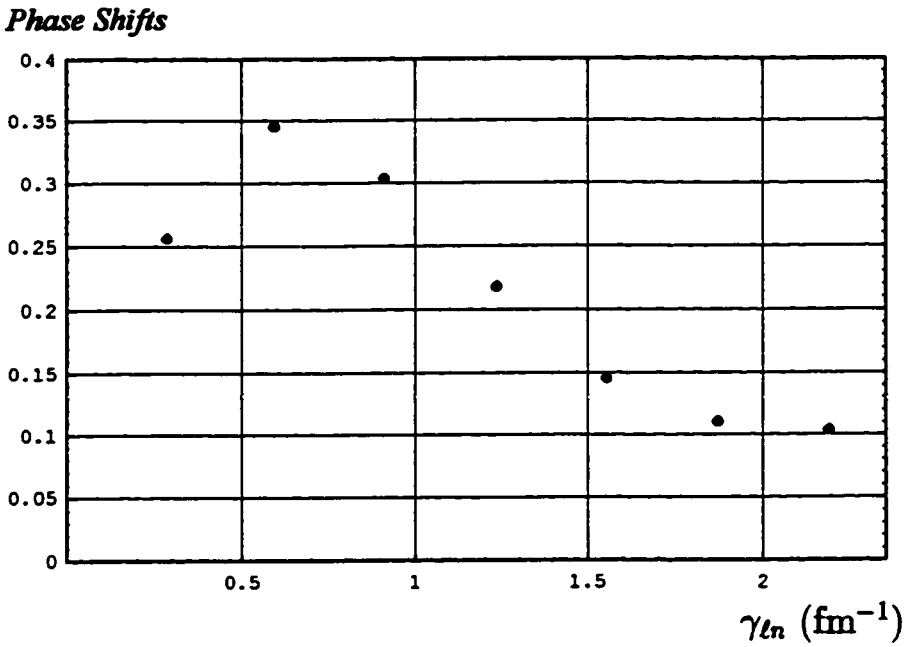

Fig. 7.9a : Discrete phase shifts produced by a nucleon scattered from a square well potential of depth $V = -10$ MeV and range $d = 2$ fm in $\ell = 0$. The discrete energies were obtained by solving the transcendental equation 7.6 for $a = 10$ fm.

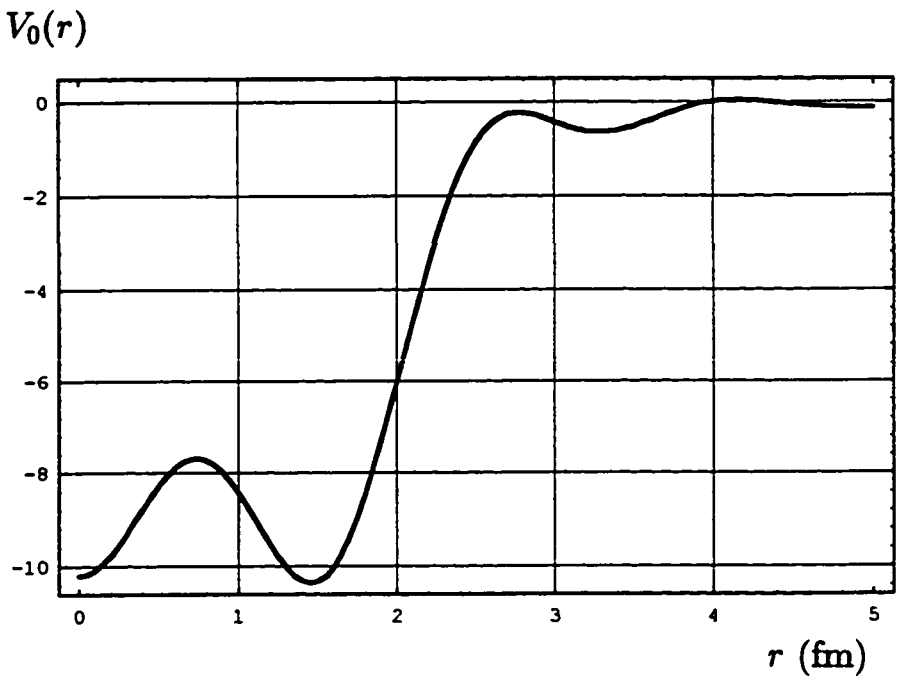

Fig. 7.9b : Potential calculated from eqn. (7.5) using the discrete perturbed energy states obtained in the above figure.

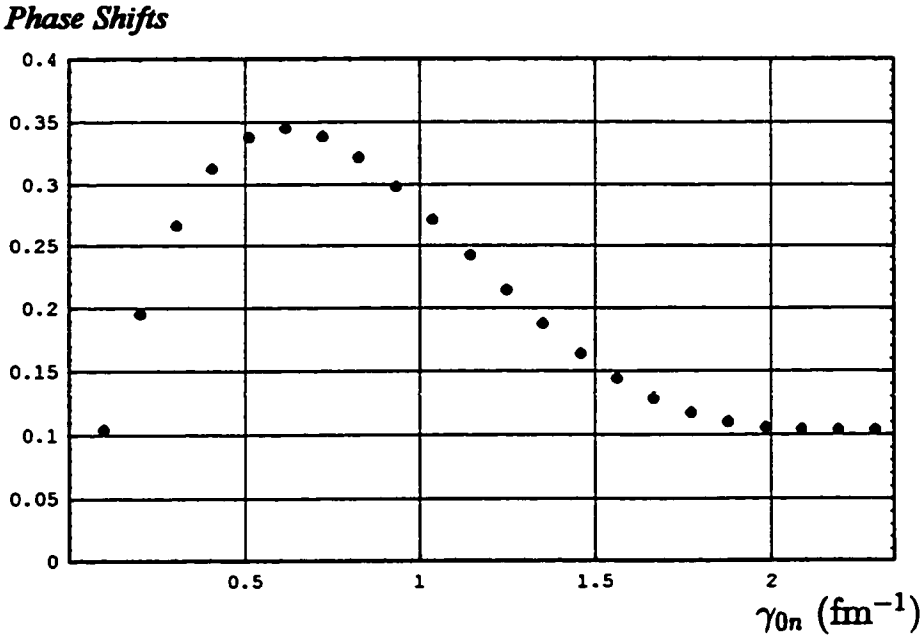

Fig. 7.10a : Discrete phase shifts produced by a nucleon scattered from a square well potential of depth $V = -10$ MeV and range $d = 2$ fm in $\ell = 0$. The discrete energies were obtained by solving the transcendental equation 7.6 for $a = 30$ fm.

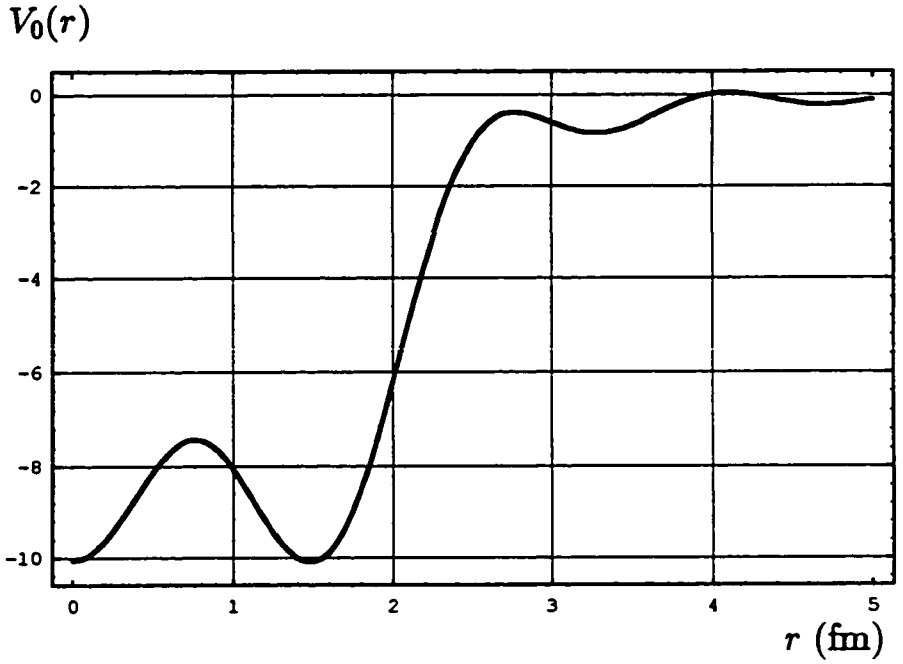

Fig. 7.10b : Potential calculated from eqn. (7.5) using the discrete perturbed energy states obtained in the above figure.

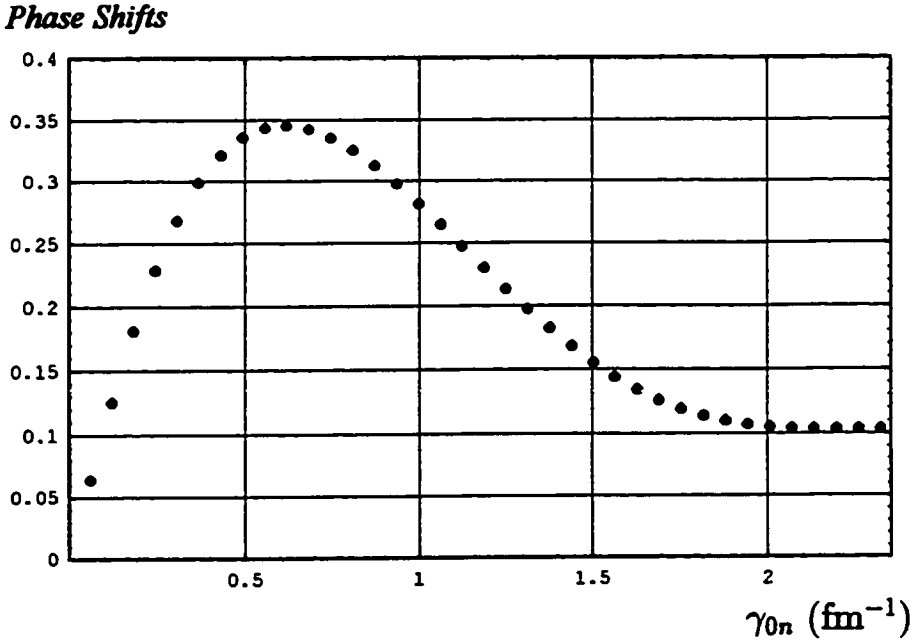

Fig. 7.11a : Discrete phase shifts produced by a nucleon scattered from a square well potential of depth $V = -10$ MeV and range $d = 2$ fm in $\ell = 0$. The discrete energies were obtained by solving the transcendental equation 7.6 for $a = 50$ fm.

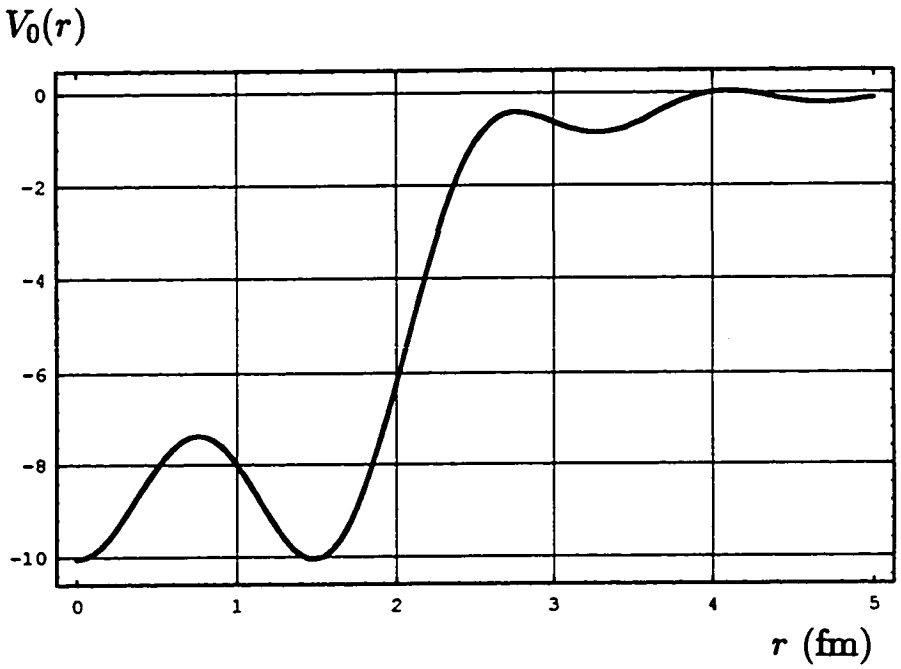

Fig. 7.11b : Potential calculated from eqn. (7.5) using the discrete perturbed energy states obtained in the above figure.

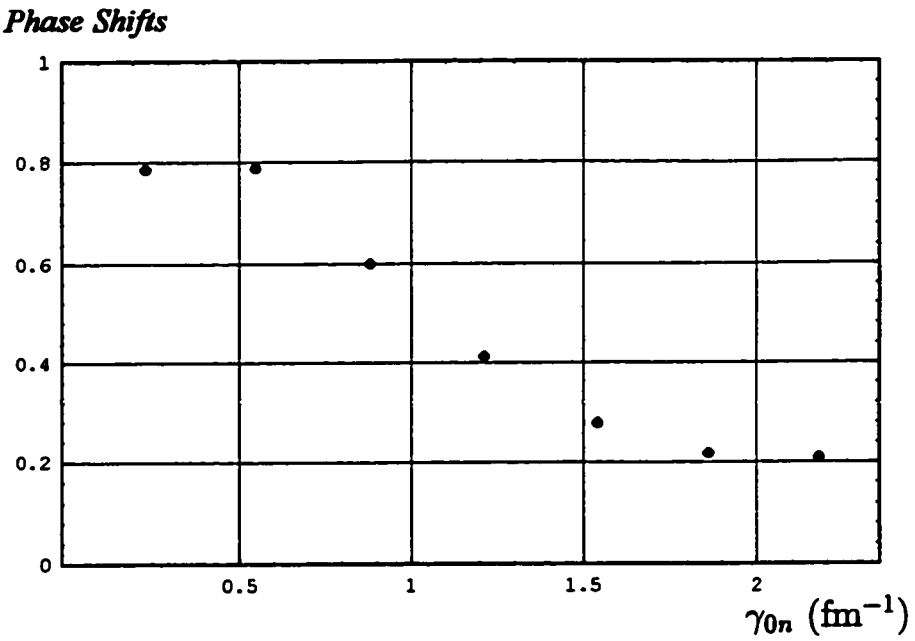

Fig. 7.12a : Discrete phase shifts produced by a nucleon scattered from a square well potential of depth $V = -20$ MeV and range $d = 2$ fm in $\ell = 0$. The discrete energies were obtained by solving the transcendental equation 7.6 for $a = 10$ fm.

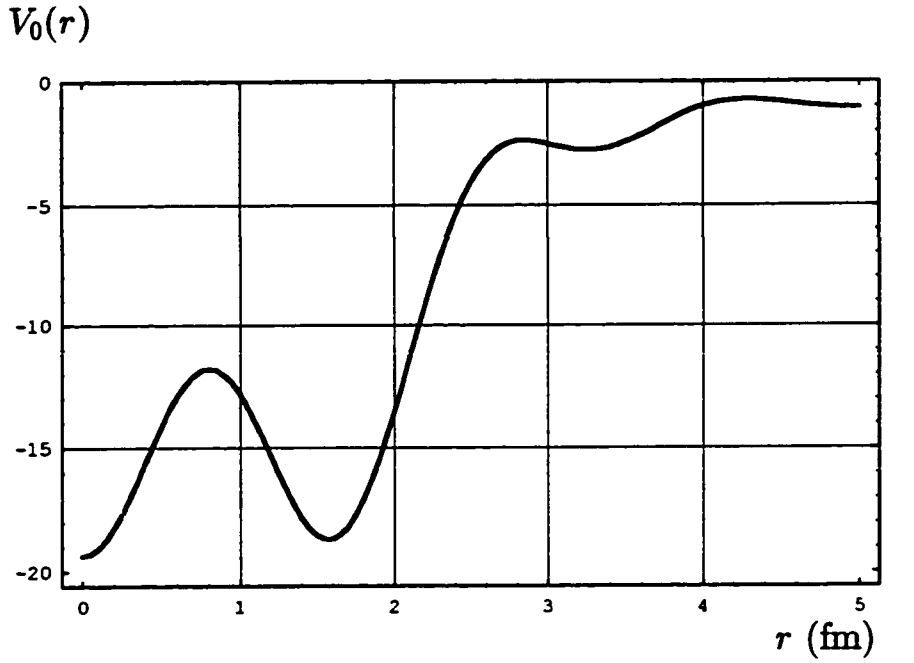

Fig. 7.12b : Potential calculated from eqn. (7.5) using the discrete perturbed energy states obtained in the above figure.

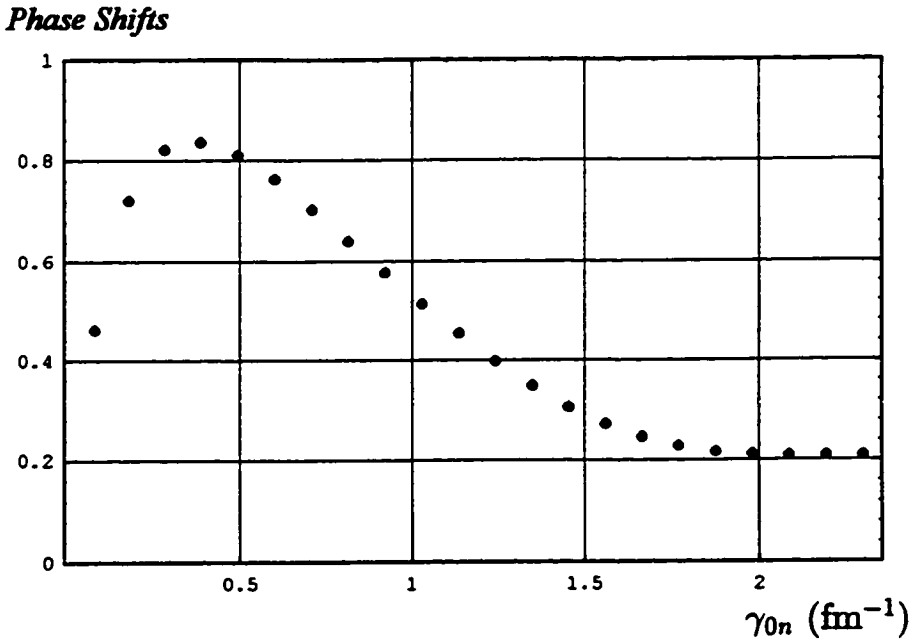

Fig. 7.13a : Discrete phase shifts produced by a nucleon scattered from a square well potential of depth $V = -20$ MeV and range $d = 2$ fm in $\ell = 0$. The discrete energies were obtained by solving the transcendental equation 7.6 for $a = 30$ fm.

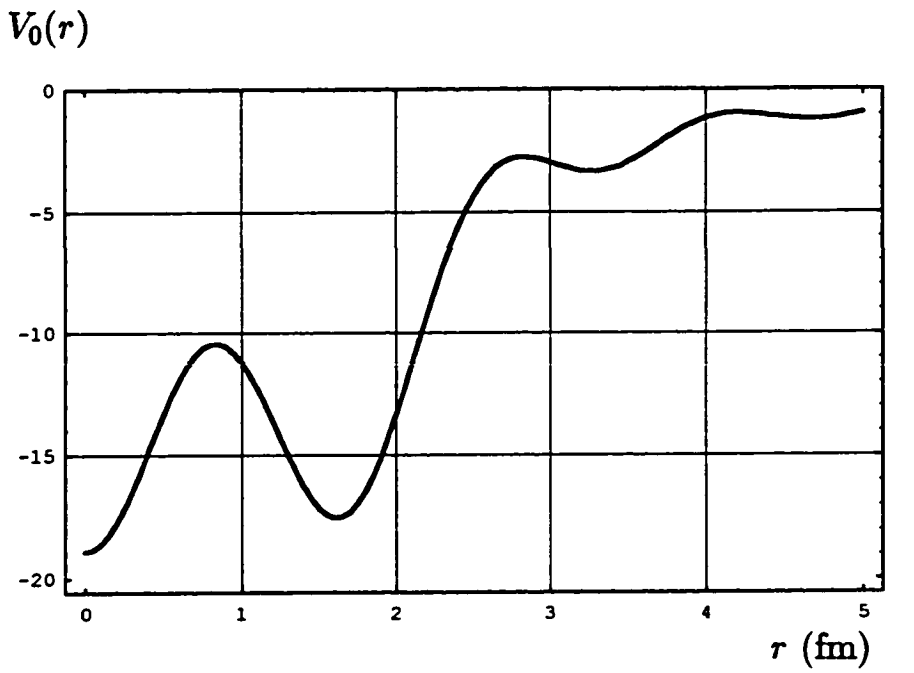

Fig. 7.13b : Potential calculated from eqn. (7.5) using the discrete perturbed energy states obtained in the above figure.

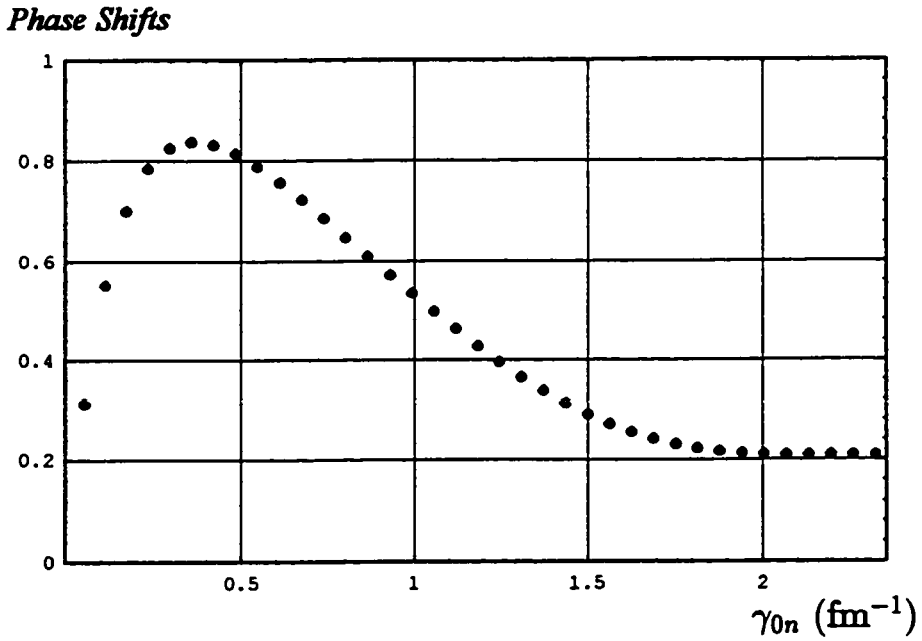

Fig. 7.14a : Discrete phase shifts produced by a nucleon scattered from a square well potential of depth $V = -20$ MeV and range $d = 2$ fm in $\ell = 0$. The discrete energies were obtained by solving the transcendental equation 7.6 for $a = 50$ fm.

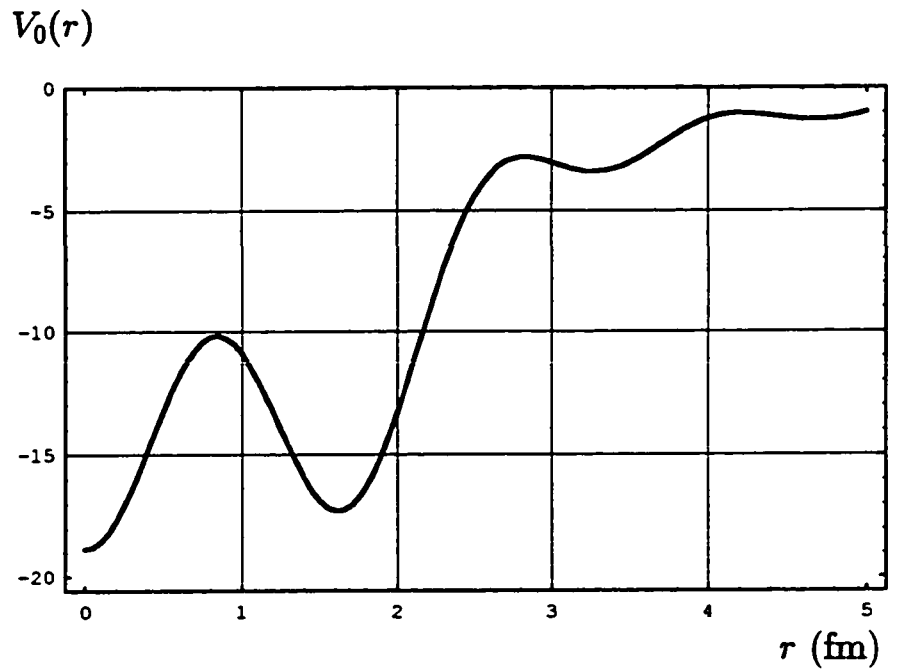

Fig. 7.14b : Potential calculated from eqn. (7.5) using the discrete perturbed energy states obtained in the above figure.

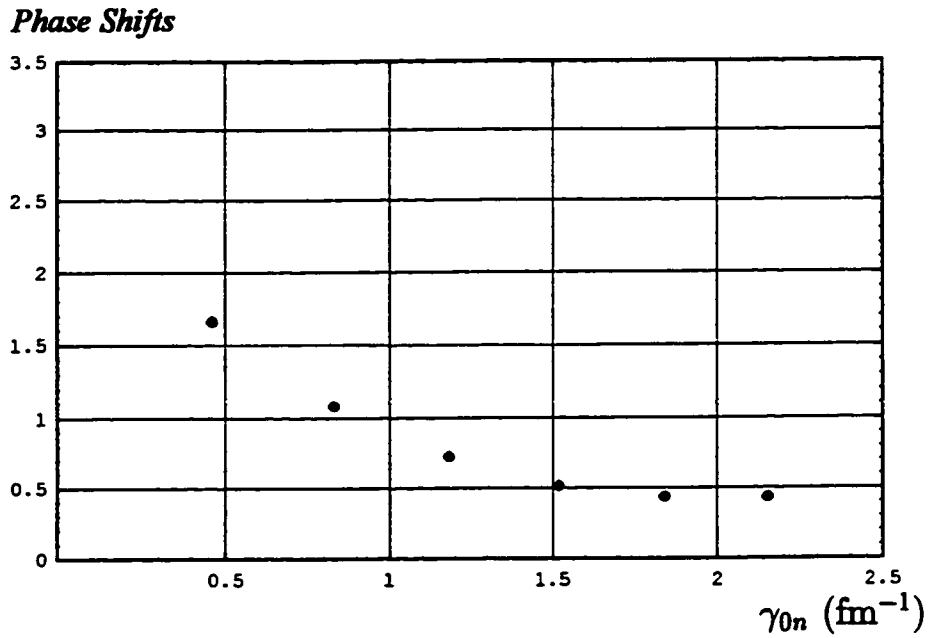

Fig. 7.15a : Discrete phase shifts produced by a nucleon scattered from a square well potential of depth $V = -40$ MeV and range $d = 2$ fm in $\ell = 0$. The discrete energies were obtained by solving the transcendental equation 7.6 for $a = 10$ fm.

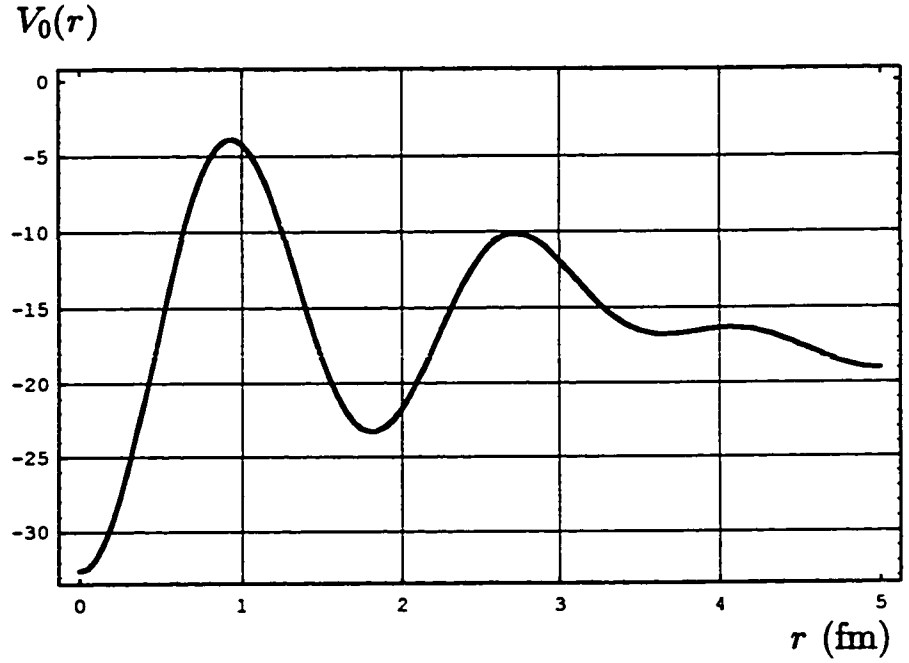

Fig. 7.15b : Potential calculated from eqn. (7.5) using the discrete perturbed energy states obtained in the above figure.

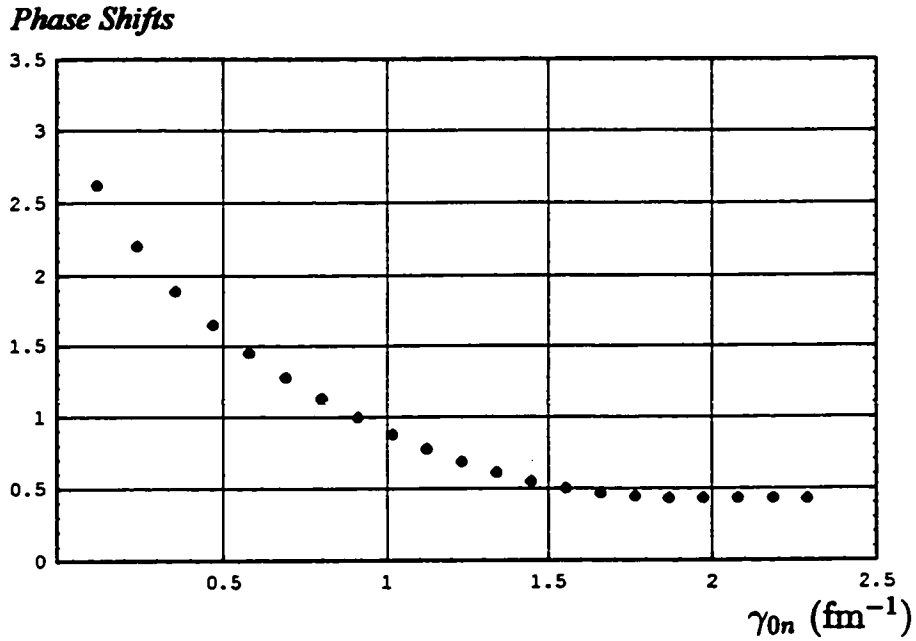

Fig. 7.16a : Discrete phase shifts produced by a nucleon scattered from a square well potential of depth $V = -40$ MeV and range $d = 2$ fm in $\ell = 0$. The discrete energies were obtained by solving the transcendental equation 7.6 for $a = 30$ fm.

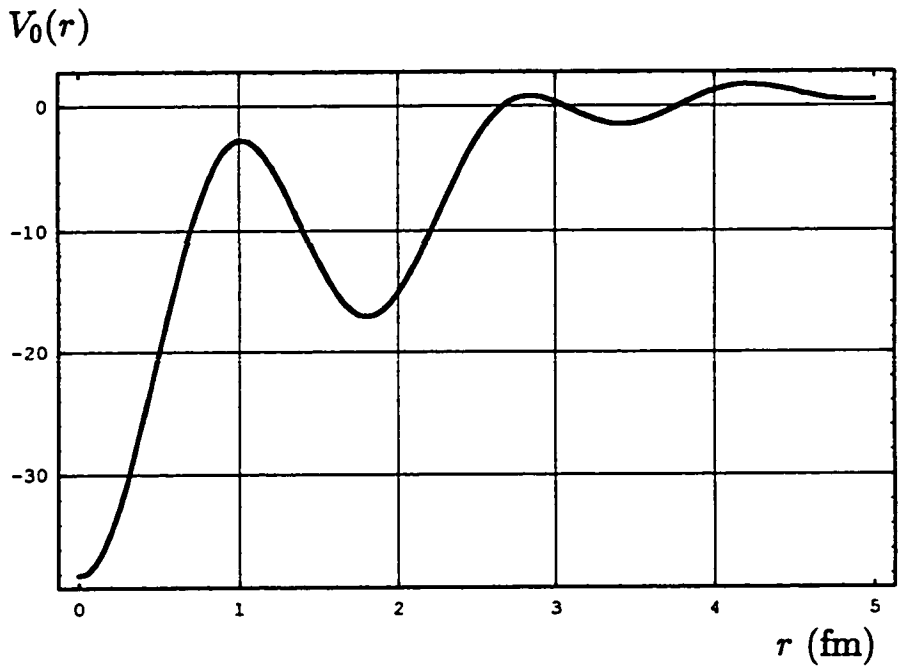

Fig. 7.16b : Potential calculated from eqn. (7.5) using the discrete perturbed energy states obtained in the above figure.

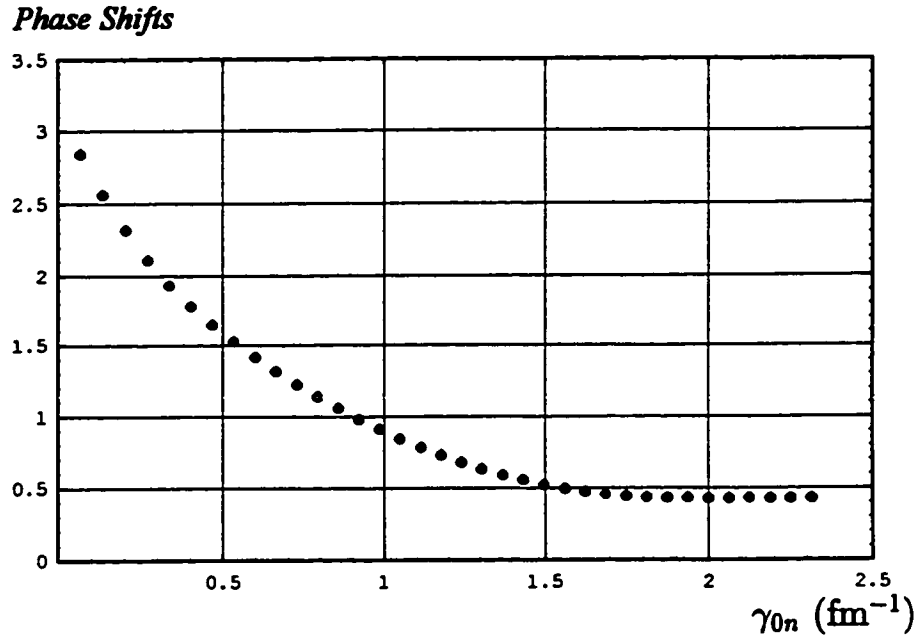

Fig. 7.17a : Discrete phase shifts produced by a nucleon scattered from a square well potential of depth $V = -40$ MeV and range $d = 2$ fm in $\ell = 0$. The discrete energies were obtained by solving the transcendental equation 7.6 for $a = 50$ fm.

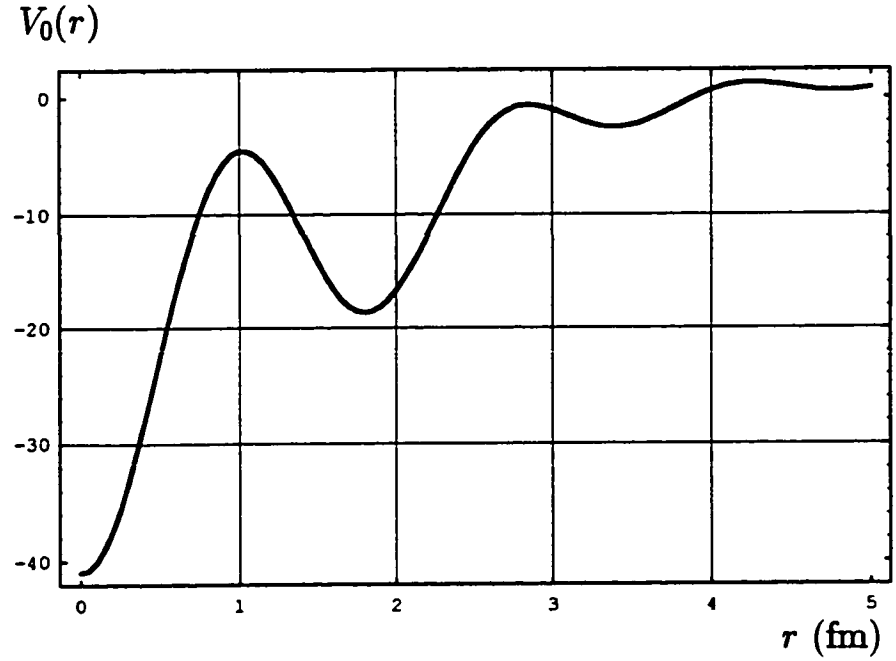

Fig. 7.17b : Potential calculated from eqn. (7.5) using the discrete perturbed energy states obtained in the above figure.

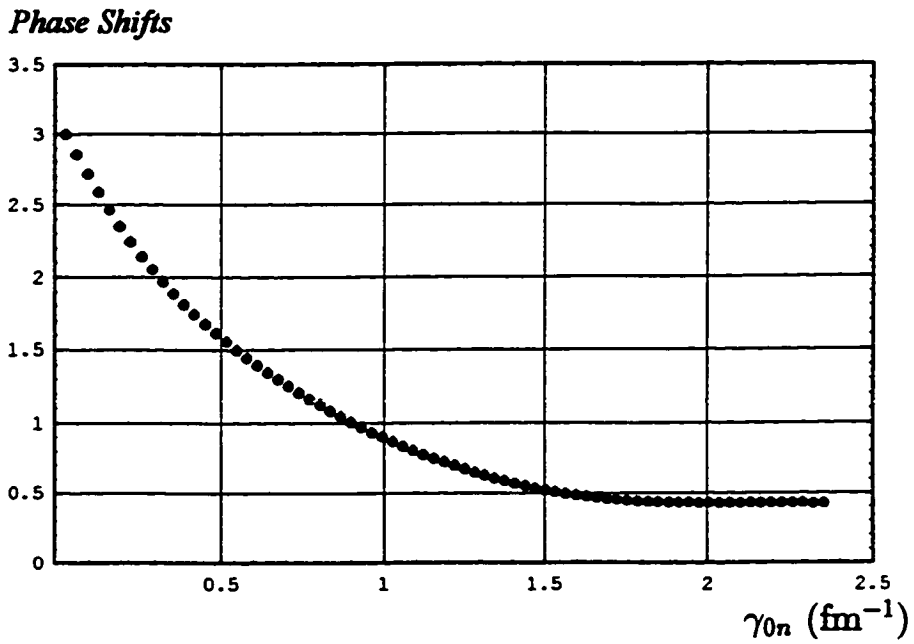

Fig. 7.18a : Discrete phase shifts produced by a nucleon scattered from a square well potential of depth $V = -40$ MeV and range $d = 2$ fm in $\ell = 0$. The discrete energies were obtained by solving the transcendental equation 7.6 for $a = 100$ fm.

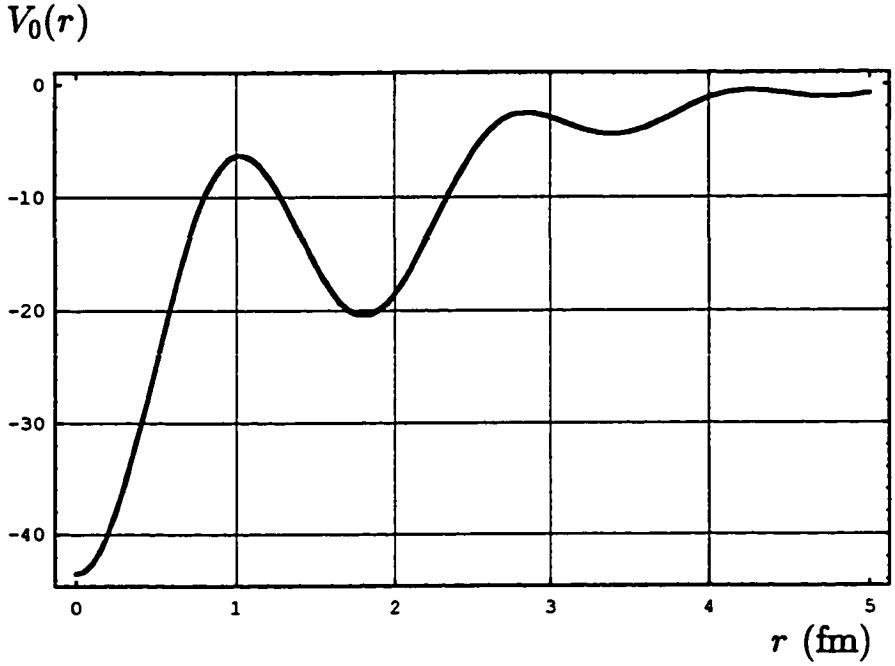

Fig. 7.18b : Potential calculated from eqn. (7.5) using the discrete perturbed energy states obtained in the above figure.

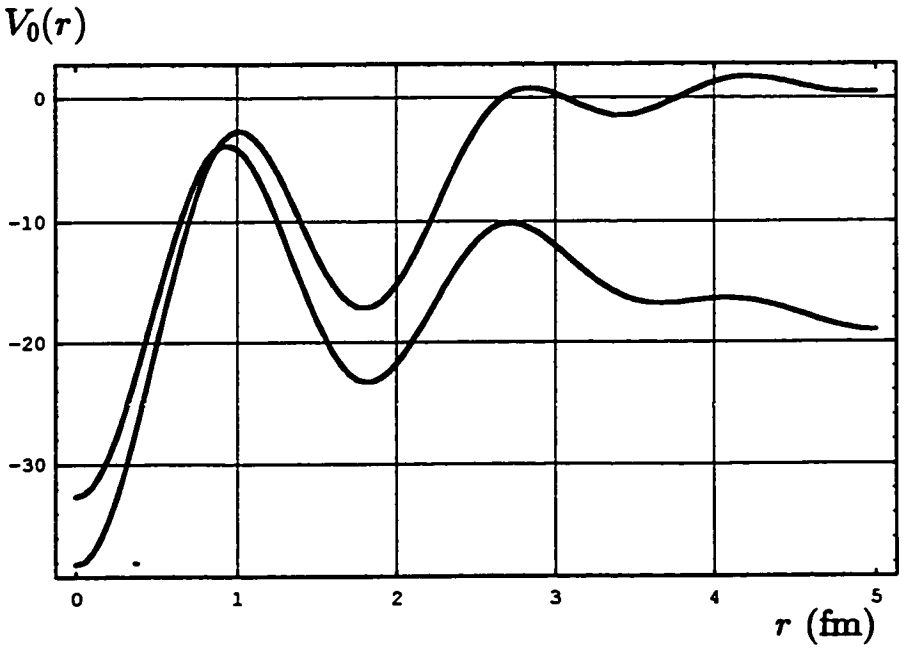

Fig. 7.19 : Comparison between potentials calculated using discrete phase shifts of a square well potential of depth $V = -40$ MeV and range $d = 2$ fm, in $\ell = 0$ for $a = 10$ and 30 fm.

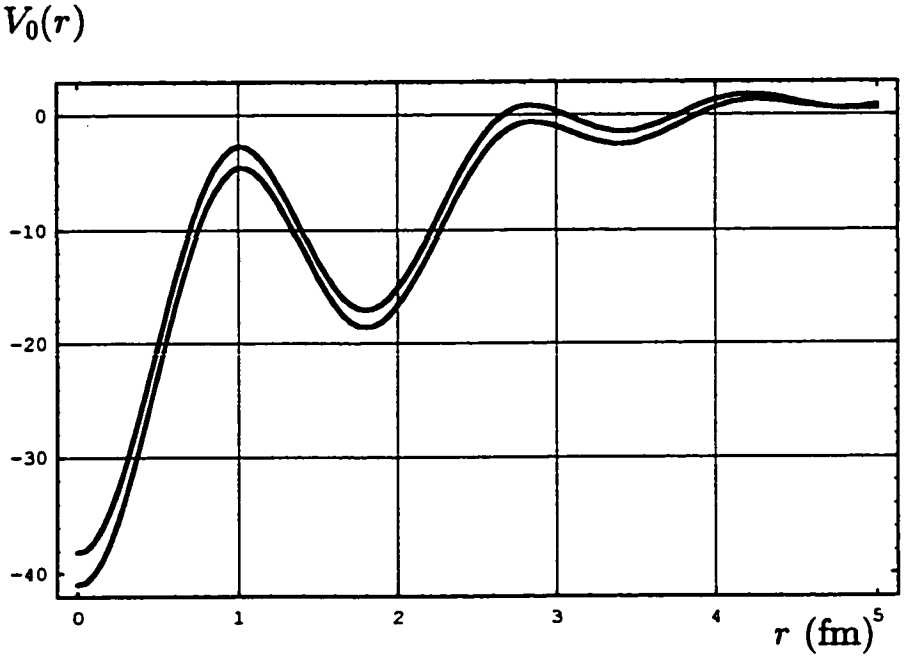

Fig. 7.20 : Comparison between potentials calculated using discrete phase shifts of a square well potential of depth $V = -40$ MeV and range $d = 2$ fm, in $\ell = 0$ for $a = 30$ and 50 fm.

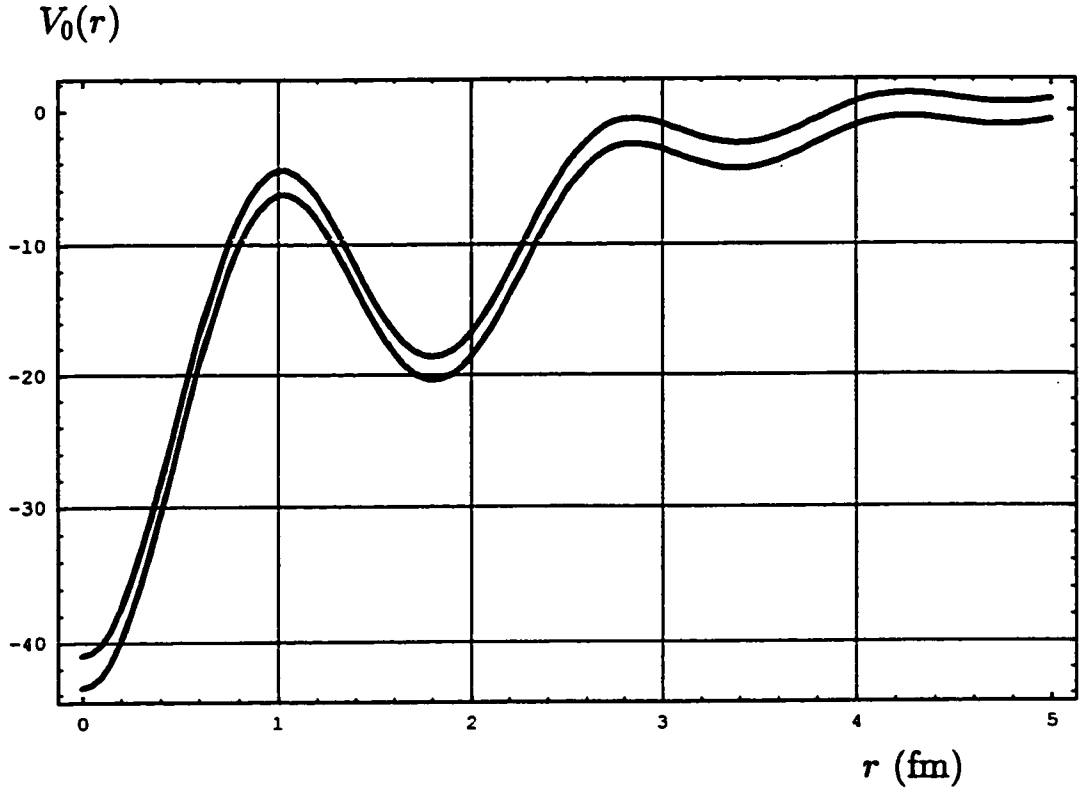

Fig. 7.21 : Comparison between "experimental" potentials produced using discrete phase shifts of a square well potential of depth $V = -40$ MeV and range $d = 2$ fm in the angular momentum channel ℓ=0 for $a = 50$ and 100 fm.

Example 7.2 :

Consider a particle of mass $\mu = 469.5$ MeV/c^2 scattered off a square well potential of depth V and range $d = 2$ fm in the angular momentum channel $\ell = 1$, in a sphere of radius a. In this case, the finite space phase shift, eqn. (7.1), reduces to[3]

$$\delta_1(\gamma_{1n}) = \tan^{-1}(\gamma_{1n}a) - \gamma_{1n}a. \tag{7.9}$$

The plot of eqn. (7.9) for different values of n is given in fig. 7.22.

The potential $V_1(r)$, is given by

$$V_1(r) = \frac{4k_{11}L}{3\pi} + \sum_{n=1}^{n=m}\left[\frac{\hbar^2}{2\mu}\left(\frac{\gamma_{1n}^2 - k_{1n}^2}{\aleph_{1n}^2}\right) - L\right]\frac{g_1(k_{1n}r)}{k_{1n}^2 r^2}\Delta k_{1n}, \tag{7.10}$$

where the sum in eqn. (7.10) was truncated for the reasons discussed previously.

Let us study the following cases :

Case I) : Consider a square well potential of depth $V = -5$ MeV in a sphere of radius $a = 10$ fm. The "experimental" phase shifts $\delta_1^{ex}(k)$ of this potential is given in fig. 7.23. Solving the transcendental equation

$$\delta_1^{ex}(k)|_{k=\gamma_{1n}} = \tan^{-1}(\gamma_{1n}a) - \gamma_{1n}a, \quad n = 1, 2, \ldots, m, \tag{7.11}$$

graphically, as in fig. 7.24, or numerically, one can obtain the discrete phase shifts at the discrete perturbed energy states, see fig. 7.25a. substituting the obtained discrete perturbed energy states γ_{1n} in eqn. (7.10), one can obtain the potential

[3]See chapter 4, eqn. (4.63)

$V_1(r)$, see fig. 7.25b. As can be seen from fig. 7.25b, the potential obtained is, to a good approximation, a square well potential of depth $V = -5$ MeV. Figures 7.26a and 7.27a, show the discrete finite space phase shifts for the same potential but for $a = 30$ and 50 fm respectively while figures 7.26b and 7.27b show the corresponding potentials. As can be seen from figures 7.28 and 7.29, increasing the radius of the sphere from $a = 10$ fm to $a = 30$ fm results in improving the tail of the potential while increasing a from 30 to 50 fm does not result in any considerable changes in the shape of the potential.

Case II) : Consider a square well potential of depth $V = -10$ MeV. One can use the argument above to obtain the discrete phase shifts at the corresponding perturbed energies. The discrete phase shifts for $a = 50$ fm are shown in fig. 7.30a while the corresponding potential is given in fig. 7.30b.

Case III) : Consider a square well potential of depth $V = -20$ MeV. Using the argument in case I, one can obtain the discrete phase shifts and the corresponding potentials. Fig. 7.31a shows the discrete phase shifts for $a = 50$ fm while the corresponding potential is shown in fig. 7.31b. Increasing the radius of the sphere from $a = 10$ fm to $a = 30$ fm results in improving the tail of the potential while increasing a from 30 to 50 fm does not result in any considerable changes in the shape of the potential.

Case IV) : Consider a square well potential of depth $V = -40$ MeV. The discrete phase shifts for $a = 50$ fm are shown in fig. 7.32a while the corresponding potential is given in fig. 7.32b. Increasing the radius of the sphere from $a = 10$ fm to $a = 30$ fm results in improving the tail of the potential while increasing a from 30 to 50 fm does not result in any considerable changes in the shape of the potential.

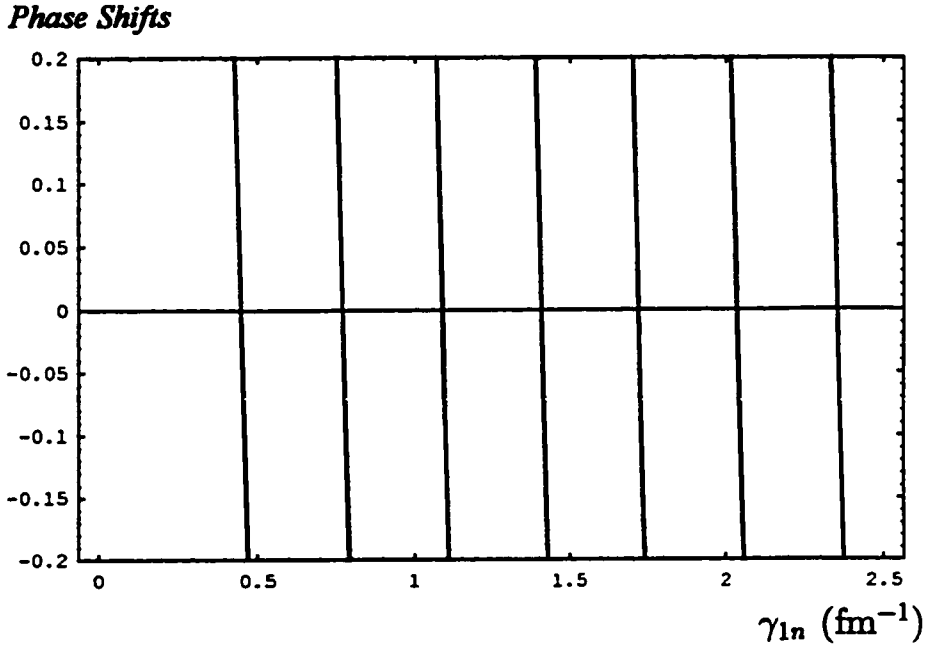

Fig. 7.22 : Plot of eqn. (7.9) for $n = 1$ to $n = 7$.

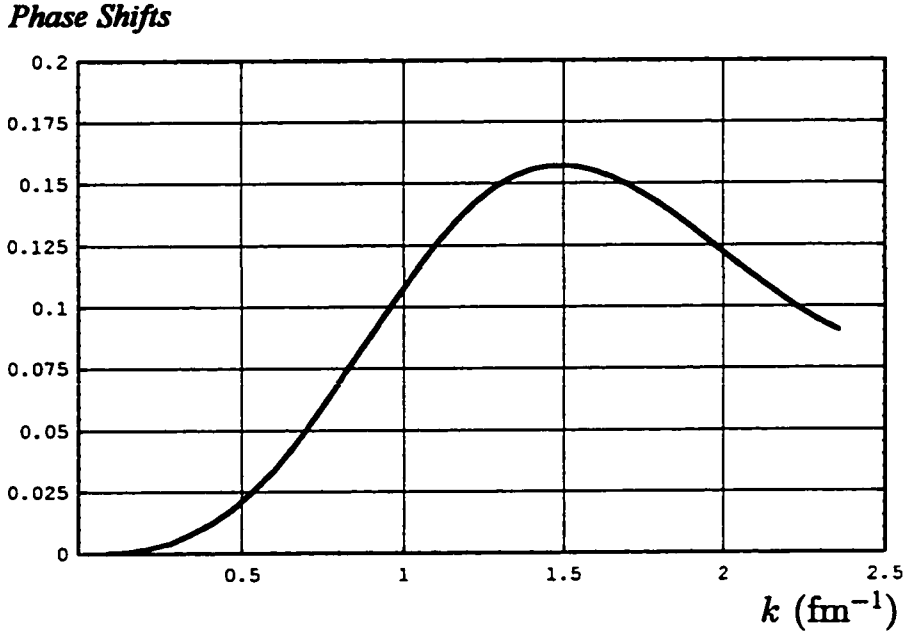

Fig. 7.23 : "Experimental" phase shifts produced by a nucleon scattered off a square well potential of depth $V = -5$ MeV and range $d = 2$ fm, in the angular momentum channel $\ell = 1$.

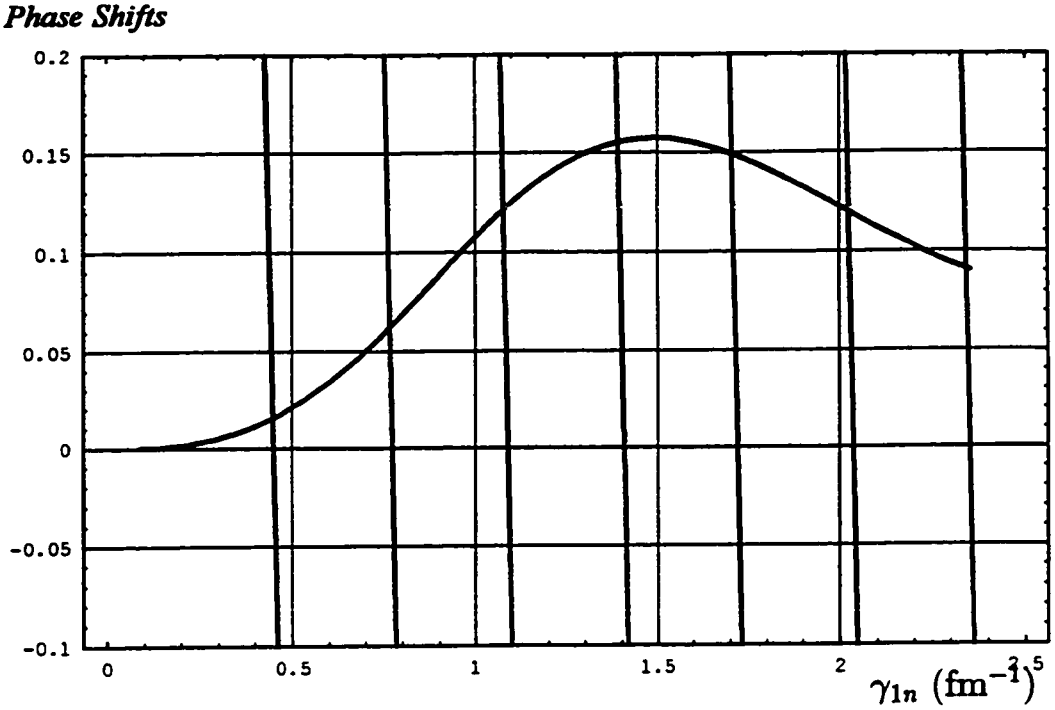

Fig. 7.24 : Graphical solution of the transcendental equation (7.11). The energies at which the intersections of the curve, which represents the "experimental" phase shifts, with the straight lines, which represents the discrete phase shifts, occur represents the discrete perturbed energy states.

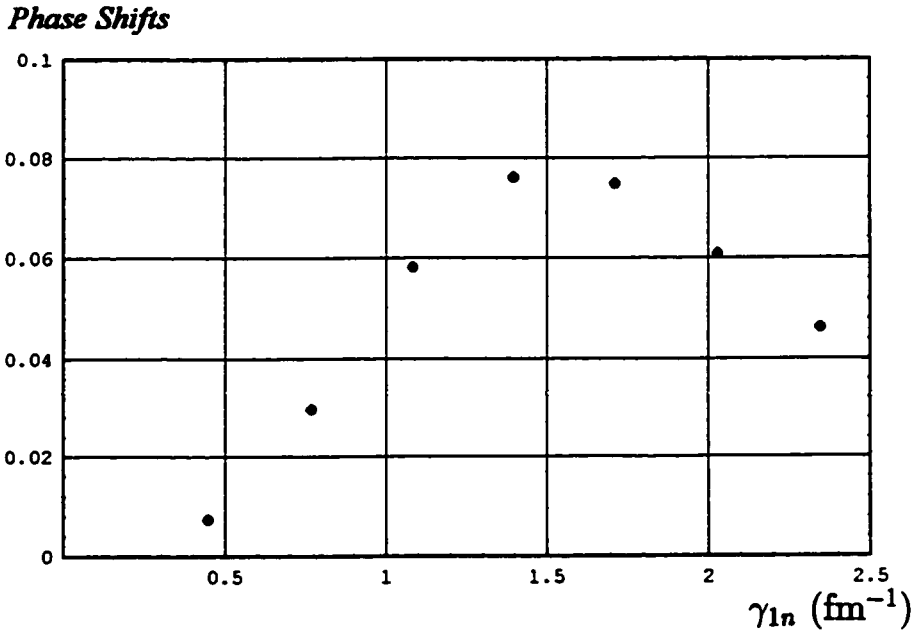

Fig. 7.25a : Discrete phase shifts produced by a nucleon scattered from a square well potential of depth $V = -5$ MeV and range $d = 2$ fm in $\ell = 1$. The discrete energies were obtained by solving the transcendental equation 7.11 for $a = 10$ fm.

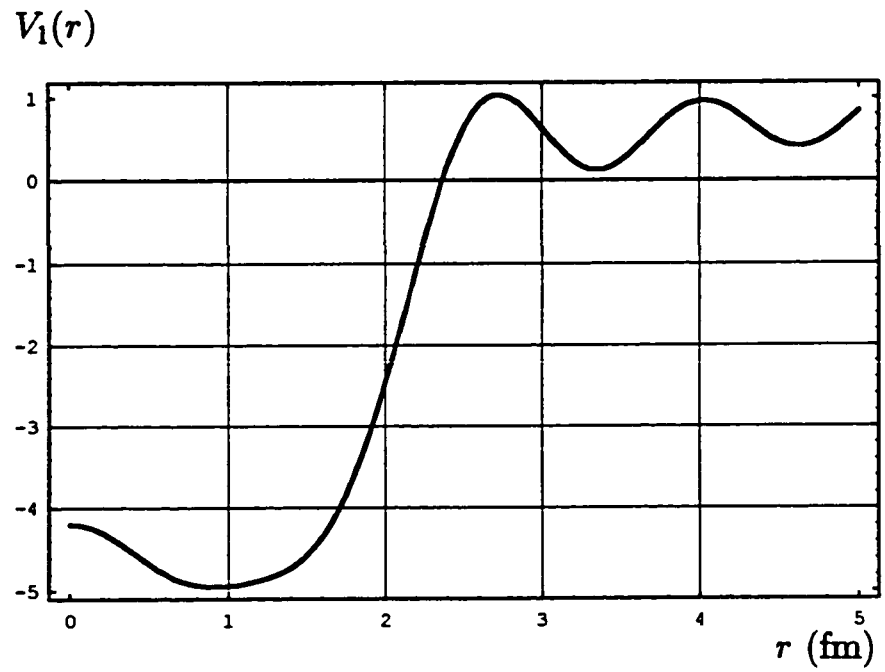

Fig. 7.25b : Potential calculated from eqn. (7.10) using the discrete perturbed energy states obtained in the above figure.

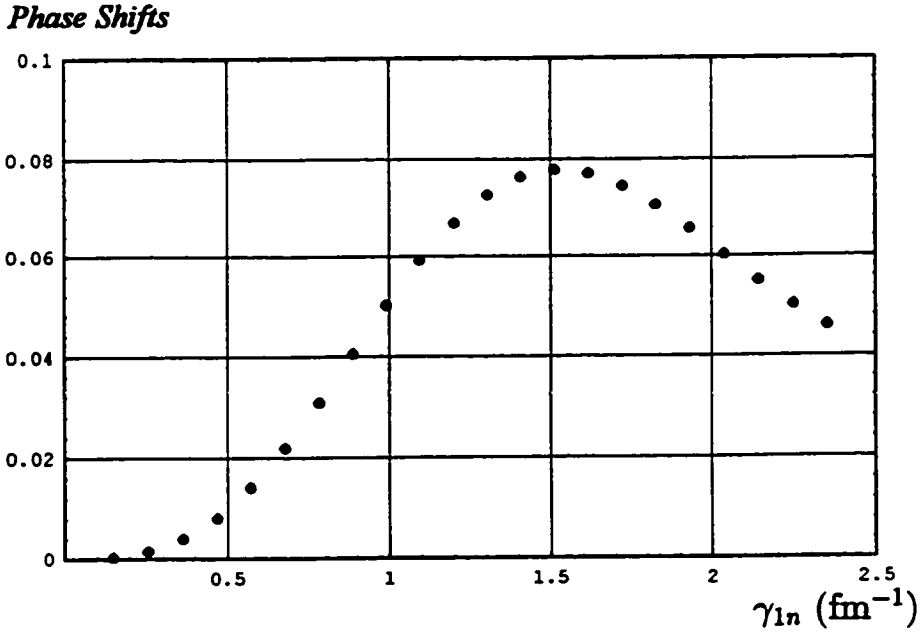

Fig. 7.26a : Discrete phase shifts produced by a nucleon scattered from a square well potential of depth $V = -5$ MeV and range $d = 2$ fm in $\ell = 1$. The discrete energies were obtained by solving the transcendental equation 7.11 for $a = 30$ fm.

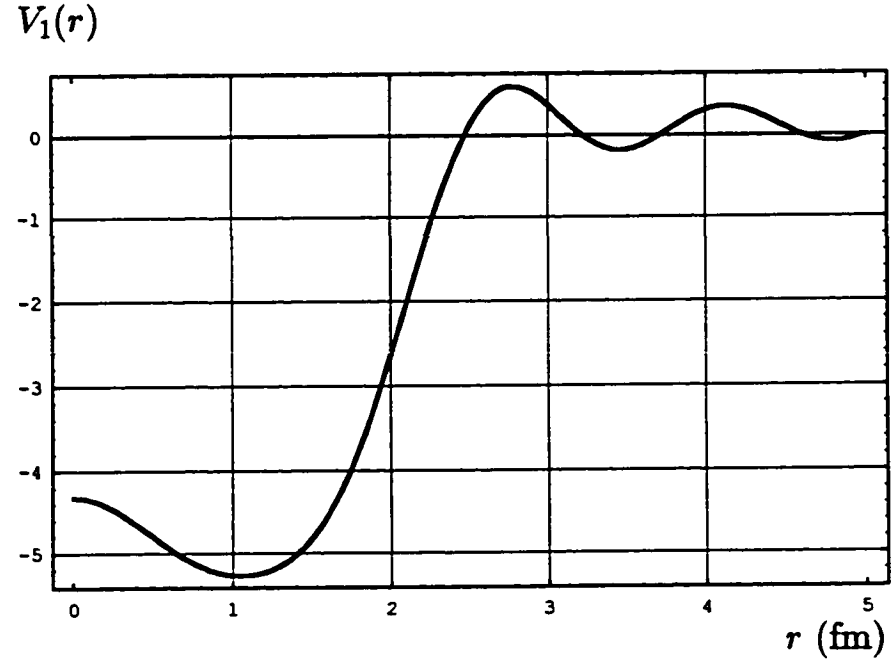

Fig. 7.26b : Potential calculated from eqn. (7.10) using the discrete perturbed energy states obtained in the above figure.

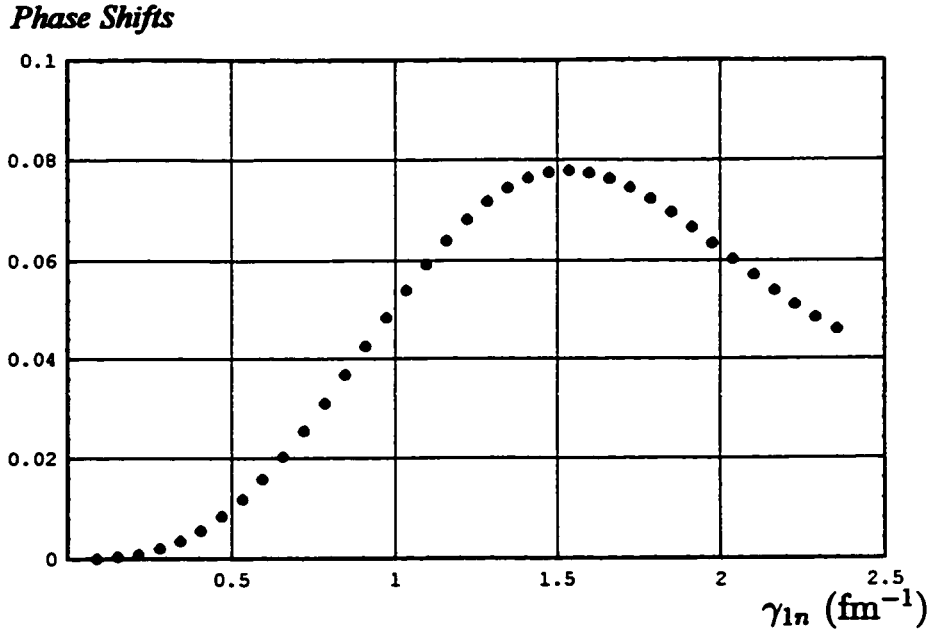

Fig. 7.27a : Discrete phase shifts produced by a nucleon scattered from a square well potential of depth $V = -5$ MeV and range $d = 2$ fm in $\ell = 1$. The discrete energies were obtained by solving the transcendental equation 7.11 for $a = 50$ fm.

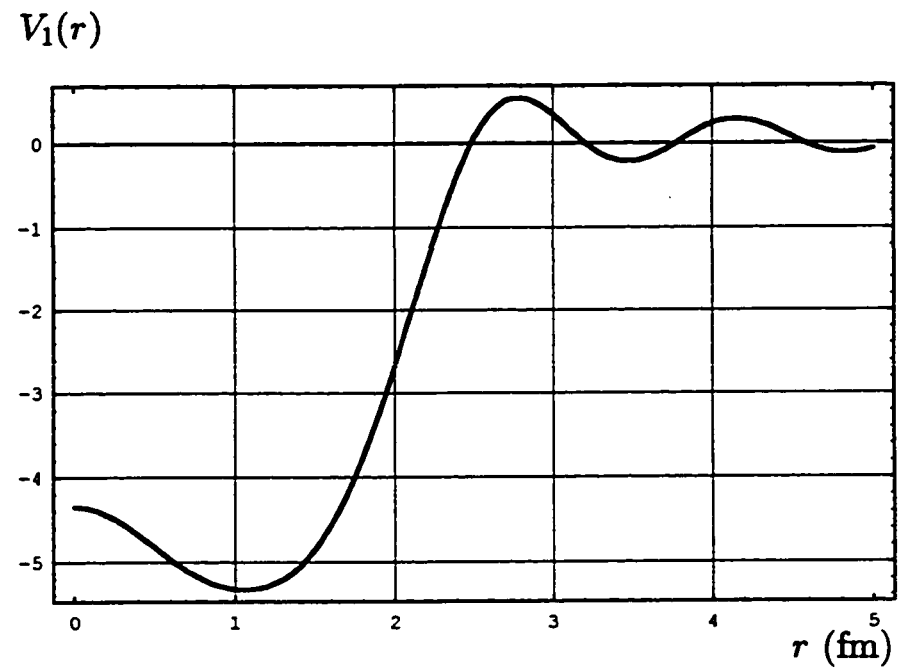

Fig. 7.27b : Potential calculated from eqn. (7.10) using the discrete perturbed energy states obtained in the above figure.

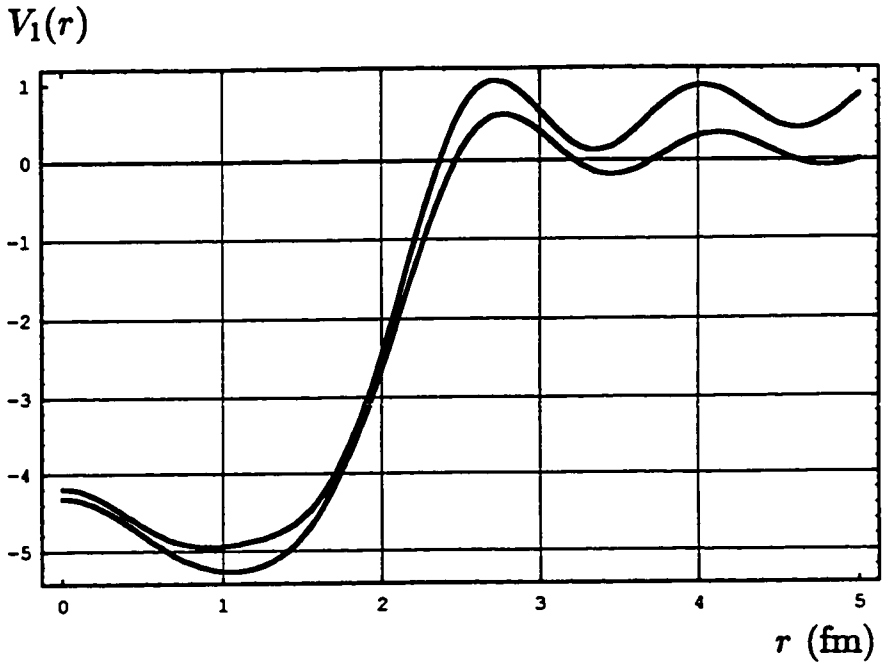

Fig. 7.28 : Comparison between potentials obtained in figs. 7.25b and 7.26b.

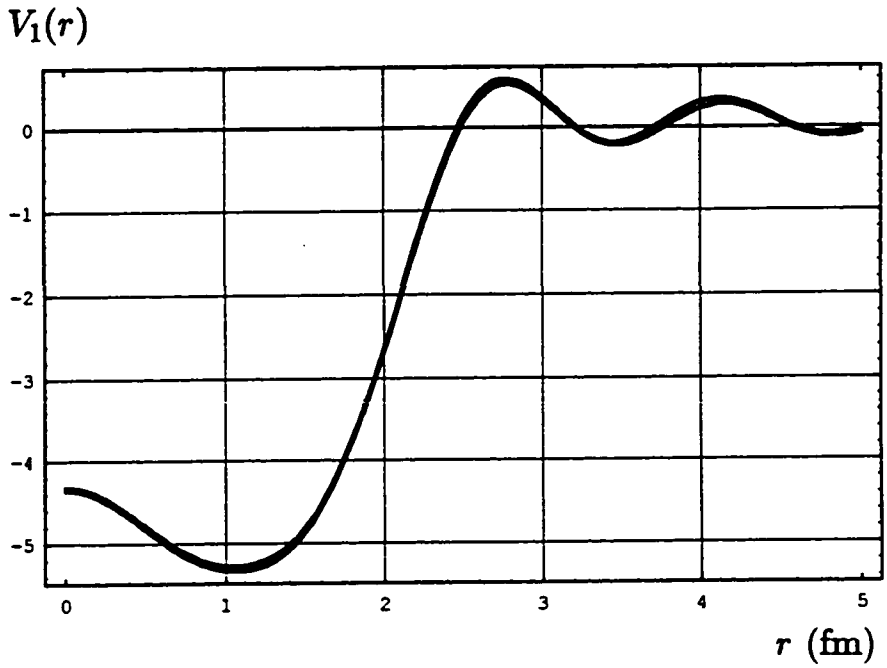

Fig. 7.29 : Comparison between potentials obtained in figs. 7.26b and 7.27b.

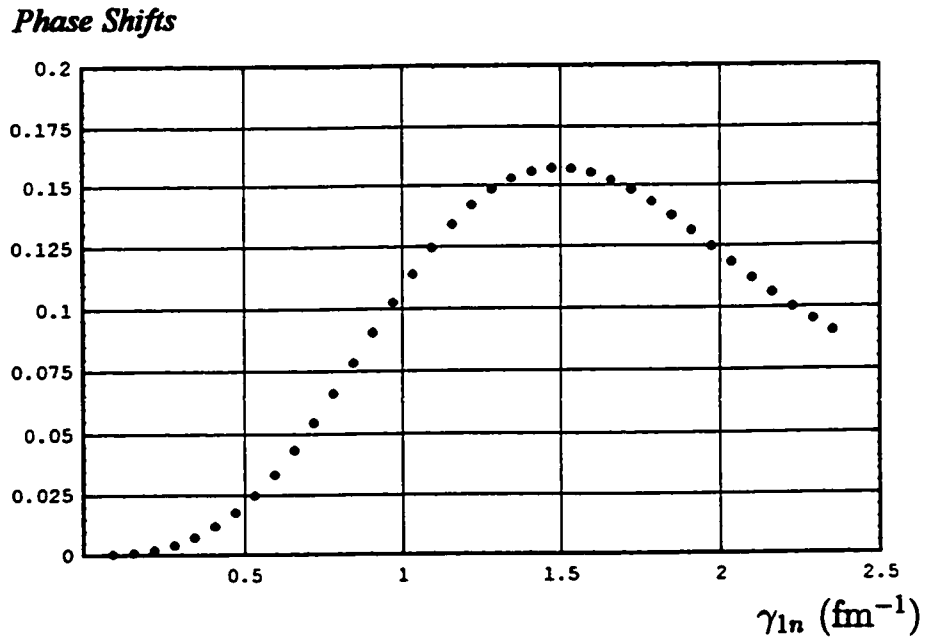

Fig. 7.30a : Discrete phase shifts produced by a nucleon scattered from a square well potential of depth $V = -10$ MeV and range $d = 2$ fm in $\ell = 1$. The discrete energies were obtained by solving the transcendental equation 7.11 for $a = 50$ fm.

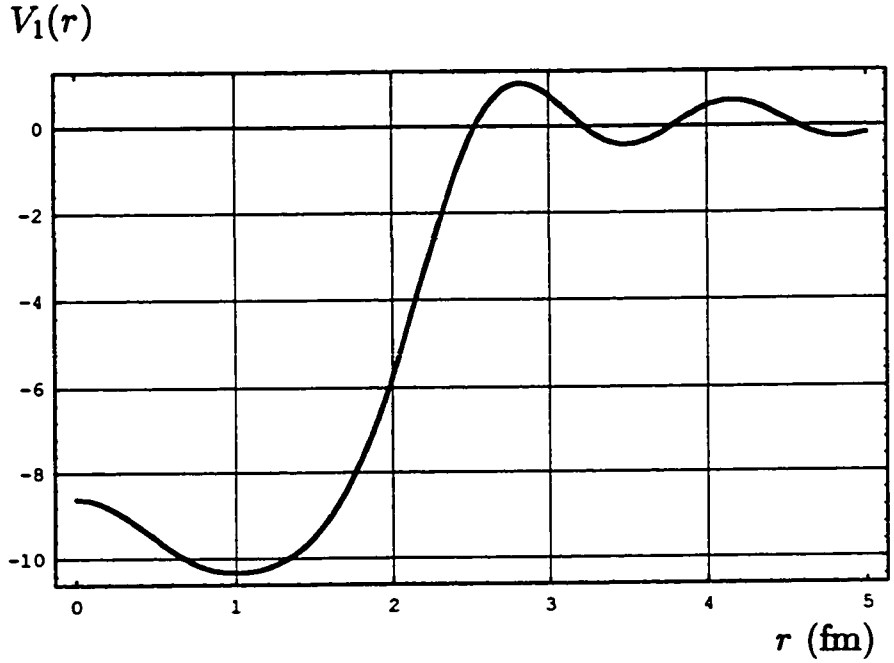

Fig. 7.30b : Potential calculated from eqn. (7.10) using the discrete perturbed energy states obtained in the above figure.

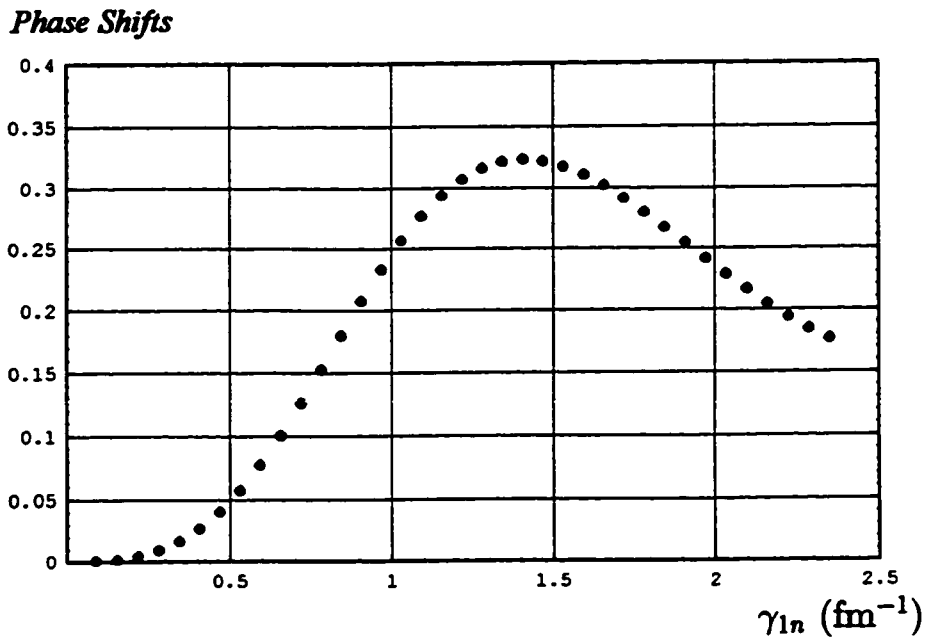

Fig. 7.31a : Discrete phase shifts produced by a nucleon scattered from a square well potential of depth $V = -20$ MeV and range $d = 2$ fm in $\ell = 1$. The discrete energies were obtained by solving the transcendental equation 7.11 for $a = 50$ fm.

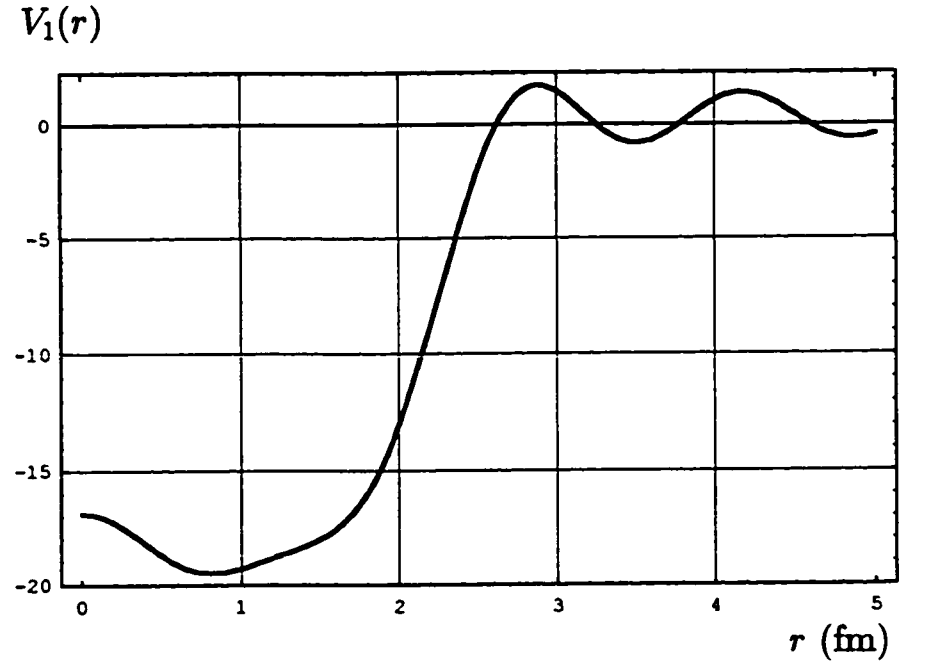

Fig. 7.31b : Potential calculated from eqn. (7.10) using the discrete perturbed energy states obtained in the above figure.

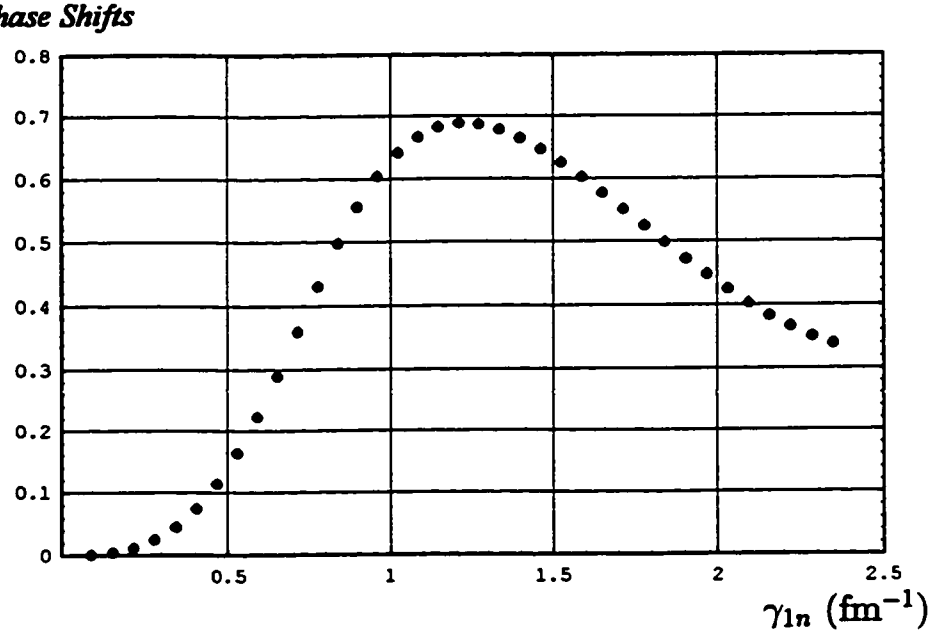

Fig. 7.32a : Discrete phase shifts produced by a nucleon scattered from a square well potential of depth $V = -40$ MeV and range $d = 2$ fm in $\ell = 1$. The discrete energies were obtained by solving the transcendental equation 7.11 for $a = 50$ fm.

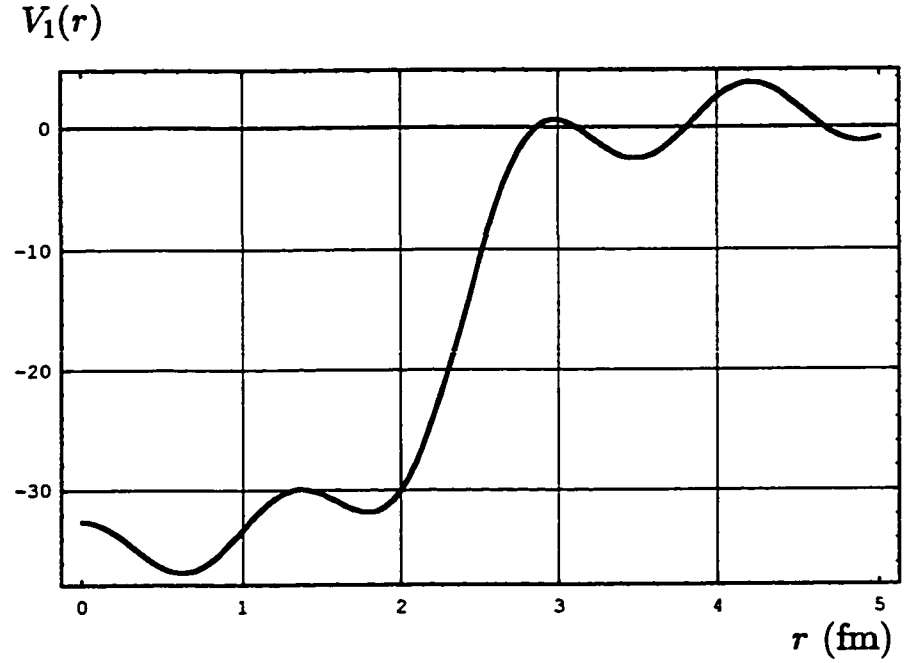

Fig. 7.32b : Potential calculated from eqn. (7.10) using the discrete perturbed energy states obtained in the above figure.

Example 7.3 :

Consider a particle of mass $\mu = 469.5\ \mathrm{MeV}/c^2$ scattered off a square well potential of depth V and range $d = 2$ fm in the angular momentum channel $\ell = 2$, in a sphere of radius a. In this case, the finite space phase shift, eqn. (7.1), reduces to[4]

$$\delta_2(\gamma_{2n}) = \tan^{-1}\left\{\frac{3\gamma_{2n}a}{3-(\gamma_{2n}a)^2}\right\} - \gamma_{2n}a. \tag{7.12}$$

The plot of eqn. (7.12) for different values of n is given in fig. 7.33.

The potential $V_2(r)$, is given by

$$V_2(r) = \frac{4k_{21}L}{5\pi} + \sum_{n=1}^{n=m}\left[\frac{\hbar^2}{2\mu}\left(\frac{\gamma_{2n}^2 - k_{2n}^2}{\aleph_{2n}^2}\right) - L\right]\frac{g_2(k_{2n}r)}{k_{2n}^2 r^2}\Delta k_{2n}, \tag{7.13}$$

where the sum in eqn. (7.13) was truncated for the reasons discussed previously.

Let us study the following cases :

Case I) : Consider a square well potential of depth $V = -5$ MeV in a sphere of radius $a = 10$ fm. The "experimental" phase shifts $\delta_2^{ex}(k)$ of this potential is given in fig. 7.34. Solving the transcendental equation

$$\delta_2^{ex}(k)|_{k=\gamma_{2n}} = \delta_2(\gamma_{2n}) = \tan^{-1}\left\{\frac{3\gamma_{2n}a}{3-(\gamma_{2n}a)^2}\right\} - \gamma_{2n}a, \quad n = 1, 2, \ldots, m, \tag{7.14}$$

graphically, as in fig. 7.35, or numerically, one can obtain the discrete phase shifts at the discrete perturbed energy states, see fig. 7.36a. substituting the obtained discrete perturbed energy states γ_{1n} in eqn. (7.13), one can obtain the potential

[4]See chapter 4, eqn. (4.64)

$V_1(r)$, see fig. 7.36b. As can be seen from fig. 7.36b, the potential obtained is, to a good approximation, a square well potential of depth $V = -5$ MeV. Figures 7.37a and 7.38a, show the discrete finite space phase shifts for the same potential but for $a = 30$ and 50 fm respectively while figures 7.37b and 7.38b show the corresponding potentials. As can be seen from figures 7.39 and 7.40, increasing the radius of the sphere from $a = 10$ fm to $a = 30$ fm results in improving the tail of the potential while increasing a from 30 to 50 fm does not result in any considerable changes in the shape of the potential.

Case II) : Consider a square well potential of depth $V = -10$ MeV. One can use the argument above to obtain the discrete phase shifts at the corresponding perturbed energies. The discrete phase shifts for $a = 50$ fm are shown in fig. 7.41a while the corresponding potential is given in fig. 7.41b.

Case III) : Consider a square well potential of depth $V = -20$ MeV. Using the argument in case I, one can obtain the discrete phase shifts and the corresponding potentials. Fig. 7.42a shows the discrete phase shifts for $a = 50$ fm while the corresponding potential is shown in fig. 7.42b. Increasing the radius of the sphere from $a = 10$ fm to $a = 30$ fm results in improving the tail of the potential while increasing a from 30 to 50 fm does not result in any considerable changes in the shape of the potential.

Case IV) : Consider a square well potential of depth $V = -40$ MeV. The discrete phase shifts for $a = 50$ fm are shown in fig. 7.43a while the corresponding potential is given in fig. 7.43b. Similarly, increasing the radius of the sphere from $a = 10$ fm to $a = 30$ fm results in improving the tail of the potential while increasing a from 30 to 50 fm does not result in any considerable changes in the shape of the potential.

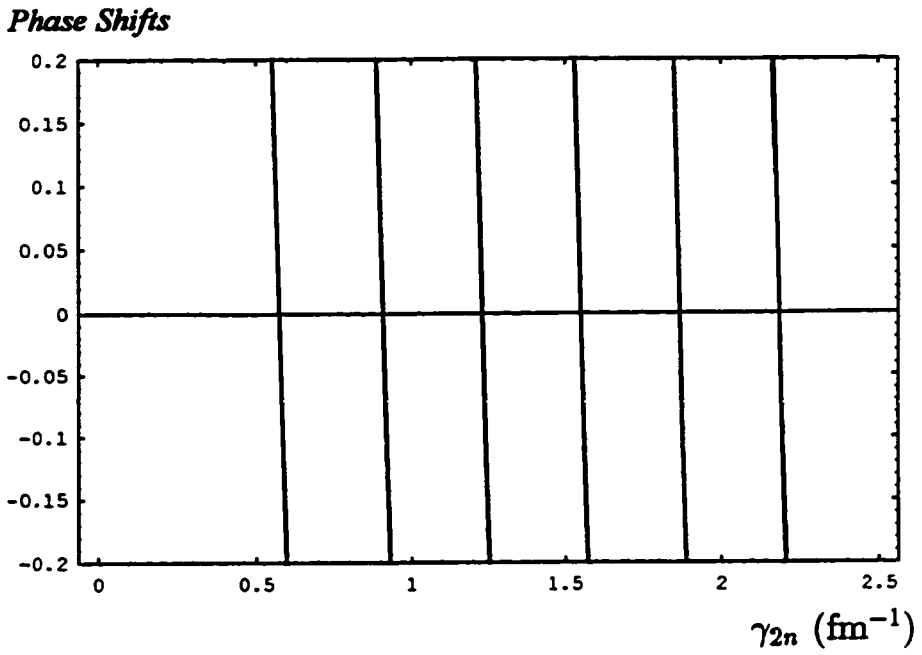

Fig. 7.33 : Plot of eqn. (7.12) for $n = 1$ to $n = 7$.

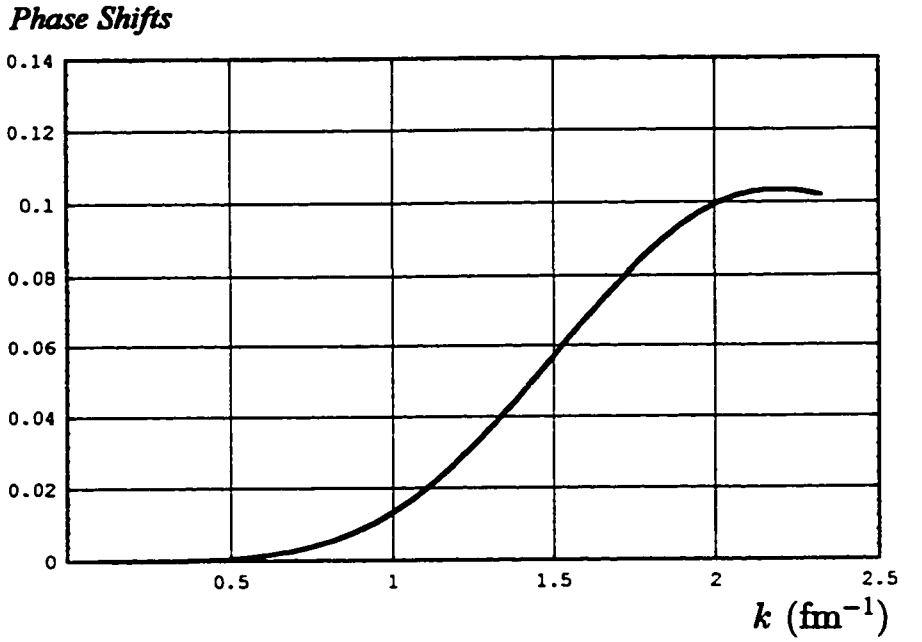

Fig. 7.34 : "Experimental" phase shifts produced by a nucleon scattered off a square well potential of depth $V = -5$ MeV and range $d = 2$ fm, in the angular momentum channel $\ell = 2$.

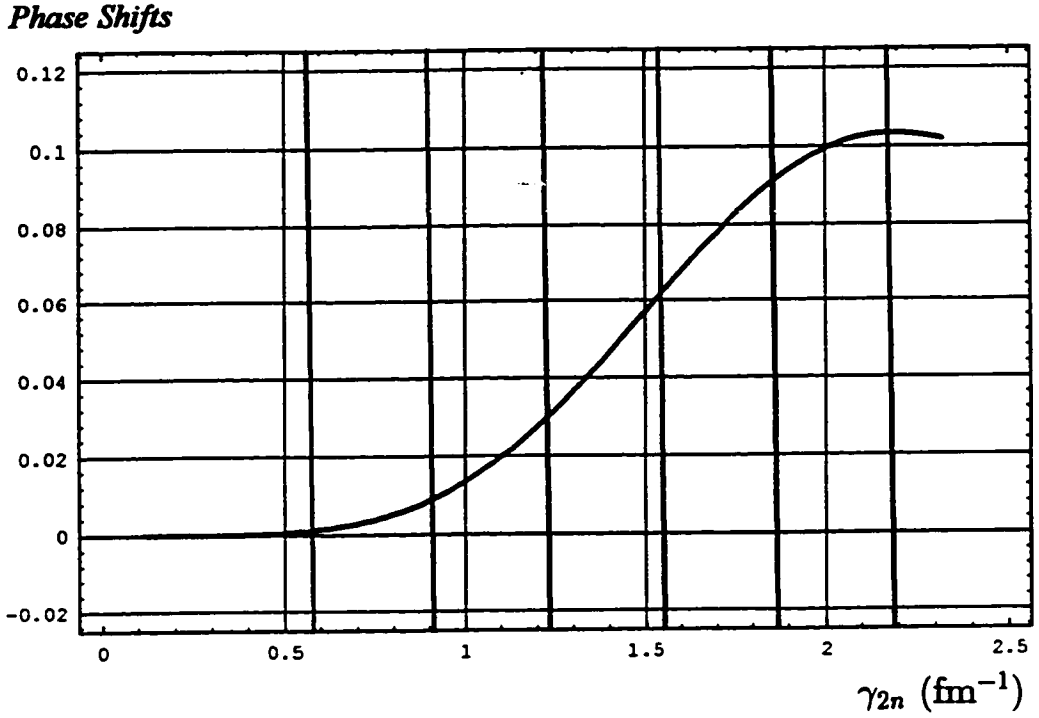

Fig. 7.35 : Graphical solution of the transcendental equation (7.14). The energies at which the intersections of the curve, which represents the "experimental" phase shifts, with the straight lines, which represents the discrete phase shifts, occur represents the discrete perturbed energy states.

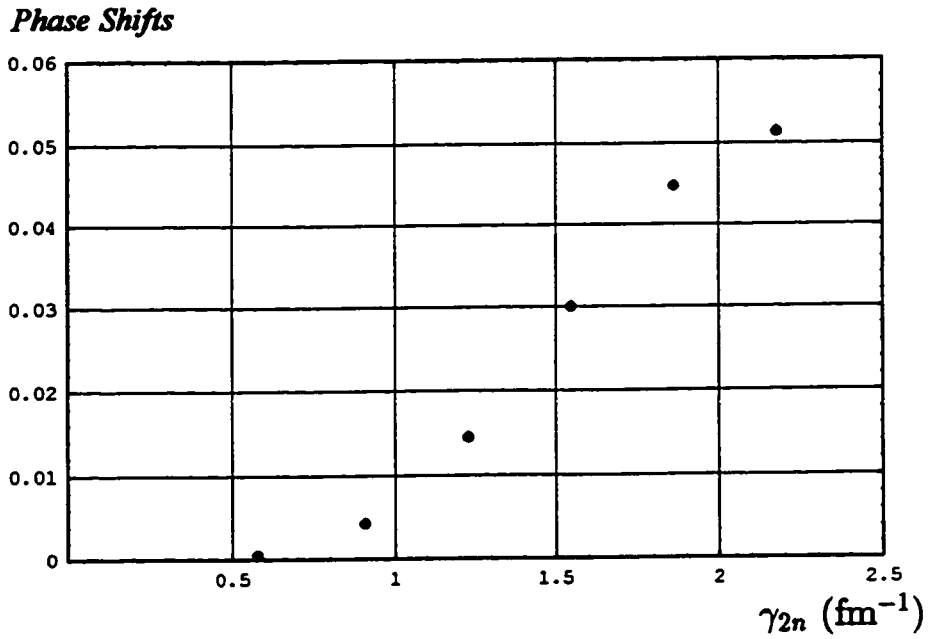

Fig. 7.36a : Discrete phase shifts produced by a nucleon scattered from a square well potential of depth $V = -5$ MeV and range $d = 2$ fm in $\ell = 2$. The discrete energies were obtained by solving the transcendental equation 7.14 for $a = 10$ fm.

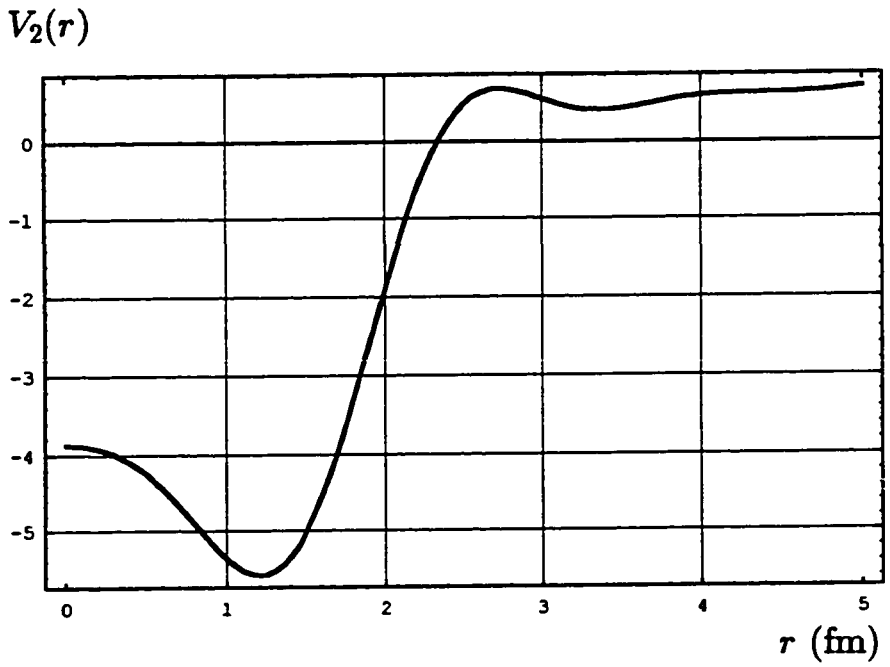

Fig. 7.36b : Potential calculated from eqn. (7.13) using the discrete perturbed energy states obtained in the above figure.

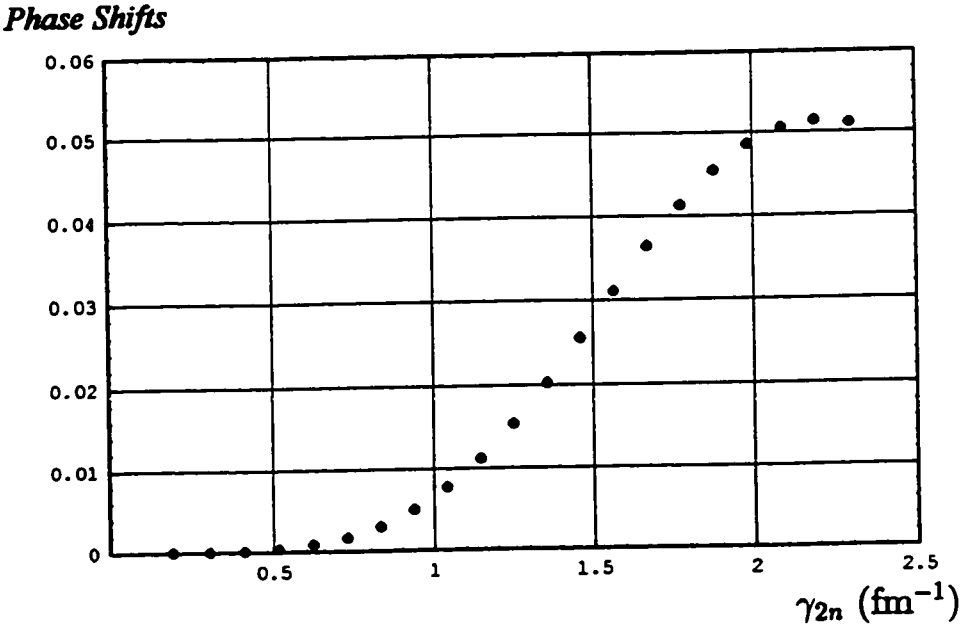

Fig. 7.37a : Discrete phase shifts produced by a nucleon scattered from a square well potential of depth $V = -5$ MeV and range $d = 2$ fm in $\ell = 2$. The discrete energies were obtained by solving the transcendental equation 7.14 for $a = 30$ fm.

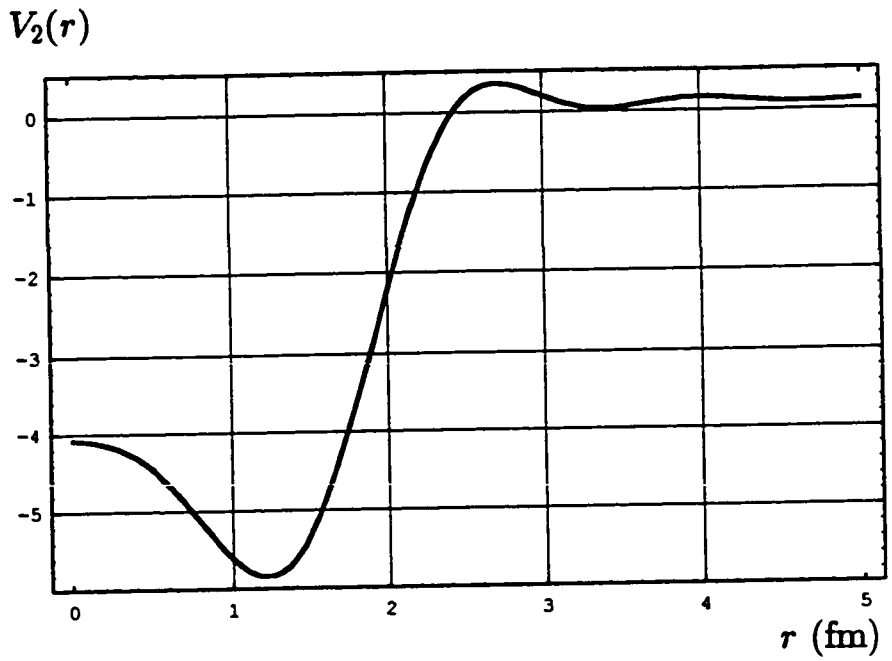

Fig. 7.37b : Potential calculated from eqn. (7.13) using the discrete perturbed energy states obtained in the above figure.

Phase Shifts

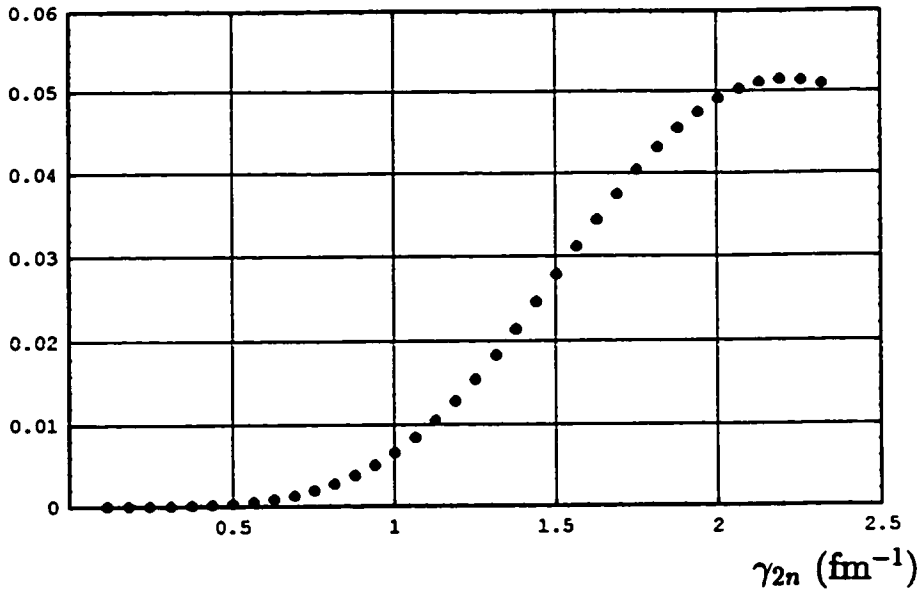

Fig. 7.38a : Discrete phase shifts produced by a nucleon scattered from a square well potential of depth $V = -5$ MeV and range $d = 2$ fm in $\ell = 2$. The discrete energies were obtained by solving the transcendental equation 7.14 for $a = 50$ fm.

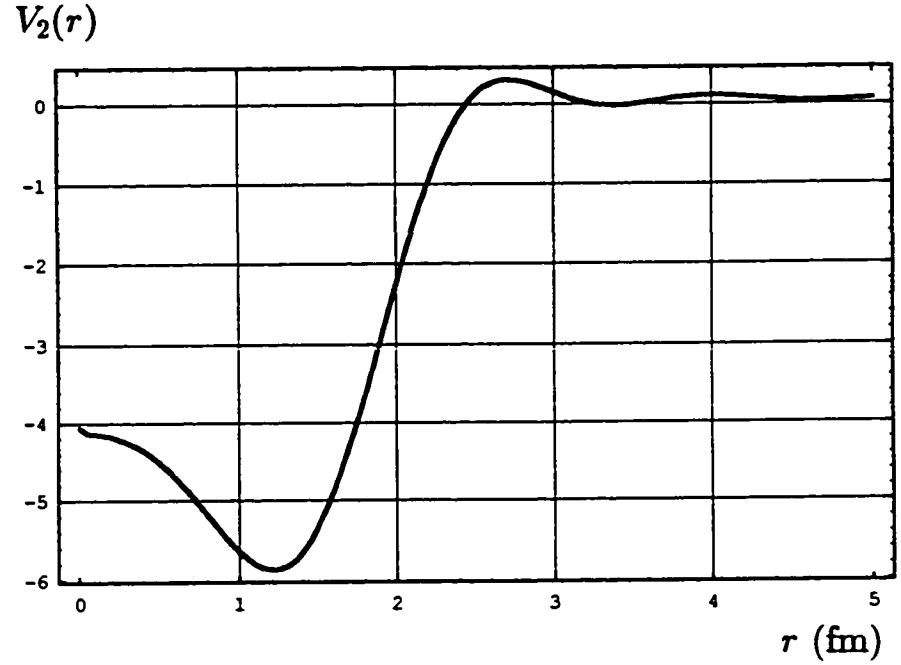

Fig. 7.38b : Potential calculated from eqn. (7.13) using the discrete perturbed energy states obtained in the above figure.

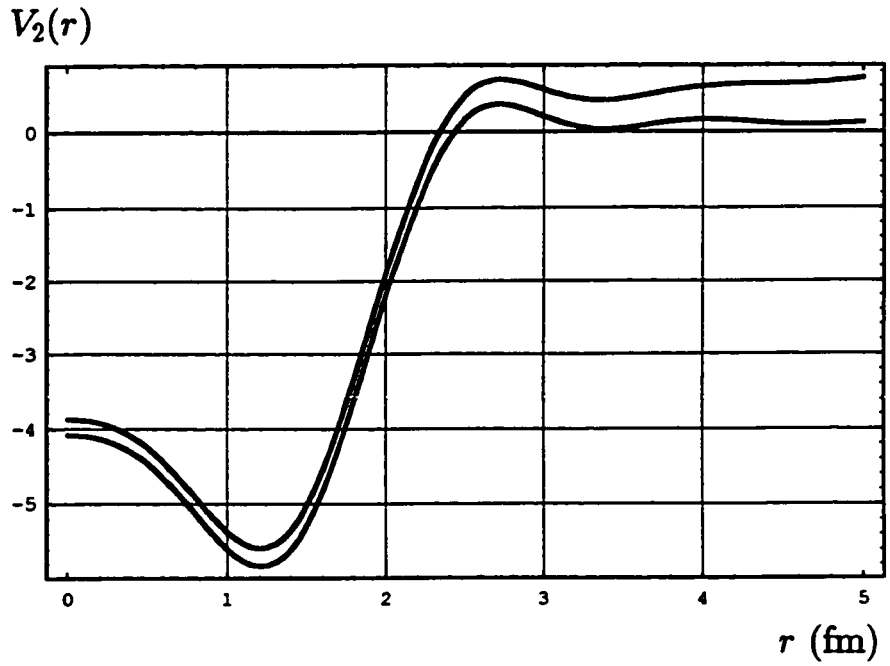

Fig. 7.39 : Comparison between potentials obtained in figs. 7.36b and 7.37b.

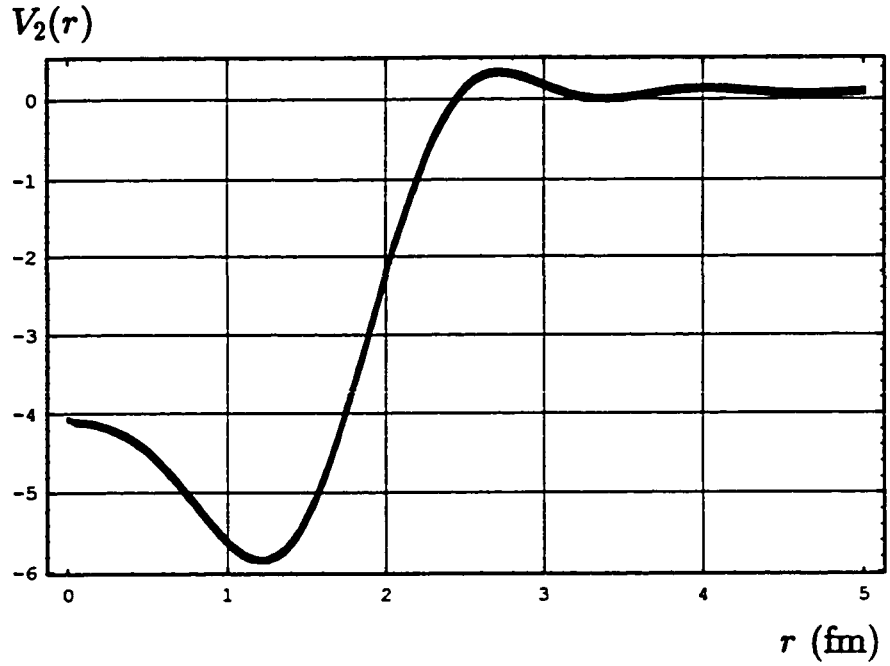

Fig. 7.40 : Comparison between potentials obtained in figs. 7.37b and 7.38b.

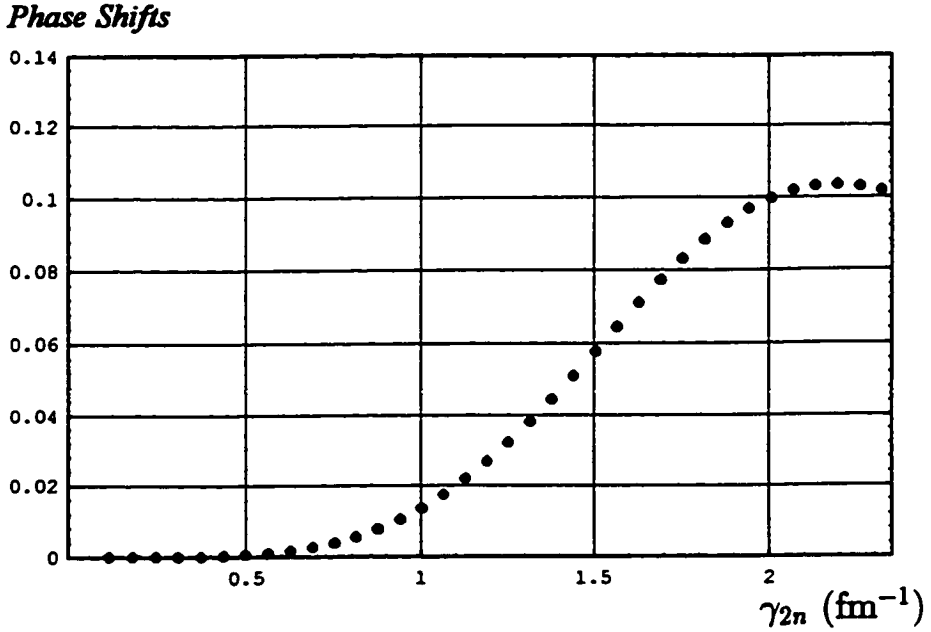

Fig. 7.41a : Discrete phase shifts produced by a nucleon scattered from a square well potential of depth $V = -10$ MeV and range $d = 2$ fm in $\ell = 2$. The discrete energies were obtained by solving the transcendental equation 7.14 for $a = 50$ fm.

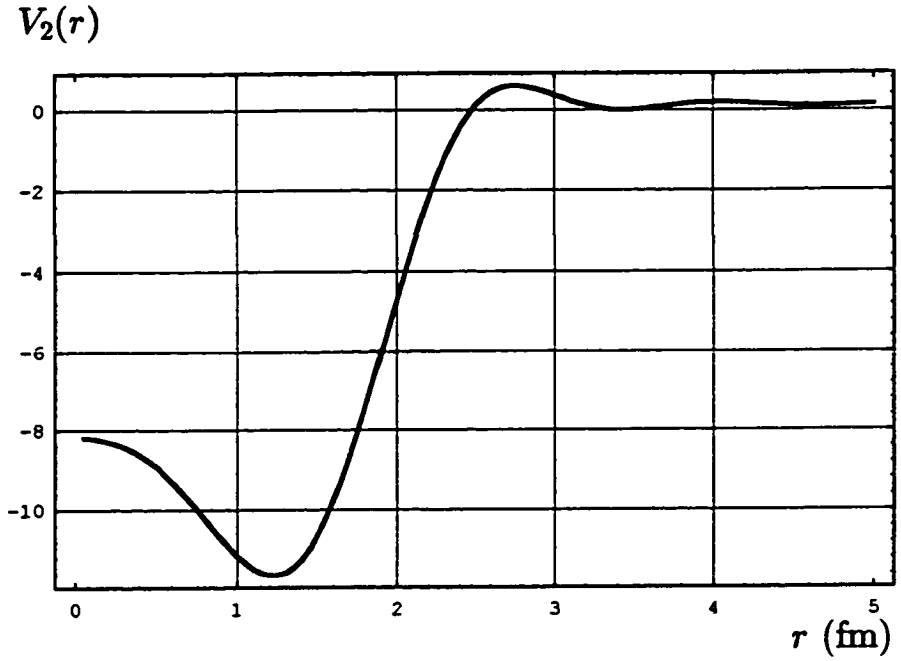

Fig. 7.41b : Potential calculated from eqn. (7.13) using the discrete perturbed energy states obtained in the above figure.

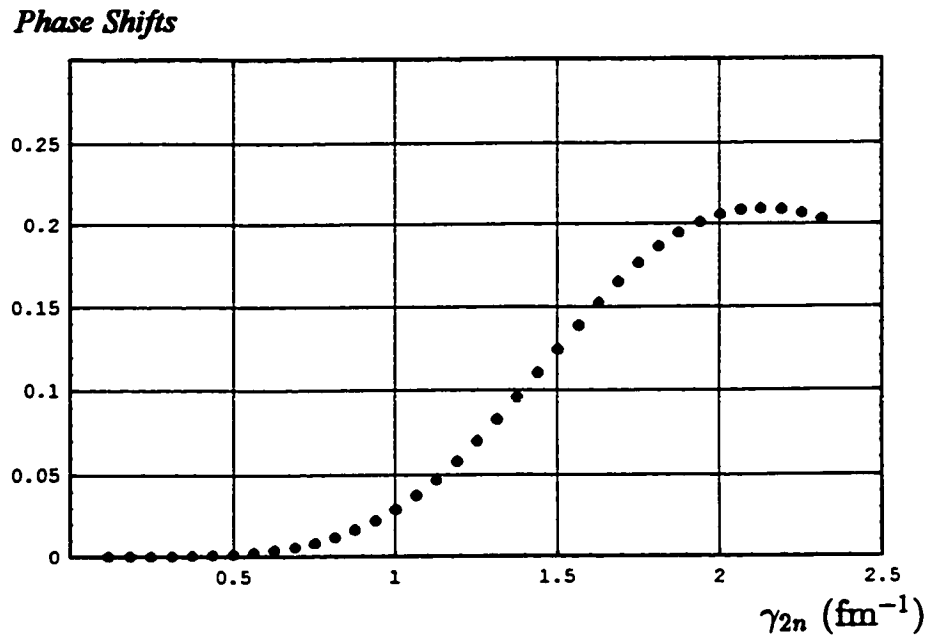

Fig. 7.42a : Discrete phase shifts produced by a nucleon scattered from a square well potential of depth $V = -20$ MeV and range $d = 2$ fm in $\ell = 2$. The discrete energies were obtained by solving the transcendental equation 7.14 for $a = 50$ fm.

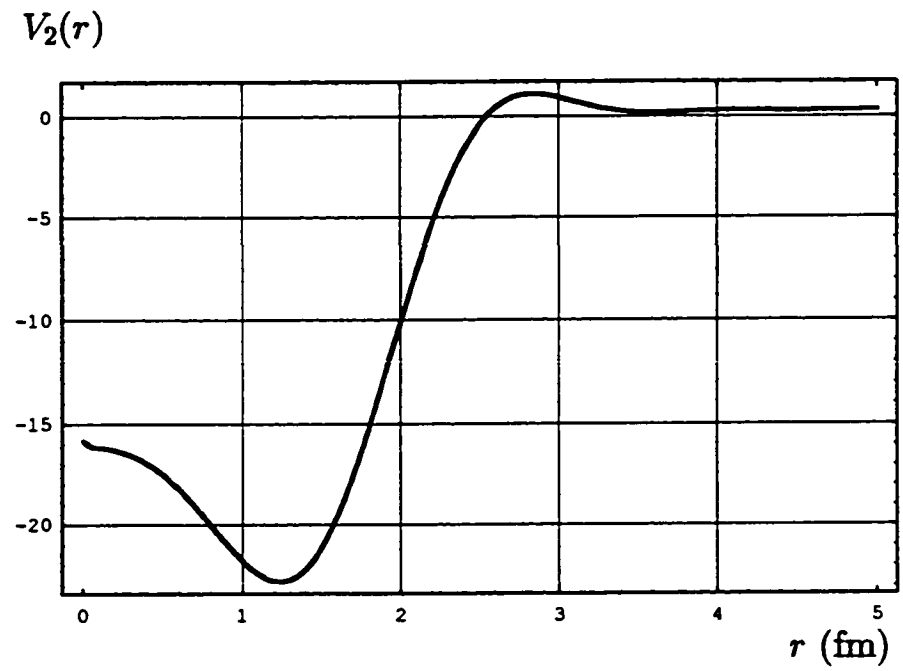

Fig. 7.42b : Potential calculated from eqn. (7.13) using the discrete perturbed energy states obtained in the above figure.

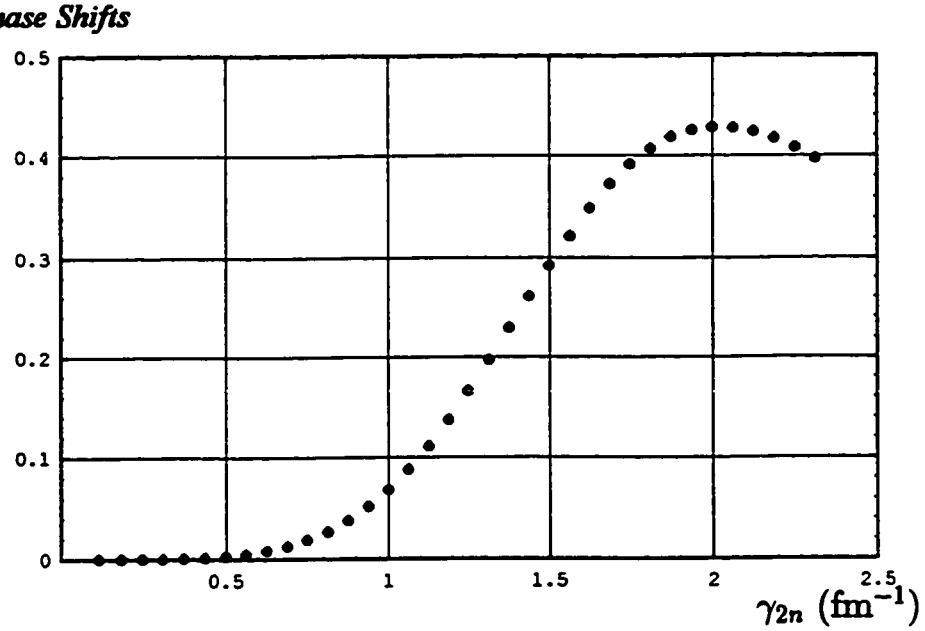

Fig. 7.43a : Discrete phase shifts produced by a nucleon scattered from a square well potential of depth $V = -40$ MeV and range $d = 2$ fm in $\ell = 2$. The discrete energies were obtained by solving the transcendental equation 7.14 for $a = 50$ fm.

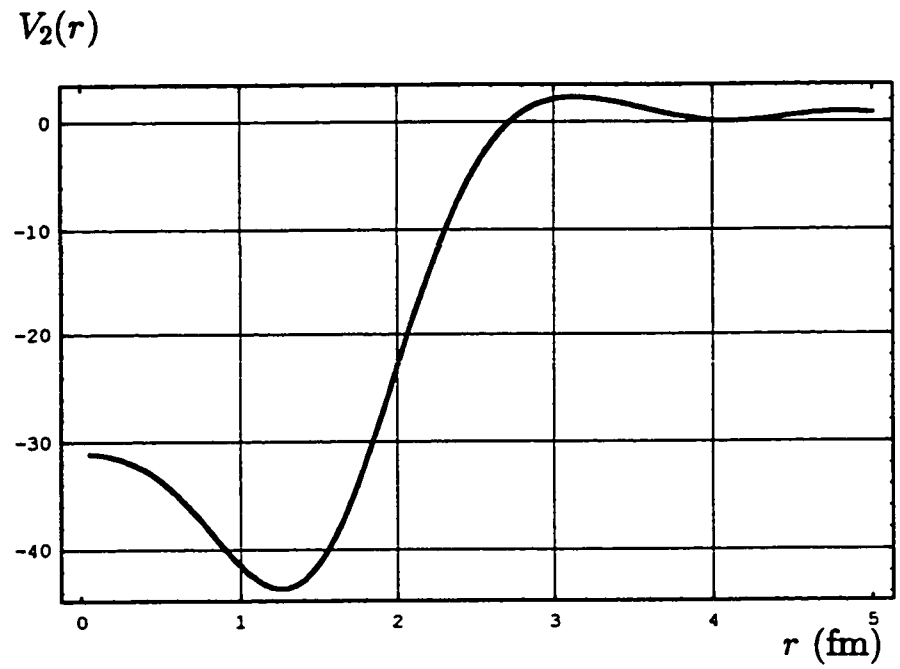

Fig. 7.43b : Potential calculated from eqn. (7.13) using the discrete perturbed energy states obtained in the above figure.

7.2 Potential Expansion Approach

Example 7.4 :

Consider a particle of mass $\mu = 469.5$ MeV/c^2 scattered off a square well potential of depth $V = -10$ MeV and range $d = 2$ fm in the angular momentum channel $\ell = 0$, in a sphere of radius a.

In this approach, the potential is expanded in terms of a complete set $\left\{U_p\left(\alpha_{pq}\frac{r}{a}\right)\right\}$, i.e.

$$V_0(r) = \sum_{q=1}^{q=m} b_q U_p\left(\alpha_{pq}\frac{r}{a}\right),$$

where α_{pq} is the qth root of U_p. We will expand the potential in terms of $j_0\left(\frac{n\pi}{a}r\right)$. Recall that the roots of j_0 are $\alpha_{0n} = n\pi$, n =1, 2,.... One could equally well expand $V_0(r)$ in terms of any orthonormal set e.g. $g_\ell(k_{\ell n}r)$ (see chapter 1).

7.2.1 $j_0(k_{0n}r)$−Expansion

One can expand the potential in terms of $j_0(k_{0n}r)$, i.e.

$$V_0(r) = \sum_{q=1}^{q=m} b_q j_0(k_{0q}r) = \sum_{q=1}^{q=m} b_q \frac{\sin(k_{0q}r)}{k_{0q}r} = \sum_{q=1}^{q=m} \beta_q \frac{\sin(k_{0q}r)}{r}, \qquad (7.15)$$

where

$$k_{0q} \equiv \frac{\alpha_{0q}}{a} = \frac{q\pi}{a},$$

and

$$\beta_q \equiv \frac{b_q}{k_{0q}}$$

As mentioned before, α_{0q} is the qth root of j_0. In this case, eqn. (6.39) becomes

$$\frac{a\hbar^2}{4\mu}\left(\gamma_{0n}^2 - \left(\frac{n\pi}{a}\right)^2\right) = \sum_{q=1}^{q=m} \beta_q M_{nq}, \tag{7.16}$$

where

$$M_{nq} = \int_0^a k_{0n}^2 r^2 j_0^2(k_{0n}r) k_{0q} j_0(k_{0q}r).$$

or in a matrix form, eqn. (7.16) can be written as

$$d = Mb \tag{7.17}$$

where

d : is an $m \times 1$ column vector with vector elements

$$d_n \equiv \frac{a\hbar^2}{4\mu}\left(\gamma_{0n}^2 - \left(\frac{n\pi}{a}\right)^2\right).$$

M : is an $m \times m$ matrix with M_{nq} as a matrix element.

b : is an $m \times 1$ column vector with vector elements β_n.

Multiplying both sides of eqn. (7.17) by the inverse of M, M^{-1}, one obtains the set $\{\beta_q\}$, which is given in a matrix form as

$$b = M^{-1}d. \tag{7.18}$$

Then, these β_q are substituted in eqn. (7.15) to get the potential $V_0(r)$

The matrix elements M_{nq} can be written in an explicit form as follows

$$\begin{aligned} M_{nq} &= \int_0^a k_{0n}^2 r^2 j_0^2(k_{0n}r) k_{0q} j_0(k_{0q}r) \\ &= \int_0^a \frac{\sin^2\left(\frac{n\pi}{a}r\right)\sin\left(\frac{q\pi}{a}r\right)}{r}\,dr \end{aligned} \tag{7.19}$$

Let

$$\xi = \frac{\pi r}{a} \quad \Rightarrow \quad dr = \frac{a}{\pi}d\xi.$$

Making the above transformation, eqn. (7.19) becomes

$$\begin{aligned} M_{nq} &= \int_0^\pi \frac{\sin^2(n\xi)\sin(q\xi)}{\frac{a}{\pi}\xi}\frac{a}{\pi}\,d\xi \\ &= \int_0^\pi \frac{\sin^2(n\xi)\sin(q\xi)}{\xi}\,d\xi \end{aligned} \tag{7.20}$$

Notice that the matrix elements M_{nq} do not depend on the details of the problem; the depth of the potential V, the range of the potential d, the radius of the sphere a and the mass of the particle μ, which means that one can study different situations using the same matrix.

Let us study the following cases :

Case I) : Let $a = 10$ fm. Recall that one should consider phase shifts in the range $E \approx 0$–225 MeV since this inversion technique is valid where the inelastic effects are small. This condition is satisfied for $m = 7$ since $\gamma_{07} = 198.60$ MeV[5].

In order to obtain the inverse of the matrix M, one should calculate the determinant of M. For this 7×7 matrix, the determinant is -1.607458×10^{-9}, which

[5]This was obtained by solving eqn. (7.6). See also fig. 7.8

implies that M is singular. In this case one can use the singular value decomposition technique (see chapter 1) to invert this singular 7×7 matrix. In this technique, M (which is of rank 7) is decomposed into $U \in \mathbf{R}^{7\times7}$, $\Sigma \in \mathbf{R}^{7\times7}$ and $W \in \mathbf{R}^{7\times7}$, such that U and W are orthogonal, Σ has the form

$$\Sigma = \begin{pmatrix} \sigma_1 & & & 0 \\ & \sigma_2 & & \\ & & \ddots & \\ 0 & & & \sigma_7 \end{pmatrix}$$

where $\sigma_1 \geq \sigma_2 \geq \cdots \geq \sigma_7 > 0$, and

$$M = U\Sigma W^T \tag{7.21}$$

The singular values σ_i, i =1, 2,..., 7 are given in table 7.1[6].

The singularity of the matrix M is indicated in the singular values where one can see that σ_6 is small and σ_7 is very small. In order to obtain the inverse of M using the singular value decomposition technique, one should construct the diagonal matrix Σ^+ with σ_i^{-1}, $i = 1, 2, \ldots, 7$ as the diagonal elements (recall that $M^{-1} = W\Sigma^+U^T$) and it is obvious that the small singular values will cause the singularity.

[6]The singular value decomposition and all of the subsequent numerical calculations were evaluated using either *Mathematica* or Matlab programs.

Table 7.1: Singular values of the matrix M which were obtained by solving eqn. (7.21).

i	σ_i
1	4.7717
2	0.22307
3	0.698606
4	0.539351
5	0.0401307
6	0.00138326
7	0.0000131683

The pseudoinverse of M, M^+, is given by

$$M^+ = W\Sigma^+ U^T \tag{7.22}$$

where

$$\Sigma^+ = \begin{pmatrix} \sigma_1^{-1} & & & 0 \\ & \sigma_2^{-1} & & \\ & & \ddots & \\ 0 & & & \sigma_7^{-1} \end{pmatrix}$$

Using this inverse, eqn. (7.18) becomes

$$b = W\Sigma^+ U^T d \tag{7.23}$$

Although the coefficients β_q, and consequently the potential, were calculated, the solution of the problem, namely the potential, is **irregular**. This is because the singularity is inherent in the problem and one cannot get rid of this singularity

even if the inverse is obtained. The irregularity of the problem is illustrated in fig. 7.44 where the potential $V_0(r)$ is plotted using the coefficients calculated from eqn. (7.23), which is given in table 7.2. As can be seen from fig. 7.44, the potential obtained is very far away from the "experimental" one. In fact, this irregularity can be observed from the coefficients β_i, where one can observe that all of the β_i's are much larger than the depth of the "experimental" potential.

Table 7.2: Irregular coefficients β_i calculated using eqn. (7.23).

i	β_i	i	β_i
1	13364.1	2	−38709.9
3	6947.95	4	20635.5
5	−5979.4	6	−2142.18
7	437.08		

However, *this irregularity can be removed by setting the singular values which cause the singularity to zero.* Suppose that there are ν singular values which cause the singularity. Then **regular singular value decomposition** of the matrix M is given by

$$M = U\Sigma' W^T \tag{7.24}$$

where

$$\Sigma' = \left(\begin{array}{ccc|c} \sigma_1 & & 0 & \\ & \sigma_2 & & 0 \\ & & \ddots & \\ 0 & & \sigma_{7-\nu} & \\ \hline & 0 & & 0 \end{array}\right) \begin{array}{l} \left.\begin{array}{l} \\ \\ \\ \end{array}\right\} 7-\nu \\ \left.\begin{array}{l} \\ \end{array}\right\} \nu \end{array}$$

$$\underbrace{\qquad\qquad}_{\nu}$$

and $\sigma_1 \geq \sigma_2 \geq \cdots \geq \sigma_{7-\nu} > 0$. Then, the **regular pseudoinverse** of M is given by

$$M^+ = W\Sigma'^+U^T \tag{7.25}$$

where

$$\Sigma'^+ = \left(\begin{array}{ccc|c} \sigma_1^{-1} & & 0 & \\ & \sigma_2^{-1} & & 0 \\ & & \ddots & \\ 0 & & \sigma_{7-\nu}^{-1} & \\ \hline & 0 & & 0 \end{array}\right) \begin{array}{l} \left.\begin{array}{l} \\ \\ \\ \end{array}\right\} 7-\nu \\ \left.\begin{array}{l} \\ \end{array}\right\} \nu \end{array}$$

$$\underbrace{\qquad\qquad}_{\nu}$$

and consequently the **regular coefficients** are given by

$$b = W\Sigma'^+U^Td \tag{7.26}$$

Let us consider the following cases to illustrate how one can determine the value of ν and consequently how one can obtain a regular solution from the irregular one.

a) Let $\nu = 1$. Solving eqn. (7.26), one obtains the coefficients β_i which are given in table 7.3. These coefficients can be substituted in eqn. (7.15) to get

the potential, see fig. 7.45. Fig. 7.45 shows that by setting the last singular value, namely σ_7, to zero, the amplitude of the obtained potential drops from around -10400 MeV, in the case of irregular solution, to -70. Although the potential obtained is improved, it is still far away from the "experimental" potential and the coefficients obtained, see table 7.3, are still larger than the depth of the "experimental" potential.

Table 7.3: The coefficients β_i obtained by solving eqn. (7.26) for $\nu = 1$

i	β_i	i	β_i
1	41.038	2	-107.705
3	124.767	4	-238.376
5	40.1999	6	138.748
7	-44.4632		

b) Let $\nu = 2$. Solving eqn. (7.26), one obtains the coefficients β_i which are given in table 7.4. These coefficients can be substituted in eqn. (7.15) to get the potential, see fig. 7.46. As can be seen from fig. 7.46, the amplitude of the potential obtained lies within the expected range (around -10 MeV) but the coefficients β_i are still larger than the depth of the "experimental" potential, which indicates that the solution is still irregular.

Table 7.4: The coefficients β_i obtained by solving eqn. (7.26) for $\nu = 2$

i	β_i	i	β_i
1	−4.20093	2	0.58614
3	−10.1597	4	5.55353
5	−20.7575	6	37.59
7	−14.9895		

c) Let $\nu = 3$. Solving eqn. (7.26), one obtains the coefficients β_i which are given in table 7. 5. These coefficients can be substituted in eqn. (7.15) to get the potential, see fig. 7.47. Fig. 7.47 shows that the amplitude of the potential obtained lies within the expected range (around −10 MeV) and the coefficients β_i are less than the depth of the "experimental" potential, which indicates that the solution is now regular. In fact, one cannot determine whether the solution obtained is regular by just comparing the values of the β_i's with the amplitude of the "experimental" potential since practically the amplitude of the "experimental" potential is not known, but here we follow this comparison procedure to show the dependence of the regularity of the solution on the values of the β_i's. The practical method of making a solution regular will be discussed later in this section. Fig. 7.48 shows that this inversion technique does not contain the ambiguity contained in the $g_\ell(k_{\ell n})$−inversion technique where the potential obtained in the latter technique is reliable on $0 \leq r \leq a/2$ while in this technique the solution is physical in the whole space since the potential dies off as the relative distance between the nucleons increases.

Table 7.5: The coefficients β_i obtained by solving eqn. (7.26) for $\nu = 3$.

i	β_i	i	β_i
1	−2.5224	2	−2.594
3	−4.21291	4	−2.48701
5	−2.12893	6	−0.137897
7	2.07964		

d) Let $\nu = 4$. Solving eqn. (7.26), one obtains the coefficients β_i which are given in table 7.6. These coefficients can be substituted in eqn. (7.15) to get the potential, see fig. 7.49. As can be seen from fig. 7.49, the potential obtained is exactly as the one obtained when $\nu = 3$. fig. 7.50 compares the potential obtained when $\nu = 3$ with the one obtained when $\nu = 4$.

Table 7.6: The coefficients β_i obtained by solving eqn. (7.26) for $\nu = 4$.

i	β_i	i	β_i
1	−2.49156	2	−2.60608
3	−4.27757	4	−2.48583
5	−2.05873	6	−0.129627
7	2.0391		

e) Let $\nu = 5$. Solving eqn. (7.26), one obtains the coefficients β_i which are given in table 7.7. These coefficients can be substituted in eqn. (7.15) to get the

potential, see fig. 7.51. As can be seen from fig. 7.51, increasing the value of ν more than a certain limit results in some deviation from the regular solution. This is because the more singular values one sets equal to zero, the more information one looses.

Table 7.7: The coefficients β_i obtained by solving eqn. (7.26) for $\nu = 5$.

i	β_i	i	β_i
1	−4.18382	3	−2.557
3	−2.62007	4	−1.50243
5	−0.867238	6	−0.436175
7	0.122519		

From the above discussion, one can conclude that the value of ν of the regular solution is not unique and one can determine a value for ν by assigning a value to ν and then increasing this value by one. If the solutions obtained do not change dramatically, then the solution is regular. The calculated coefficients, β_i, can be used to identify the regular solution. If β_i for ν and $\nu + 1$ are in the same range, then the solution is regular.

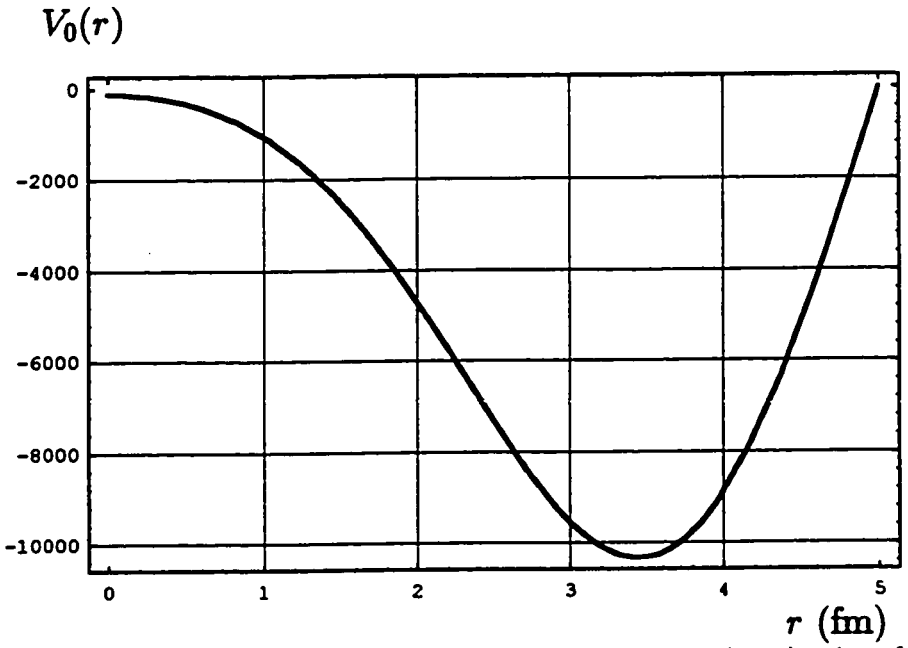

Fig. 7.44 : Irregular potential obtained by solving eqn. (7.23) using the irregular coefficients β_i given in table 7.2.

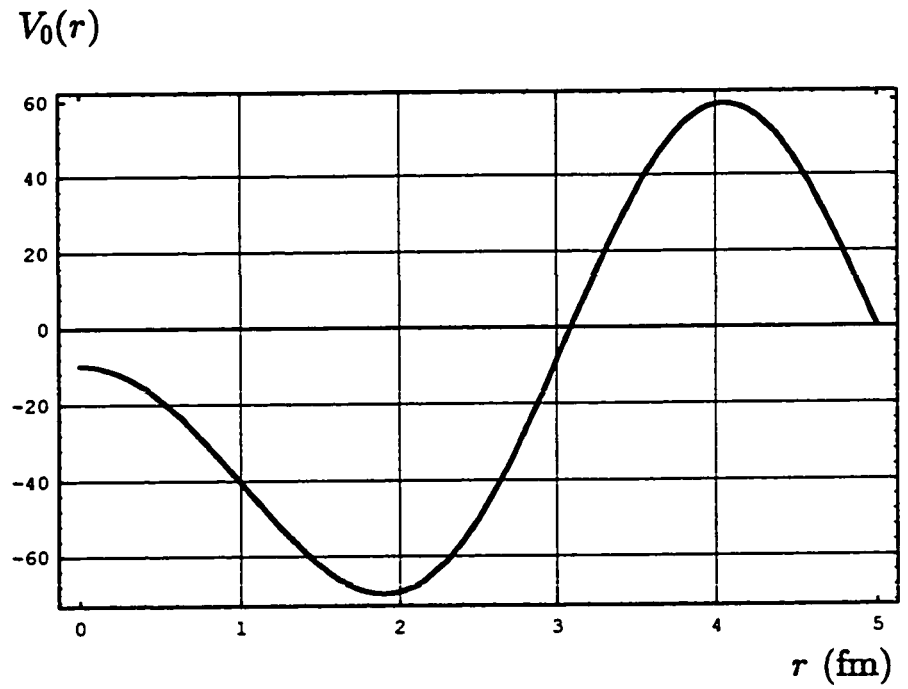

Fig. 7.45 : Potential obtained by solving eqn. (7.26) for $\nu = 1$, using the coefficients β_i given in table 7.3.

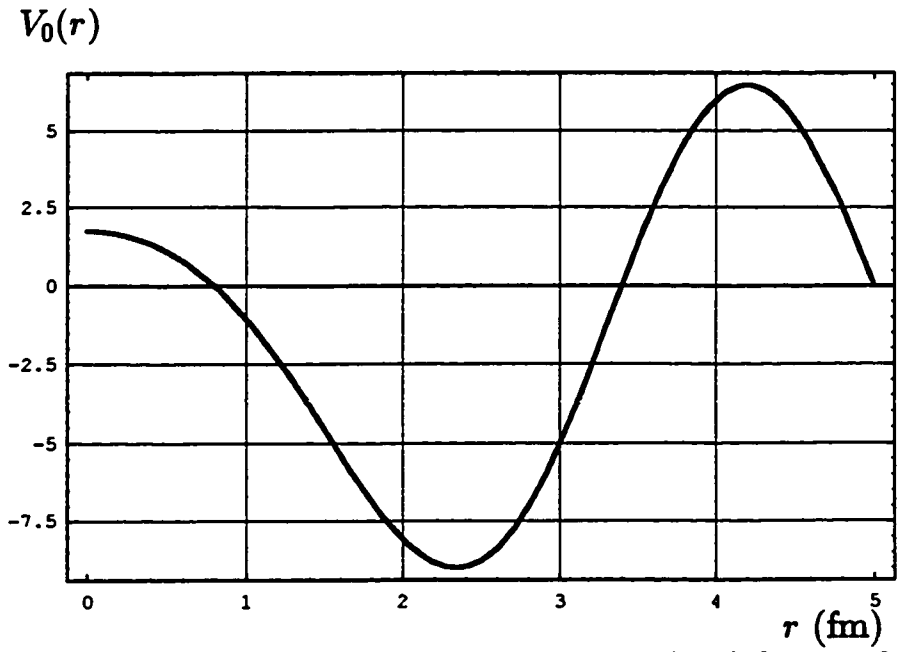

Fig. 7.46 : Potential obtained by solving eqn. (7.26) for $\nu = 2$, using the coefficients β_i given in table 7.4.

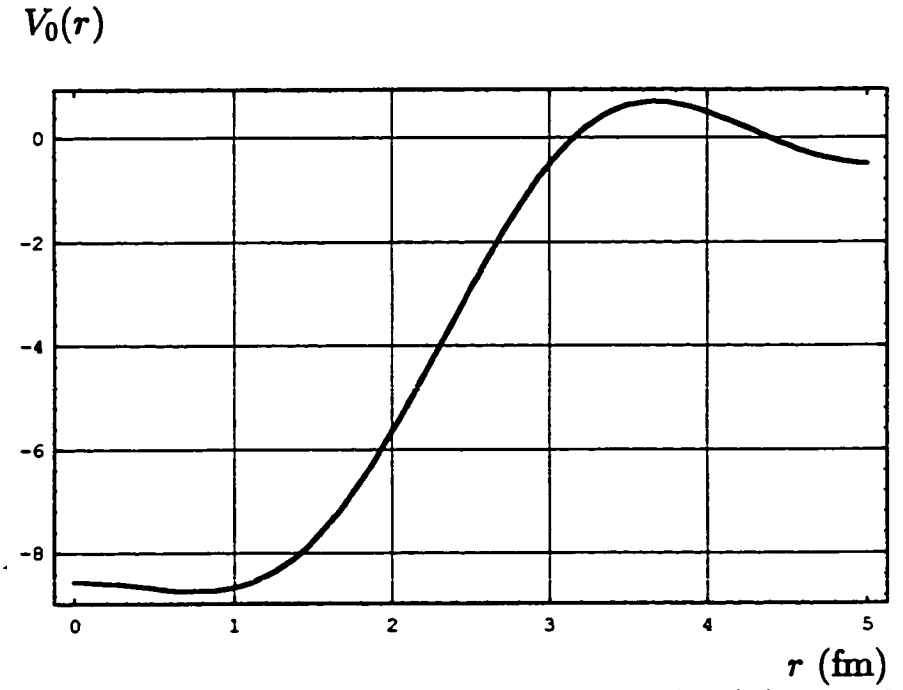

Fig. 7.47 : Potential obtained by solving eqn. (7.26) for $\nu = 3$, using the coefficients β_i given in table 7.5.

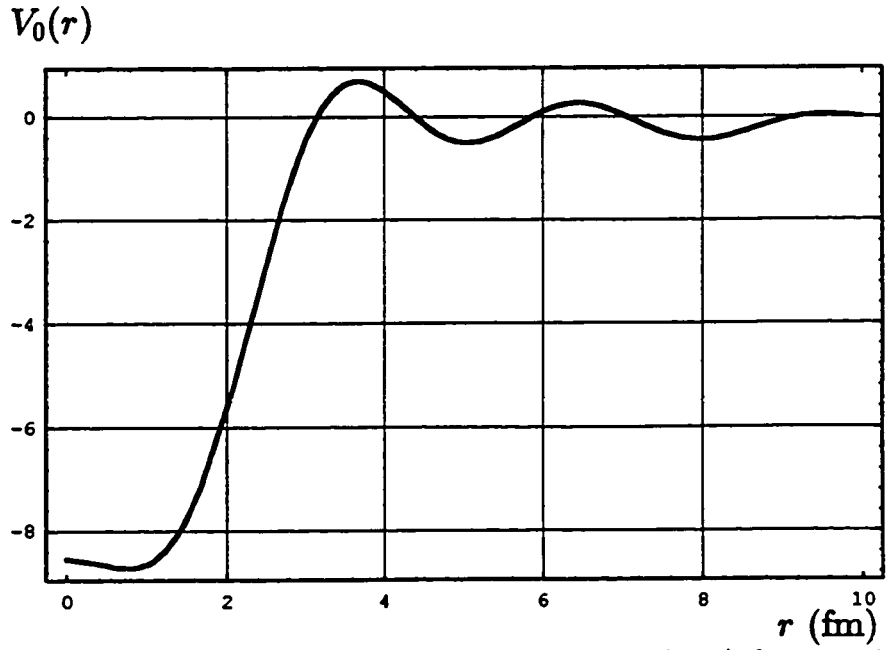

Fig. 7.48 : Potential obtained by solving eqn. (7.26) for $\nu = 3$, using the coefficients β_i given in table 7.5. The potential in this figure was calculated over the whole space.

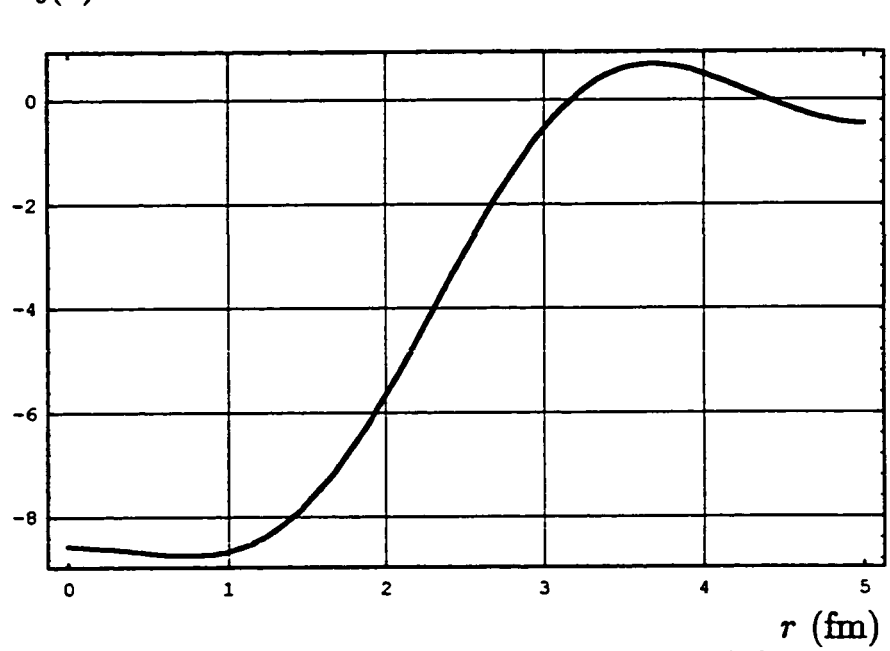

Fig. 7.49 : Potential obtained by solving eqn. (7.26) for $\nu = 4$, using the coefficients β_i given in table 7.6.

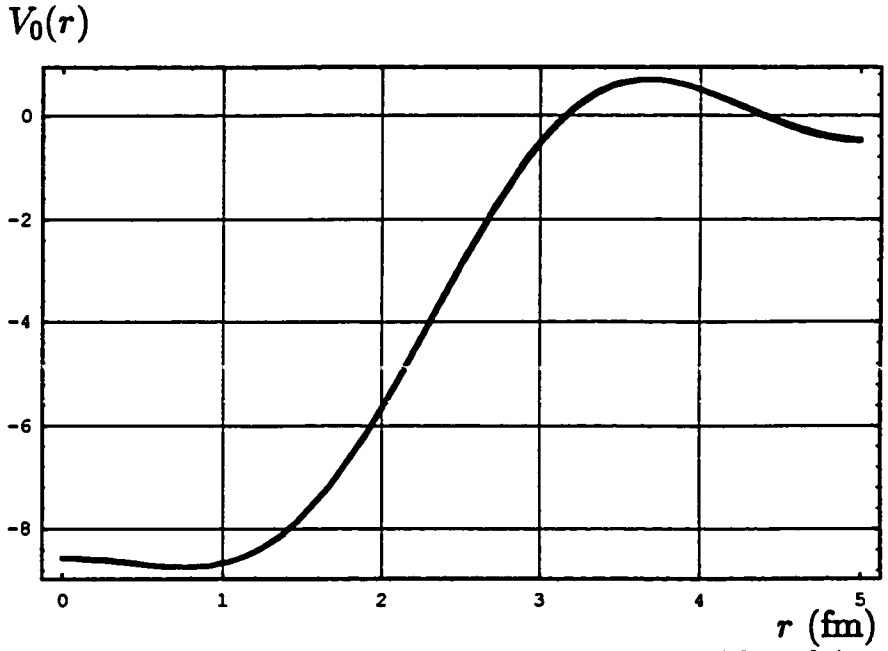

Fig. 7.50 : Comparison between the potential obtained by solving eqn. (7.26) for $\nu = 3$ and the one obtained for $\nu = 4$.

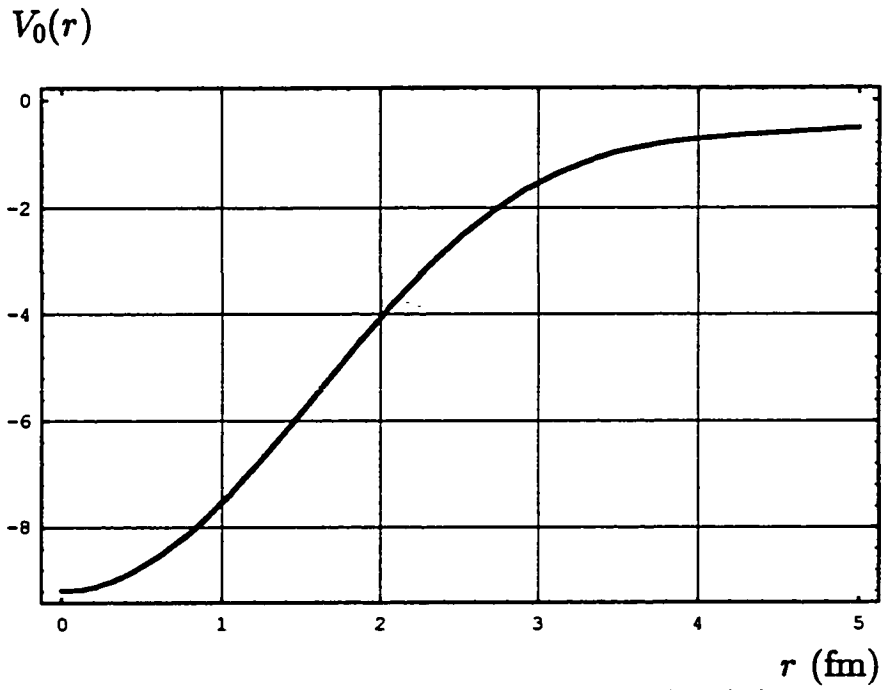

Fig. 7.51 : Potential obtained by solving eqn. (7.26) for $\nu = 5$, using the coefficients β_i given in table 7.7.

Case II) : Let $a = 30$ fm. The energy of the 22nd state is 219.38 MeV which implies that one can choose the truncation number m to be 22. The determinant of the resultant 22×22 matrix, M, with matrix elements given by eqn. (7.20), namely

$$M_{nq} = \int_0^\pi \frac{\sin^2(n\xi)\,\sin(q\xi)}{\xi}\,d\xi,$$

is -2.266×10^{-79}, which indicates that the matrix M is singular. In this case one can use the singular value decomposition technique to invert this singular 22×22 matrix. In this technique, M (which is of rank[7]20) is decomposed into U, Σ and $W \in \mathbf{R}^{22\times 22}$, such that U and W are orthogonal, Σ has the form

$$\Sigma = \left(\begin{array}{ccc|c} \sigma_1 & & 0 & \\ & \sigma_2 & & 0 \\ & \ddots & & \\ 0 & & \sigma_{20} & \\ \hline & 0 & & 0 \end{array}\right) \begin{array}{l} \left.\begin{array}{l}\\\\\\\\\end{array}\right\} 20 \\ \left.\begin{array}{l}\\\end{array}\right\} 2 \end{array}$$

$$\underbrace{\qquad\qquad}_{2}$$

where $\sigma_1 \geq \sigma_2 \geq \cdots \geq \sigma_{20} > 0$, and

$$M = U\Sigma W^T. \tag{7.27}$$

The singular values σ_i, $i = 1, 2, \ldots, 20$ are given in table 7.8. Substituting these values of σ_i in eqn. (7.27), one can obtain the coefficients β_i and consequently the potential. From table 7.8, one can see clearly that the potential obtained is irregular, see fig. 7.52.

[7]Using *Mathematica*

Table 7.8: Sigular values of the 22×22 matrix.

i	σ_i	i	σ_i
1	14.4400	2	3.6181
3	1.9297	4	1.3116
5	0.9989	6	0.8140
7	0.69491	8	0.6150
9	0.56107	10	0.5261
11	0.5064	12	0.3197
13	0.02497	14	0.002040
15	0.000118	16	4.7934×10^{-6}
17	1.3531×10^{-7}	18	2.5944×10^{-9}
19	3.2250×10^{-11}	20	2.3913×10^{-13}

The **regular pseudoinverse** of M is given by

$$M^{+} = W\Sigma'^{+}U^{T} \tag{7.28}$$

where

$$\Sigma'^{+} = \left(\begin{array}{ccc|c} \sigma_1^{-1} & & 0 & \\ & \sigma_2^{-1} & & 0 \\ & \ddots & & \\ 0 & & \sigma_{20-\nu}^{-1} & \\ \hline & 0 & & 0 \end{array}\right) \begin{array}{l} \left.\begin{array}{l}\\\\\\\end{array}\right\} 20-\nu \\ \left.\begin{array}{l}\\\end{array}\right\} \nu+2 \end{array}$$

$$\underbrace{\qquad\qquad}_{\nu+2}$$

and consequently the **regular coefficients** are given by

$$b = W\Sigma'^{+}U^{T}d \tag{7.29}$$

Let us consider the following cases:

a) Let $\nu = 7$. Solving eqn. (7.29), one obtains the coefficients β_i. These coefficients can be substituted in eqn. (7.15) to get the potential, see fig. 7.53. To determine whether this solution is regular or not, one should consider the calculated potential using eqn. (7.29) for $\nu = 8$.

b) Let $\nu = 8$. Solving eqn. (7.29), one obtains the coefficients β_i. These coefficients can be substituted in eqn. (7.15) to get the potential, see fig. 7.54. Comparing the potential obtained for $\nu = 8$ with the one obtained for $\nu = 7$, one can see clearly that the potential obtained in case a, with $\nu = 7$, is not regular. To determine whether this solution is regular or not, one should consider the calculated potential using eqn. (7.29) for $\nu = 9$.

c) Let $\nu = 9$. Using the procedure discussed in the previous cases, one can calculate the potential for $\nu = 9$, see fig. 7.55. Comparing the potential obtained for $\nu = 9$ with the one obtained for $\nu = 8$, see fig. 7.56, one can see clearly that the potentials obtained with $\nu = 8$ and $\nu = 9$ are approxiamtely the same, which implies that the potentials obtained for $\nu = 8$ and $\nu = 9$ are regular.

d) Going one step further by calculating the potential for $\nu = 10$, see fig. 7.57, one can see clearly that the potential obtained with $\nu = 9$ is regular. As can be seen from fig. 7.58, the calculated potential for $\nu = 9$ is exactly the same as the one calculated for $\nu = 10$.

e) Let $\nu = 13$. Fig. 7.59, shows the calculated potential for $\nu = 13$ and it can be seen that the calculated potential is exactly as the one obtained for $\nu = 9$. This illustrates that the value of ν is not unique and several values of ν can make the solution regular. As discussed in case I, one expect that by increasing the value of ν more than a certain value, the calculated potential will deviate from the regualr solution. This is illustrated in figs. 7.60 and 7.62, where the potentials are calculated for $\nu = 16$ and 17 respectively. figs. 7.61 compares the potential calculated for $\nu = 16$ with the one obtained for $\nu = 9$ and fig. 7.63 compares the potential calculated for $\nu = 17$ with the one obtained for $\nu = 16$.

Case III) : Let $a = 10$ fm and $V = -5$ MeV. Using the argument applied in case I, one can obtain a regular solution. Fig. 7.64 shows the potential obtained by solving eqn. (7.26) for $\nu = 3$.

Case IV) : Let $a = 10$ fm and $V = -20$ MeV. Using the argument applied in case I, one can obtain a regular solution. Fig. 7.65 shows the potential obtained by solving eqn. (7.26) for $\nu = 3$.

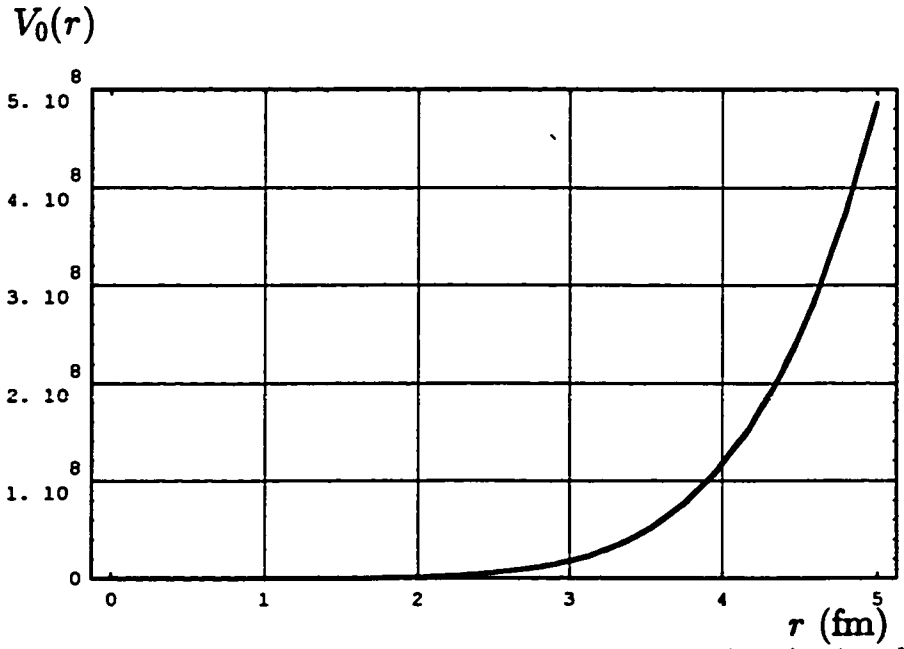

Fig. 7.52 : Irregular potential obtained by solving eqn. (7.27) using the irregular coefficients β_i.

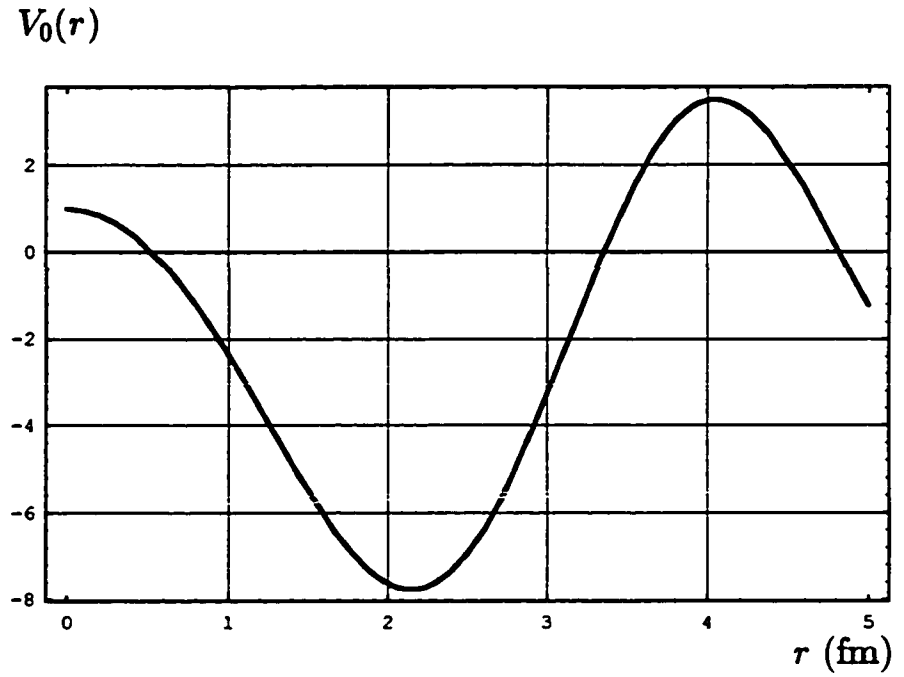

Fig. 7.53 : Potential obtained by solving eqn. (7.29) for $\nu = 7$.

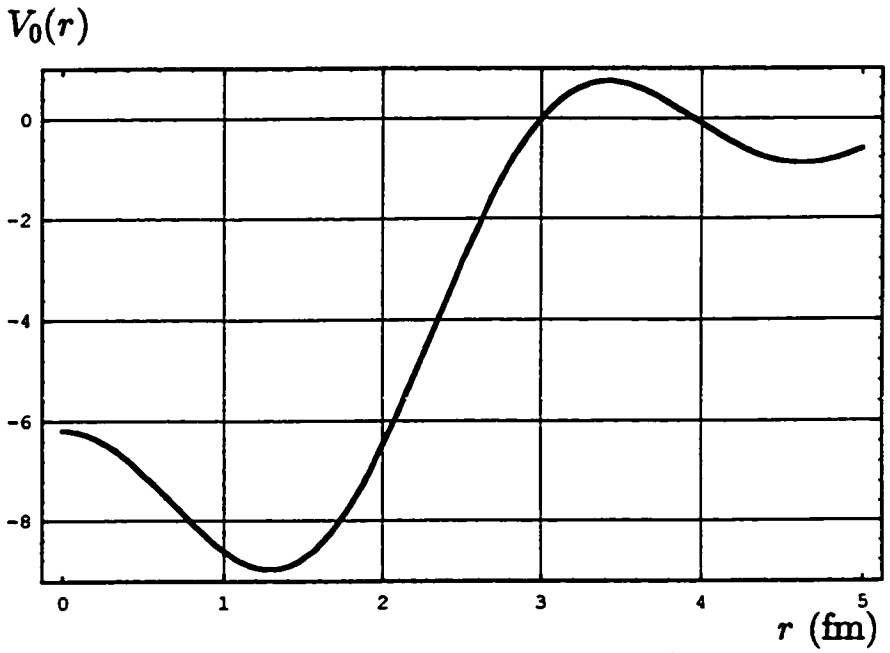

Fig. 7.54 : Potential obtained by solving eqn. (7.29) for $\nu = 8$.

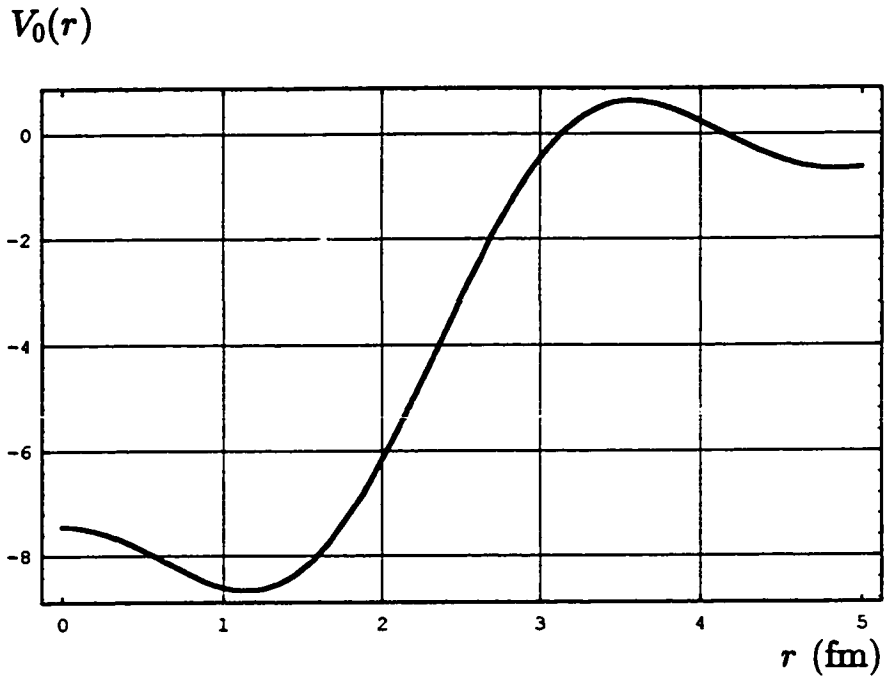

Fig. 7.55 : Potential obtained by solving eqn. (7.29) for $\nu = 9$.

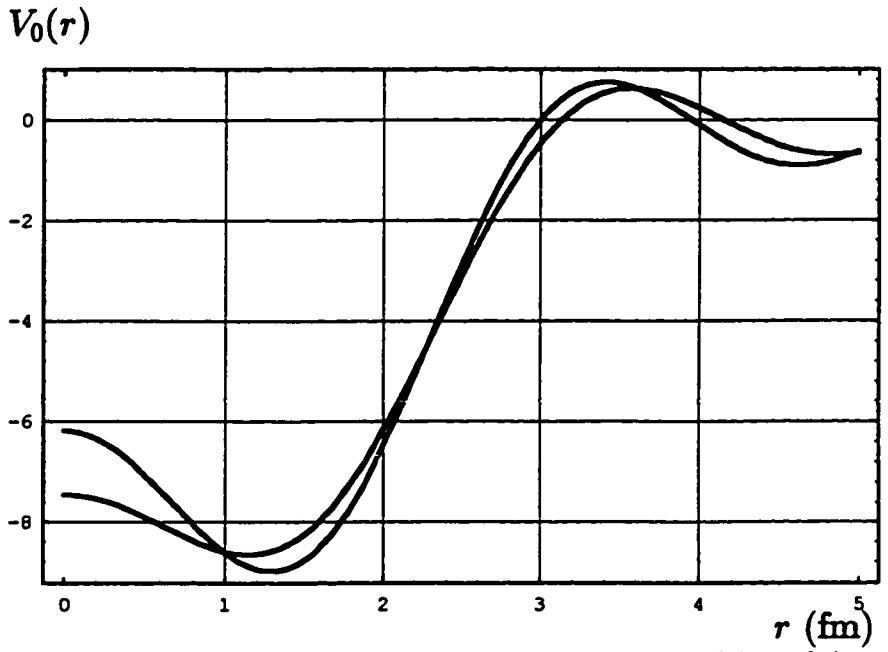

Fig. 7.56 : Comparison between the potential obtained by solving eqn. (7.29) for $\nu = 8$ and the one obtained for $\nu = 9$.

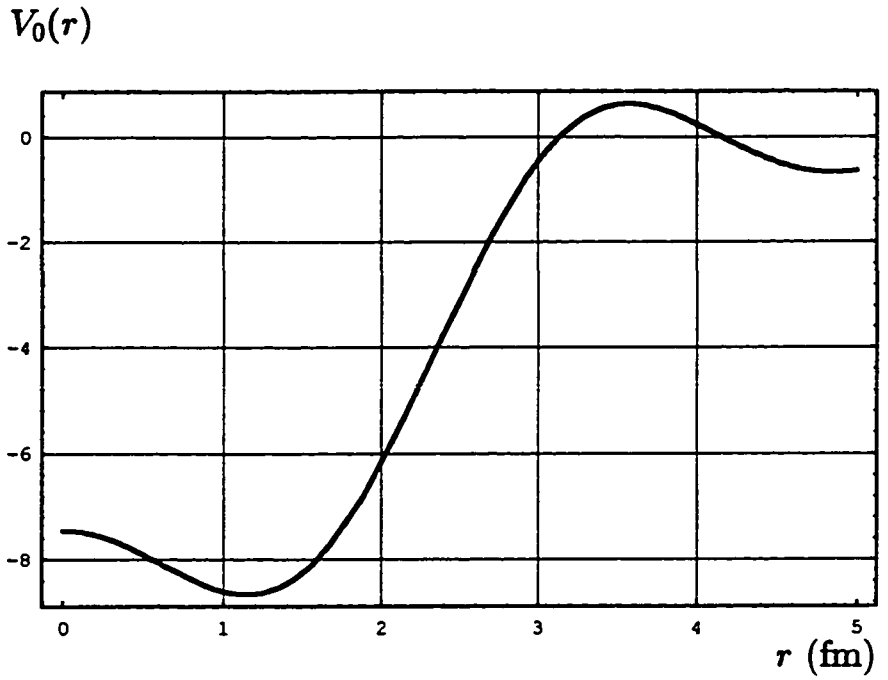

Fig. 7.57 : Potential obtained by solving eqn. (7.29) for $\nu = 10$.

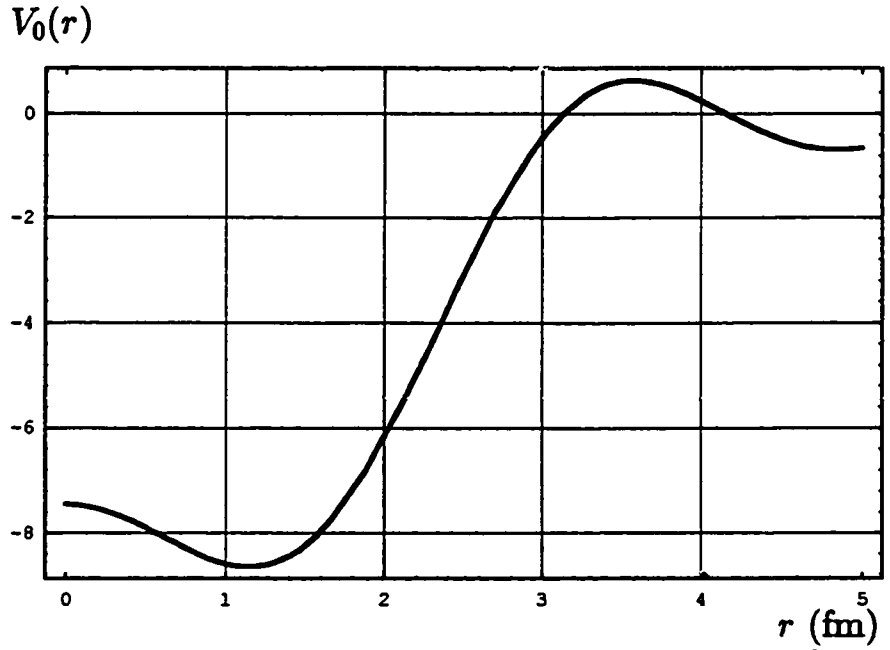

Fig. 7.58 : Comparison between the potential obtained by solving eqn. (7.29) for $\nu = 9$ and the one obtained for $\nu = 10$.

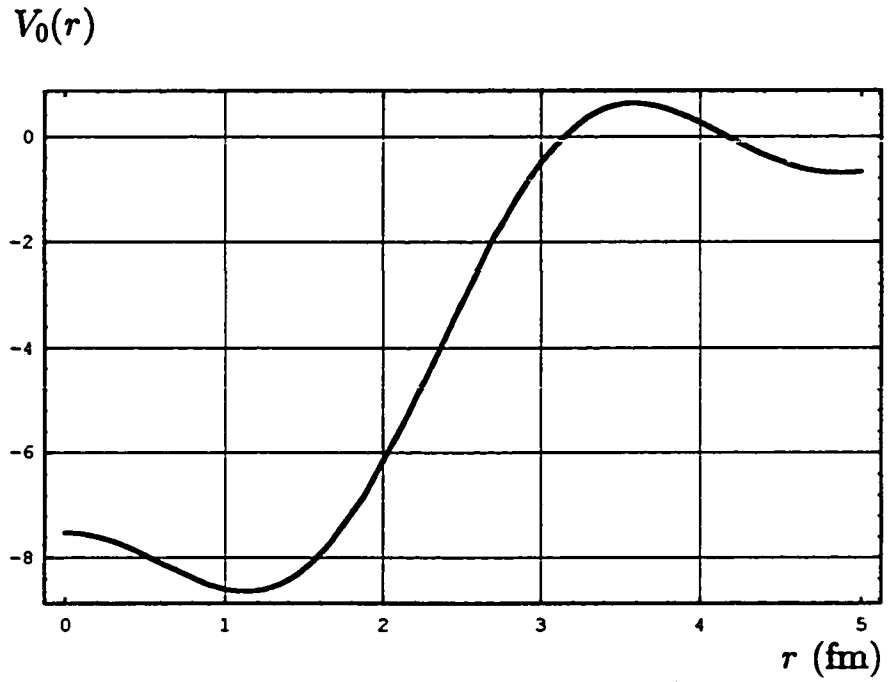

Fig. 7.59 : Potential obtained by solving eqn. (7.29) for $\nu = 13$.

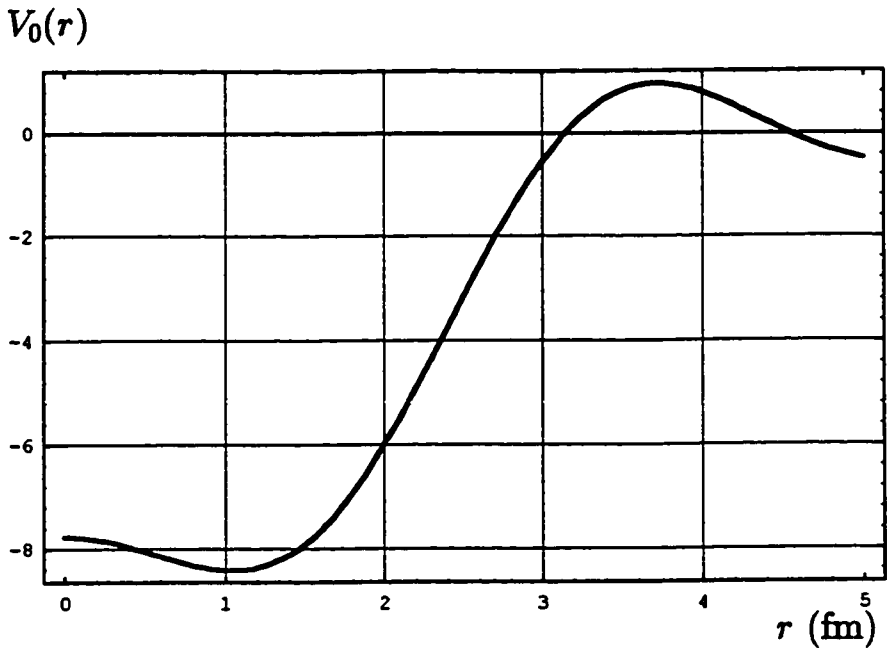

Fig. 7.60 : Potential obtained by solving eqn. (7.29) for $\nu = 16$.

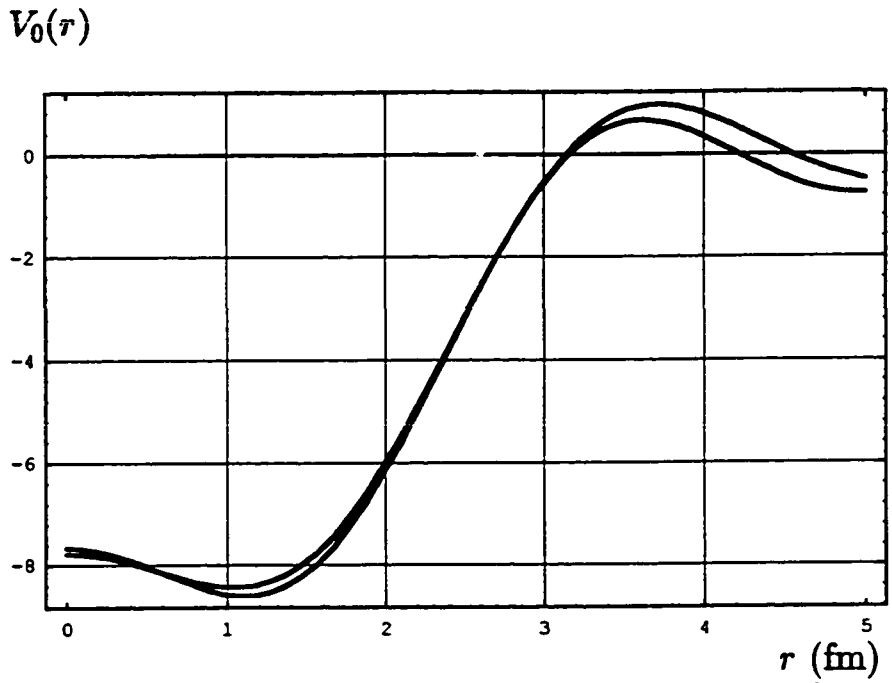

Fig. 7.61 : Comparison between the potential obtained by solving eqn. (7.29) for $\nu = 16$ and the one obtained for $\nu = 9$.

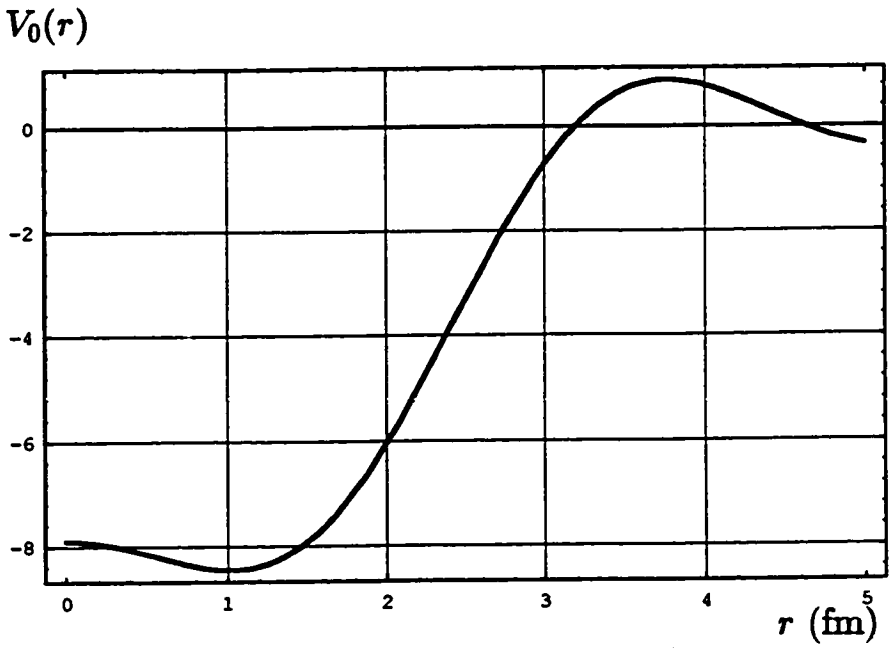

Fig. 7.62 : Potential obtained by solving eqn. (7.29) for $\nu = 17$.

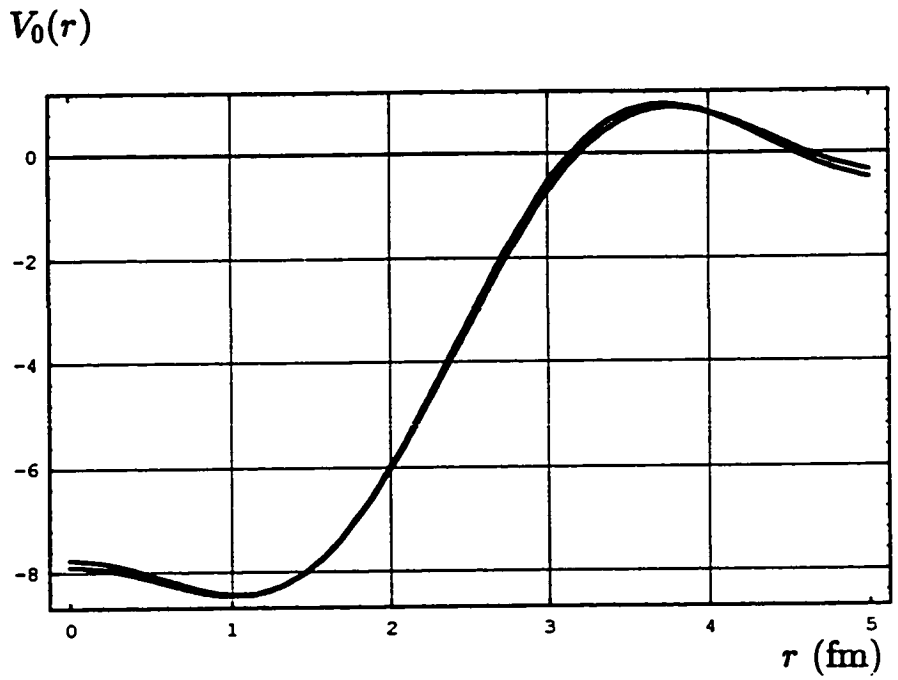

Fig. 7.63 : Comparison between the potential obtained by solving eqn. (7.29) for $\nu = 17$ and the one obtained for $\nu = 16$.

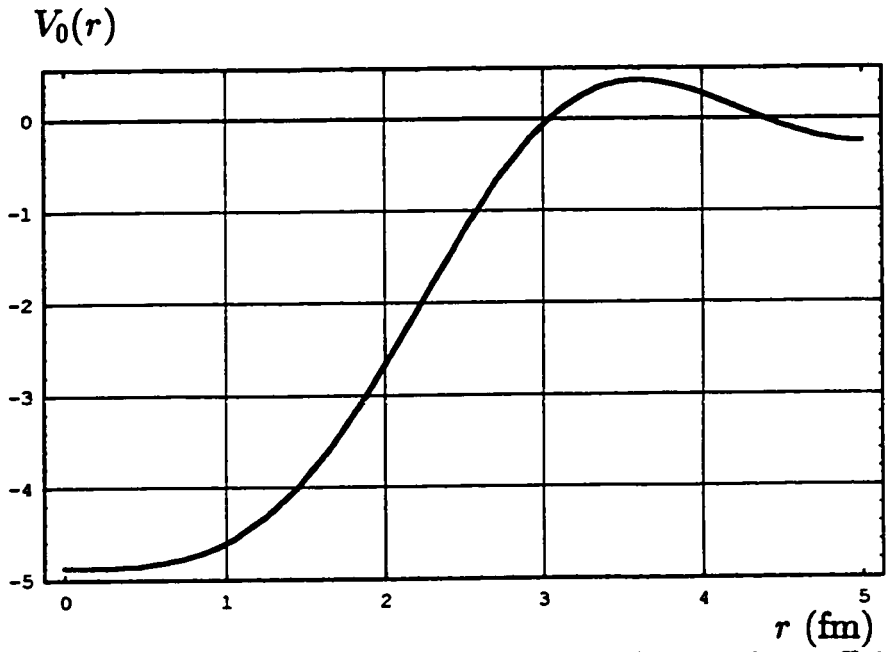

Fig. 7.64 : Potential calculated from eqn. (7.15) using the coefficients β_i calculated from eqn. (7.26) for a nucleon in a sphere of radius $a = 10$ fm, scattered from a square well potential of depth $V = -5$ MeV and range $d = 2$ fm, in $\ell = 0$.

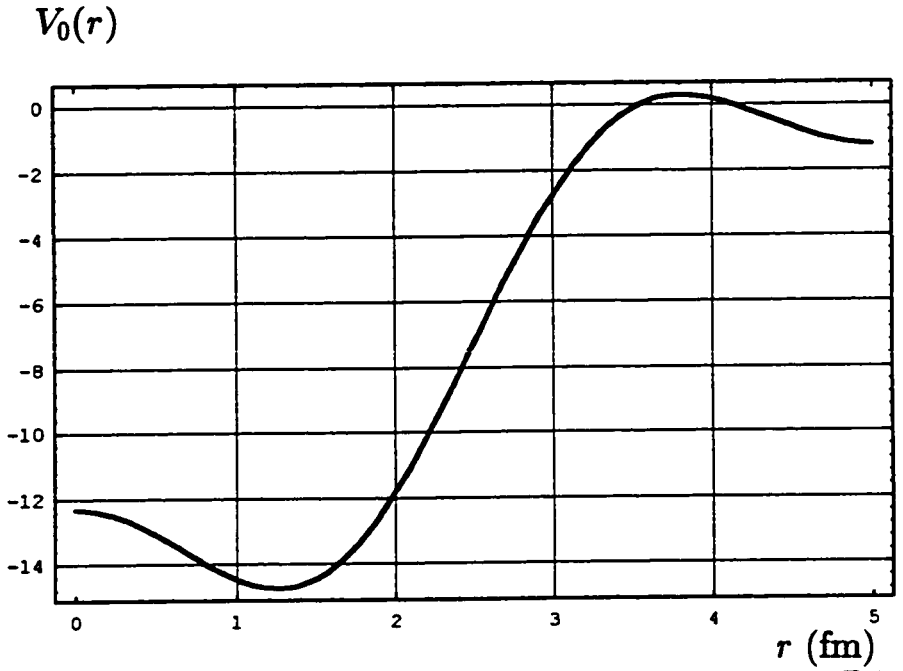

Fig. 7.65 : Potential calculated from eqn. (7.15) using the coefficients β_i calculated from eqn. (7.26) for a nucleon in a sphere of radius $a = 10$ fm, scattered from a square well potential of depth $V = -20$ MeV and range $d = 2$ fm, in $\ell = 0$.

7.3 Comparison Between The Two Inversion Techniques

Comparing the potential obtained using the two inversion techniques, one can observe that the first inversion technique, namely the $g_\ell(k_{\ell n}r)$−approach, gives quite good results in the range $0 \leq r \leq a/2$ while the second one, namely the potential expansion approach, gives slightly less accurate results because of the singularity of the matrix obtained. Figs. 7.66, 7.67 and 7.68 compare the potential obtained using the two inversion techniques for a nucleon confined within a three-dimensional sphere of radius $a = 10$ fm, and scattered off a square well potential of range $d = 2$ fm and depths $V = -5$, -10 and -20 MeV respectively, in the angular momentum channel $\ell = 0$. From these figures, one can see clearly that the results obtained using the first technique is better than those obtained using the second one. However, the second inversion technique is more general than the first and can be applied in many inverse problems which occur in many different fields of science such as Astronomy, while the first technique is restricted to inverse problems which contain an integral involving $j_\ell^2(k_{\ell n}r)$.

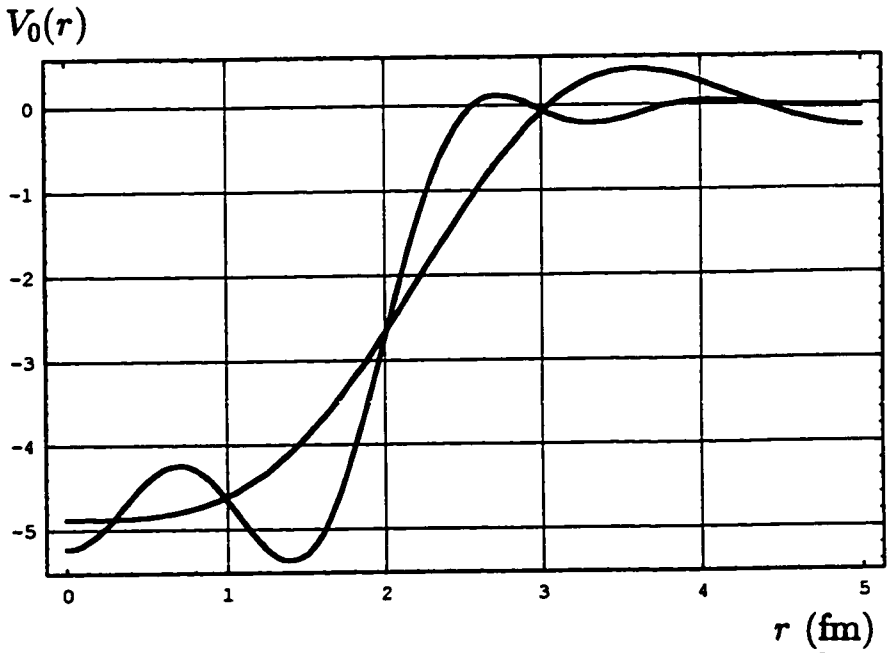

Fig. 7.66 : Comparison between the potential obtained using the two inversion techniques for a nucleon in a sphere of radius $a = 10$ fm, scattered from a square well potential of depth $V = -5$ MeV and range $d = 2$ fm, in $\ell = 0$.

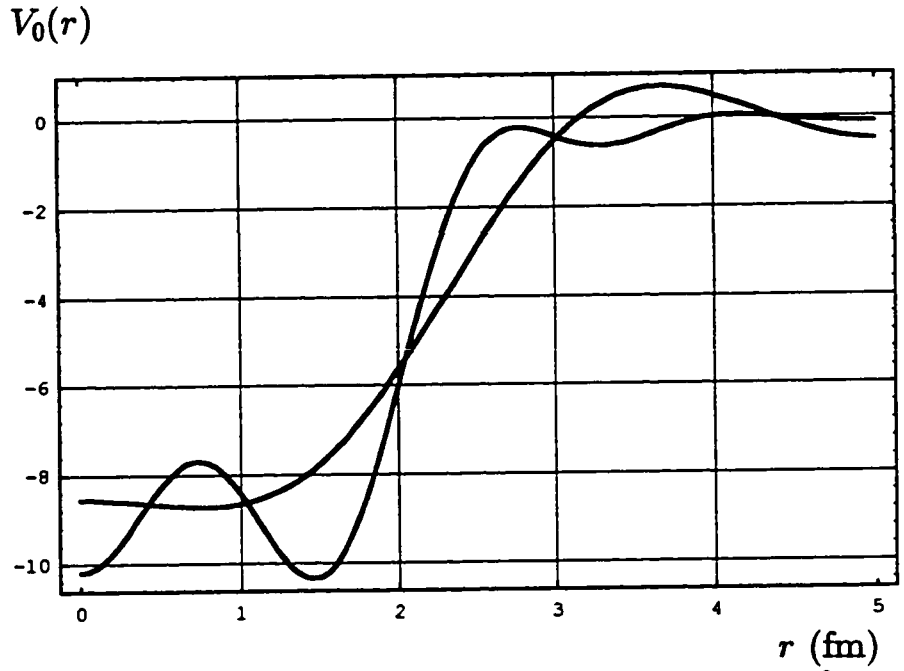

Fig. 7.67 : Comparison between the potential obtained using the two inversion techniques for a nucleon in a sphere of radius $a = 10$ fm, scattered from a square well potential of depth $V = -10$ MeV and range $d = 2$ fm, in $\ell = 0$.

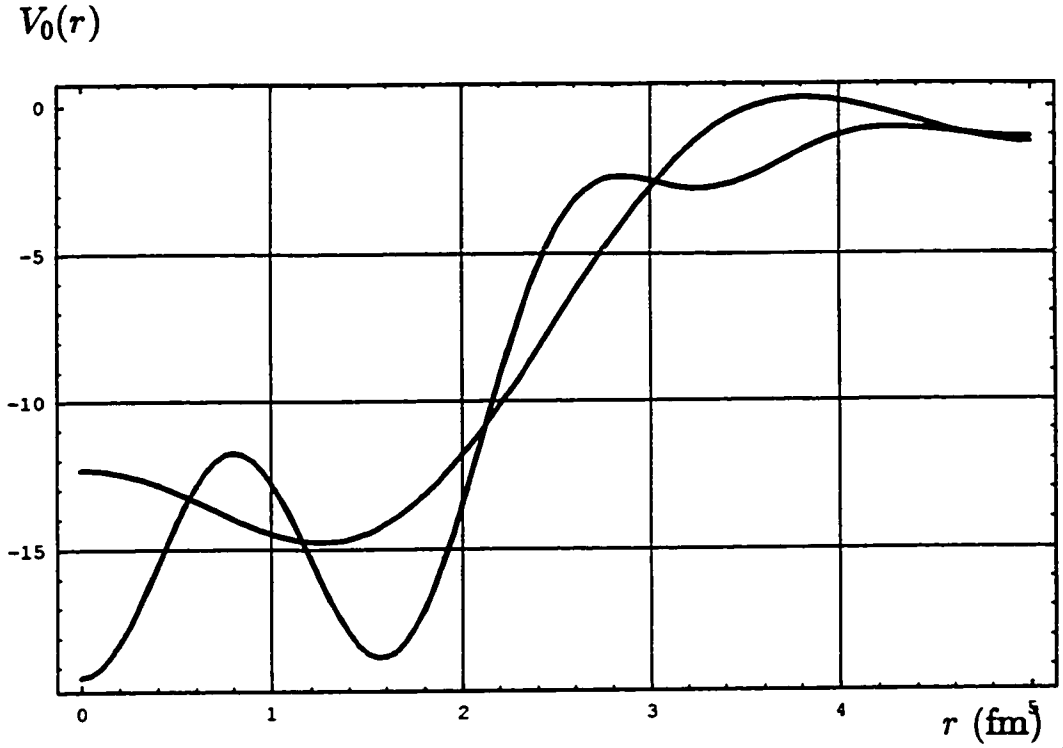

Fig. 7.68 : Comparison between the potential obtained using the two inversion techniques for a nucleon in a sphere of radius $a = 10$ fm, scattered from a square well potential of depth $V = -20$ MeV and range $d = 2$ fm, in $\ell = 0$.

7.4 Mass Dependence

The inversion techniques which extract the potential from the partial wave Born approximation in finite and infinite spaces is mass dependent. To illustrate this mass dependence, let us consider two particles of masses $\mu_1 = 469.5$ MeV/c^2 and $\mu_2 = 1000$ MeV/c^2, scattered off a square well potential of depth $V = -10$ MeV and range $d = 2$ fm in the angular momentum channel $\ell = 0$. As an example, let us consider the finite $g_\ell(k_{\ell n}r)$−approach to illustrate this mass dependence.

The "experimental" phase shifts (up to $E \approx 225$ MeV) produced by the particle μ_1, scattered off the above potential and the corresponding potential calculated from eqn. (7.5) are given in figs. (7.69) and (7.70) respectively while the "experimental" phase shifts (up to $E \approx 225$ MeV/c^2) produced by the particle μ_2, scattered off the same potential and the corresponding potential calculated from eqn. (7.5) are given in figs. (7.71) and (7.72) respectively. From fig. (7.73) one can observe clearly that the calculated potential of mass μ_1, which is of smaller mass, approximates the "experimental" potential much better than that of μ_2.

This mass dependence is expected since the partial wave Born approximation is most appropriate for phase shifts which are small or in other words for particles with wave functions of small deviation from the free particle wave function. For two particles of different masses scattered from the same potential, the lighter particle feels the potential less than the heavier one and consequently the phase

shifts of the lighter particle is smaller than that of the heavier particle, see figs. 7.69 and 7.71, which means that the lighter particle satisfies the partial wave Born approximation better than the heavier one.

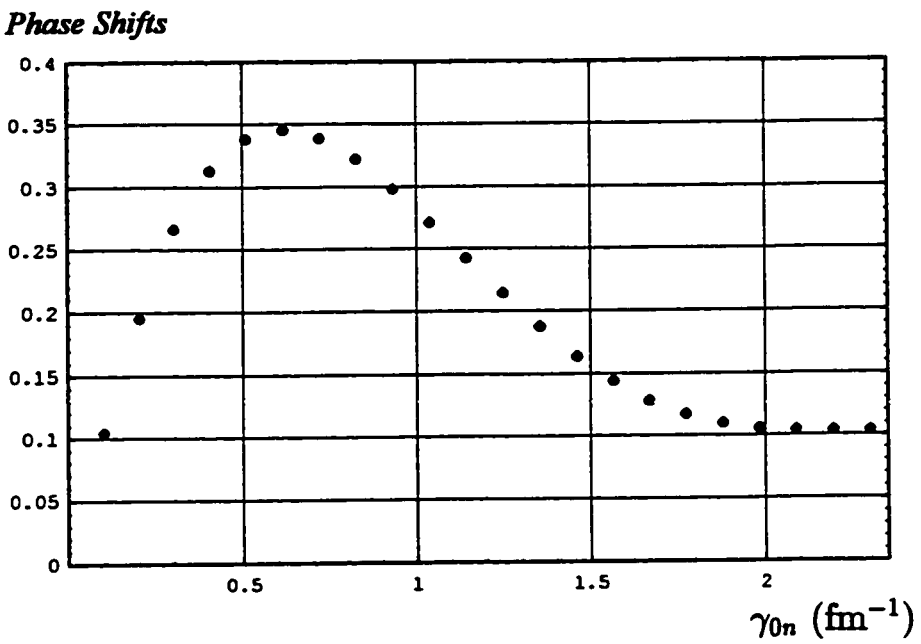

Fig. 7.69 : Discrete phase shifts produced by a particle of mass $\mu_1 = 469.5$ MeV/c^2 scattered from a square well potential of depth $V = -10$ MeV and range $d = 2$ fm in $\ell = 0$ in a sphere of radius $a = 30$ fm.

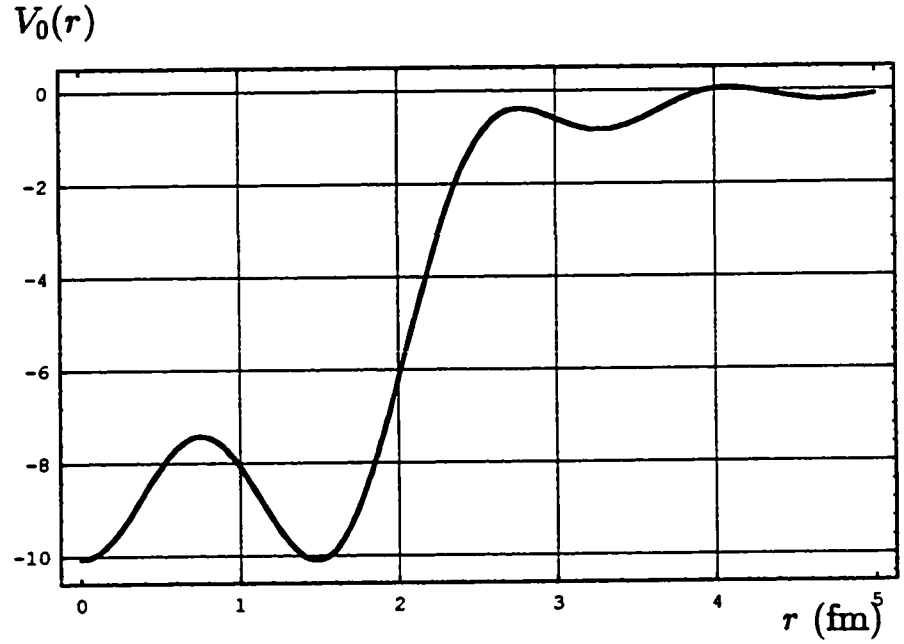

Fig. 7.70 : Potential calculated from eqn. (7.5) using the discrete perturbed energy states obtained in the above figure.

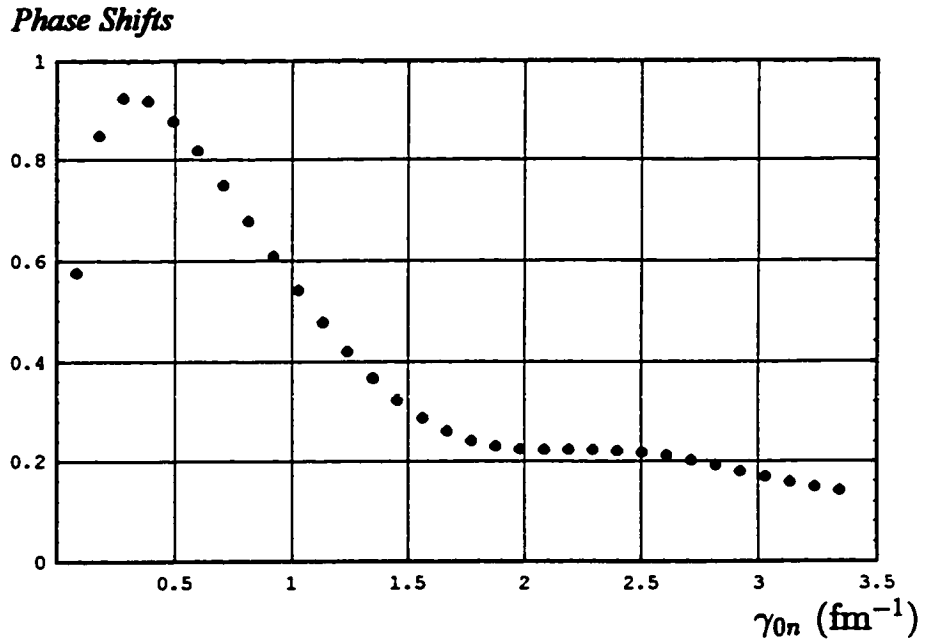

Fig. 7.71 : Discrete phase shifts produced by a particle of mass $\mu_2 = 1000$ MeV/c^2 scattered from a square well potential of depth $V = -10$ MeV and range $d = 2$ fm in ℓ=0 in a sphere of radius a=30 fm.

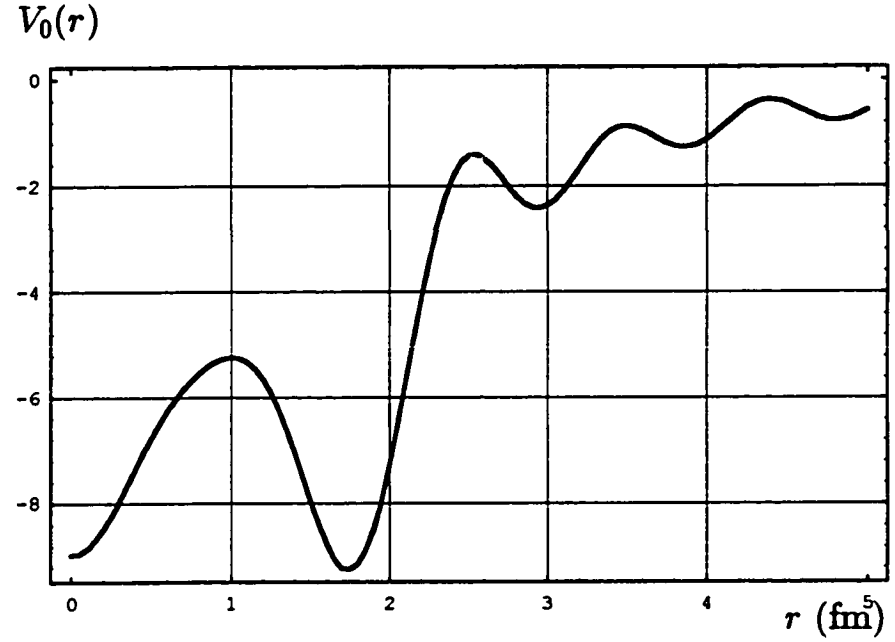

Fig. 7.72 : Potential calculated from eqn. (7.5) using the discrete perturbed energy states obtained in the above figure.

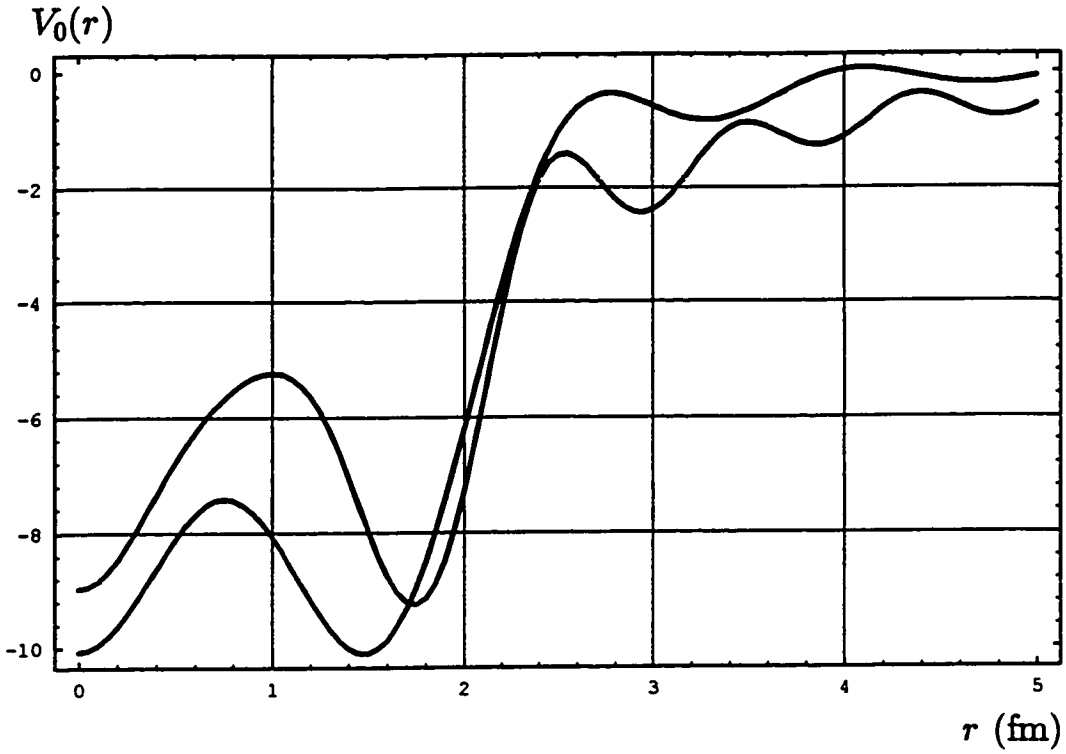

Fig. 7.73 : Comparison between the two potentials given in figs. (7.70) and (7.72).

CONCLUSIONS

Two inversion techniques were developed to invert the finite-space partial-wave Born approximation. The first technique, involves using the inverse function of $j_\ell^2(r)$, namely $g_\ell(r)$ while the second technique involves expanding the potential in terms of a complete set and then reducing the problem to solving the matrix equation $Mb = d$, eqn. (6.41). To obtain the potential $V_\ell(r)$, one needs to invert the matrix M which turns out to be *singular. Although the matrix M is singular, we inverted it using generalized inverse concepts and techniques.*

The first technique gives quite good results in the range $0 \leq r \leq a/2$ while the second gives slightly less accurate results because of the singularity of the matrix obtained. One should notice that the second technique is more general than the first and can be applied in many inverse problems which occur in many different fields of science such as Astronomy, while the first technique is restricted to inverse

problems which contain an integral involving $j_\ell^2(k_{\ell n}r)$.

Our approach, namely inverting the partial wave Born approximation in finite spaces, is valid for weak potentials and is mass dependent, as in infinite spaces. However, our approach improves for large angular momentum channels and light masses. In fact, our results are much better than the results obtained in [7], since in that paper the authors considered a particle of mass $\mu = 931$ MeV/c^2 in the relative coordinate system while one should consider a particle of mass $\mu \approx 469.5$ MeV/c^2, which is around a half of the rest mass of the nucleon, since our aim is to test the inversion techniques to obtain the potentials using the experimental phase shifts produced by *nucleon−nucleon scattering.* Furthermore, the infinite space inversion techniques developed in ref. [7] were improved by inverting the second partial wave Born approximation rather than the first partial wave Born approximation.

REFERENCES

1. K. Chadan and P. C. Sabatier, *Inverse Problems in Quantum Scattering Theory*, (Springer-Verlag, 1989).
2. F. Calogero and A. Degasperis, *Spectral Transform and Solitons*, (North Holland, Amsterdam, 1982).
3. K. M. Case and M. Kac, J. Math. Phys. 14, 1973, p. 594.
4. K. M. Case, J. Math. Phys. 14, 1973, p. 916.
5. K. M. Case and S. C. Chiu, J. Math. Phys. 14, 1973, p. 1643.
6. E. Merzbacher, *Quantum Mechanics* (Wiley, New York, 1970), 2nd ed., p. 244.
7. H.A. Mavromatis and A.M. Al-Jalal, J. Math. Phys. 31, 1991, p. 1181.
8. M. A. Preston and R. K. Bhaduri, *Structure of the Nucleus*, (Addison Wesley Publishing Company, 1982), p. 165.
9. J. D. Jackson, *Classical Electrodynamics*, (John Wiley & Sons, Inc., 1975), 2nd ed., p. 65.
10. J. Mathews and R. Walker, *Mathematical Methods of Physics*, (Addison Wesley, 1970), 2nd ed., p. 187.
11. F. W. Olver, *Royal Society Mathematical Tables*, Vol. 7, (University Press, Cambridge, 1960).
12. J. Mathews and R. Walker, Ref. 10, p. 182.
13. G. Arfken, *Mathematical Methods for Physicists*, (Academic Press, 1970), 2nd ed., p. 495.

14. H.A. Mavromatis and K. Schilcher, J. Math. Phys. 9, 1968, p. 1627.
15. H.A. Mavromatis and K. Schilcher, Ref. 14.
16. J. Mathews and R. Walker, Ref. 10, p. 187.
17. H.A. Mavromatis and A.M. Jalal, Ref. 7, p. 1187.
18. S.B. Al-Ruwaili, M.S. thesis, Phys. Dept. KFUPM, Dhahran, Saudi Arabia. p. 10.
19. H.A. Mavromatis and A.M. Al-Jalal, Ref. 7, p. 1181.
20. H.A. Mavromatis and A.M. Al-Jalal, Ref. 7, p. 1182.
21. S.B. Al-Ruwaili, Ref. 18, p. 19.
22. I. S. Gradshteyn and I. M. Ryzhik, *Tables of Integrals, Series, and Products*, (Academic Press, New York, 1980), p. 747.
23. J. Mathews and R. Walker, Ref. 10, p. 187.
24. I. S. Gradshteyn and I. M. Ryzhik, Ref. 22, p. 692.
25. J. Mathews and R. Walker, Ref. 10, p. 77.
26. G Barton, *Elements of Green's Functions and Propagation*, (Clarendon Press, Oxford, 1989), p. 8.
27. R. A. Horn and C. A. Johnson, *Matrix Analysis*, (Cambridge University Press, 1985), p. 12.
28. A. Ben-Israel and T. Greville, *Generalized Inverses, Theory and Applications*, (John Wiley & Sons, Inc., 1974), p. 1.
29. D. Watkins, *Fundamentals of Matrix Computations*, (John Wiley & Sons, Inc., 1991), p. 232.
30. D. Watkins, Ref. 29, p. 391.
31. S. L. Campbell, *Recent Applications of Generalized Inverses*, (Pitman Adcanced Publishing Program, 1982).
32. M. Z. Nashed, *Generalized Inverses and Applications*, (Academic Press, 1976).
33. I. Fredholm, Acta. Math., 27, 1903, pp. 365-390.

34. A. Ben-Israel and T. Greville, Ref. 28, p. 2.

35. R. Penrose, Proc. Cambridge Philos. Soc., 51, 1955, pp. 406-413.

36. S. Biswas, *Topics in Algebra of Matrices*, (Academic Publications, 1984), p. 84.

37. D. Watkins, Ref. 29, p. 421.

38. C. J. Joachain, *Quantum Collision Theory*, (North Holland, Amsterdam, 1983). p. 46.

39. E. Merzbacher, Ref. 6, p. 232.

40. M. A. Preston and R. K. Bhaduri, Ref. 8, p.29.

41. H.A. Mavromatis and A.M. Al-Jalal, Ref. 7, p. 1182.

42. C. J. Joachain, Ref. 38, p. 121.

43. E. Merzbacher, Ref. 6, p. 194.

44. E. Merzbacher, Ref. 6, p. 232.

45. G. Arfken, Ref. 13, p. 525.

46. G. Arfken, Ref. 13, p. 525.

47. M. A. Preston and R. K. Bhaduri, Ref. 8, p. 24.

48. M. A. Preston and R. K. Bhaduri, Ref. 8, p. 154.